

Investigating the Antibody Immune Response to Ebola Virus Vaccination in Humans

Inaugural-Dissertation

zur

Erlangung des Doktorgrades

der Mathematisch-Naturwissenschaftlichen Fakultät

der Universität zu Köln

vorgelegt von

Stefanie Alexandra Ehrhardt

aus Mainz

Bonn, 2021

Berichterstatter: Prof. Dr. Florian Klein
(Gutachter) Prof. Dr. Michael Lässig
Prof. Dr. Michael Nothnagel

Tag der Disputation:

Erklärung zur Dissertation

Ich versichere, dass ich die von mir vorgelegte Dissertation selbständig angefertigt, die benutzten Quellen und Hilfsmittel vollständig angegeben und die Stellen der Arbeit – einschließlich Tabellen, Karten und Abbildungen –, die anderen Werken im Wortlaut oder dem Sinn nach entnommen sind, in jedem Einzelfall als Entlehnung kenntlich gemacht habe; dass diese Dissertation noch keiner anderen Fakultät oder Universität zur Prüfung vorgelegen hat; dass sie – abgesehen von unten angegebenen Teilpublikationen – noch nicht veröffentlicht worden ist, sowie, dass ich eine solche Veröffentlichung vor Abschluss des Promotionsverfahrens nicht vornehmen werde. Die Bestimmungen der Promotionsordnung sind mir bekannt. Die von mir vorgelegte Dissertation ist von Prof. Dr. Florian Klein betreut worden.

Teilpublikationen:

Stefanie A. Ehrhardt, Matthias Zehner, Verena Krähling, Hadas Cohen-Dvashi, Christoph Kreer, Nadav Elad, Henning Gruell, Meryem S. Ercanoglu, Philipp Schommers, Lutz Gieselmann, Ralf Eggeling, Christine Dahlke, Timo Wolf, Nico Pfeifer, Marylyn M. Addo, Ron Diskin, Stephan Becker, and Florian Klein. *Polyclonal and convergent antibody response to Ebola virus vaccine rVSV-ZEBOV*. **Nat Med** 25, 1589–1600 (2019).

Hadas Cohen-Dvashi, Matthias Zehner, **Stefanie A. Ehrhardt**, Michael Katz, Nadav Elad, Florian Klein, and Ron Diskin. *Structural Basis for a Convergent Immune Response against Ebola Virus*. **Cell Host Microbe** 27, 418-427 (2020).

Bonn, den 15. November 2021



Stefanie Alexandra Ehrhardt

Summary

As the most advanced Ebola virus vaccine candidate, recombinant vesicular stomatitis virus–Zaire Ebola virus (rVSV-ZEBOV) has been used under compassionate use to combat two Ebola virus disease (EVD) outbreaks. Before licensing, more than 350,000 individuals at risk had been administered the vaccination until 2020. Importantly, a detailed molecular analysis of the vaccine-induced humoral immunity was not available.

In this thesis, the B cell and antibody immune response is elucidated in an unprecedented depth in a cohort of human volunteers that were enrolled in a phase 1 rVSV-ZEBOV vaccination trial. Sera of all vaccinees and across different vaccination doses showed higher reactivity compared to non-vaccinated individuals. Advanced and comprehensive single B cell sorts and sequence analyses further revealed that all individuals exhibited polyclonal B cell responses with numerous specific B cells. Albeit the response was diverse, it was highly reproducible and amongst vaccinees, convergent B cell responses were observed with B cell clones that shared sequence characteristics to a remarkable degree. Moreover, in all vaccinated subjects, convergent antibodies were identified that combined heavy chains with IGHV3-15 with lambda light chains comprising IGLV1-40, arguing for an eminent yet previously unnoticed role of this group of antibodies in the defense against Ebola viruses. Detailed epitope mapping showed that vaccination induced B cell responses against all domains of EBOV GP.

Moreover, vaccination-induced antibodies had overlapping target epitopes with antibodies isolated from EVD survivors, which was shown by competition for EBOV GP epitopes and electron microscopy structure analyses suggesting that vaccination authentically triggers B cell immunity. Importantly, EBOV GP-specific antibodies also cross-reacted with other Filovirus species, which might indicate positive effects on antibody-mediated immunity against other Filoviruses. Moreover, in all vaccinees, we detected highly potent EBOV-neutralizing antibodies including antibodies combining the IGHV3–15/IGLV1–40 immunoglobulin gene segments. Some of them exerted EBOV-neutralizing activities comparable or even superior to previously reported monoclonal antibodies such as the survivor-derived mAb114, which has recently been licensed as EVD therapy. These findings provide the first comprehensive analysis of the rVSV-ZEBOV-induced B cell response and will help to evaluate and direct current and future means against EVD and potentially other viral diseases.

Zusammenfassung

Als fortschrittlichster Impfstoffkandidat gegen das Ebola Virus wurde rVSV-ZEBOV (rekombinantes vesikuläre Stomatitis-Virus mit Zaire Ebola Virus Glykoprotein) bereits vor der Zulassung außerordentlich eingesetzt, um zwei Ausbrüche der Ebola-Virus-Krankheit (engl.: Ebola virus disease EVD) zu bekämpfen. So erhielten bis 2020 mehr als 350.000 gefährdete Personen den experimentellen Impfstoff. Zu diesem Zeitpunkt gab es jedoch keine detaillierte, molekulare Analyse der Impfstoff induzierten humoralen Immunität.

In dieser Arbeit sollte daher die Immunantwort von B-Zellen und Antikörpern in einer Kohorte Freiwilliger untersucht werden, die an einer Phase-1 Studie für das rVSV-ZEBOV Vakzin teilgenommen hatten. Unabhängig von der Impfstoffdosis zeigten die Seren aller Geimpften im Vergleich zu nicht geimpften Personen eine höhere Reaktivität gegen das Ebolavirus Glykoprotein. Spezifische B-Zellisolationen auf Einzelzellebene und nachfolgende umfangreiche Sequenzanalysen zeigten ferner, dass alle Individuen polyklonale B-Zell-Antworten mit zahlreichen Ebola virus Glykoprotein-spezifischen B-Zellen ausbildeten. Die Vakzinierung führte zur Expansion unterschiedlicher B-Zellen innerhalb einzelner Individuen, war jedoch hoch reproduzierbar im Vergleich zwischen verschiedenen Individuen. In unterschiedlichen Probanden wurden konvergente B-Zell-Reaktionen und B-Zell-Klone beobachtet, die Sequenzmerkmale in bemerkenswertem Maße teilten. Darüber hinaus wurden bei allen geimpften Probanden konvergente Antikörper identifiziert, die schwere Ketten mit Gensegment IGHV3-15 und leichten Lambda-Ketten des Gensegments IGLV1-40 kombinierten. Die herausragende Rolle einer bestimmten Gruppe von Antikörpern bei der Abwehr von Ebola Viren war bisher unbekannt. Die detaillierte Analyse der Zielepitope zeigte, dass die Impfung spezifische Antikörper gegen alle Domänen des EBOV GP induzierte. Darüber stimmten die Zielepitope der durch Impfung induzierten Antikörper teilweise oder in Gänze mit denen in EVD-Überlebenden überein, was durch die kompetitive Bindungsexperimente um EBOV-GP-Epitope sowie elektronenmikroskopische Strukturanalysen gezeigt wurde. Es konnte demnach gezeigt werden, dass die B-Zell-Antwort nach rVSV-ZEBOV Impfung und natürlicher Infektion vergleichbar sind.

Darüber hinaus, waren EBOV GP-spezifische Antikörper auch mit Glykoproteinen anderer Filoviren kreuzreaktiv, weshalb eine Impfung mit rVSV-ZEBOV möglicherweise einen positiven Einfluss auf die Antikörper-vermittelte Immunität gegen andere Filoviren haben könnte. In allen Probanden konnten wir hochwirksame EBOV-neutralisierende Antikörper nachweisen. Hierzu gehörte auch die verbreitete Gruppe der Antikörper, die die Immunglobulin-Gensegmente IGHV3-15/IGLV1-40 kombinieren. Einige Antikörper neutralisierten bei vergleichbaren oder sogar bei geringeren Mengen als bereits publizierte

monoklonale Antikörper wie mAb114, der aus einem Überlebenden isoliert und kürzlich als EVD-Therapie zugelassen wurde. Diese Ergebnisse liefern die erste umfassende Analyse der rVSV-ZEBOV-induzierten B-Zell-Antwort und werden dazu beitragen, aktuelle und zukünftige Therapien und Vakzine gegen EVD und potenziell andere Viruserkrankungen zu bewerten und zu optimieren.

Abbreviations

°C	degree Celsius
A	Adenosine
A	Alanine
aa	Amino acid
Ab	Antibody
ADCC	Antibody-dependent cellular cytotoxicity
ADCP	Antibody-dependent cellular phagocytosis
ADNP	Antibody-dependent neutrophil phagocytosis
AF700	Alexa Fluor 700
AID	Activation induced deaminase
AIDS	Acquired immune deficiency syndrome
AM	Affinity maturation
AmpR	Ampicillin Resistance gene
APC	Allophycocyanin
APE1	Apurinic/aprimidinic endonuclease 1
BCR	B cell receptor
BDBV	<i>Bundibugyo ebolavirus</i>
BEBOV	Former abbreviation of <i>Bundibugyo ebolavirus</i> (BDBV)
Bis-Tris	Bis (2-hydroxyethyl) imino-tris (hydroxymethyl) methane-HCl
BLOSUM	BLOCKS Substitution Matrix
bNAb	broadly NAb
BOMV	<i>Bombali ebolavirus</i>
bp	base pair(s)
C	Cysteine
CaCl ₂	Calcium chloride
CAG	CMV enhancer, chicken beta-Actin and rabbit beta-Globin splice acceptor site
CatL/B	Cathepsins L and B
CD	Cluster of differentiation
CDC	Complement-dependent cytotoxicity
CDC	Centers for Disease Control and Prevention
cDNA	complementary DNA
CDR	Complementary determining region
CDRH	CDR of HC
CDRL	CDR of LC

CH	Heavy chain constant region
CIEBOV	<i>Côte d'Ivoire virus</i> ; former abbreviation of <i>Bundibugyo ebolavirus</i> (BDBV)
CL	Light chain constant region
CLP	Common lymphoid progenitor
CMV	Cytomegalovirus
COVID-19	Coronavirus disease of 2019
CPE	Cytopathic effect
CSR	Class switch recombination
C-terminal	Carboxy-terminal
D	Aspartic acid
D	Diversification gene
DAPI	4',6-diamidino-2-phenylindole
DMEM	Dulbecco's Modified Eagle's medium
DMF	Dimethyl formamide
DMSO	Dimethyl sulfoxide
DNA	Deoxyribonucleic acid
dNTPs	Deoxyribonucleotide triphosphates
DPBS	Dulbecco's phosphate buffered saline
DRC	Democratic Republic of the Congo
DTT	Dithiothreitol
E	Glutamic acid
<i>E. coli</i>	<i>Escherichia coli</i>
EBOV	<i>Zaire ebolavirus</i>
EC	Effective concentration
EDTA	Ethylenediamine tetraacetic acid
ELISA	Enzyme-linked immunosorbent assay
ER	Endoplasmatic reticulum
ESRF	European Synchrotron Radiation Facility
EtOH	Ethanol
EV	rVSV-ZEBOV-immunized donor
EVD	Ebola virus disease
F	Phenylalanine
Fab	Fragment antigen binding
FACS	Fluorescence activated cell sorting
FBS	Fetal bovine serum
Fc	Fraction crystallizable

FcnR	Neonatal FcR
FcR	Fc receptor
FDA	Food and Drug Administration
FITC	Fluorescein isothiocyanate
FP	Frankfurt patient
FSC	Forward scatter
FSC-A	FSC-Area
FSC-H	FSC-Height
fw	forward
FWR	Framework region
G	Glycine
g	gravity
GCN4	General Control Nonderepressible 4
Gly-Cap	Glycan cap
GP	Glycoprotein
GPcl	Cleaved GP
H	Histidine
H ₂ O	Water
<i>HBS</i>	HEPES <i>buffered</i> saline
HC	Heavy chain
HCl	Hydrogen chloride
HEK	Human embryonic kidney
HEPES	Hydroxyethyl piperazineethanesulfonic acid
HIV	Human immunodeficiency virus
HR1/2	Heptad repeat 1 and 2
HRP	Horseradish peroxidase
I	Isoleucine
IC	Inhibitory concentration
IFL	Internal fusion loop, also referred to as fusion loop
Ig	Immunoglobulin
IgA	Ig HC of the α isotype; also describing full antibody comprising isotype α HC
IgD	Ig HC of the δ isotype; also describing full antibody comprising isotype δ HC
IgE	Ig HC of the ϵ isotype; also describing full antibody comprising isotype ϵ HC

IgG	Ig HC of the γ isotype; also describing full antibody comprising isotype γ HC
IgH	Ig HC
IgK	Ig LC of the κ isotype; also describing full antibody comprising isotype κ LC
IgL	Ig LC of the λ isotype; also describing full antibody comprising isotype λ LC
IgM	Ig HC of the μ isotype; also describing full antibody comprising isotype μ HC
imgt	ImMunoGeneTics database
IRB	Institutional review board
IRES	Internal ribosomal entry site
J	Junctional gene
JH	Junctional gene of the HC
JL	Junctional gene of the LC
K	Lysine
KCl	Potassium chloride
kDa	kilo Dalton
KH ₂ PO ₄	Monopotassium dihydrogen phosphate
L polymerase	Large polymerase
L	Leucine
LB	Lysogeny broth
LC	Light chain
LDS	Lithium dodecyl sulfate
LLOV	<i>Lloviu cuevavirus</i>
M	Methionine
mAb	Monoclonal Ab
MACS	Magnetic activated cell sorting
MARV	Marburg virus
MFI	Mean fluorescence intensity
MID	Molecular identifier
MLD	Mucin(-like) domain
MOPS	3-(N-Morpholino) propane sulphonic acid
MPER	Membrane proximal external region
mRNA	Messenger RNA
MSF	Médecins Sans Frontières

MWCO	Molecular weight cut off
N	Asparagine
N-	Non-templated
n.d.	Not determined or not detected
n.m.	No match
N/A	Not analyzed
Na ₂ HPO ₄	Disodium hydrogen phosphate
NAb	Neutralizing mAb
NaCl	Sodium chloride
NaOH	Sodium hydroxide
NGS	Next generation sequencing
NHEJ	Non-homologous end joining
NHP	Non-human primate
Ni-NTA	Nickel nitrilotriacetic acid
NK cell	Natural killer cell
NK	Nucleoprotein
NPC1	Niemann-Pick C1
NPI	Sodium phosphate imidazole
N-terminal	Amino-terminal
OD	Optical density
ori	Origin of replication
p	Promoter
P	Palindromic nucleotide sequence
P	Proline
P/S	Penicillin/Streptomycin
PAGE	Polyacrylamide gelectrophoresis
PBMC	Peripheral blood mononuclear cell
PBS	Phosphate buffered saline
PBST	PBS with Tween 20
PCR	Polymerase chain reaction
PDGF-R	Platelet-derived growth factor receptor
PEI	Polyethylenimine, 25 kDA
pfu	Plaque forming units
PI	Propidium iodide
Pre-	Precursor
Q	Glutamine
R	Arginine

RAG1/2	Recombination activating genes 1 and 2
RAVV	Ravn virus
rev	reverse
RNA	Ribonucleic acid
RPMI	Roswell Park Memorial Institute, 1640 medium, with L-Glutamine
RS	Restriction site
RSS	Recombination signal sequences
RT	Room temperature
rVSV	Recombinant vesicular stomatitis virus
rVSV-ZEBOV	recombinant vesicular stomatitis virus with EBOV GP
rxn	reaction
S	Serine
S	Survivor of EVD
SARS	Severe acute respiratory syndrome
SARS-CoV-2	SARS-Coronavirus-2
SD	Standard deviation
SDS	Sodium dodecyl sulfate
SEBOV	Former abbreviation of <i>Sudan ebolavirus</i> (SUDV)
SEC	Size exclusion chromatography
sGP	Secreted GP
SHM	Somatic hypermutation
SLIC	Sequence- and ligation-independent cloning
SOC medium	Super optimal broth with catabolite repression medium
SOC	Standard of care
SP	Signal peptide
SSC	Sideward scatter
SSC-A	SSC-Area
SSC-H	SSC-Height
ssGP	Small sGP
ssRNA	Single-stranded RNA
SUDV	<i>Sudan ebolavirus</i>
SV40	Simian vacuolating virus 40
T	Threonine
TAE	Tris-Acetate EDTA <i>buffer</i>
TAFV	<i>Tai Forest ebolavirus</i>
Taq	<i>Thermophilus aquaticus</i>
TdT	Terminal deoxynucleotidyl transferase

TM	Transmembrane domain
TRIS	<i>Tris</i> (hydroxymethyl)aminomethane
Tween 20	Polyoxyethylene-20-sorbitan monolaurate
U	Uridine
UMI	Unique molecular identifier
UNG	Uracil DNA glycosylase
V	Valine
V	Variable gene
VH gene	Variable gene of the HC, or V gene segment (Cave: in the literature, this abbreviation is also used to describe the variable region of the heavy chain. For the sake of clearness in this thesis, the variable region of the heavy chain is referred to as V region)
VH region	Variable region of the HC
VL gene	Variable gene of the LC
VL region	Variable region of the LC
VP	Viral protein
W	Tryptophan
WHO	World Health Organization
Y	Tyrosine
ZEBOV	Former abbreviation of <i>Zaire ebolavirus</i> (EBOV)

Table of Contents

Erklärung zur Dissertation	III
Summary.....	V
Zusammenfassung	VI
Acknowledgements.....	VIII
Abbreviations.....	IX
Table of Contents	XVI
1 Introduction.....	1
1.1 <i>The role of B cells and antibodies in the immune system</i>	1
1.1.1 B cell development	2
1.1.2 B cell receptor structures.....	3
1.1.3 B cell receptor diversity	6
1.1.3.1 Somatic recombination.....	7
1.1.3.2 Combinatorial diversity.....	8
1.1.3.3 Junctional diversity	8
1.1.3.4 Somatic hypermutation	9
1.1.3.5 Class switch recombination	10
1.1.4 Antibody characteristics and effector functions.....	10
1.2 <i>Ebolaviruses and Ebola Virus Disease</i>	12
1.2.1 Ebola virus taxonomy and epidemiology	13
1.2.2 Ebola virus structure and genome organization	15
1.2.2.1 Ebola virus sGP/GP gene products.....	16
1.2.3 Ebola virus glycoprotein (GP) binding and fusion	18
1.2.4 Immune responses against Ebolaviruses	20
1.2.5 Countermeasures to Ebolaviruses	21
1.2.5.1 Therapy	21
1.2.5.2 Vaccinations	22
1.3 <i>Aim of this thesis</i>	24

2	Materials and methods	25
2.1	<i>Materials</i>	25
2.1.1	Laboratory equipment	25
2.1.2	Consumables	26
2.1.3	Chemicals, biologicals, and reagents	27
2.1.4	Buffer, media and solutions	29
2.1.5	Commercial kits	30
2.1.6	Antibodies	31
2.1.7	Enzymes	31
2.1.8	Oligonucleotides	32
2.1.9	Human samples, cell lines, and bacterial or viral strains	36
2.1.10	Software	36
2.2	<i>Methods</i>	37
2.2.1	Molecular biology	37
2.2.1.1	Restriction digestion	37
2.2.1.2	Gel electrophoresis	37
2.2.1.3	DNA purification	38
2.2.1.4	DNA quantification	38
2.2.1.5	DNA ligation	38
2.2.1.6	Transformation of chemically competent bacteria	38
2.2.1.7	Colony PCR	38
2.2.1.8	Mini preparation of plasmid DNA	40
2.2.1.9	Midi and maxi preparation of plasmid DNA	40
2.2.1.10	Sequencing	41
2.2.1.11	Preparation of glycerol stocks	41
2.2.1.12	Cloning strategies	42
2.2.2	Cell culture	46
2.2.2.1	Human samples	46
2.2.2.2	Cultivation of cell lines	47
2.2.3	Protein biology	48
2.2.3.1	Protein expression	48
2.2.3.2	Protein purification	48
2.2.3.3	Buffer exchange	49
2.2.3.4	Gel electrophoresis	49
2.2.3.5	Silver staining	49
2.2.3.6	Protein quantification	50
2.2.3.7	Protein modification	50
2.2.3.8	Protein analysis	50

2.2.4	Cellular assays	53
2.2.4.1	Analysis of cell surface-expression of anti-EBOV GP-specific antibodies as a model of EBOV GP-specific B cells to test EBOV GP Δ TM	53
2.2.4.2	Isolation of anti-Ebolavirus glycoprotein-specific B cells	53
2.2.4.3	Neutralization assay	55
2.2.5	Quantification and statistics	55
2.2.6	Sequence analyses	56
2.2.6.1	Ig heavy/light chain sequence analysis	56
2.2.6.2	Unbiased B cell repertoire analyses	57
2.3	<i>List of contributions</i>	58
3	Results	60
3.1	<i>Generation and validation of Ebola virus glycoprotein as a sorting bait</i>	60
3.1.1	Glycoprotein cloning and production	60
3.1.2	Purified protein binds to previously reported anti-EBOV GP-specific antibodies in ELISA	61
3.1.3	Produced GP is bound by HEK293T cells transiently expressing anti-EBOV GP-specific antibodies on their cell surface.....	63
3.2	<i>B cell immune response to rVSV-ZEBOV vaccination</i>	64
3.2.1	Subjects and serum response	65
3.2.2	Flow cytometric analysis and sort.....	66
3.2.3	Sequence analysis of EBOV GP-specific B cell receptors.....	70
3.2.4	Comparison of EBOV GP-specific population and total IgG B cell repertoire	73
3.2.5	Convergent development of EBOV GP Δ TM-specific antibody sequences.....	77
3.2.5.1	Among rVSV-ZEBOV-vaccinated individuals	77
3.2.5.2	Among rVSV-ZEBOV-vaccinated individuals and EVD survivors	80
3.2.6	rVSV-ZEBOV-induced antibodies bind to EBOV and are cross-reactive to other Filoviruses	81
3.2.7	rVSV-ZEBOV-induced antibodies target a broad spectrum of epitopes	84
3.2.7.1	Epitope distribution in cross-reactive or EBOV-specific antibodies.....	88
3.2.8	rVSV-ZEBOV-induced antibodies neutralize EBOV.....	90
3.2.8.1	Neutralization by serum.....	90
3.2.8.2	Neutralization by monoclonal antibodies.....	91
3.2.8.3	Epitope spectrum of neutralizing antibodies and link to cross-reactivity.....	92
3.2.8.4	Recurrent generation of an IGHV3-15/IGLV1-40 antibody class across donors	94
3.2.9	Structural analysis of rVSV-ZEBOV induced antibodies	98
3.2.9.1	IGHV3-15/IGLV1-40 antibody class	98
3.2.9.2	Strong neutralizers 3T0331 and 4m0368.....	101

4	Discussion	105
4.1	<i>Analysis of the rVSV-ZEBOV antibody response</i>	105
4.1.1	Objectives	105
4.1.2	Considerations for characterizing the rVSV-ZEBOV-induced antibody response	105
4.1.3	Analyzing the serum IgG response after vaccination is not a reliable determinant of immunity 105	
4.1.4	GP-specific memory B cells are less abundant after vaccination than after infection	106
4.1.5	rVSV-ZEBOV vaccination induces infrequent mutations in antibodies comparable to natural infection	107
4.1.6	rVSV-ZEBOV vaccination induces cross-reactive neutralizing antibodies with a broad epitope spectrum comparable to natural infection	107
4.2	<i>Analysis of sequence convergence in antibodies</i>	110
4.2.1	IGHV3-15/IGLV1-40 class antibodies are recurrently induced by rVSV-ZEBOV vaccination ...	110
4.2.2	Shared antibodies with nearly identical HC and LC sequences occur across donors after rVSV- ZEBOV vaccination	112
4.3	<i>Achieving cross-protection – the holy grail?</i>	115
4.4	<i>Conclusions</i>	117
5	References	119
6	Appendix	133

1 Introduction

1.1 The role of B cells and antibodies in the immune system

The leading causes of death within the 19th century were infectious diseases (Rahlf, 2015). In an attempt to find a treatment against diphtheria and tetanus, Emil von Behring, Paul Ehrlich and Shibasaburo Kitasato infected rabbits with the causative pathogens *Corynebacterium diphtheriae* or *Clostridium tetani*, respectively. They found that some rabbits survived injections with the bacteria and developed immunity against the diseases. Notably, immunity turned out to be transferrable to other subjects. On the one hand, it prevented healthy animals from being infected upon later challenge (E. v. K. Behring, Shibasaburo, 1890). Moreover, the transfer of blood sera of convalescent animals was able to cure mice that already had been infected (E. v. Behring, 1890; E. v. K. Behring, Shibasaburo, 1890). This soon led to an effective therapy against diphtheria for humans, which reduced mortality rates in patients from >50% to ~20% (Behring, 1893; P. K. Ehrlich, Hermann; von Wassermann, August Paul, 1894).

Von Behring and Kitasato found that the protective agents mediating this immunity were not cells, but substances comprised in cell-free blood sera (E. v. Behring, 1890; E. v. K. Behring, Shibasaburo, 1890). Knowing that diphtheria and tetanus were caused by bacterial toxins, the toxin-neutralizing agents within sera were termed antitoxins or antibodies. Accordingly, substances that triggered the development of antibodies were termed antigens, for they led to *antibody generation* (**Figure 1**). With his side-chain or receptor theory, Paul Ehrlich proposed that certain cells contained receptors that chemically reacted with toxins thereby neutralizing them (P. Ehrlich, 1908; Silverstein, 1999). He believed that the consumption of side-chains dictated the cells to reproduce such. By recurrent immunization with the toxin, cells could be trained to preserve this immunity and reproduce side-chains. As a result, these were available at a quantity too large for the cells to carry and secreted into blood in the form of antibodies (P. Ehrlich, 1900, 1908).

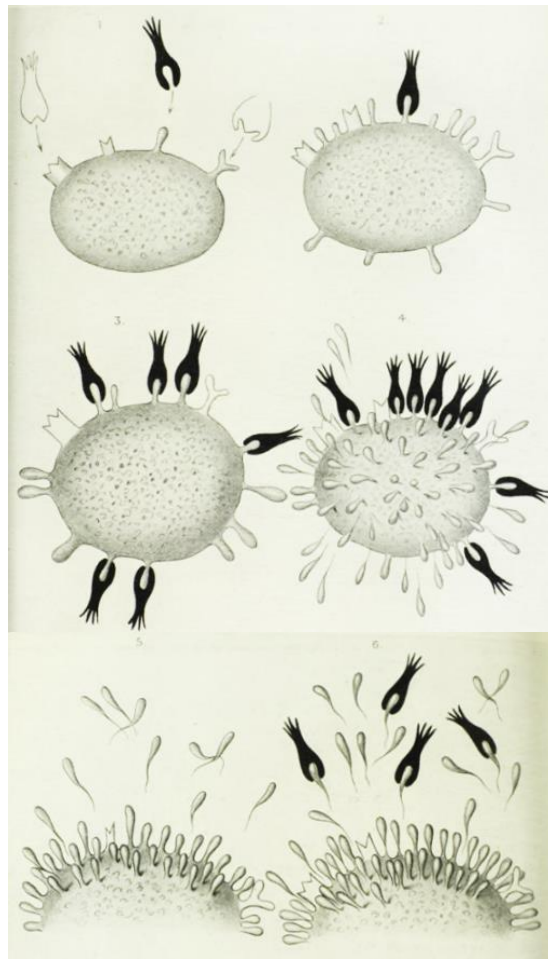


Figure 1. Side-chain theory. Originally: Seitenkettentheorie.

(1) Nutrients (white) and toxins (black) can bind nutriceptors or side-chains expressed on cell membranes. (2) Toxin attached to side-chain. (3) Increasing amounts of toxin consume side-chains and prevent uptake of nutrients. (4) The cell reacts by reproducing side-chains. (5) Side-chains are secreted as antibodies. (6) Antibodies neutralize toxin. Adapted from (P. Ehrlich, 1900). By courtesy of the Paul-Ehrlich-Institut.

1.1.1 B cell development

In many aspects, Ehrlich's explanation of antibody-mediated immunity comes close to what we know today. In fact, his drawings of antigens and membrane-bound side-chains or nutriceptors look remarkably similar to schemes of today. He understood the binding of antigen to side-chains as exploitation, as he believed that side chains that he also termed nutriceptors had the task to take up nutrients into the cell. Since then, the side-chains responsible for antigen binding have been identified as B cell antigen receptors (BCRs) and the binding of antigen is not an unwanted process but the means to combat antigens considered to be foreign or harmful.

BCRs are produced by a specialized cell type of the immune system belonging to the lymphoid lineage giving rise to cells of the adaptive immune system. This cell type was first identified in the bursa fabrica of chickens, which gave them the name B lymphocytes or B cells (Cooper, Peterson, & Good, 1965; Murphy, 2011). In humans, this lineage is built in the fetal liver and later in the bone marrow from pluripotent hematopoietic stem cells, which also give rise to the myeloid lineage of immune cells forming the innate immune system (Asma, Langlois van den Bergh, & Vossen, 1984; Murphy, 2011; Rajewsky, 1996). From a common lymphoid progenitor (CLP), the cells undergo an early B stage, several pro- and pre-B cell developmental stages in the bone marrow. During these differentiation steps, the BCR is generated, and B cells are cautiously selected and tested for functionality and absent autoreactivity. The different B cell developmental stages are defined by the surface expression of certain cluster of differentiation (CD) markers and the state of BCR development. Immature B cells that match all selection criteria then migrate to peripheral lymphoid organs such as the spleen and differentiate to mature naïve B cells (Hystad et al., 2007).

1.1.2 B cell receptor structures

B cell receptors (BCRs) are composed of four polypeptides. Two identical polypeptides termed heavy chains (HC) and two identical polypeptides called light chains (LC) assemble to symmetrical structures known as immunoglobulins (Ig) via disulfide bonds (**Figure 2A**) (Edelman & Poulik, 1961). Every HC and LC contain two functionally different regions: the variable (V) and the constant (C) region (Murphy, 2011; Schroeder & Cavacini, 2010; Tonegawa, 1983). These names reflect the genetic diversity of the regions. The C region of HC (C_H) consists of three or four domains (C_{H1} - C_{H4}). Five different main classes of the C_H are encoded by C_{μ} , C_{δ} , C_{γ} , C_{ϵ} and C_{α} gene segments and the resulting proteins are termed isotypes IgM, IgD, IgG1-4, IgE or IgA1-2 accordingly (Murphy, 2011). All isotypes can be produced as a membrane-bound version (BCR) or as a secreted version (antibody) via alternative splicing (Alt et al., 1980). In LC, two isotypes exist, which can be combined to the HC: the kappa (κ) and the lambda (λ) LC. Only one C_L region has been discovered per chain type (Murphy, 2011; Schroeder & Cavacini, 2010). A single B cell can only produce BCRs or antibodies harboring the same C_H isotype. Exceptions are co-expressions of M and D-harboring BCRs on the same mature naïve B cell. The C_H region of an antibody can initiate a variety of anti-microbial effector functions which will be addressed below (p. 10).

Before effector functions can be initiated, it is elementary that invading pathogens are recognized. This is facilitated by the V regions of HC and LC, which are combined from a set of gene segments termed variable (V), diversity (D) and junction (J) (**Figure 2A, C and D**). The IgH locus harbors a set of HC V (V_H), D and J (J_H) gene segments (**Figure 2A and C**).

The two LC loci IgK and IgL for kappa LC and lambda LC, respectively, are missing the D gene segment and contain V and J gene segments (V_L and J_L) only (**Figure 2A and D**) (Schroeder & Cavacini, 2010; Tonegawa, 1983). The resulting antibody can be enzymatically digested with the protease papain, cleaving the Ig into two antigen-binding fragments (Fab) and a crystallizable fragment (Fc). The V regions of HC and LC in a Fab can also be separated into the complementary determining regions 1, 2 and 3 (CDR1, CDR2 and CDR3) and the so-called framework regions 1-4 (FWR1-4) around them (**Figure 2B-D**) (Schroeder & Cavacini, 2010; Tonegawa, 1983). The CDRs and especially CDR3 have been identified as the domains mainly responsible for antigen binding and the analysis of their sequences is therefore of high interest (**Figure 2C and D**). Sequences can be analyzed utilizing the ImMunoGeneTics (imgt) database (M.-P. Lefranc, 2011). In HC and LC, respectively, V gene segments build FWR1, CDRH1 and CDRL1, FWR2, CDRH2 and CDRL2, FWR3 and contribute to CDRH3 and CDRL3. The entire D gene segment of HC is part of the CDRH3. Finally, the JH and JL gene segments also add to the CDRH3 and CDRL3 sequence, respectively, and make up the FWR4 until the start of the C region (Schroeder & Cavacini, 2010; Tonegawa, 1983).

Of note, both the HC V region and the HC V gene segment are abbreviated by V_H for historical reasons. However, they describe different parts of the antibody. While the entire V_H gene segment is always part of the V_H region, the V_H region in return spans more gene segments than the V_H gene segment (**Figure 2A and C**). For the sake of clearness, here, the variable antibody domain of a HC comprising V, D and J gene segments will be referred to as HC *V region* or V_H *region*, while the variable gene segment of a HC will always be termed HC *V gene segment* or V_H *gene segment*. If a specific V_H gene segment is to be named, it will be referred to as IGHV family-gene i.e., IGHV3-15. Likewise, the variable region of a LC and the gene segment of a LC are both abbreviated by V_L . In this work, the LC domain comprising V and J gene segments will be referred to as V_L *region*. The V gene segment of a LC will be distinguished by V_L *gene segment*.

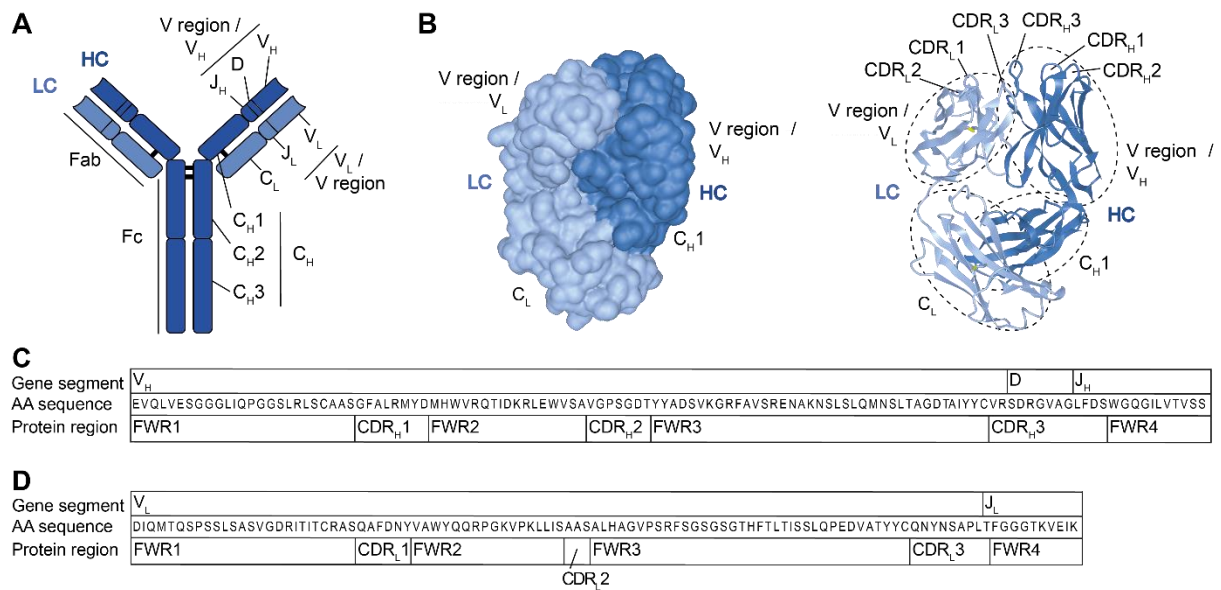


Figure 2. Antibody structure.

(A) Schematic structure of a representative antibody. Every immunoglobulin (Ig) consists of two identical heavy chains (HC; dark blue) and two smaller identical light chains (LC; light blue) assembling to symmetrical Y-shaped structures via disulfide bonds (black). Antibodies can be enzymatically digested with the protease papain, cleaving the antibody in two antigen-binding fragments (Fab) and a fragment crystallizable (Fc). HC and LC comprise a variable (V) region (V_H and V_L, respectively) and a constant (C) region (C_H and C_L, respectively). The CH region contains three (C_{H1-3}) or four domains. V_H regions are built from variable (V_H), diversity (D) and junctional (J_H) gene segments, while V_L regions are made from merely the variable (V_L) and junctional (J_L) gene segments. (B) Crystal structure of one Fab of the anti-Ebolavirus antibody mAb114 (GenBank: PDB ID 5FHA) as surface (left) and ribbon representation (right) generated using the tool iCn3d MMDB (Madej et al., 2014). Dashed lines visualize the V and C regions of HC and LC. Complementary determining regions (CDR) of HC (CDR_{H1-3}) and LC (CDR_{L1-3}) are exposed regions building the paratope responsible for antigen binding. Colors as in (A). (C and D) Exemplary sequence analysis of mAb114 HC variable domain (GenBank: KU594603.1) and kappa LC variable domain (GenBank: KU594604.1) using the tool IgBlast (Ye, Ma, Madden, & Ostell, 2013) based on the ImMunoGeneTics (IMGT) database (M. P. Lefranc et al., 1999). Top lines indicate the gene segments encoding the amino acid (AA) sequence of mAb114 HC (C) and LC (D) V regions (middle line). Bottom lines show the resulting domains of the protein, which are framework regions (FWR1-4) and CDR_{H1-3} or CDR_{L1-3}, respectively.

1.1.3 B cell receptor diversity

As the counterpart to the huge variety of viruses, bacteria, fungi and parasites, the repertoire of V regions must be highly diverse itself. In contrast to only five C region representatives, the human immune system can generate approximately 10^8 different V regions in mature naïve B cells, that have not encountered their antigen yet (Murphy, 2011). This tremendous variability is achieved by several mechanisms: Somatic recombination (**Figure 3A**), junctional diversity (**Figure 3A**), combinatorial diversification, somatic hypermutation (SHM; **Figure 3B**) and class switch recombination (CSR; **Figure 3C**). The first three are processes found in the developing B cell and therefore account for the primary antibody diversity. In contrast, SHM and CSR are induced in the mature B cell that has encountered its antigen and therefore contribute to the secondary antibody diversity (Di Noia & Neuberger, 2007; Murphy, 2011). These mechanisms will be described in the following sections.

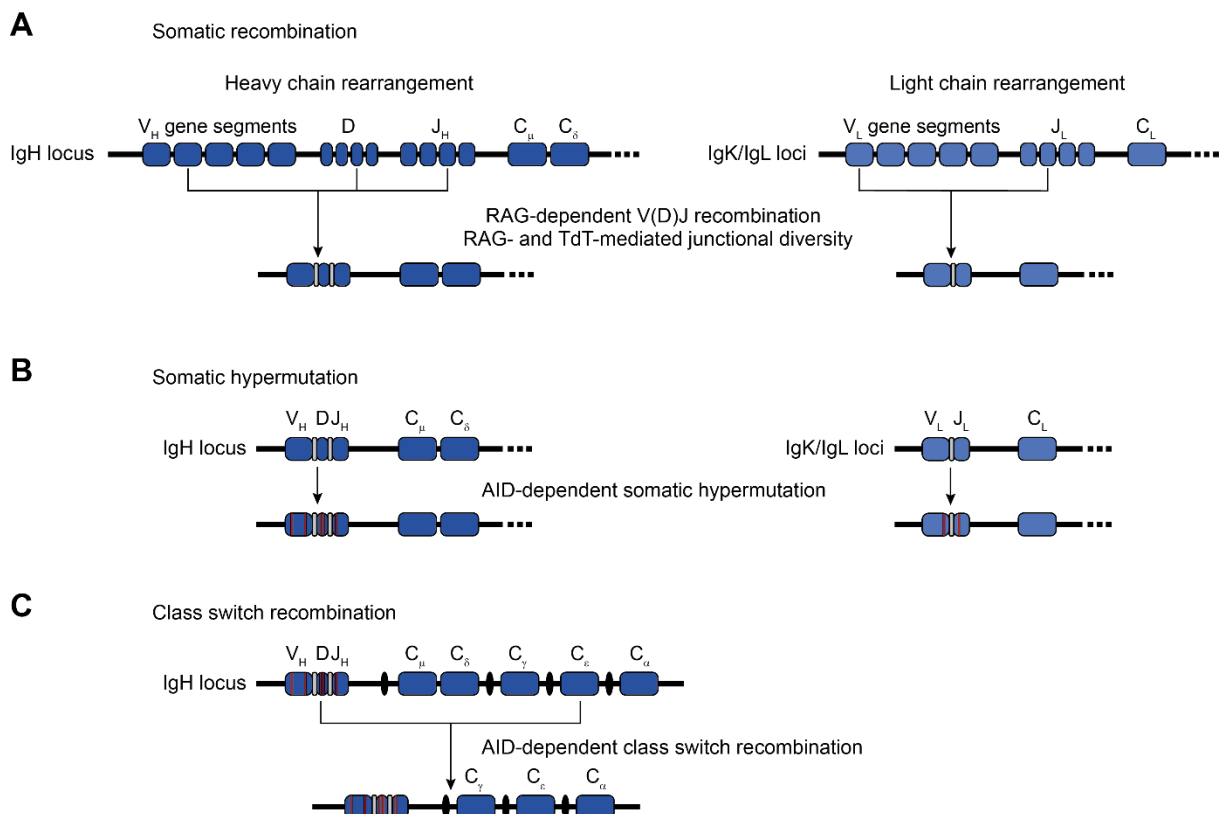


Figure 3. Mechanisms mediating B cell receptor diversity.

Schematic representation of permanent changes in the somatic DNA of immunoglobulin (Ig) heavy chains at the IgH locus (left), and Ig light chains at the IgK and IgL loci (right). Loci are indicated as black strands with respective gene segments as dark (heavy chain) or light blue (light chain) boxes. The number of boxes does not reflect the actual number of identified gene segments. (A) Somatic recombination or V-(D-)J recombination of gene segments. Recombination activating genes 1 and 2 (RAG1/2) introduce double strand DNA breaks at recombination signal sequences (not shown) flanking the gene segments according to the 12/23 rule. RAG1/2, terminal deoxynucleotidyl transferase (TdT) and other DNA repair enzymes additionally insert and/or delete non-templated nucleotides (P-, and T-nucleotides; grey lines) and lead to non-homologous end joining (NHEJ) of DNA strands that increase the junctional diversity (Murphy, 2011; Schatz & Ji, 2011). (B) Somatic hypermutation (SHM) of activated B cells in germinal centers. Activation induced deaminase (AID) introduces single-point mutations (red lines) into gene segments of the variable region at the IgH and IgK/IgL loci in a process known as SHM that increase BCR diversity and lead to affinity maturation of a B cell clone (Di Noia & Neuberger, 2007) (C) Class switch recombination (CSR) of the C_H region of activated B cells in- or outside germinal centers. Individual guanosine-rich repeats known as S regions (black ellipses) precede gene segments C_μ, C_δ, C_γ, C_ε and C_α (the subclasses of C_γ and C_α are not shown). An exception are C_μ and C_δ, which follow a shared S region. AID introduces double strand breaks at S regions (black ellipses) and DNA repair machinery including uracil DNA glycosylase (UNG) and apurinic/apyrimidinic endonuclease 1 (APE1) somatically joins the remaining C gene segment and the remaining locus to the VDJ gene segment upstream of C_γ, C_ε or C_α (Alt, Zhang, Meng, Guo, & Schwer, 2013).

1.1.3.1 Somatic recombination

Somatic recombination – also known as V(D)J recombination – describes one of the most fundamental processes of adaptive immunity to generate effective strategies to combat nearly any pathogen. It first explained how the immune system can generate a seemingly unlimited variety of antigen receptors on B and T cells without encoding the same number of genes in the germline (Tonegawa, 1976, 1983). To this end, 56 different V_H gene segments, 23 D gene segments, and six J_H gene segments have been identified on the IgH locus (M. P. Lefranc et al., 1999). By different V_HDJ_H combinations, a theoretical $56 \times 23 \times 6 = 7728$ different HC variable regions can be generated. For the IgK and IgL loci, 41 or 33 V_L gene segments, and 5 J_L gene segments have been described, respectively (M. P. Lefranc et al., 1999). In total, a variety of $(41 + 33) \times 5 = 370$ different LC variable regions can be combined.

The selection and assembly of one V, (D,) and J gene segment, respectively, to an individual Ig chain requires reorganization of the germline encoding genes and several events of DNA double strand breaks (**Figure 3A**). This is in line with the observation that every B cell carries BCRs of the same specificity and that only a single BCR is passed on to progeny cells. These reorganizational events occur during B cell development in the bone marrow starting at

the stage of pro-B cells (Hystad et al., 2007). The main enzymes facilitating somatic recombination are the recombination activating genes 1 and 2 (RAG1 and RAG2) (Oettinger, Schatz, Gorka, & Baltimore, 1990). In several rounds, double DNA strand breaks are introduced at recombination signal sequences (RSS). Non-selected gene segments are excised, while selected ones are jointly reassembled. First, D and J_H gene segments are joined, before joining of to V_H to DJ_H gene segments (Murphy, 2011).

At the stage of pre-B cells, HC are combined with surrogate LC to test HC functionality. Subsequently, once a functional V_HDJ_H molecule has been rearranged, V_LJ_L genes are joint and replace the surrogate LC (Murphy, 2011). In humans, typically the IgK locus rearranges first and somatic recombination at the IgL locus occurs if no productive kappa LC could be arranged. Therefore, in humans the kappa to lambda ratio is usually 2:1 (Murphy, 2011). The recombinations at IgH, IgK and IgL loci are somatic and hence permanent. Thus, a given B cell will only express BCRs or antibodies of one antigen specificity and pass on the genetic information to progeny cells (Burnet, 1976; Jerne, 1955; Rajewsky, 1996; Talmage, 1959).

1.1.3.2 Combinatorial diversity

Through the different possibilities of pairing the 7728 HC and 370 LC, approximately 2.86×10^6 distinct B cells can be generated by genetic rearrangements from the germline encoded gene segments.

1.1.3.3 Junctional diversity

As described above, somatic recombination of selected V, D and J gene segments to joint genes requires the excision of other gene segments via DNA strand breaks. During this process, RAG1/2 enzymes may add palindromic (P) nucleotides (**Figure 3A**, grey lines) (Lafaille, Decloux, Bonneville, Takagaki, & Tonegawa, 1989). The ends of broken double stranded DNA are repaired by enzymes belonging to the cellular DNA repair machinery including terminal deoxynucleotidyl transferase (TdT). The TdT may randomly add non-templated (N-) nucleotides (**Figure 3A**, grey lines), which are not encoded, to join the gene segments (Komori, Okada, Stewart, & Alt, 1993). Additional enzymes may delete nucleotides before joining V(D)J gene segments. This process is therefore referred to as non-homologous end joining (NHEJ) (Ma, Pannicke, Schwarz, & Lieber, 2002). The additional modifications alone increase the variety of the possible B cell repertoire known as junctional diversity by 3×10^7 (Schatz & Ji, 2011) and lead to a final range of $\sim 5 \times 10^{13}$ different BCRs that can theoretically be found on naïve B cells (Murphy, 2011).

1.1.3.4 Somatic hypermutation

Fully developed mature naïve B cells migrate through the lymphatic vessels and germinal centers of lymphoid tissues such as the spleen or lymph nodes. Once a B cell encounters its matching antigen it needs two further signals to achieve B cell activation. B cells either require signals from T helper cells or clustering of BCRs on the cell surface. Moreover, either cytokines or Toll-like receptor activation is required as a third signal (Ruprecht & Lanzavecchia, 2006). After activation, several proliferation and differentiation processes are initiated. The activated B cell proliferates and gives rise to further B cells of identical specificity and affinity in a process called clonal expansion. This amplifies the number of B cells successfully combating the pathogenic or dangerous agent (Burnet, 1976; Murphy, 2011; Nossal & Lederberg, 1958; Talmage, 1959).

Moreover, the enzyme activation induced deaminase (AID) initiates the introduction of somatic DNA mutations in the newly formed B cells (Maul & Gearhart, 2010; Muramatsu et al., 2000; Weigert, Cesari, Yonkovich, & Cohn, 1970) (**Figure 3B**, red lines). The alterations of germline-encoded V, D and/or J gene segments of the variable region are either silent or change the germline sequence to encode another amino acid in this position and lead to the diversification of BCRs in the different cells of a given clone (Burnet, 1976; Jacob, Kelsoe, Rajewsky, & Weiss, 1991). Rarely, the introduced mutations do not alter a single nucleotide but cause in-frame insertions or deletions of several bases in the V region (Wilson & Donald Capra, 1998). The mutations are largely found in the CDRs and may directly influence the binding affinity between the B cell and the matching antigen. After the introduction of mutations, which may be repeated several times, the B cell undergoes further selection processes. B cells with increased affinity for the identical antigen and the absence of a newly introduced autoreactivity are selected for survival. This process called somatic hypermutation (SHM) will eventually lead to affinity maturation (AM) of the clone and generate BCRs and antibodies that bind the appropriate antigen or toxin with increased affinity (Di Noia & Neuberger, 2007). This V region-mediated effector function known as neutralization is one of the most important mechanisms to prevent pathogen-induced infection or toxin-mediated cellular damage. If a cell proliferates after these mutations are introduced, they are passed on to progeny cells (Burnet, 1976; Jacob et al., 1991). Therefore, clonally related cells which developed from a common ancestor cell can be identified by sequence analysis with special attention to the presence of nucleotide mutations at the same position.

1.1.3.5 Class switch recombination

Initially, every naïve B cell co-expresses C_H regions of the isotypes C_{μ} and C_{δ} . After an activated B cell has proliferated to generate clonal progeny, the clone may additionally exchange the somatic DNA of its BCR C_H region, which is referred to as class switch recombination (CSR) or isotype class switch. This process facilitates the production of even more functionally specialized B cells and antibodies (Murphy, 2011; Schroeder & Cavacini, 2010). Similar to somatic recombination, double strand DNA breaks are initiated by the enzyme AID (Muramatsu et al., 2000) and introduced at guanosine-rich repeats known as S region (**Figure 3C**, black ellipses). Subsequently, enzymes belonging to the DNA repair machinery such as uracil DNA glycosylase (UNG) and apurinic/apyrimidinic endonuclease 1 (APE1) somatically excise C_{μ} and C_{δ} and may join the C gene segment to the VDJ gene segment upstream of C_{γ} , C_{ϵ} or C_{α} (Alt et al., 2013; Imai et al., 2003; Schrader, Linehan, Mochevova, Woodland, & Stavnezer, 2005; Stavnezer, Guikema, & Schrader, 2008). As a result of CSR, either membrane-bound or secreted IgG, IgE or IgA antibodies are produced.

Unlike the previously described mechanisms somatic recombination, combinatorial diversity, junctional diversity and SHM, CSR does not alter the diversity enabling antigen binding. In contrast, it allows that clonal B cells of a certain antigen specificity can differentiate to produce antibodies comprising other C_H regions, thereby developing distinct characteristics, and mediating different effector functions (Murphy, 2011) which will be briefly described in the following.

1.1.4 Antibody characteristics and effector functions

Secreted antibodies mediate humoral immunity in different ways. A very potent way to combat invading pathogens and particularly viruses, intracellular bacteria and toxins is the V region-mediated binding of antibodies to pathogenic antigens. This process termed neutralization blocks the surface-exposed proteins of many viruses such as Ebola virus, Marburg virus, HIV-1, or SARS-CoV-2 (Andrew I. Flyak et al., 2015; Maruyama et al., 1999; Pinto et al., 2020; Scheid et al., 2009), thereby blocking viral entry to host cells. Another antibody-mediated way to counteract pathogens is called opsonization. Here, pathogens are marked as foreign or dangerous and attract cells of the innate immune system carrying the respective Fc receptors on their surface. Binding may trigger phagocytosis by monocytes and macrophages known as antibody-dependent cellular phagocytosis (ADCP), or by neutrophils termed antibody-dependent neutrophil phagocytosis (ADNP). Similarly, also natural killer (NK) cells can be recruited by opsonization and exert antibody-dependent cellular cytotoxicity (ADCC). Moreover, antibody binding to antigens can activate the complement system initiating

complement-dependent cytotoxicity (CDC) (Murphy, 2011; Nimmerjahn & Ravetch, 2010; Saphire, Schendel, Fusco, et al., 2018).

Neutralization is exclusively mediated by the antigen-specific V region of the antibody. In contrast, opsonization and recruitment of phagocytes, cytotoxic cells and proteins of the complement system additionally requires the C_H region of an antibody. Depending on the isotype class, different effector functions are initiated due to the differential expression of the matching Fc receptors on different immune cells. To this end, the C_L regions of κ and λ LC have not been found to exert any effector functions.

Apart from these effector functions, the C_H region may expand the body compartments accessible to antibodies and determines the half-life of a secreted antibody and thereby the duration of the response. For example, the primarily produced antibodies are IgM and IgD antibodies with a short serum half-life of 10 and 3 days, respectively. IgM antibodies exhibit relatively low affinity for their cognate antigen but may initiate CDC. The role of IgD antibodies is not fully understood but it is hypothesized that IgD BCRs serve as auxiliary receptors increasing the bioavailability of antigens to IgM BCRs (Murphy, 2011). The Fc portion of IgA binds to the neonatal Fc receptor (FcRn) which facilitates the transfer of IgA antibodies to mucosal tissue surfaces and secreted fluids such as milk thereby expanding the area of antibody-mediated immunity (Murphy, 2011). IgE antibodies can be bound by mast cells, basophil and eosinophil granulocytes expressing the Fcε receptor. Thereby, IgE antibodies with a serum half-life of only 2 days are involved in several inflammatory immune responses from allergic reactions to defense against parasites (Murphy, 2011).

IgG antibodies are the most abundant and long-lived isotype with a serum half-life of 7 days for subtype IgG3 and 20-21 days for subtypes IgG1, IgG2 and IgG4 (Murphy, 2011). They are initially expressed by short-lived IgG-positive plasma cells, which may undergo numerous rounds of SHM, steadily increasing their affinity for the antigen. They can mature to potently neutralizing antibodies. On the other hand, they effectively opsonize pathogens and antigens, thereby inducing ADCP, ADNP, ADCC and CDC. Towards the end of an acute infection, effector memory cells are built in the form of long-lived IgG-positive plasma cells, which contribute to potent and sustained humoral immunity against re-challenges (Bernasconi, Traggiai, & Lanzavecchia, 2002; Manz, Thiel, & Radbruch, 1997). The generation of highly affine, long-lived, and neutralizing IgG-secreting B cells is therefore considered a determinant of protective immunity that is also the goal of vaccination.

1.2 Ebolaviruses and Ebola Virus Disease

Viral zoonoses such as HIV/AIDS, Influenza, COVID-19, SARS, and Ebola have become global challenges with emerging frequency during the last 80 years (Han, Kramer, & Drake, 2016; K. E. Jones et al., 2008). Ebola virus disease (EVD) formerly called Ebola hemorrhagic fever has been identified first at the Ebola River in the Democratic Republic of Congo (DRC) during two simultaneous but unrelated outbreaks in 1976 (K. M. Johnson, Lange, Webb, & Murphy, 1977). In the 44 years since their identification, Ebolaviruses have caused iterative outbreaks with increasing significance (**Figure 4**). Before 2013, 23 EVD outbreaks together have led to a total of 2386 cases and 1589 deaths with individual case fatality between from 25 and 90% (WHO, 2021a). With the first infection in Guinea December 2013, an international epidemic developed that has outreached any EVD outbreak seen before. In total, 28,646 cases and 11,323 deaths have been reported mainly in Guinea, Sierra Leone and Liberia (Sylvain Baize et al., 2014; WHO, 2018b). Only two years later, the world's second largest outbreak of EVD in history began in the DRC in August 2018. Yet before it had been declared contained (WHO, 2020a), another independent outbreak had already been communicated (MSF, 2020; WHO, 2020b).

The incubation time, that is the time from infection to disease onset, strongly varies between 2-21 days but is mostly observed between four and ten days (WHO, 2021a). Typically, patients suffer from headache, fever, fatigue, vomiting, and diarrhea resulting in dehydration. Internal bleedings, which led to the name Ebola hemorrhagic fever, occur in 50% of cases. Eventually the disease may lead to multiorgan failure and death occurs six to nine days after disease onset (Bah et al., 2015).

EVD is a zoonosis thought to be transmitted to humans by fruit bats, in which the viruses are endemic. However, a spillover from fruit bat to human has not been documented (Forbes et al., 2019; Leroy et al., 2005). Viruses have also been discovered in pigs (Barrette et al., 2009), monkeys (Le Guenno et al., 1995) and antelopes (WHO, 2021a). The disease is not air-borne but transmitted via direct contact to patients and people who died from EVD, contaminated surfaces, or fluids. Importantly, viral RNA has been detected in body fluids for up to 18 months after infection and may cause delayed transmission and flare-ups of the disease (Deen et al., 2017; Diallo et al., 2016). In February 2021, two new outbreaks of EVD have been declared. As of March 24th 2021, 12 cases and 6 deaths caused by EBOV have been reported in the DRC (CDC, 2021d). While WHO states that it remains to be investigated whether this case is the result of a new spillover event or represents a flare-up of the 2018-2020 EBOV outbreak, the CDC classifies the outbreak as flare-up (CDC, 2021a; WHO, 2021b). A second outbreak was declared in Guinea and is likewise caused by EBOV. As of March 24th 2021, 18 cases and 9 deaths caused by EBOV have been reported (CDC, 2021d). The CDC

proposes this outbreak to be linked to the 2014-2016 West African epidemic as evidenced by a mutual nucleotide mutation in samples from the West African epidemic and samples from 2021 (CDC, 2021b). To this end, this hypothesis should be considered with caution, as no survivor could be identified to be the contact of the index case of this outbreak. Hence, it remains unclear, whether viral RNA has been transmitted from a survivor as late as 5 years after convalescence, or whether the index case might have become infected years ago without developing clinical signs until recently (Kupferschmidt, 2021).

1.2.1 Ebolavirus taxonomy and epidemiology

The genus Ebolavirus belongs to the family of Filoviridae. To this end, six distinct Ebolavirus species have been identified. The nomenclature of these has been changed several times and shall be clarified here: The six species are *Zaire ebolavirus* (EBOV; formerly ZEBOV (WHO, 1978b)), *Sudan ebolavirus* (SUDV, formerly SEBOV (WHO, 1978a)), *Reston ebolavirus* (RESTV, formerly REBOV (Jahrling et al., 1990)), *Bundibugyo ebolavirus* (BDBV, formerly BEBOV (Towner et al., 2008)), *Tai Forest ebolavirus* (TAFV; formerly *Côte d'Ivoire virus* (CIEBOV) (Le Guenno et al., 1995), and the recently described *Bombali ebolavirus* (BOMV (Goldstein et al., 2018)). For each of these species, a single member has been identified, which are Ebola virus, Sudan virus, Reston virus, Bundibugyo virus, Tai Forest virus, and Bombali virus, respectively. Beyond this classification, viruses are subdivided into variants commonly referred to as strains; For EBOV, some examples are strains *Mayinga*, *Makona* or *Kikwit*, named after the regions they have first been identified (Kuhn et al., 2010). To this end, three of the six known species have caused severe infections in humans, i.e., EBOV, SUDV and BDBV. RESTV was identified in imported macaques, in which it caused severe infection. Several animal workers have developed antibodies against RESTV but showed no signs of illness (CDC, 1990; Miranda et al., 1991). Moreover, a case of TAFV in a human individual with mild symptoms is documented, which has been caused by contact with an infected chimpanzee (Le Guenno et al., 1995). The pathogenicity of BOMV for humans remains elusive, as no cases have been reported so far (Goldstein et al., 2018) (**Figure 4**).

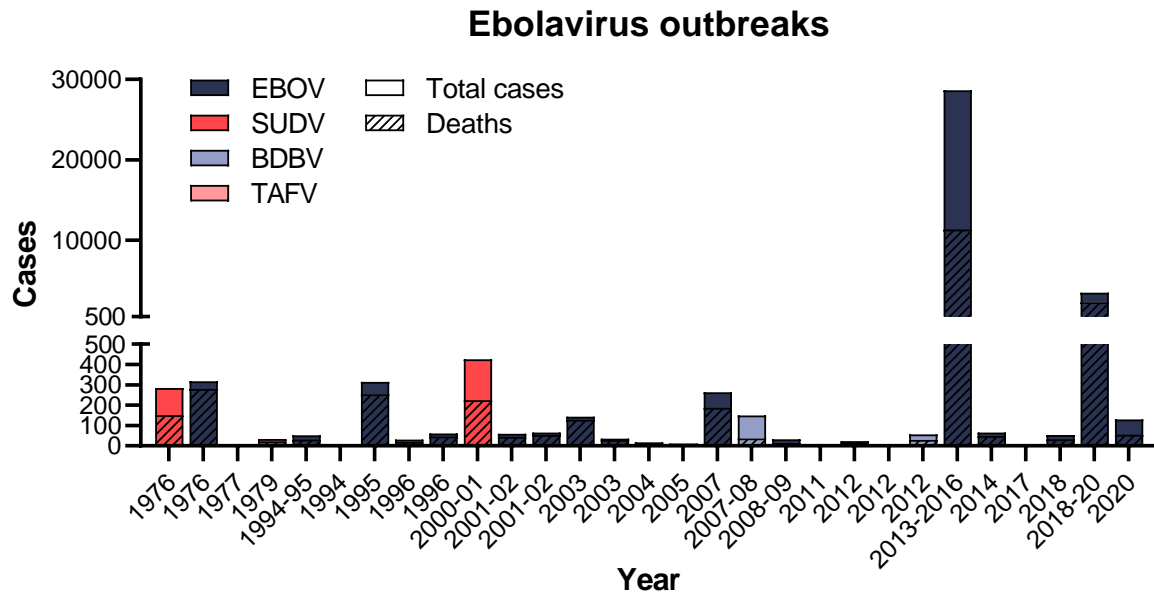


Figure 4. Ebolavirus outbreaks in humans since the identification in 1976.

Filoviruses of the genus *Ebolavirus* were first identified during two simultaneous outbreaks of Ebola virus disease (EVD) in the Democratic Republic of the Congo and Sudan. Most EVD outbreaks are caused by Zaire ebolavirus (EBOV, dark blue) in 1976, 1977, 1994, 1995, 2x 1996, 2x 2001, 2003, 2005, 2007, 2008, 2013-2016, 2014, 2017, 2018, 2018-2020, and 2020. Sudan ebolavirus (SUDV, medium blue) caused outbreaks in 1976, 1979, 2000, 2004, 2011, and 2x in 2012. Bundibugyo ebolavirus (BDBV, light blue) led to EVD in 2007 and 2012. The only Tai Forest ebolavirus (TAFV, grey) infection occurred in 1994. Laboratory-associated infections are not shown. Bars represent total cases with dashed part indicating the fatalities. Dates as of January 28, 2021. (CDC, 2021c; Kuhn et al., 2010; Le Guenno et al., 1995; Towner et al., 2008; WHO, 1978a, 1978b, 2021a, 2021b).

In addition to Ebolaviruses, the family of Filoviridae homes two more genera. These are *Cuevavirus* represented by the species *Lloviu cuevavirus* (LLOV) homing the member *Lloviu virus* (Negredo et al., 2011), as well as the genus *Marburgvirus* with the species *Marburg marburgvirus* and its members *Marburg virus* (MARV) and *Ravn virus* (RAVV), which both cause Marburg virus disease. Like Ebolaviruses, Marburgviruses are highly pathogenic to humans and have caused outbreaks in the past (E. D. Johnson et al., 1996; Siebert, Shu, Slenczka, Peters, & Muller, 1967). LLOV has been identified in dead bats in Spain but did not cause any documented human infections (Negredo et al., 2011).

1.2.2 Ebolavirus structure and genome organization

The family of Filoviruses is named after their filamentous structure with a diameter of ~80 nm and a length of 805-1,400 nm (Geisbert & Jahrling, 1995) (**Figure 5A**). Ebolaviruses are enveloped and carry single stranded RNA genomes of negative polarity (-ssRNA) and a length of ~19 kb. All Ebolavirus species share a common genome organization, which harbors seven genes (**Figure 5B**); These encode the nucleoprotein (NP), the membrane-associated protein viral protein (VP) 24, the polymerase matrix proteins VP30 and VP35, the matrix protein VP40, the large (L) RNA-dependent RNA polymerase, and the secreted glycoprotein (sGP) gene (Muhlberger, 2007).

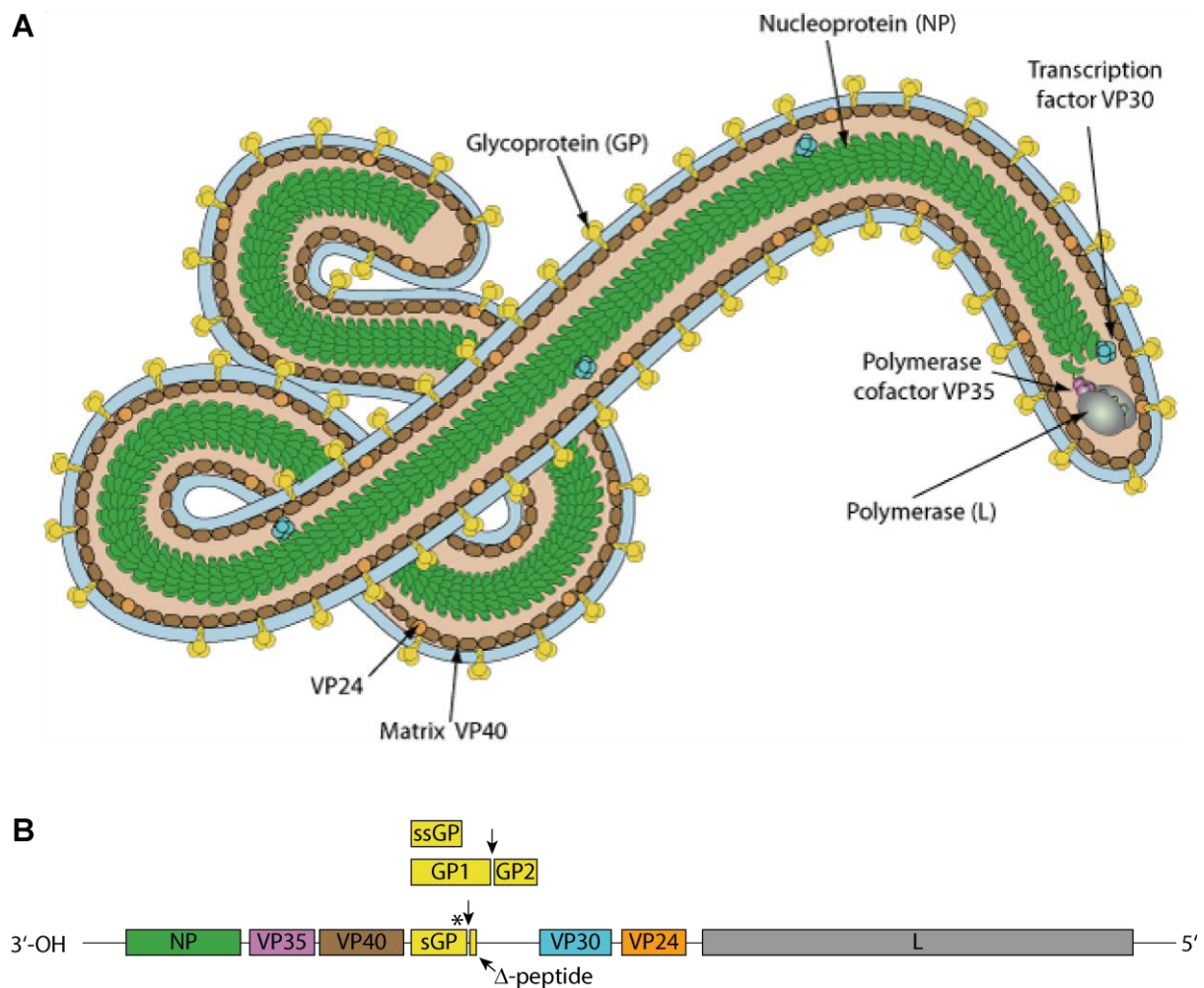


Figure 5. Schematic Ebolavirus structure and genome organization.

(A) Schematic presentation of EBOV structure. The RNA genome is wrapped and accompanied by nucleocapsid proteins NP (green), viral proteins VP35 (pink) and VP30 (turquoise) and RNA-dependent RNA polymerase L (grey). Viral proteins VP40 (brown) and VP24 (orange) build the viral matrix. Glycoprotein (GP) trimers (yellow) are anchored within the envelope originating from the host cell's membrane (blue). (B) Schematic diagram of Ebola virus (EBOV) genome. The single-stranded RNA of negative polarity (-ssRNA) harbors seven genes (boxes) as well as flanking (leader and trailer) and intergenic nontranscribed regions (black line). The mRNA editing site within the EBOV GP gene is indicated by an asterisk and the different resulting proteins are indicated in boxes above sGP. Furin-mediated cleavage of precursor proteins pre-sGP into sGP and Δ -peptide, as well as GP0 into GP1 and GP2 is indicated by arrows. Schemes adapted from (Philippe Le Mercier, 2014 and 2017).

1.2.2.1 Ebolavirus sGP/GP gene products

From the Ebolavirus sGP gene four different proteins are produced, namely sGP, Δ -peptide, small sGP (ssGP), and GP (**Figure 5B**). sGP represents the actually encoded protein of this gene and is transcribed with a probability of 70-75%. It is 364 aa long and forms homodimers that are secreted from infected cells (Sanchez, Trappier, Mahy, Peters, & Nichol, 1996; Volchkova, Feldmann, Klenk, & Volchkov, 1998). sGP is initially translated as precursor protein (pre-sGP) and subsequently cleaved by furin to yield the mature sGP (**Figure 5B**, indicated by an arrow). For a long time, it was hypothesized that sGP serves as an immune evasion mechanism by capturing antibodies released by the hosts immune system (de La Vega, Wong, Kobinger, & Qiu, 2015). However, a recent comprehensive study analyzing 186 different monoclonal antibodies showed that antibodies targeting sGP are not hampered in neutralizing the virus (Saphire, Schendel, Fusco, et al., 2018).

As a side product of pre-SP cleavage, a heavily glycosylated 40 aa long C-terminal Δ -peptide is generated (Volchkova, Klenk, & Volchkov, 1999). Little is known about its biological function; however, it appears to reduce viral entry into host cells, presumably by preventing superinfection and assisting budding of novel virions (Radoshitzky et al., 2011; Zhu, Banadyga, Emeterio, Wong, & Qiu, 2019).

Thirdly, ssGP originates from the sGP/GP gene and is produced by alternative transcription. During transcribing a sequence of seven consecutive uridines (U) in the viral genome into adenosines (A), the viral L polymerase may stutter and in 5% of transcriptions either skip an adenosine or insert two additional adenosines into the transcript, termed 6A or 9A-version (**Figure 5B**, position indicated by an asterisk). The resulting smaller protein ssGP presumably remains in monomeric or dimeric conformation, but its function remains elusive (A. M. Q. A. King, M. J.; Carstens, E. B.; Lefkowitz E. J. , 2011; Volchkov et al., 1995; Volchkova et al., 1999; Zhu et al., 2019)

The fourth protein originating from the sGP gene, is the membrane-anchored glycoprotein (GP). Like ssGP, it is the result of polymerase slippage during transcribing the sequence of seven uridines and produced by a single insertion of a non-templated adenosine (8A-version) (**Figure 5B**, position indicated by an asterisk). This leads to the transcription of a distinct and longer sequence, which is translated with a frameshift and a postponed stop codon (A. M. Q. A. King, M. J.; Carstens, E. B.; Lefkowitz E. J. , 2011; Zhu et al., 2019) (**Figure 6A**). Although it is not encoded as a main product, the 8A-version is transcribed in 20-25% of cases. Initially, it is produced as pre-GP or GP0 of 676 aa length (**Figure 6A**). Subsequently, it is post-translationally cleaved into the N-terminal GP1 and the C-terminal GP2 proteins by the protease furin (**Figure 5B**, indicated by an arrow). The two proteins assemble to heterodimers, which in turn form trimers, referred to as GP (**Figure 6B**). As it is produced co-transcriptional editing at from the same gene, GP1 shares a large proportion of its amino acid sequence with sGP. Only from position 295 the aa sequence differs (**Figure 6A**). The trimeric GP is embedded in the viral envelope where it facilitates both binding to the host cell receptor and fusion with the cell membrane (Lee & Saphire, 2009; Sanchez et al., 1998; Zhu et al., 2019).

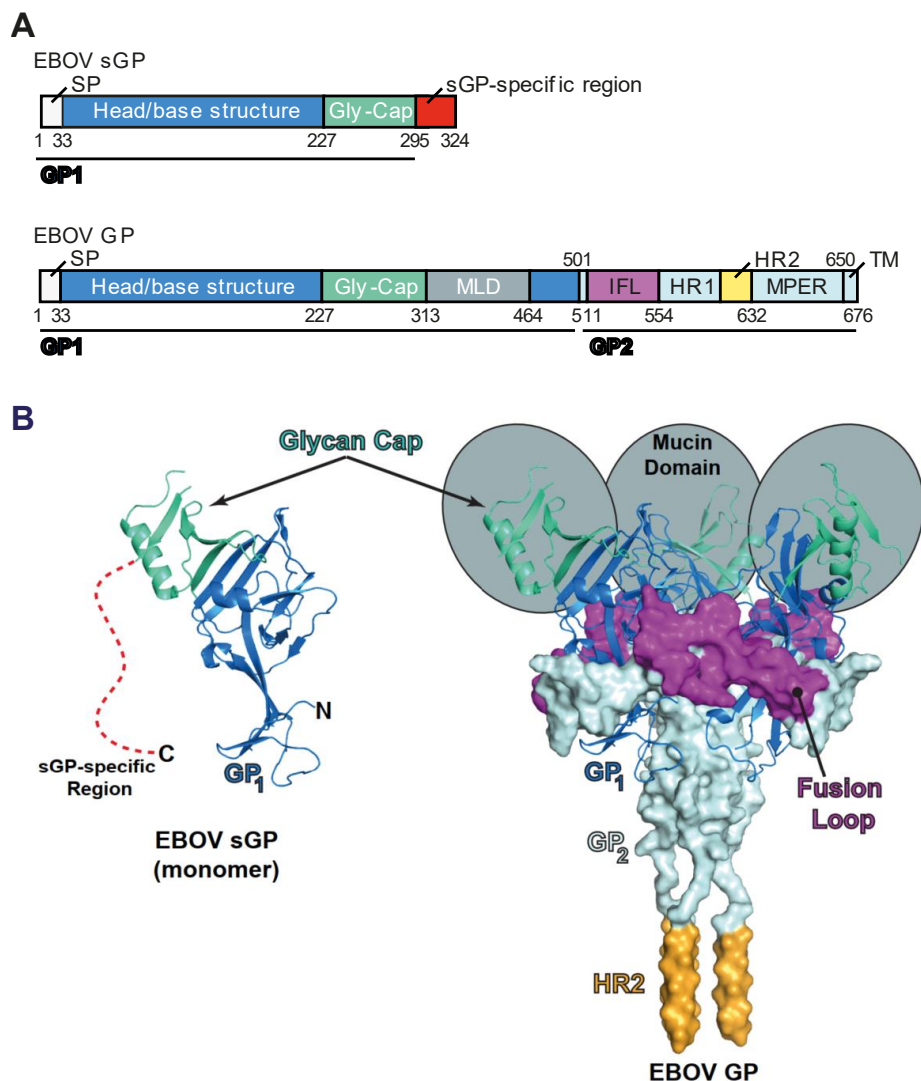


Figure 6. Transcripts and schematic structure of the EBOV sGP and GP.

(A) Transcripts of the Ebola virus sGP (top) and GP (bottom). Both transcripts share the N-terminal signal peptide (SP), the Head/base (blue) structure and partially the glycan-cap (Gly-Cap; turquoise). The sGP transcript terminates with the sGP-specific region (red). The GP sequence continues with the mucin-like domain (MLD; grey). The GP2 domain comprises the internal fusion loop (IFL; purple), heptad repeats 1 (HR1; light blue) and 2 (HR2; yellow), the membrane proximal external region (MPER; light blue) and transmembrane domain (TM). Numbers indicate nucleotide position and lines below transcripts indicate affiliation to GP1 or GP2. (B) Predicted protein structure of sGP monomer (left) and solved GP trimer structure (right). sGP- and GP-overlapping N-terminal Head/base and are shown as ribbon. The sGP structure is predicted based on the solved GP1 structure (PDB ID: 3CSY). The sGP-specific C-terminal region has structurally not been solved and is depicted as dashed line (red). The MLD is shown as grey spheres. The GP2 domain is shown in surface representation (PDB ID: 3CSY), including the IFL, HR1, HR2 (modeled in silico). The MPER and TM are not shown. Adapted from (Bornholdt et al., 2016).

1.2.3 Ebolavirus glycoprotein (GP) binding and fusion

Once an individual comes in contact with Ebolaviruses, the virus primarily infects dendritic cells, monocytes and macrophages (**Figure 7**; step 1). The virus also enters myeloid cells and endothelial cells of the liver, lymph nodes and bone marrow (Alvarez et al., 2002; Dominguez-Soto et al., 2007; Gramberg et al., 2008; Simmons et al., 2003). The broad tropism of target cells is explained by the utilization of several abundant cellular carbohydrate receptors and attachment factors.

Driven by the membrane-distal glycoprotein (GP) domain 1 (GP1) including the highly glycosylated mucin-like domain (MLD; **Figure 6**), the virus attaches to one of the several possible carbohydrate receptors. The virus is subsequently engulfed via macropinocytosis and enters the endocytic pathway (Nanbo et al. (2010) (**Figure 7**; step 2). Cathepsins L and B (CatB/L) cleave the heterotrimeric GP (Chandran, Sullivan, Felbor, Whelan, & Cunningham, 2005), thereby trimming the GP1 glycan cap domain and reducing the dimension of the MLD, formerly also referred to as glycan shield (step 3). Indeed, among facilitating viral attachment to the host cell, the MLD moreover hides the majority of structures and epitopes of the GP, reducing the amount of potential target sites for host antibodies or therapeutic agents (Zhu et al., 2019). CatB/L-mediated degradation of the MLD reduces the size of GP1 to 19 kDA and initiates conformational changes in the cleaved GP (GPcl), uncovering the receptor binding site referred to as internal fusion loop (IFL) of the GP2 domain (step 4). Thereby, the IFL is primed for binding to the cholesterol transporter Niemann-Pick C1 (NPC1) and fusion with the vesicular membrane in the acidic environment of late endosomes (Carette et al., 2011; Chandran et al., 2005; Cote et al., 2011; Lee & Saphire, 2009; H. Wang et al., 2016; White & Schornberg, 2012; Zhu et al., 2019).

The viral genome is then released into the cytosol, where replication, transcription and translation of viral RNA and proteins take place (steps 5-7). Translation of mRNA encoding the GP additionally involves the endoplasmic reticulum (ER) and Golgi compartments (steps 8-9). Large numbers of dimeric sGP are released from the cell and new enveloped virions are formed at the host's cell membrane by budding (steps 10-11) (White & Schornberg, 2012).

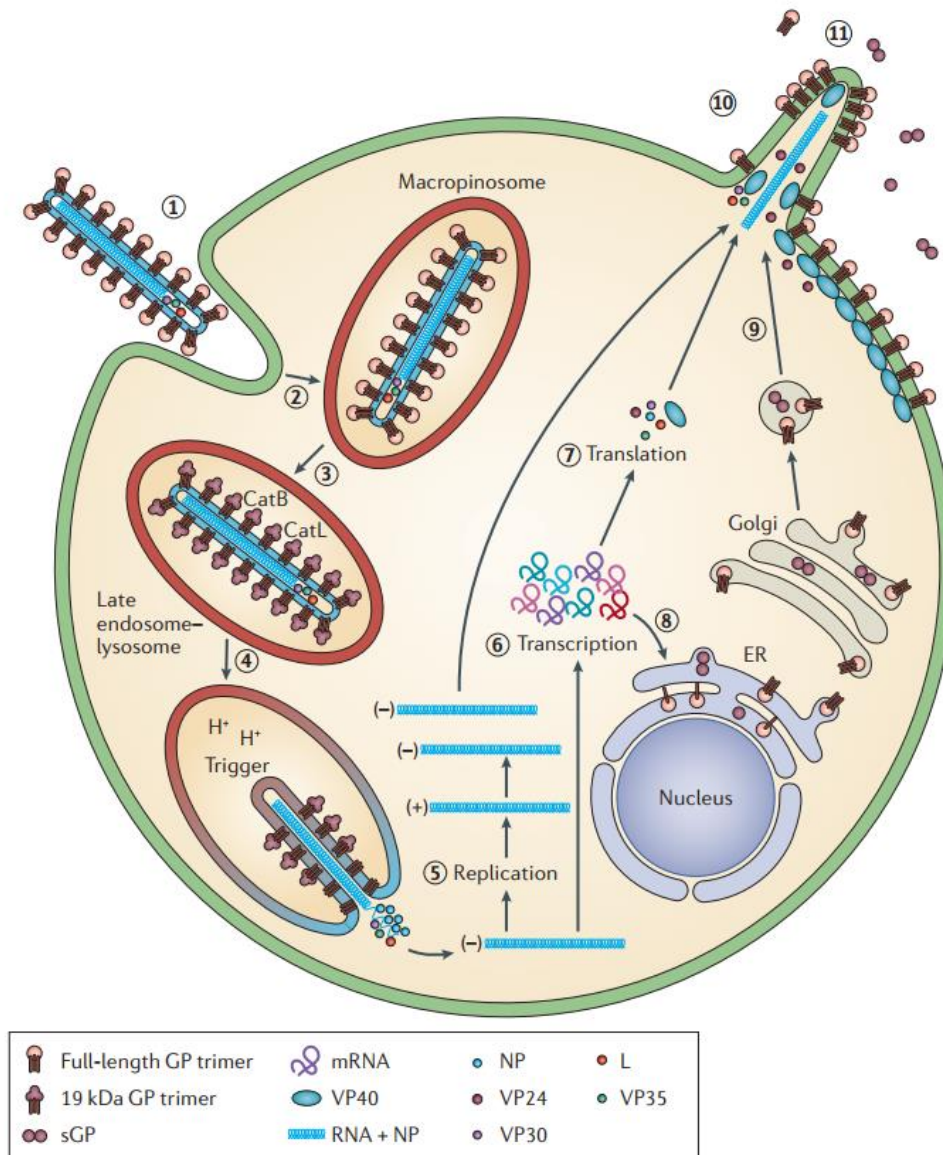


Figure 7. Ebolavirus life cycle.

An invading Ebola virus (EBOV) binds to a host cell with the surface-exposed glycoprotein (GP) (step 1). By macropinocytosis it enters the endocytic pathway (step 2). Cathepsins L and B (CatB/L) trim the glycoprotein 1 (GP1) glycan cap domain and reduce the dimension of the mucin-like domain (MLD; step 3). Cathepsins B and L (CatB/L) degrade the MLD and cause conformational changes in the cleaved GP (GPcl), uncovering the receptor binding site referred to as internal fusion loop (IFL) of the GP2 domain (step 4). The internal fusion loop (IFL) can then fuse with the cholesterol transporter Niemann-Pick C1 (NPC1) of the vesicular membrane in the acidic environment of late endosomes. After release of the viral genome into the cytosol, replication of viral RNA (step 5) as well as transcription (step 6) and translation (step 7) of proteins take place. Translation of mRNA encoding the GP additionally involves the endoplasmic reticulum (ER) and Golgi compartments (steps 8-9). From the host cell membrane, newly developed virions bud (step 10). Also, large numbers of dimeric sGP are released from the cell (step 11). Figure from (White & Schornberg, 2012).

1.2.4 Immune responses against Ebolaviruses

Being the only viral molecule on the virus' surface, GP represents the interface between virus and host. In this exposed position it is, therefore, likely to be the target of antiviral immune reactions. Several studies increased interest in the understanding of GP-directed immune responses and particularly the antibody response. The characterization of animal models of EVD showed that antibodies were found in animals that survived the viral challenge (Takada, Ebihara, Jones, Feldmann, & Kawaoka, 2007) and antibodies mediated virus clearance (Gupta et al., 2004). As early as in 1996 passive immunization of rodents has been described by the transfer of immunoglobulins (Jahrling et al., 1996). Similar observations were made in infected humans, where defective humoral responses in general and particularly an absent IgG response was associated with fatal outcome of EVD (S. Baize et al., 1999). Moreover, in an infected human the mounting of the EBOV GP-specific serum antibodies coincided with the reduction of viral RNA (Wolf et al., 2015). As a result, survivors of EVD outbreaks have been analyzed more closely and several groups have identified highly potent neutralizing mAbs directed against the viral GP. Importantly, they protected rodents and NHP from infection upon viral challenge and were moreover, effective as post-exposure prophylaxis (Bornholdt et al., 2019; Bornholdt et al., 2016; Damon, 2018; A. I. Flyak et al., 2018; A. I. Flyak et al., 2016; Marzi et al., 2015; Maxmen, 2018; Murin et al., 2014; Pascal et al., 2018; Qiu et al., 2014; Warfield et al., 2018). Therefore, GP-specific neutralizing antibodies are promising candidates to prevent and combat infection in humans.

1.2.5 Countermeasures to Ebolaviruses

When beginning this project, no licensed therapy or vaccine had existed. Methods to prevent and control EVD were mostly limited to the identification and isolation of Ebolavirus-infected or exposed individuals and non-specific medical care. However, several vaccine candidates and therapeutic agents were experimentally investigated and tested in animal models. The unprecedented dimensions of the West African outbreak from 2013-2017 further accelerated efforts to develop effective means against the virus. A few of them will be outlined in the following.

1.2.5.1 Therapy

Due to the lack of licensed therapeutics, until 2015 the standard of care (SOC) for EVD patients was mostly aiming for symptomatic treatment (WHO, 2021a). In NHP models, only direct-acting antivirals in form of nucleoside analogs and monoclonal antibodies have proven efficacy (Hansen, Feldmann, & Jarvis, 2021). Here, antibodies had moreover shown that they could protect from infection if administered before or after challenge (Bornholdt et al., 2019; Bornholdt et al., 2016; Damon, 2018; A. I. Flyak et al., 2018; A. I. Flyak et al., 2016; Marzi et al., 2015; Maxmen, 2018; Murin et al., 2014; Pascal et al., 2018; Qiu et al., 2014; Warfield et al., 2018). One of them was the cocktail ZMapp, which comprises the three human-mouse chimeric monoclonal antibodies called 13C6, c2G4, and c4G7 (Qiu et al., 2014). Although it had not been licensed, the devastating circumstances of the West African outbreak made the cocktail available for compassionate use (Group et al., 2016). 71 patients were enrolled in a rapidly set up clinical trial to evaluate the efficacy of ZMapp. Due to the containment of the epidemic, the trial did not reach statistical significance, but the results were promising; In the group that received the current SOC, 37% of cases were fatal. The rate was reduced to 22% in patients that received ZMapp in addition to SOC. (Group et al., 2016; WHO, 2021a).

Additional antibodies and cocktails have been evaluated for their safety and tolerability in humans. One of them is REGN-EB3 a combination of three antibodies obtained from immunized mice (Pascal et al., 2018), which was tested in a phase I clinical trial (Sivapalasingam et al., 2018). In addition, the monoclonal antibody mAb114, which was isolated from a human survivor of the 1995 EVD outbreak 10 years after infection was found to be safe, well-tolerated and immunogenic in study participants (Corti et al., 2016; Gaudinski et al., 2019). However, for several years ZMapp remained the only anti-Ebolavirus treatment providing efficacy data in humans. Then, during the 2018-2020 EVD outbreak in the DRC, four therapeutic candidates were evaluated for efficacy in a clinical trial. Three of them were monoclonal antibody (cocktails) ZMapp, REG-EB3 and mAb114 (Kupferschmidt, 2019; Mulangu et al., 2019). The fourth candidate was the nucleotide-analogue Remdesivir (Warren

et al., 2016), which has recently also proven beneficial as a treatment option against SARS-CoV-2 (Beigel et al., 2020). The clinical trial was halted when the first interim results were presented. The candidates ZMapp and Remdesivir, which had led to a reduction of mortality from 67% in untreated patients to 49% and 53%, respectively, were excluded from further investigation. The candidates REG-EB3 and mAb114 had delivered more promising results, reducing fatality to 29% and 34%, respectively (Kupferschmidt, 2019; Mulangu et al., 2019).

These results paved the way for their licensing. As the first available therapy the REG-EB3 cocktail was approved for treatment of EVD under the trade name Inmazeb™ (comprising the monoclonal antibodies Atoltivimab, Odesivimab and Maftivimab) in February 2020 (FDA, 2020b). Ten months later, also mAb114 has been licensed under the trade name Ebanga (generic name Ansuvimab) in December 2020 (FDA, 2020a). Despite this success, efforts to find even more potent antibodies and new combinations are needed to further reduce mortality rates in outbreaks. Moreover, the therapies introduced above are only directed against EBOV. No antibody-based countermeasures against SUDV, BDBV or MARV have shown efficacy in humans to date.

1.2.5.2 Vaccinations

Antibodies are well-described means for passive immunization and can be administered as prophylaxis before viral challenge. Nevertheless, the protection they confer is transient and only active immunization and the generation of humoral memory will provide long-lasting immunity against disease. To complement passive immunotherapy, numerous vaccine candidates have been developed and some have been tested in clinical trials (Ana Maria Henao-Restrepo et al., 2017; Ledgerwood et al., 2017; Medaglini & Siegrist, 2017; Regules et al., 2017; Reynolds & Marzi, 2017; Suschak & Schmaljohn, 2019; Wong et al., 2018).

Among them, the replication-competent recombinant vesicular stomatitis virus (rVSV)-based vector (Schnell, Buonocore, Kretzschmar, Johnson, & Rose, 1996) carrying the EBOV glycoprotein (rVSV-ZEBOV) is the most advanced vaccine. It utilizes rVSV and replaces its surface glycoprotein complex by the one of Ebola virus strain *Kikwit*. Therefore, it is referred to as rVSV-ZEBOV (also known as VSV-EBOV or rVSV Δ G-EBOV GP). rVSV-ZEBOV has been demonstrated to be protective against lethal EBOV challenges in rodents and NHPs (Marzi et al., 2015; Suder, Furuyama, Feldmann, Marzi, & de Wit, 2018; Wong et al., 2014). The mechanism by which the vaccine conferred protection to NHPs was found to rely on antibodies (Marzi et al., 2013). Several phase I studies including a multicenter study with participation of the University Hospital Hamburg-Eppendorf have demonstrated its safety, tolerability and immunogenicity (Agnandji et al., 2017; Agnandji et al., 2016; A. Huttner, 2017; A. Huttner et al., 2015; Regules et al., 2017). During the 2013-16 West African outbreak rVSV-

ZEBOV has been evaluated for safety and efficacy in the first phase II/III study. The results of the cluster-randomized ring vaccination trial were promising as none of 4,539 vaccinated contacts of index cases became infected (Ana Maria Henao-Restrepo et al., 2017; A. M. Henao-Restrepo et al., 2015).

Being the first vaccine candidate to provide efficacy data, rVSV-ZEBOV had been designated as lead candidate for administration in current and future EVD outbreaks (WHO, 2018a, 2018c). During the outbreak in the DRC, it has been administered to individuals at risk of EBOV infection. Before its licensing under the trade name Ervebo in December 2019, more than 350,000 individuals had received the vaccine candidate under compassionate use protocols (FDA, 2019; WHO, 2021a). The efficacy of rVSV-ZEBOV is found to reach 100% (FDA, 2019; Ana Maria Henao-Restrepo et al., 2017; WHO, 2019, 2021a). However, despite its broad application and licensing, a detailed understanding of the rVSV-ZEBOV immune response is limited and no analysis has been performed to elucidate the molecular composition of the induced antibody response.

1.3 Aim of this thesis

The rVSV-ZEBOV vaccine has been administered to >350,000 individuals and has been licensed in December 2019. However, our understanding of the detailed humoral response that is conferring protection is still limited.

The aim of this project was, therefore, to provide the first comprehensive characterization of the rVSV-ZEBOV vaccination-induced human memory B cell and antibody response to Ebolaviruses and their surface-exposed glycoproteins. It should be addressed i) whether rVSV-ZEBOV vaccination induces clonal expansion and memory formation of EBOV GP-specific B cells; ii) whether the vaccination-induced antibody response was reproducible among vaccinees with regards to quality, quantity, durability, genetic as well as functional characteristics; and iii) how vaccine-induced antibodies compare to those induced by natural EVD infection.

2 Materials and methods

2.1 Materials

2.1.1 Laboratory equipment

Table 1 shows the laboratory equipment used in this work.

Table 1. Laboratory equipment used in this work.

Device	Specification and vendor
10 μ L Multichannel pipette PCR room	Research Plus, Eppendorf
100 μ L Multichannel pipette PCR room	Research, Eppendorf
1000 μ L pipette	Pipetman, Gilson
125 mL Erlenmeyer cell culture flask	CLS431143-50EA, Corning, Sigma-Aldrich
2 μ L pipette	Pipetman, Gilson
20 μ L pipette	Pipetman, Gilson
-20 °C freezer	Premium, Liebherr
200 μ L pipette	Pipetman, Gilson
200 μ L Rainin multichannel pipette	Pipet-Lite XLS, Rainin
300 μ L Multichannel pipette	Transferpette S-12, Brand
4 °C fridge	Premium BioFresh, Liebherr
-80 °C freezer	MDF-DU700VH-PE, Panasonic
Alarm clock	Carl Roth
Balance	Mettler PC 4400
Cell culture hood	Mars Safety Class 2, Scanlaf
Centrifuge	Avanti J-26S XP, Beckman Coulter
Centrifuge	5810R, Eppendorf
Centrifuge rotor	JS-5.3, Beckman Coulter
CO ₂ Incubator (cell culture)	MCO-19AICUV-PE, Panasonic
CO ₂ Incubator shaker (cell culture)	New Brunswick S41i, Eppendorf
Coffee machine	Melitta Optima Timer
Counting chamber	ZK06 Neubauer improved, Laborversand A. Hartenstein
Electrical multichannel pipette	Xplorer, Eppendorf
Flow cytometer	FACSAria Fusion, BD Bioscience
Fluorescence light microscope	Leica DMI6000B, Leica Biosystem
Fluorescence light source	X-Cite 120PC, Olympus
Gel detection and imaging system	Gel Doc XR+, BioRad
Gel detection table	ECX-F20.Skylight, Peqlab
Horizontal nucleic acid gelelectrophoresis chamber large	OWL 3-14, Thermo Fisher Scientific
Horizontal nucleic acid gelelectrophoresis chamber small	OWL B2, Thermo Fisher Scientific
Incubator (bacteria)	Binder
Incubator shaker (bacteria)	Multitron Pro, INFORS HT

MACS MultiStand	Miltenyi Biotec
MACS Quadro Magnet	Miltenyi Biotec
Microscope	CKX53, Olympus
Mini table centrifuge	D-8550 SU Sunlab, neoLab
Multistep pipette	Multipette M4, Eppendorf
Nucleic acid sample preparator	QIAcube, Qiagen
PCR room hood	PCR UV2 Workstation, Analytic Jena
pH Meter	pH 3110 PLUS, WTW
Pipette boy	Accu-jet pro, Brand
Plate spectrophotometer	Sunrise, Tecan
Plate washer	Hydrospeed, Tecan
Power supply	PowerEase 90W, Life Technologies
Rotator	Gyro-Rocker, Stuart Scientific
Rotator	RM10W 30V, CAT
Rotator	SB3, Stuart Equipment
Spectrophotometer	NanoDrop One, Thermo Fisher Scientific
Stirrer	MSH-20D WiseStir, Wisd Laboratory Instruments
Table centrifuge	5424, Eppendorf
Thermocycler	Veriti, AppliedBiosystems, Thermo Fisher Scientific
Thermomixer	Thermomixer comfort, Eppendorf
Vacuum aspiration system	AC02, Hettich Benelux
Vertical protein gelelectrophoresis chamber	XCell SureLock Electrophoresis Cell, Novex, Life Technologies
Vortexer	Mixer Uzusio VTX-3000L, LMS Laboratory & Medical Supplies
Water bath	AquaLine AL18, Lauda

2.1.2 Consumables

Table 2 shows the consumables used in this work.

Table 2. Consumables used in this work.

Consumable	Order no. and vendor
1.5 mL reaction tube	30120086, Eppendorf
10 µL filter tip	70.1130.210, Sarstedt
10 mL serological pipette	86.1254.001, Sarstedt
1000 µL filter tip	70.762.211, Sarstedt
15 mL reaction tube	62.554.502, Sarstedt
2 mL reaction tube	30120094, Eppendorf
2 mL serological pipette	86.1252.001, Sarstedt
2.5 µL filter tip	70.1130.212, Sarstedt
20 µL filter tip	70.760.213, Sarstedt
200 µL filter tip	70.760.202, Sarstedt
200 µL tip tower	17005093 Rainin LTS, Mettler Toledo
25 mL reservoir	EKT6.1, Carl Roth
25 mL reservoir, sterile and single-packed	EKT8.1, Carl Roth

25 mL serological pipette	86.1685.001, Sarstedt
300 µL filter tip	70.765.200, Sarstedt
5 mL reaction tube, sterile and single-packed	Z768744-50EA, Eppendorf, Sigma Aldrich
5 mL round bottom polystyrene tube with cap	352063, Falcon, Corning
5 mL round bottom polystyrene tube with cell strainer snap cap	734-0001, Falcon, Corning
5 mL serological pipette	86.1253.001, Sarstedt
50 mL reaction tube	62.547.254, Sarstedt
50 mL reservoir	EKT9.1, Carl Roth
50 mL serological pipette	86.1256.001, Sarstedt
6-well tissue culture plate	83.3920.005, Sarstedt
96-well deep well plate	Z688738-32EA, Nunc, Sigma-Aldrich
96-well high binding PS plate, flat bottom	3369 Easy Wash, Corning
96-well PCR plate	72.1979.102, Sarstedt
96-well plate adhesive sealing foil	PEQL82-0626-A, Peqlab, VWR
96-well plate, conical bottom, non-sterile	82.1583, Sarstedt
Adhesive label, silver	L6008-20, Avery Zweckform
Adhesive label, white	L7871, Avery Zweckform
Arm sleeves	113-0494 Tyvek, VWR
Autoclave tape	H7202, SRM
Facial tissues	224995, Tapira Plus
Flat cap strips	82-0784-A, Peqlab
Gloves	D1401-26, Dermagrip Ultra Long
Parafilm	PM-996, Carl Roth
Petri dishes 100 mm	664161, Greiner Bio One
Petri dishes 60 mm	628161, Greiner Bio One
Protein concentrator, Amicon 4 mL, MWCO 10 kDa	UFC801096, Merck
Protein concentrator, Amicon 4 mL, MWCO 30 kDa	UFC803096, Merck
Protein concentrator, Pierce 2-6 mL, MWCO 30 kDa	88522, Thermo Fisher Scientific
Removable label, white	L4731REV-25, Avery Zweckform
Removable round tube lid label, white	L6019REV-25, Avery Zweckform
Self-adhesive film, transparent	2500, Avery Zweckform
Table waste	E705.1, Carl Roth
Tissue culture dishes 100 mm	83.3902, Sarstedt
Tissue culture dishes 150 mm	TPP93150, SRM
Tissues	Kolibri, SAP 224644, UK SRM
Waste bags	E706.1, Carl Roth

2.1.3 Chemicals, biologicals, and reagents

Table 3 shows the chemicals, biologicals and reagents used in this work.

Table 3. Chemicals, biologicals and reagents used in this work.

Reagent	Order no. and vendor
25 kDa polyethylenimine (PEI)	23966, Polysciences
3-(N-Morpholino) propane sulphonic acid (MOPS)	6979, Carl Roth

4',6-Diamidino-2-phenylindole (DAPI)	D1306, RRID: AB_2629482, Thermo Fisher Scientific
40 kDa polyethylenimine (PEI MAX)	24765, Polysciences
4-12% Bis-Tris [Bis (2-hydroxyethyl) imino-tris (hydroxymethyl) methane-HCl] protein gels	NuPAGE NP0322BOX, Thermo Fisher Scientific
Acetic acid, 100%	6755.2, Carl Roth
Agar	X969.3, Carl Roth
Agarose	3810.3, Carl Roth
Albumin fraction V	8076.3, Carl Roth
Antibiotic-Antimycotic, 100x	15240096, Gibco, Thermo Fisher Scientific
Bovine serum albumine	A2153, Sigma-Aldrich
Calcium chloride (CaCl ₂)	HN04.2, Carl Roth
Cresol red	KK15.1, Carl Roth
Deoxyribonucleotide triphosphate (dNTPs, 25 mM)	R1122, Thermo Fisher Scientific
D-Glucose	HN06.2, Carl Roth
Dimethyl formamide (DMF)	803068, Merck
Dimethyl sulfoxide (DMSO)	116743, Merck
Disodium hydrogen phosphate (Na ₂ HPO ₄)	4984.1, Carl Roth
Dithiothreitol (DTT), 10 mM	P1171, Promega
D-Sucrose	4621.1, Carl Roth
Dulbecco's Modified Eagle's medium (DMEM), high glucose (4.5 g/L), without L-Glutamine	11960-044, Thermo Fisher Scientific
Dulbecco's phosphate buffered saline (DPBS)	14190-169 Gibco, Thermo Fisher Scientific
Ethanol Rotipuran, ≥99,8 %,	9065.5, Carl Roth
Ethanol, 70%	T868.3, Carl Roth
Ethanol, denatured	K928.4, Carl Roth
Ethylenediaminetetraacetic acid (EDTA), 0.5 M, pH 8.0	Ambion, Thermo Fisher Scientific
FACS Clean Solution	340345, BD Biosciences
Fetal bovine serum (FBS)	F4135, Merck
FreeStyle 239 Expression medium	12338-026, Life Technologies, Thermo Fisher Scientific
GeneRuler 1 kb Plus DNA ladder	SM1331, Invitrogen, Thermo Fisher Scientific
Glycine	3187.3, Carl Roth
HistoPaque	H8889, Merck
Hydrogen chloride (HCl)	6792.1, Carl Roth
Hydroxyethyl piperazineethanesulfonic acid (HEPES)	6763.1, Carl Roth
Imidazole	3899.3, Carl Roth
Kifunensine (Mannosidase inhibitor)	10009437, Cayman Chemical
L-Glutamine	25030081, Gibco, Thermo Fisher Scientific
Lithium dodecyl sulfate (LDS) sample buffer, 4x	NuPAGE NP0007, Thermo Fisher Scientific
Monopotassium dihydrogen phosphate (KH ₂ PO ₄)	3904.1, Carl Roth
Nuclease-free H ₂ O	AM9937 Ambion, Thermo Fisher Scientific
PageRuler Plus Prestained Protein Ladder	26619, Thermo Fisher Scientific
Penicillin/Streptomycin (P/S)	15140122 Gibco, Thermo Fisher Scientific
Phosphate buffered saline (PBS) for cell culture	10010-015 Gibco, Thermo Fisher Scientific

Polyoxyethylene-20-sorbitan monolaurate (Tween 20)	9127.1, Carl Roth
Potassium chloride (KCl)	P017.1, Carl Roth
Protein G Sepharose 4 Fast Flow	GE17-0618-05, GE Healthcare, Sigma-Aldrich
Protino Ni-NTA Agarose	745400, Macherey-Nagel
RNase away	A998.2, Carl Roth
RNaseOUT	10777019, Thermo Fisher Scientific
RNasin	N2515, Promega
Roswell Park Memorial Institute (RPMI) 1640 medium, with L-Glutamine	1875-093, Life Technologies
Sample reducing agent, 10x	NuPAGE NP0009, Thermo Fisher Scientific
Sodium chloride (NaCl)	3957.1, Carl Roth
Sodium chloride (NaCl), 0.9% for FACS	101900, SRM
Sodium dihydrogen phosphate (NaH ₂ PO ₄)	T878.2, Carl Roth
<i>Sodium dodecyl sulfate (SDS)</i>	1057.1, Carl Roth
Sodium hydroxide (NaOH)	6771.1, Carl Roth
Sodium pyruvate	11360070, Gibco, Thermo Fisher Scientific
Streptavidin, HRP-conjugated	N100, Thermo Fisher Scientific
Super optimal broth with catabolite repression (SOC) medium	15544034, Thermo Fisher Scientific
SYBRSafe DNA stain, 10,000x	S33102, Invitrogen, Thermo Fisher Scientific
<i>Tris(hydroxymethyl)aminomethane (TRIS)</i>	4855.2, Carl Roth
Trypan blue	T8154, Sigma-Aldrich
Trypsin 0.05% / EDTA 0.02%, phenol red	25300054 Gibco, Thermo Fisher Scientific
Tryptone	8952.2, Carl Roth
Yeast extract	2363.4, Carl Roth

2.1.4 Buffer, media and solutions

Table 4 shows the buffers, media and solutions used in this work.

Table 4. Commercial or self-made buffers, media and solutions used in this work.

Buffer, medium or solution	Composition
10x PBS	H ₂ O, 1.37 M NaCl, 27 mM KCl, 100 mM Na ₂ HPO ₄ , 18 mM KH ₂ PO ₄
1x NPI-10	H ₂ O, 50 mM NaH ₂ PO ₄ , 300 mM NaCl, 10 mM imidazole, pH = 8
1x TAE	950 mL H ₂ O + 50 mL 50x TAE
20x MOPS buffer	H ₂ O, 1 M MOPS, 1 M Tris, 20 mM EDTA, 2% (w/v) SDS, dilute to 1 x with ddH ₂ O before use
2x HBS buffer	500 mL, 8 g NaCl, 5 g HEPES, 1 g Glucose, 0.38 g KCl, 0.1 g Na ₂ HPO ₄ , pH = 7.05 with NaOH
2x NPI-10	H ₂ O, 100 mM NaH ₂ PO ₄ , 600 mM NaCl, 20 mM imidazole, pH = 8
50x TAE	H ₂ O, 2 M Tris base, 0.1 M EDTA, 1 M Acetic acid, autoclave

Cresol red loading dye, 0.03%	49 mL H ₂ O, 17 g Sucrose, 1 mL Cresol red
Developer working solution (Silver stain)	25 mL Silver stain developer, 0.5 mL Silver stain enhancer
ELISA blocking buffer	ELISA wash buffer, 5% BSA (w/v)
ELISA wash buffer (PBST)	PBS, 0.05% Tween 20 (v/v)
FACS buffer	PBS, 2% FBS (v/v), 2 mM EDTA
Fixation buffer (Silver stain)	H ₂ O, 30% Ethanol (v/v), 10% Acetic acid (v/v)
HEK293F cell medium	FreeStyle 293 expression medium, 0.2% P/S (v/v)
HEK293T cell medium	DMEM, 10% FBS (v/v), 1% Antibiotic-Antimycotic (v/v), 1% Sodium pyruvate (v/v) and 1% L-Glutamine (v/v)
LB agar	LB medium, 1.5% (w/v) agar, autoclaved, with antibiotic if required
Lysogeny broth (LB) medium	1 L H ₂ O, 10 g Tryptone, 5 g Yeast extract, 10 g NaCl autoclaved
MACS buffer	PBS, 2% BSA (w/v), 2 mM EDTA
NPI-100	H ₂ O, 50 mM NaH ₂ PO ₄ , 300 mM NaCl, 100 mM imidazole, pH = 8
NPI-20	H ₂ O, 50 mM NaH ₂ PO ₄ , 300 mM NaCl, 20 mM imidazole, pH = 8
PEI working solution	H ₂ O, 0.45 mg/mL PEI, sterile-filtred and stored at -80 °C
Sensitizer working solution (Silver stain)	25 mL H ₂ O, 50 µL Silver stain sensitizer
Stain working solution (Silver stain)	25 mL Silver stain, 0.5 mL Silver stain enhancer
Stop solution (Silver stain)	H ₂ O, 5% Acetic acid (v/v)

2.1.5 Commercial kits

Table 5 shows the commercial kits used in this work.

Table 5. Commercial kits used in this work.

Kit	Order no. and vendor
CD19 MicroBeads, human	130-050-301, Miltenyi Biotec
EZ-Link™ Sulfo-NHS-Biotin	21326, Thermo Fisher Scientific
GeneJET Gel Extraction and DNA Cleanup Micro Kit	K0832, Thermo Fisher Scientific
Microscale Antibody Labeling Kit DyLight 488	53025, Thermo Fisher Scientific
NEBuilder HiFi DNA Assembly Mix	E2621S, New England Biolabs
NOVA Lite Hep-2 ANA Kit	066708100, Inova Diagnostics / Werfen
Pierce Silver Stain Kit	24612, Thermo Fisher Scientific
PureLink HiPure Plasmid Maxiprep kit	K210007, Invitrogen, Thermo Fisher Scientific
PureLink HiPure Plasmid Midiprep kit	K210005, Invitrogen, Thermo Fisher Scientific
QIAprep Miniprep kit	27106, Qiagen
RNeasy Micro Kit	74004, Qiagen

2.1.6 Antibodies

Table 6 shows the commercial antibodies used in this work.

Table 6. Commercial antibodies used in this work.

Antibody	Species	Clone	Conju- gate	Dilution	Order no. and vendor	Application
anti-human CD20	mouse	2H7	AF700	1:20	560631, BD Bioscience	Flow cytometry
anti-human IgG	mouse	G18-145	APC	1:20	550931, BD Bioscience	Flow cytometry
anti-human IgG	goat	Polyclonal	HRP	1:1000	2040-05, Southern Biotech	ELISA
anti-human IgM	mouse	G20-127	FITC	1:20	555782, BD Bioscience	Flow cytometry

2.1.7 Enzymes

Table 7 shows the Nucleic acid- or protein-modifying enzymes used in this work.

Table 7. Enzymes used in this work.

Enzyme	Order no. and vendor
AfeI	R0652S, New England Biolabs
AflII	R0520S, New England Biolabs
AgeI	R3552L, New England Biolabs
BamHI	R3136S, New England Biolabs
BsiWI	R3553S, New England Biolabs
EcoRI	R3101S, New England Biolabs
NotI	R3189S, New England Biolabs
Papain	3125, Merck
Platinum Taq polymerase	11304029, Thermo Fisher Scientific
PlatinumTaq Green HotStart polymerase	11966034, Thermo Fisher Scientific
Q5 High Fidelity DNA polymerase	M0493, New England Biolabs
Sall	R3138S, New England Biolabs
Self-made Taq	Christoph Kreer, Klein Lab
SgrAI	R0603S, New England Biolabs
SuperScript IV Reverse Transcriptase	18090200, Thermo Fisher Scientific
T4 DNA polymerase	M0203, New England Biolabs
T4 ligase	M0202S, New England Biolabs
Taq polymerase	201203, Qiagen
XhoI	R0146S, New England Biolabs

2.1.8 Oligonucleotides

Table 8 shows the commercial antibodies used in this work. All primers were purchased as custom DNA oligos at Invitrogen, Thermo Fisher Scientific and solved in nuclease-free H₂O to a stock concentration of 50 µM.

Table 8. Oligonucleotides used in this work.

Mix	Name	Sequence (5' → 3')	Reference
	5' Ab-sense	GCTTCGTTAGAACGCGGCTAC	(T. Tiller et al., 2008)
	5' plgH_K_L seq primer 1	ATCCACTTTGCCTTTCTCTC	Klein Lab
	IGHV_Opt5_1_fw	CACCTGTGGTTCTTCCTCCTCC	Klein Lab
	IGHV_Opt5_2_fw	CACCTGTGGTTCTTCCTCCTGC	Klein Lab
	IGHV_Opt5_3_fw	ATGGAGTTTGGGCTGAGCTGG	Klein Lab
	IGHV_Opt5_4_fw	ATGGAGTTGGGCTGAGCTG	Klein Lab
	IGHV_Opt5_5_fw	TGGAGTTTTGGCTGAGCTGGG	Klein Lab
	IGHV_Opt5_6_fw	ACTTTGCTCCACGCTCCTGC	Klein Lab
	IGHV_Opt5_7_fw	ATGGACTGGACCTGGAGCATC	Klein Lab
5' Opt5 Mix	IGHV_Opt5_8_fw	ATGGACTGGACCTGGAGTTCC	Klein Lab
	IGHV_Opt5_9_fw	ATGGACTGCACCTGGAGGATC	Klein Lab
	IGHV_Opt5_10_fw	ATGGACTGGACCTGGAGGGTCTTC	Klein Lab
	IGHV_Opt5_11_fw	TCTGTCTCCTTCCTCATCTTCCTGC	Klein Lab
	IGHV_Opt5_12_fw	GGACTGGATTTGGAGGGTCCTCTTC	Klein Lab
	IGHV_Opt5_13_fw	GCTCCGCTGGGTTTTCTTG	Klein Lab
	IGHV_Opt5_14_fw	TGGGGTCAACCGCCATCC	Klein Lab
	IGHV_Opt5_15_fw	GGCCTCTCCACTTAAACCCAGG	Klein Lab
	IGHV_Opt5_16_fw	TGGACACACTTTGCTACACACTCC	Klein Lab
	3' Ozawa_cg_rt	AGGTGTGCACGCCGCTGGTC	(Ozawa, Kishi, & Muraguchi, 2006)
	3' IgG (Internal)	GTTCGGGGAAGTAGTCCTTGAC	(T. Tiller et al., 2008)
	5' L-Vκ 1/2	ACAGGTGCCACTCCCAGGTGCAG	(T. Tiller et al., 2008)
5' LVκ Mix	5' L-Vκ 3	AAGGTGTCCAGTGTGARGTGCAG	(T. Tiller et al., 2008)
	5' L-Vκ 4/6	CCCAGATGGGTCCTGTCCCAGGTGCAG	(T. Tiller et al., 2008)
	5' L-Vκ 5	CAAGGAGTCTGTTCCGAGGTGCAG	(T. Tiller et al., 2008)
	5' Pan Vκ	ATGACCCAGWCTCCABYCWCCCTG	(T. Tiller et al., 2008)
	3' Cκ543	GTTTCTCGTAGTCTGCTTTGCTCA	(T. Tiller et al., 2008)
	3' Cκ 494	GTGCTGTCCCTTGCTGTCTGCT	(T. Tiller et al., 2008)
	5' L-Vλ 1	GGTCCTGGGCCAGTCTGTGCTG	(T. Tiller et al., 2008)
	5' L-Vλ 2	GGTCCTGGGCCAGTCTGCCCTG	(T. Tiller et al., 2008)
5' LVλ Mix	5' L-Vλ 3	GCTCTGTGACCTCCTATGAGCTG	(T. Tiller et al., 2008)
	5' L-Vλ 4/5	GGTCTCTCTCSCAGCYTGTGCTG	(T. Tiller et al., 2008)
	5' L-Vλ 6	GTTCTTGGCCAATTTTATGCTG	(T. Tiller et al., 2008)
	5' L-Vλ 7	GGTCCAATTCYCAGGCTGTGGTG	(T. Tiller et al., 2008)
	5' L-Vλ 8	GAGTGGATTCTCAGACTGTGGTG	(T. Tiller et al., 2008)
	3' Cλ	CACCAGTGTGGCCTTGTTGGCTTG	(T. Tiller et al., 2008)
	3' XhoI Cl	CTCCTCACTCGAGGGYGGGAACAGAGTG	(T. Tiller et al., 2008)

5' AgeI SLIC VH 1	CTAGTAGCAACTGCAACCGGTGTACATTCC CAGGTGCAGCTGGTGCAG	(T. Tiller et al., 2008)
5' AgeI SLIC VH 1/5	CTAGTAGCAACTGCAACCGGTGTACATTCC GAGGTGCAGCTGGTGCAG	(T. Tiller et al., 2008)
5' AgeI SLIC VH 1-18	CTAGTAGCAACTGCAACCGGTGTACATTCC CAGGTTTCAGCTGGTGCAG	(T. Tiller et al., 2008)
5' AgeI SLIC VH 1-24	CTAGTAGCAACTGCAACCGGTGTACATTCC CAGGTCCAGCTGGTACAG	(T. Tiller et al., 2008)
5' AgeI SLIC VH 3	CTAGTAGCAACTGCAACCGGTGTACATTCT GAGGTGCAGCTGGTGGAG	(T. Tiller et al., 2008)
5' AgeI SLIC VH 3-11	CTAGTAGCAACTGCAACCGGTGTACATTCT CAGGTGCAGCTGGTGGAG	(T. Tiller et al., 2008)
5' AgeI SLIC VH 3-23	CTAGTAGCAACTGCAACCGGTGTACATTCT GAGGTGCAGCTGTTGGAG	(T. Tiller et al., 2008)
5' AgeI SLIC VH 3-33	CTAGTAGCAACTGCAACCGGTGTACATTCT CAGGTGCAGCTGGTGGAG	(T. Tiller et al., 2008)
5' AgeI SLIC VH 3-9	CTAGTAGCAACTGCAACCGGTGTACATTCT GAAGTGCAGCTGGTGGAG	(T. Tiller et al., 2008)
5' AgeI SLIC VH 4	CTAGTAGCAACTGCAACCGGTGTACATTCC CAGGTGCAGCTGCAGGAG	(T. Tiller et al., 2008)
5' AgeI SLIC VH 4-34	CTAGTAGCAACTGCAACCGGTGTACATTCC CAGGTGCAGCTACAGCAGTG	(T. Tiller et al., 2008)
5' AgeI SLIC VH 4-39	CTAGTAGCAACTGCAACCGGTGTACATTCC CAGCTGCAGCTGCAGGAG	(T. Tiller et al., 2008)
5' AgeI SLIC VH 6-1	CTAGTAGCAACTGCAACCGGTGTACATTCC CAGGTACAGCTGCAGCAG	(T. Tiller et al., 2008)
3' Sall SLIC JH 1/2/4/5	CCGATGGGCCCTTGGTTCGACGCTGAGGAG ACGGTGACCAG	(T. Tiller et al., 2008)
3' Sall SLIC JH 3	CCGATGGGCCCTTGGTTCGACGCTGAAGAG ACGGTGACCATTG	(T. Tiller et al., 2008)
3' Sall SLIC JH 6	CCGATGGGCCCTTGGTTCGACGCTGAGGAG ACGGTGACCGTG	(T. Tiller et al., 2008)
5' AgeI SLIC V _K 1–5	CTAGTAGCAACTGCAACCGGTGTACATTCT GACATCCAGATGACCCAGTC	(T. Tiller et al., 2008)
5' AgeI SLIC V _K 1–9	CTAGTAGCAACTGCAACCGGTGTACATTCA GACATCCAGTTGACCCAGTCT	(T. Tiller et al., 2008)
5' AgeI SLIC V _K 1D–43	CTAGTAGCAACTGCAACCGGTGTACATTGT GCCATCCGGATGACCCAGTC	(T. Tiller et al., 2008)
5' AgeI SLIC V _K 2–24	CTAGTAGCAACTGCAACCGGTGTACATGG GGATATTGTGATGACCCAGAC	(T. Tiller et al., 2008)
5' AgeI SLIC V _K 2–28	CTAGTAGCAACTGCAACCGGTGTACATGG GGATATTGTGATGACTCAGTC	(T. Tiller et al., 2008)
5' AgeI SLIC V _K 2–30	CTAGTAGCAACTGCAACCGGTGTACATGG GGATGTTGTGATGACTCAGTC	(T. Tiller et al., 2008)

5' AgeI SLIC V _K 3–11	CTAGTAGCAACTGCAACCGGTGTACATTCA GAAATTGTGTTGACACAGTC	(T. Tiller et al., 2008)
5' AgeI SLIC V _K 3–15	CTAGTAGCAACTGCAACCGGTGTACATTCA GAAATAGTGATGACGCAGTC	(T. Tiller et al., 2008)
5' AgeI SLIC V _K 3–20	CTAGTAGCAACTGCAACCGGTGTACATTCA GAAATTGTGTTGACGCAGTCT	(T. Tiller et al., 2008)
5' AgeI SLIC V _K 4–1	CTAGTAGCAACTGCAACCGGTGTACATTCCG GACATCGTGATGACCCAGTC	(T. Tiller et al., 2008)
3' BsiWI SLIC J _K 1/4	GAAGACAGATGGTGCAGCCACCGTACGTT TGATYTCCACCTTGGTGTC	(T. Tiller et al., 2008)
3' BsiWI SLIC J _K 2	GAAGACAGATGGTGCAGCCACCGTACGTT TGATCTCCAGCTTGGTGTC	(T. Tiller et al., 2008)
3' BsiWI SLIC J _K 3	GAAGACAGATGGTGCAGCCACCGTACGTT TGATATCCACTTTGGTCTGTC	(T. Tiller et al., 2008)
3' BsiWI SLIC J _K 5	GAAGACAGATGGTGCAGCCACCGTACGTT TAATCTCCAGTCGTGTC	(T. Tiller et al., 2008)
3' BsiWI SLIC J _K 1/4	GAAGACAGATGGTGCAGCCACCGTACGTT TGATYTCCACCTTGGTGTC	(T. Tiller et al., 2008)
5' AgeI SLIC V _λ 1	CTAGTAGCAACTGCAACCGGTTCTGGGC CCAGTCTGTGCTGACKCAG	(T. Tiller et al., 2008)
5' AgeI SLIC V _λ 2	CTAGTAGCAACTGCAACCGGTTCTGGGC CCAGTCTGCCCTGACTCAG	(T. Tiller et al., 2008)
5' AgeI SLIC V _λ 3	CTAGTAGCAACTGCAACCGGTTCTGTGAC CTCCTATGAGCTGACWCAG	(T. Tiller et al., 2008)
5' AgeI SLIC V _λ 4/5	CTAGTAGCAACTGCAACCGGTTCTCTCTCS CAGCYTGTGCTGACTCA	(T. Tiller et al., 2008)
5' AgeI SLIC V _λ 6	CTAGTAGCAACTGCAACCGGTTCTGGGC CAATTTTATGCTGACTCAG	(T. Tiller et al., 2008)
5' AgeI SLIC V _λ 7/8	CTAGTAGCAACTGCAACCGGTTCCAATTCY CAGRCTGTGGTGACYCAG	(T. Tiller et al., 2008)
3' XhoI SLIC C _λ	GAAGCTCCTCACTCGAGGGYGGGAACAGA GTG	(T. Tiller et al., 2008)
fwd seq pCAGGS upstr EcoRI	GTGCTGGTTATTGTGCTGTC	Self-made
rev seq pCAGGS downstr NotI	CACCAGCCACCACCTTC	Self-made
fwd pMX–SgrAI–VK KZ52	TGTTCCAGATTACGCCGGTG GAACTGGTGATGACTCAGAGCC	Self-made
fwd pMX–SgrAI–VK mAb114	TGTTCCAGATTACGCCGGTG GACATCCAGATGACCCAGTCTC	Self-made
fwd pMX–SgrAI–VK ADI- 15758	TGTTCCAGATTACGCCGGTG GAAATTGTATTGACACAGTCTCCAGC	Self-made
fwd pMX–SgrAI–VK ADI- 15999	TGTTCCAGATTACGCCGGTG GATATTGTGATGACGCAGACTCCA	Self-made

fwd pMX-SgrAI-VL mAb100	TGTTCCAGATTACGCCGGTG TCCTATGAGCTGACTCAGCCA	Self-made
fwd pMX-SgrAI-VL ADI- 16037	TGTTCCAGATTACGCCGGTG CAGCCTGTGCTGACTCAGC	Self-made
rev kappa constant_2A	AGTTCAGAGTCTGTTTCACGCTAGC ACACTCTCCCCTGTTGAAGCTC	Self-made
rev lambda constant_2A	AGTTCAGAGTCTGTTTCACGCTAGC TGAACATTCTGTAGGGGCCAC	Self-made
fwd 2A - IgH leader	GCTAGCGTGAAACAGACTCTG	Self-made
rev 2A - IgH leader	GAATGTACACCGTTGCAGT	Self-made
fwd Leader_VH_KZ52	AGCAACTGCAACCGGTGTACATTCT GAGGTTCAACTTCTGGAGTCAGG	Self-made
fwd leader_VH_114_15999_16 037	AGCAACTGCAACCGGTGTACATTCT GAGGTGCAGCTGGTGGAGT	Self-made
fwd Leader_VH_ADI- 15758	AGCAACTGCAACCGGTGTACATTCT CAGGTGCAGCTGGTGGAGT	Self-made
fwd Leader_VH_mAb100	AGCAACTGCAACCGGTGTACATTCT CAGGTGCAGCTGCAGGAGT	Self-made
rev heavy constant-Afel- pMX NEW	AGTCCTTGACCAGGCAGCCAGCGCTGCT GTGCCCCAGAGGTG	Self-made
fwd seq primer PMX upstr BamHI	CTTACACAGTCCTGCTGAC	Self-made
90 fwd seq primer PMX upstr VL	CATGGAGACAGACACACTCCTG	Self-made
fwd pMX_BamHI-SgrAI	GGGGTGGACCATCCTCTAGAC	Self-made
rev pMX_BamHI-SgrAI	CACCGGCGTAATCTGGAACATC	Self-made
fwd seq primer kappa constant	GCACCATCTGTCTTCATCTTC	Self-made
fwd seq primer lambda constant	CCCTCGGTCACTCTGTTC	Self-made
rev PDGF myc heavy constant	CCTAACGTGGCTTCTTCTG	Self-made
rev seq PMX downstr NotI	CTAGAAGGCACAGTCGAGG	Self-made
Random Hexamer Primer Mix		SO142, Invitrogen

2.1.9 Human samples, cell lines, and bacterial or viral strains

Table 9 shows the human samples, cell lines and bacterial/viral strains used in this work.

Table 9. Human samples, cell lines and bacterial/viral strains.

Category	Specification	Vendor/Provider	Order no./Identifier
Human samples	rVSV-ZEBOV-vaccinated individuals (EV01-EV07)	This project, Addo Lab, Clinical Trial Center North, Hamburg-Eppendorf	Clinical trial: NCT02283099 (Agnandji et al., 2016)
	Frankfurt patient: Serum and PBMCs	Dr. Timo Wolf, University of Frankfurt	N/A
	EVD survivor sera	M.W. Carroll; Becker Lab, Phillips University, Marburg	N/A
Cell lines	HEK293T	ATCC	CRL-3216, RRID: CVCL_0063
	HEK293F	National Research Council Canada	www.nrc-cnrc.gc.ca/eng/solutions/licensing/10894.html
	FreeStyle™ 293-F Cells	Thermo Fisher Scientific	R79007
	Vero C1008	ATCC	CRL-1586, RRID: CVCL_0574
Bacterial strains	<i>E. coli</i> DH5α	Thermo Fisher Scientific	18263012
Virus strains	EBOV (strain <i>Mayinga</i>)	Becker Lab, Phillips University, Marburg	GenBank: NC_002549

2.1.10 Software

Table 10 shows software used in this work.

Table 10. Software used in this work.

Name	Source/Reference	Identifier or website
Abpredict tool	(Norn, Lapidoth, & Fleishman, 2017)	N/A
Adobe Illustrator CC 2018	Adobe	https://www.adobe.com
Aimless	(Evans & Murshudov, 2013b)	N/A
Clustal Omega 1.2.3	(Sievers et al., 2011)	https://www.ebi.ac.uk/Tools/msa/clustalo/ RRID: SCR_001591
Codon optimization	IDT Codon optimization	http://www.idtdna.com/CodonOpt
Coot	(Emsley, Lohkamp, Scott, & Cowtan, 2010)	N/A
cryoSPARC V2 suite	(Punjani, Rubinstein, Fleet, & Brubaker, 2017)	N/A
CTFFIND4	(Rohou & Grigorieff, 2015)	N/A
FlowJo 10.5.3	FlowJo, LLC	https://www.flowjo.com
Geneious 10.2.6	Geneious	https://www.geneious.com

iCn3D (MMDB)	(Madej et al., 2014)	https://www.ncbi.nlm.nih.gov/Structure/icn3d/full.html
IgBLAST 1.13.0	(Ye et al., 2013)	https://www.ncbi.nlm.nih.gov/igblast/ RRID: SCR_002873
Image Lab	BioRad	
MacVector 16.0.9	MacVector	https://www.macvector.com
NEBuilder Assembly Tool 1.12.19	NEB	http://nebuilder.neb.com/!
Phaser	(McCoy et al., 2007)	N/A
Phenix real-space refinement tool	(Adams et al., 2010)	N/A
Phenix refine	(Adams et al., 2010)	N/A
pRESTO 0.5.11	(Vander Heiden et al., 2014)	RRID: SCR_001782
Prism 7	GraphPad	https://www.graphpad.com/
Python 3.6.8	Python Software Foundation	https://www.python.org/ RRID: SCR_008394
UCSF chimera	(Pettersen et al., 2004)	N/A
WebLogo3	(Crooks, Hon, Chandonia, & Brenner, 2004)	http://weblogo.berkeley.edu/info.html
Xia2	(Winter, 2010)	N/A

2.2 Methods

2.2.1 Molecular biology

2.2.1.1 Restriction digestion

Preparative restriction digests were prepared according to NEB's instructions. Briefly, reactions were set up in a volume of 50 μ L and contained 5-20 μ g of vectors. For inserts typically 100 ng of ordered fragments (~400 fmol) or purified PCR product were digested. Reactions were 10x over digests and to reduce amount of enzyme, incubated for ~16 h if no star activity was reported. Enzymes were heat-inactivated at 65 °C for 10 min if required.

2.2.1.2 Gel electrophoresis

Nucleic acids were separated on agarose gel after PCR or restriction digest. DNA of expected size below 500 bp were applied to 2% (w/v) agarose gels, nucleic acids of larger size on 0.8-1% agarose gels. Agarose was melted in 1x TAE buffer and supplied with SYBR Safe (1:20,000 v/v) after cooling below 60 °C. Following polymerization, gels were transferred to electrophoresis chamber and fully covered with 1x TAE buffer. Samples were supplied with 6x Loading dye if not contained in PCR reaction and transferred to lanes. To evaluate fragment sizes, 6 μ L of 1 kb DNA

ladder was applied. Electrophoresis was exerted at typically 150 V (7 V/cm gel length) and separation monitored on a gel documentation and imaging system. If DNA was to be purified from gel, it was cut on a gel detection table and full excision documented afterwards.

2.2.1.3 DNA purification

DNA was purified using GeneJET Gel Extraction and DNA Cleanup Micro Kit. Depending on upstream reaction, different protocols were followed for cleanup. Restriction digests were purified using protocol A, PCR products via protocol B, and protocol C was applied for extraction from gel. Nucleic acids were eluted in 11 μ L nuclease-free H₂O.

2.2.1.4 DNA quantification

DNA content was determined by measuring absorption at 260 nm via NanoDrop One. Nuclease-free H₂O was used as a blank.

2.2.1.5 DNA ligation

Purified fragments from restriction digests were ligated at a vector to insert molar ratio of 1:5, typically using 50 fmol vector and 250 fmol insert. Reaction was performed using 1 μ L T4 ligase (400 U) in 1x T4 ligation buffer (NEB) and in a final volume of 10 μ L and incubated at RT for 30 min or at 16 °C for 20 min. Afterwards, enzyme was heat-inactivated at 65 °C for 10 min.

2.2.1.6 Transformation of chemically competent bacteria

Plasmid DNA was transformed into chemically competent *Escherichia coli* (*E. coli*) strain DH5 α using standard protocol. Briefly, 2-5 μ L ligation reaction, 2 μ L of SLIC reaction, or 1 μ L of mini, midi or maxi preparation were added to 50 μ L bacteria and incubated on ice for 15-30 min. Bacteria were heat-shocked at 42 °C for 45 sec and briefly put back on ice. 50 μ L LB or SOC medium was added, and samples were incubated at 37 °C whilst shaking at 400-600 rpm. Cells were spun at 2,000 x g for 1 min, 50 μ L supernatant discarded, pellet resuspended in rest volume and plated on LB agar plates with required antibiotic – typically ampicillin at a final concentration of 50 μ g/mL. Plates were incubated at 37 °C upside down over night.

2.2.1.7 Colony PCR

Colony PCRs were performed on *E. coli* after transformation. Reactions were prepared on ice and set up in 25 μ L volume. For downstream DNA preparations and sequencing, it was necessary to be able to trace back colonies selected for PCR. Therefore, colonies were simultaneously transferred to a new master plate. Briefly, sterile pipette tips were used to transfer colonies from original plates by briefly tipping a defined “well” on a new agar plate that was subdivided into 96

areas using a grid. The same tip was then used to inoculate a well on a PCR plate containing PCR solution. Master plate was incubated overnight at 37 °C. PCR reactions were set up as described in **Table 11**, **Table 12** and **Table 13** depending on DNA polymerase used. PCRs were performed at cycling conditions summarized in **Table 14**. Afterwards, 8 µL of amplimers were analyzed via gel electrophoresis.

Table 11. Colony PCR reaction master mix using Taq DNA polymerase.

Reagent	Volume/well (µL)
H ₂ O	11.775
Cresol red loading dye	10
10x Taq buffer	2.5
25 nM dNTPs	0.125
Forward primer (50 µM)	0.2
Reverse primer (50 µM)	0.2
Taq DNA polymerase (Qiagen)	0.2

Table 12. Colony PCR reaction master mix using Platinum DNA polymerase.

Reagent	Volume/well (µL)
H ₂ O	19.75
10x Platinum Green Taq buffer	2.5
kb Extender	0.75
25 nM dNTPs	1.5
Forward primer (50 µM)	0.2
Reverse primer (50 µM)	0.1
Platinum Taq DNA polymerase (Qiagen)	0.1

Table 13. Colony PCR reaction master mix using self-made Taq DNA polymerase.

Reagent	Volume/well (µL)
H ₂ O	19.75
10x self-made Taq buffer	2.5
6x loading dye	0.75
25 nM dNTPs	1.5
Forward primer (50 µM)	0.2
Reverse primer (50 µM)	0.1
Taq DNA polymerase (self-made)	0.5

For analysis of heavy and kappa and lambda light chain variable regions within expression plasmids:

HC: fw: 5' Ab-sense rev: 3' IgG Internal

KC: fw: 5' Ab-sense rev: 3' Ck494

LC: fw: 5' Ab-sense rev: 3' *Xho*I Cl

Table 14. Colony PCR cycling condition.

Cycle step	Process	Temperature	Time	Cycles
1	Initial denaturation	94 °C	5 min	x1
2	Denaturation	94 °C	30 sec	x25
	Annealing	57-58 °C	30-60 sec/kb	
	Extension	72 °C	1-2 min	
3	Final extension	72 °C	10 min	x1
4	Storage	4 °C	hold	x1

2.2.1.8 Mini preparation of plasmid DNA

Plasmid DNA was isolated using the QIAprep spin mini prep kit (Qiagen) following manufacturer's instructions. Briefly, tubes of 3 mL LB medium supplemented with required antibiotic were inoculated with single clones picked from agar plates. Cultures were allowed growing for 12-18 h whilst shaking at 200 rpm at 37 °C in incubators reserved for bacterial cultures. After incubation, 1-1.5 mL were transferred to a 1.5 mL reaction tube and cells were harvested by centrifugation (6,800 x g, RT, 3 min). Supernatant was discarded and pellet resuspended in 250 µL resuspension buffer P1. Subsequently, 250 µL of lysis buffer P2 were added, and tubes inverted six times. To neutralize sample pH, 350 µL of buffer N3 was added, and reaction tubes inverted six times immediately. Lysates were cleared of precipitate by centrifugation at 13,000 x g for 10 min. Supernatant was transferred to QIAprep spin column and spun (18,000 x g for 1 min). Flow-through was discarded, 750 µL of wash buffer were added to membrane and spun. Washing step was repeated. After discarding flow-through, columns were spun at full speed for 1 min to elute residual wash buffer. Finally, columns were transferred to clean 1.5 mL reaction tube, 50 µL of nuclease-free H₂O was added, and after 1 min incubation plasmid DNA was eluted by centrifugation (18,000 x g for 1 min). Remaining bacterial overnight cultures were discarded or stored at 4 °C to subsequent inoculation of cultures for midi or maxi preparation or the preparation of glycerol stocks.

2.2.1.9 Midi and maxi preparation of plasmid DNA

Midi and maxi preparations of plasmid DNA were performed according to manual with minor changes using PureLink HiPure midi or maxi prep kits (Thermo Fisher Scientific). Volumes for overnight cultures and buffers for respective kits are listed in **Table 15** below. Overnight cultures of LB media supplemented with antibiotic were inoculated with single colonies or left-over mini prep overnight cultures. After shaking at 200 rpm at 37 °C for 14-18 h, bacteria were pelleted in 50 mL reaction tubes or 250 mL conical bottles tubes by centrifugation (4,000 x g, 10 min). Supernatant was discarded and pellet resuspended thoroughly in resuspension buffer R3. Lysis buffer L7 was added, and tubes inverted six times. After 5 min of incubation, precipitation buffer N3 was added to lysate, tubes immediately inverted six times, and samples spun (6,800 x g, 4 °C, 30 min). Cell debris-free supernatant was transferred to midi columns, equilibrated with

equilibration buffer EQ1. After solution drained by gravity flow, columns were washed with wash buffer W8 twice. Finally, plasmid DNA was eluted with elution buffer E4 into 50 mL reaction tubes prefilled with isopropanol. Tubes were mixed by inverting and spun at 12,000 x g for 30-45 min. Supernatant was carefully aspirated with vacuum pump, and pellet washed with 70% ethanol. Ethanol was added with a 1000 μ L pipette and a pipette tip with shortened tip. Thereby, the tip opening was widened, and DNA pellets could be taken up. Plasmid DNA was transferred to 1.5 mL or 2 mL reaction tubes together with ethanol they were washed in. After centrifugation (6,800 x g, 4 °C, 5 min), ethanol was carefully aspirated, and tubes put in heat block at 40 °C for a few minutes to remove residual alcohol. Finally, pellets were resuspended in H₂O by overnight storage at 4 °C and subsequent vortexing.

Table 15. Volumes of buffers and solutions used for midi and maxi preps.

Buffer or solution	Midi prep	Maxi prep
Overnight culture volume	100 mL	250 mL
Resuspension buffer R3	4 mL	10 mL
Lysis buffer L7	4 mL	10 mL
Precipitation buffer N3	4 mL	10 mL
Equilibration buffer EQ1	10 mL	30 mL
Wash buffer W8	10 mL	60 mL
Elution buffer	5 mL	15 mL
Isopropanol	3.5 mL	10.5 mL
70% EtOH (v/v)	1 mL	1-2 mL
H ₂ O for solving DNA	200 μ L	1 mL

2.2.1.10 Sequencing

Nucleic acid sequence was determined by Eurofins or GATC according to company's requirements. If sample size was larger than 40, samples were sent in 96-well plates covered by plate lid strips. Usually, plasmid DNA was sent as premixed sample and diluted to 50-100 ng/ μ L with nuclease-free H₂O in a total volume of 15 μ L. 2 μ L of a 10 μ M primer were added. PCR reactions were filled up to 15-20 μ L with nuclease-free H₂O and purified by the company. Primers were sent in separate tubes.

2.2.1.11 Preparation of glycerol stocks

For long-time storage of colonies harboring plasmids with validated sequences, residual bacterial cultures were used for preparation of glycerol stocks. Equal volumes of bacterial culture were mixed with 50% glycerol and stored at -80 °C.

2.2.1.12 Cloning strategies

2.2.1.12.1 Glycoprotein expression

Filovirus glycoprotein DNA selected for experiments were EBOV strain *Makona*, EBOV strain *Mayinga*, BDBV (codon optimized), SUDV *Gulu* (codon optimized) and MARV (**Table 16**).

Table 16. Filovirus glycoprotein sequences and proteins used in this work.

Name	Genus	Species	Strain	Conformation	GenBank or source	Ref.
EBOV GP Δ TM	<i>Ebolavirus</i>	<i>Zaire ebola virus</i>	<i>Makona</i>	trimeric	KJ660347	(Sylvain Baize et al., 2014)
EBOV GP Δ MLD Δ TM	<i>Ebolavirus</i>	<i>Zaire ebola virus</i>	<i>Makona</i>	trimeric	KJ660347	(Sylvain Baize et al., 2014)
EBOV sGP	<i>Ebolavirus</i>	<i>Zaire ebola virus</i>	<i>Makona</i>	dimeric	KJ660347	(Sylvain Baize et al., 2014) (Bukreyev, Volchkov, Blinov, & Netesov, 1993)
EBOV GP Δ TM <i>Mayinga</i>	<i>Ebolavirus</i>	<i>Zaire ebola virus</i>	<i>Mayinga</i>	trimeric	AF086833.2	(A. I. Flyak et al., 2016)
BDBV GP Δ TM	<i>Ebolavirus</i>	<i>Bundibugyo ebolavirus</i>	<i>Uganda</i>	trimeric	FJ217161	(Sanchez & Rollin, 2005)
SUDV GP Δ TM	<i>Ebolavirus</i>	<i>Sudan ebolavirus</i>	<i>Gulu</i>	trimeric	AY729654.1	
MARV GP Δ TM	<i>Marburg-virus</i>	<i>Marburg marburgvirus</i>		trimeric	Becker Lab, Phillips University, Marburg	

All constructs were modified to contain a GCN4 trimerization domain for complex formation (except sGP), His-Tag for purification and Avi-Tag for labeling (Corti et al., 2016). Full length EBOV strain *Makona* GP in pCAGGS backbone (pCAGGS-EBOV_GP_C7_Gueckedou-Xmal-NotI) was provided by Prof. Stephan Becker, Phillips University, Marburg and served as a starting point for cloning constructs containing different variants of glycoproteins. Vector maps are shown the Appendix (**Fehler! Verweisquelle konnte nicht gefunden werden., p.Fehler! Textmarke nicht definiert.**).

pCAGGS-EBOV_GP_C7_Gueckedou-Xmal-NotI contained an AgeI restriction site (RS) within the EBOV GP1 sequence, and a NotI RS downstream of the transmembrane domain (TM), which were used to insert the fragment EBOV *Makona* GP Δ MLD Δ TM. The resulting plasmid was termed pCAGGS-EBOV-Makona_GP Δ MLD Δ TM and lacked the mucin-like domain (MLD; Δ 313-464) and the TM (Δ 651-676). It contained C-terminal GCN4, His- and Avi-Tags.

A similar construct, additionally harboring the MLD but lacking the TM (Δ 651-676; (pCAGGS-EBOV_GP Δ TM) was cloned by digesting pCAGGS-EBOV-Makona_GP Δ MLD Δ TM

with restriction enzymes AgeI and AflIII, followed by insertion of a fragment spanning the AgeI RS, EBOV FFM GP Δ TM and GCN4 until the RS AflIII.

The construct containing sGP should not contain a trimerization domain as sGP forms homodimers. Additionally, sGP is the main product resulting from gene expression and contains a 7A sequence. Therefore, fragment AgeI-EBOV sGP was designed to contain 7 alanines in contrast to GP constructs with 8 alanines that are the result of transcriptional editing. The fragment AgeI-sGP-His-Avi was introduced by AgeI and NotI into the digested and purified pCAGGS-EBOV-Makona_GP Δ MLD Δ TM. Wild-type fragments of EBOV *Mayinga* GP Δ TM and MARV GP Δ TM, as well as codon optimized fragments of BDBV GP Δ TM and SUDV GP Δ TM sequences (**Table 16**) were designed to be flanked with RS 5'EcoRI and 3'NotI restriction sites and ordered at Eurofins. By restriction digest of pCAGGS-EBOV_GP Δ TM, they were subcloned into pCAGGS backbone resulting in the plasmids pCAGGS-EBOV-Mayinga_GP Δ TM, pCAGGS-MARV_GP Δ TM, pCAGGS-BDBV_GP Δ TM, pCAGGS-SUDV_GP Δ TM, respectively.

2.2.1.12.2 Surface expression of Ebolavirus GP-specific antibodies

Constructs allowing the expression of anti-Ebolavirus GP-specific antibodies on the surface of transfected cells should be cloned. After transient transfection into HEK293T cells, these could be used as a model recapitulating EBOV-specific B cells and their binding to produced glycoproteins. Previously reported human EBOV-specific antibodies targeting different epitopes on the Ebolavirus GP were selected for this experiment. These were KZ52 (Maruyama et al., 1999), mAb114, mAb100 (Corti et al., 2016), ADI-15758, ADI-15999, and ADI-16037 (Bornholdt et al., 2016). This approach ensured that produced glycoproteins were suitable to be used for single cell sorts of specific B cells.

pMX-PG16-mCherry plasmid harboring a platelet-derived growth factor receptor (PDGFR) transmembrane domain TM and the reporter protein mCherry was provided by Florian Klein and served as starting point to clone plasmids. pMX-PG16-mCherry originated from a pDisplay vector and contained a leader sequence, the HIV-specific PG16 antibody light chain variable and constant regions, self-cleaving F2A signal, a second leader sequence, PG16 heavy variable and constant regions and C-terminal myc-Tag and PDGFR TM domain (Gaebler et al., 2013). Because suitable restriction sites were missing at required positions or were present on the vector multiple times, variable regions could not be exchanged to other sequences easily. To this end, it was necessary to excise the fragment spanning the light chain leader sequence to PDGF TM domain and assemble vectors *de novo*. In an attempt to allow linearization of pMX backbone without excision of complete insert and to allow future exchange of antibody variable regions, a fragment called backbone-BamHI-NotI was designed. This fragment contained pMX backbone sequence downstream of BamHI restriction site, a leader sequence, a novel SgrAI restriction site followed by heavy chain constant region, myc-Tag and PDGF TM, and 3' NotI restriction site. In the first part of heavy constant region, a novel AfeI restriction site was included via a non-coding

mutation. For introduction of novel restriction sites sequences were selected that were neither present in other parts of the pMX backbone nor any of the antibody sequences to be introduced. Thereby, digestion with SgrAI and AfeI should allow the simple exchange of antibody variable sequences.

The fragment “backbone-BamHI-NotI” described above, was ordered at Eurofins. Both pMX-PG16 and backbone-BamHI-NotI were digested with restriction enzymes BamHI and NotI. Thereby, pMX was linearized and PG16 sequence excised. Digested vector was separated by gelelectrophoresis and empty pMX was recovered from gel. Backbone-BamHI-NotI purified from digestion reaction directly. By ligation of purified nucleic acids, plasmid “pMX-backbone-BamHI-NotI” was obtained, transformed into *E. coli*, presence of insert validated by Colony PCR using primers “fwd PMX upstr BamHI” and “rev PDGF myc heavy constant”. Plasmid DNA of colony containing insert was purified by midi preparation and sequenced.

During digestions of pMX-backbone-BamHI-NotI with SgrAI it became obvious, that the enzyme had star activity and cut the vector in two additional positions. Star activity could neither be prevented by shorter digestion time nor reduced enzyme amount. This made linearization by this enzyme unfeasible. Therefore, cloning strategy had to be changed in order to introduce light chain variable and constant regions. As an alternative, antibody light and heavy chain regions should now be introduced into pMX-backbone-BamHI-NotI by Gibson Assembly. Fragments and overhangs for assembly, as well as primers to create overhangs were designed online using the NEBuilder Assembly tool. Assembly of five fragments (**Table 17**) was carried out using the HiFi DNA Assembly Kit (NEB) according to manufacturer’s instructions and recommendations. Briefly, the first fragment was BamHI and AfeI digested vector, fragment two spanned vector downstream of BamHI to SgrAI. Fragments three and five were different for every construct and contained antibody light and heavy chains. Templates to amplify these were plgH, plgK and plgL expression plasmids. Fragment four contained the self-cleaving signal F2A and heavy chain leader and was amplified from pMX-PG16. Due to different sizes of fragments, ratios of fragments used for assembly was not equimolar.

Table 17. Fragments for Gibson Assembly of pMX-backbone-BamHI-NotI comprising distinct heavy and light chain variable and constant regions.

Fragment	Moles (pmol)	Size (nt)	Amount (ng)
pMX-backbone BamHI-NotI linearized by BamHI and AfeI	0.05	8302	270
Fragment BamHI-SgrAI	0.2	131	17
SgrAI-light chain	0.05	~700	22.75
F2A-IgH leader	0.2	137	17.8
Heavy chain variable-partial constant-AfeI	0.05	~500	16.25

Required volumes of fragments were mixed and filled up with H₂O to 10 µL. Next, 10 µL of NEBuilder Master Mix were added, the reaction was incubated at 50 °C for 60 min and 2 µL of the reaction used for transformation of *E. coli* DH5α. Correct assembly of all fragments was validated by Colony PCR using primers fwd seq primer upstr BamHI and rev seq primer downstr NotI. Annealing temperature was 58 °C and elongation time 2.5 min. PCR products of correct size were approximately 2.6 kb long. Mini preps were sequenced using primers fwd seq primer upstr BamHI, rev seq primer downstr NotI, fwd 2A-IgH leader and either fwd seq primer kappa constant or fwd seq primer lambda constant.

2.2.1.12.3 Reference antibody expression in plgH, plgK and plgL vectors

Table 18 shows previously reported human anti-EBOV GP-specific antibodies, which were used as references in this work.

Table 18. Previously reported human anti-EBOV GP-specific antibodies used as reference in this work.

Antibody	Source	Sequence information
Human anti-EBOV GP ADI-15758	(Bornholdt et al., 2016)	GenBank: KU602137-8
Human anti-EBOV GP ADI-15999	(Bornholdt et al., 2016)	GenBank: KU602605-6
Human anti-EBOV GP ADI-16037	(Bornholdt et al., 2016)	GenBank: KU602673-4
Human anti-EBOV GP mAb100	(Corti et al., 2016)	PDB: 5FHB
Human anti-EBOV GP mAb114	(Corti et al., 2016)	PDB: 5FHA
Human anti-EBOV GP KZ52	(Maruyama et al., 1999)	PDB: 3INU

2.2.1.12.4 Cloning and production of EBOV-specific mAbs in plgH, plgK and plgL vectors

Variable regions of human EBOV-specific antibodies KZ52 (Maruyama et al., 1999), mAb114, mAb100 (Corti et al., 2016), ADI-15758, ADI-15999, and ADI-16037 (Bornholdt et al., 2016) were ordered at Eurofins. Heavy chain fragments were digested with AgeI and Sall, and light chains with AgeI and BsiWI or AgeI and XhoI (all NEB) for kappa or lambda, respectively. Expression vectors plgH, plgK and/or plgL with heavy or light chain constant regions (Gaebler et al., 2013) were linearized with corresponding restriction enzymes. Fragments and vectors were purified (GeneJET Gel Extraction and DNA Cleanup Micro Kit, Protocol A, Macherey Nagel), assembled by ligation, and transduced into *E. coli* DH5α. 4-8 colonies per construct were evaluated to contain the variable region by Colony PCR and gel electrophoresis and forwarded to Sanger sequencing. Plasmids with correct antibody sequences were amplified by midi preparation (Macherey Nagel kit) according to manufacturer's protocol and stored at 4 °C (short term) or -20 °C. Antibodies were produced and purified as described below and served as reference antibodies throughout experiments.

Selected heavy and light chain variable antibody sequences from single cell analyses were cloned into mAb expression vectors by sequence- and ligation-independent cloning (SLIC) as previously described (von Boehmer et al., 2016). Briefly, amplicons for cloning were produced by PCR-

amplification using Q5 High Fidelity polymerase (NEB) by standard PCR protocols and previously described primers (Thomas Tiller et al., 2008). mAb expression vectors plgH, plgK and/or plgL (**Fehler! Verweisquelle konnte nicht gefunden werden.**) were linearized with restriction enzymes AgeI and Sall (for plgH), AgeI and BsiWI (for plgK) and AgeI and XhoI (for plgL), respectively. PCR products were purified (GeneJET Gel Extraction and DNA Cleanup Micro Kit, Protocol B, Macherey Nagel), cloned into expression vectors by SLIC reaction using T4 DNA polymerase (NEB) and transduced into *E.coli* DH5 α . Plasmid DNA was evaluated, amplified and stored as described above (Mini preparation, p.40).

Heavy and light chain-encoding plasmids were expressed in HEK293F cells, and proteins were harvested and purified as described below (Transfection of HEK293F cells, p.48ff.).

2.2.2 Cell culture

2.2.2.1 Human samples

2.2.2.1.1 Subjects and sample collection

rVSV-ZEBOV vaccinated (EV) individuals

rVSV-ZEBOV vaccinated (EV) individuals studied in this work were previously enrolled in the Phase I Trial to assess the safety, tolerability and immunogenicity of rVSV Δ G-ZEBOV-GP (**Table 9**; Clinical trial number NCT02283099) (Agnandji et al., 2016) and were vaccinated with either 3×10^5 or 3×10^6 pfu. An additional individual vaccinated with 2×10^7 pfu was enrolled. From this cohort, seven individuals (EV01-7) were enrolled in an observational study (INA; 16-054) at the University Hospital of Cologne. The protocol was approved by the Institutional Review Board (IRB) of the University of Cologne, Germany. From all participants, serum or plasma and EDTA-blood or leukapheresis samples were collected (**Table 19**) and peripheral blood mononuclear cells (PBMC) were purified by density gradient centrifugation using HistoPaque, washed three times, counted and stored at 10 to 50×10^6 cells/mL in FBS containing 10% DMSO (all Merck) at -150 °C. Serum and plasma samples were stored at -80 °C. All enrolled subjects provided written informed consent before participation in the study and all aspects of study conduct were in accordance with Good Clinical Practice. For reasons of time and cost-effectiveness, the majority of experiments has been performed for four individuals (EV01, 3, 4 and 5).

Ebolavirus disease survivor

Peripheral blood mononuclear cells (PBMCs) and serum samples from a convalescent EVD patient referred to as Frankfurt Patient (FP) were provided by Dr. Timo Wolf, University Clinics of Frankfurt (Wolf et al., 2015). PBMCs had been obtained by leukapheresis at three time points 46,

51, and 108 days after disease onset. Prior to sample collection, the patient had signed written informed consent and was twice tested negative for *Ebolavirus* RNA by PCR.

Serum samples of EVD patients were provided by Prof. Stephan Becker, Institute for Virology, Phillips University, Marburg.

2.2.2.1.2 Isolation of peripheral blood mononuclear cells (PBMCs)

PBMCs of vaccinated individuals were purified from large blood draw or leukapheresis and maintained on ice or at 4 °C during preparation. Cells were separated by density gradient centrifugation using HistoPaque. They were washed three times, counted and stored at 10 to 50 x 10⁶ cells/mL in FBS containing 10% DMSO (all Merck) at -150 °C.

2.2.2.1.3 Preparation of serum and plasma samples

EDTA-blood or fresh whole blood was spun at 2,000 x g for 10 min and aliquoted supernatant was stored at -80 °C.

2.2.2.2 Cultivation of cell lines

All human cell lines were cultivated in incubators exclusively used for cells of human origin at 37 °C and with 6% CO₂.

2.2.2.2.1 HEK293F cells

The suspension cell line HEK293F was maintained in flasks shaking at 110 rpm in FreeStyle Medium supplemented with 0.2% P/S. Cells were split every 2-3 days to have a concentration between 0.2-1 x 10⁶/mL.

2.2.2.2.2 HEK293T cells

Adherent HEK293T cells were cultivated in tissue culture treated petri-dishes with DMEN medium (DMEM supplemented with 10% FBS, 1% Antibiotic-Antimycotic, 1% Sodium pyruvate and 1% L-glutamine). Cells were passaged every 2-3 days. Plates were washed with PBS and incubated with Trypsin/EDTA at 37 °C for 2 min. Cells were further detached by tapping cell culture plates. To inactivate the enzyme, medium containing FBS was added to plates and cells resuspended and plates washed by pipetting. 3 x 10⁶ cells were seeded in 10 mL on 100 mm plates for passaging.

2.2.3 Protein biology

2.2.3.1 Protein expression

2.2.3.1.1 Transfection of HEK293F cells

At a concentration of 0.8×10^6 cells/mL HEK293F cells were transfected using 25 kDa polyethylenimine (PEI, Polysciences) with 1 μg DNA/mL cell suspension. Typically, 50 mL cultures were transfected for antibody production. 50 mL reaction tubes were prepared with 2.25 mL DPBS or 150 mM NaCl and 25 μg of heavy and light chain expression plasmids added, respectively. After briefly mixing, 170 μL of PEI solution (0.45 mg/mL) was added and samples heavily vortexed for 30-60 sec. Volumes were upscaled for increased culture volumes. Transfection mixes were incubated for 10 min at RT before droplet-wise addition to cells while carefully shaking culture flasks. After incubating for 7 days, supernatants were harvested, filtered (0.45 μm filter; Nalgene, Thermo Fisher Scientific), and stored at 4 °C or directly forwarded to protein purification.

2.2.3.1.2 Transfection of HEK293T cells

To prepare transfections, 10×10^6 cells were grown in 20 mL medium on 150 mm plates overnight. 2-4 h before transfection, medium was changed. Cells were transfected by standard calcium phosphate protocol. Briefly, for every 150 mm plate, 40 μg of DNA were added to H_2O . Then 3 mL of 2x HBS buffer were added followed by addition of 146 μL of 2.5 mM CaCl_2 . The transfection mix with a final volume of 6 mL was briefly vortexed and let rest for 2 min at RT, before droplet-wise addition to plates. Plates were carefully to distribute transfection reagent and medium was changed the next day.

2.2.3.2 Protein purification

Cell culture supernatants were always kept on ice or at 4 °C during purification and were exposed to cold buffers and solutions.

2.2.3.2.1 His-tagged proteins

Equal volumes of filtered transfection culture supernatant and 2x NPI-10 buffer were mixed and His-tagged glycoproteins were isolated using Protino Ni-NTA (nitrilotriacetic acid) agarose beads (Macherey Nagel). Briefly, 250 μL of beads per 100 mL transfection culture were washed with 10 mL PBS and centrifuged at 500 x g, 4 °C for 5 min with brakes switched off. Beads were incubated in cell culture supernatant and NPI-10 mix overnight at 4 °C while rotating. Beads were pelleted, carefully transferred into a sterile column equilibrated with PBS, washed with 1x NPI-10, and 1x NPI-20 1x buffers of 0.5x the volume of transfection culture. His-tagged glycoproteins were eluted by addition of NPI-100 buffer of 100x bead volume.

2.2.3.2.2 Antibodies

Purification of monoclonal antibodies from transfection cultures or total IgG from serum and plasma samples were conducted using Protein G sepharose beads (Sigma-Aldrich) according to manufacturer's protocol. For 50 mL transfection culture supernatant 200 μ L sepharose was prepared. Beads were washed with 10-40 mL PBS and spun at 500 x g.

2.2.3.3 Buffer exchange

Afterwards protein purification, buffer of eluates was exchanged to PBS using Amicon centrifugal filter units with molecular weight cut off (MWCO) of 30 kDa for GP Δ MLD Δ TM, GP Δ TM or antibodies, or MWCO of 10 kDa for sGP (Merck) according to protocol. Samples were always maintained on ice or 4 °C and washed with cold PBS. Briefly, centrifugal filters were equilibrated with PBS and centrifugation at 4,000 x g at for 2 min. Afterwards, eluates were applied to columns and spinned for 5-30 min. When volume was reduced to approximately 10%, columns were filled up with PBS and spun again. This was repeated two more times.

2.2.3.4 Gel electrophoresis

Protein expression was monitored via gel electrophoresis using NuPAGE 4-12% Bis-Tris protein gels. Briefly, gels were installed in horizontal gel chamber and filled with 1x MOPS buffer. Transfection culture supernatants or purified protein were supplemented with 4x LDS sample buffer, if required 10x sample reducing agent, and H₂O to a final volume of 25 μ L. Subsequently, samples were boiled at 70 °C for 10 min and transferred to gel. To evaluate protein size, 1 μ L PageRuler Plus Prestained Protein ladder were loaded onto gel. Empty gel lanes were filled with 4 μ L LDS sample buffer to prevent broadening of sample lane width during migration. Electrophoresis was performed at 200 V for approximately 45 min.

2.2.3.5 Silver staining

Bis-Tris gels were released from plastic frames and proteins stained using Pierce silver stain kit according to manufacturer's protocol. All washing steps were repeated twice by 5 min incubation in H₂O if not indicated differently. First, gel was transferred to emptied 10 μ L pipette tip box and washed. Afterwards, gel was incubated in fixation solution for 15 min twice or overnight. Gel was twice washed in 10% ethanol for 5 min, followed by regular washing steps. For 1 min gel was incubated in sensitizer working solution, washed with H₂O for 1 min twice, and stained for 30 min in stain working solution. Gel was shortly rinsed with H₂O and incubated in developer working solution until bands at expected sizes were clearly visible. Immediately, solution was removed, and reaction stopped using stop solution.

2.2.3.6 Protein quantification

Protein concentration was determined by measuring absorption at 280 nm using a NanoDrop One spectrophotometer. PBS was used as blank.

2.2.3.7 Protein modification

For downstream experiments, proteins were chemically conjugated to fluorophore or biotin. Afterwards, buffer was exchanged to PBS and proteins were stored at -80 °C

2.2.3.7.1 Conjugation to fluorophore

Glycoproteins were conjugated to DyLight 488 (Microscale Antibody Kit, Thermo Fisher Scientific) for flow cytometry experiments according to protocol. After labeling reaction buffer was exchanged to PBS and protein and fluorophore concentration determined via NanoDrop.

2.2.3.7.2 Conjugation to biotin

Antibodies were biotinylated using EZ-Link Sulfo-NHS-Biotin (Thermo Fisher Scientific) according to manufacturer's instruction for competition ELISAs. Buffer was exchanged to PBS after reaction.

2.2.3.8 Protein analysis

2.2.3.8.1 Enzyme-linked immunosorbent assay (ELISA)

ELISAs were performed for all produced monoclonal antibodies and serum IgG. Briefly, high binding assay plates (Corning) were coated with 50 µL of 2.5 µg/mL glycoprotein overnight at 4 °C. Plates were washed (Tecan or manually) 3x with 200 µL PBST and blocked with 200 µL blocking buffer for 1-1.5 h at RT. After 3x washing, plates were incubated with serial dilutions of antibodies or sera. Starting concentrations were 10 µg/mL for antibodies and 1 mg/mL for serum IgGs. Typically, dilution rows were prepared by 1:3 dilution with PBS in deep well plates (Sigma-Aldrich) to prepare volumes sufficient for testing reactivity against several glycoproteins in duplicates. Samples were incubated for 1.5 h at RT and washed 3x afterwards. Secondary goat-anti human IgG-HRP antibody (Jackson ImmunoResearch) was diluted 1:1000 in blocking buffer and incubated for 1 h at RT. Plates were washed 6x before addition of 150 µL ABTS (Thermo Fisher Scientific). Absorbance was determined as difference of 415-695 nm at several time points of development (Tecan).

2.2.3.8.2 Epitope determination

Competition ELISAs and peptide library analyses were performed by Matthias Zehner, Klein Lab to refine information of target epitopes of antibodies not binding to sGP and N-terminal part of GP1 and therefore unknown epitopes.

Competition ELISA

EBOV-specific antibodies were added to EBOV GP Δ TM-coated ELISA plates for 90 min in different concentrations. After washing, biotinylated (EZ-Link Sulfo-NHS-biotin, Thermo Fisher Scientific) competition mAbs (0.5 μ g/mL in blocking buffer) with known epitopes (ADI-15758, ADI-15999 (Bornholdt et al., 2016), KZ52 (Lee et al., 2008), and mAb100 (Corti et al., 2016)) were added for 45 min. For detection, HRP-conjugated streptavidin (1:8000; Thermo Fisher Scientific) in combination with ABTS reagent was used.

Peptide library

EBOV GP Δ TM was divided into 80 peptides with a length of 18 aa and an overlap of 10 aa. Peptides were synthesized by Thermo Fisher Scientific (PEPOTEC IMMUNO, Project BC100718.1) with an N-terminal acetylation and a C-terminal amidation. Peptides were dissolved in PBS, DMSO, or DMF, depending on their sequence characteristics. Peptides were stored at 5 mg/mL and diluted in PBS for ELISA plate coating (10 μ g/mL). ELISA was performed by Matthias Zehner, Klein Lab as described above with an antibody concentration of 30 μ g/mL.

Protein structure analysis

All methods for protein expression and structure analyses described below were performed by the Diskin Lab, Weizmann Institute, Israel.

For cloning, expression and purification of EBOV Ecto-domain for structural studies, the ectodomain of EBOV (PDB Seq ID: 5JQB_A) GP was chemically synthesized (Genscript) to eliminate the mucin-like region and to include a C-terminal trimerization domain of T4 fibrin (foldon) followed by a His-tag as previously reported (Y. Zhao et al., 2016). The truncated EBOV GP gene was subcloned into a modified pHLsec expression vector (BD Biosynthesis) and transfected using 40 kDa polyethylenimine (PEI-MAX; Polysciences) at 1 mg of plasmid DNA per 1 L of HEK293F cells (Invitrogen). To inhibit the formation of complex glycosylation, the mannosidase inhibitor kifunensine (Cayman Chemical) was added to a final concentration of 5 μ M. Media were collected after 6 days and supplemented with 0.02% (w/v) sodium azide and PMSF. Media were collected and buffer exchanged to TBS (20 mM Tris-HCl pH = 8.0, 150 mM sodium chloride) using a tangential flow filtration system (Merck Millipore). Protein was captured using a HiTrap IMAC FF Ni⁺² (GE Healthcare) affinity column followed by size exclusion chromatography (SEC) purification with a Superdex200 10/300 column (GE Healthcare).

Fabs of anti-EBOV GP-specific antibodies 3T0331 and 4m0368 were produced as described in chapters 2.2.3.1 and 2.2.3.2 with minor changes. PEI-MAX (Polysciences) was used for transfection and cell culture supernatants collected after 6 days of incubation. Antibodies were captured using protein-A affinity chromatography (Merck) and subsequently digested using Papain (Merck) with an enzyme to protein ratio of ~1:20 in 20 mM Cystein-HCl (Merck) and 10 mM EDTA pH 7.0. After digestion at 37 °C for 60 minutes. Fabs were separated from Fc

fragments by collecting the flow-through fraction from a protein-A column, followed by SEC on Superdex75 10/300 column. Fabs were mixed with EBOV ectodomain at a molar ratio of 1:2, and the complex was isolated by SEC on Superdex200 10/300.

Crystallization, data collection and structure determination of Fab 3T0331

Structural studies were performed by AG Diskin at the Weizmann Institute, Israel. Mosquito® crystallization robot (TTP labs) was used to set 60, 120, and 180 nL sitting drops of Fab 3T0331 (11 mg/ml) with 120 nL reservoir of commercially available crystallization screens. Crystallization hit for the Fab was identified using the PEGRx HT™ (Hampton). Crystals were obtained in 0.15M lithium sulfate monohydrate, 0.1M Citric Acid pH 3.5, 18% PEG 6000 at 20° C. Crystals were briefly soaked in mother liquor solution supplemented with 25 % ethylene glycol for cryo preservation before flash cooling in liquid nitrogen. X-ray diffraction data were collected at the European Synchrotron Radiation Facility (ESRF) at beamline ID23-2 using a Pilatus3 2M detector. Diffraction data were collected to a resolution of 1.56 Å. Images were indexed, integrated using Xia2 (Winter, 2010), and scaled using Aimless (Evans & Murshudov, 2013a). A molecular replacement solution was found using Phaser (McCoy et al., 2007) with a single Fab in the asymmetric unit, and the model was built and refined in an iterative manner using Coot (Emsley et al., 2010) and Phenix refine (Adams et al., 2010).

Cryo-EM image acquisition, data processing, and model building

Structural studies were performed by AG Diskin at the Weizmann Institute, Israel. Complexes of EBOV / Fabs (0.4 mg/ml) were applied to a glow-discharged C-flat 2/1-3Cu-50 holey carbon grids (EMS) and plunge frozen in liquid ethane, using ThermoFisher Vitrobot™ plunger (2.5 s blotting time, 100% humidity). Cryo-EM data were collected on a Titan Krios electron microscope (FEI) operated at 300 kV. Coma-free alignment was performed with AutoCTF (FEI) and beam size was 2.2 μM. Movies were recorded on a falcon 3EC direct detector (ThermoFisher). Movies were collected in super-resolution counting mode at a nominal magnification of 96,000X corresponding to a physical pixel size of 0.85 Å. The total dose rate was set to 1 electron per physical pixel per second and the total exposure time was 29.6 seconds, resulting in an accumulated dose of 40 electrons per Å². Each Movie was fractionated into 39 frames of 0.76 s. Nominal defocus range was -0.5 to -2.3 μM. A total of 437 and 723 movies were recorded to EBOV GP/3T0331 and EBOV GP/4m0368, respectively.

The entire data processing was conducted using the cryoSPARC V2 suite (Punjani et al., 2017). Movies were motion-corrected and contrast transfer functions were fitted using CTFFIND4 (Rohou & Grigorieff, 2015). Templates for auto picking were derived by 2D classification of manually picked particles. Following template-based autopicking a total of 109,407 and 123,880 good particles were selected for reconstruction of EBOV GP/3T0331 and EBOV GP/4m0368, respectively based on iterative reference-free 2D classifications. Initial reference maps were

calculated using Ab-initio reconstruction and high-resolution maps were obtained using the non-uniform 3D refinement, while imposing C3 symmetry. Working maps were locally filtered after calculating local resolution estimates.

Models of EBOV GP/3T0331 and EBOV GP/4m0368 were assembled by rigid-body fitting the crystallographic structure of EBOV GP (PDB: 5JQ3; (Y. Zhao et al., 2016) into electron density maps using UCSF chimera (Pettersen et al., 2004) as well as of the V_HV_L portions from crystallographic structure of 3T0331 and from a computationally modeled 4m0368. The later structure was modeled using the ABpredict tool (Norn et al., 2017). Both structures were then refined using the Phenix real-space refinement tool (Adams et al., 2010) and manually fitted into electron density maps using Coot (Emsley et al., 2010) in an iterative process.

2.2.4 Cellular assays

2.2.4.1 Analysis of cell surface-expression of anti-EBOV GP-specific antibodies as a model of EBOV GP-specific B cells to test EBOV GP Δ TM

HEK293T cells were transfected with pMX-anti-Ebolavirus_GP_antibodies-mCherry constructs that were cloned and transduced as described in chapter 2.2.3.1. An empty pMX-mCherry plasmid was used as control. Cells were harvested 1-2 days post transfection, suspended in PBS (Gibco) with 2% FBS (Merck) and 2 mM EDTA (Thermo Fisher Scientific) and subjected to fluorescence staining with 4',6-Diamidino-2-phenylindole (DAPI; Thermo Fisher Scientific), anti-huIgG-APC (BD), and EBOV GP Δ TM labeled with DyLight 488 (Microscale Antibody Kit, Thermo Fisher Scientific). Cells were stained for 20 min at 4 °C, washed, separated through cell strainer (Corning), and binding of GP Δ TM to anti-EBOV GP-specific cells was assessed by flow cytometry with FACS Aria Fusion (Becton Dickinson).

2.2.4.2 Isolation of anti-Ebolavirus glycoprotein-specific B cells

2.2.4.2.1 Isolation of CD19+ B cells

PBMCs were transferred to portable box containing liquid nitrogen and one vial at a time thawed in the 37 °C water bath for 1 min. Cells were immediately transferred to a 50 mL reaction tube on ice filled with 40 mL RPMI to dilute DMSO contained in freezing media in order to prevent cell damage. Not more than five vials of frozen cells were transferred to the same 50 mL reaction tube. Cells were spun and supernatant discarded. Thawed PBMCs were handled on ice all the time and centrifugation steps were carried out at 400 x g, 5 min, 4 °C. Frozen cell pellets were resuspended in RPMI medium. Viable cells were counted in trypan blue and cells pelleted. Cells were resuspended in 80 μ L MACS buffer per 10^7 cells and incubated with 6 μ L CD19 MicroBeads (Miltenyi Biotec) per 10^7 cells on ice and in the dark for 20 min. Meanwhile, MACS LS separation columns (Miltenyi Biotec) were installed in a QuadroMACS separator attached to a MACS

MultiStand (both Miltenyi Biotec). Cells were washed and samples transferred to columns following equilibration with MACS buffer. Sample migrated through columns by gravity flow. A part of negative fraction was collected and kept on ice. Columns with retained cells were washed three times by applying 3 mL MACS buffer. Finally, CD19+ cells were isolated adding 5 mL MACS buffer, removing LS columns from magnet and quickly putting on 15 or 50 mL reaction tubes. Cells were eluted by pressure exerted by stamp and counted.

2.2.4.2.2 Isolation of CD20+IgG+GP+ B cells

B cells were spun and suspended in PBS (Gibco) with 2% FBS (Merck) and 2 mM EDTA (Thermo Fisher Scientific) and subjected to fluorescence staining with DAPI (Thermo Fisher Scientific), anti-huCD20-Alexa Fluor 700 (BD), anti-huIgG-APC (BD), and EBOV GP Δ TM-DyLight 488 (Microscale Antibody Kit, Thermo Fisher Scientific). Cells were stained for 20 min at 4 °C and live CD20+ IgG+ EBOV GP+ cells were sorted using a FACSAria Fusion (Becton Dickinson) in a single cell manner into 96-well plates. All wells contained 4 μ L lysis buffer (0.5x PBS, 0.5 U/ μ L RNasin (Promega), 0.5 U/ μ L RNaseOUT (Thermo Fisher Scientific), and 10 mM DTT (Thermo Fisher Scientific), After sorting, plates were immediately stored at -80 °C until further processing.

2.2.4.2.3 Cell lysis and reverse transcription

Procedure for PCR amplification was performed as previously described (T. Tiller et al., 2008; von Boehmer et al., 2016) but with various adjustments (Kreer, Doring, et al., 2020). Briefly, Random Hexamers (Invitrogen), NP-40, and RNaseOUT (Thermo Fisher Scientific) were added to sorted cells in lysis buffer. The reaction was incubated for 1 min at 65 °C and cooled down for at least 2 min on ice. Afterwards, 1 x Superscript IV RT buffer, 50 U/rxn SuperScript IV Reverse Transcriptase, dNTPs, DTT, RNaseOUT (all Thermo Fisher Scientific) and RNasin (Promega) were added and incubated 10-15 min at RT, 10 min at 50 °C and 10 min at 80 °C.

2.2.4.2.4 Semi-nested PCR of single cells

cDNA of CD20+ IgG+ EBOV GP+ B cells was used to amplify light and heavy variable regions using PlatinumTaq HotStart polymerase (Thermo Fisher Scientific) according to manufacturer's protocol with 6% KB extender and 4 μ l cDNA template. Amplification was achieved by sequential semi-nested PCRs using optimized and newly developed primer sets for heavy (1st PCR: fw: 5' Opt5 Mix, rv: 3' Cg-RT (Ozawa et al., 2006), 2nd PCR: fw: 5' Opt5 Mix, rv: 3' IgG-Internal (T. Tiller et al., 2008), kappa (1st PCR: fw: 5' LVk Mix, rv: 3' Ck 543 (T. Tiller et al., 2008), 2nd PCR: fw: 5' LVk Mix, rv: 3' Ck 494) and lambda (1st PCR: fw: 5' LV λ Mix, rv: 3' C λ (T. Tiller et al., 2008), 2nd PCR: fw: 5' LV λ Mix, rv: 3' *Xho*I C λ) chain variable regions as described earlier (Kreer, Doring, et al., 2020). The results of the PCRs were analyzed by gel electrophoresis and products of correct sizes were subjected to Sanger sequencing.

2.2.4.3 Neutralization assay

Neutralization assays were performed by members of the Becker Lab in the BSL-4 laboratory of the Institute of Virology, Philipps-University Marburg, Germany. Briefly, sera or antibodies (starting at a dilution of 1:8 [sera] or a concentration of 100 µg/ml [antibodies]) were serially diluted in 96-well culture plates in Dulbecco's Modified Eagle's Medium (DMEM, Thermo Fisher Scientific) supplemented with 2% fetal calf serum, penicillin (50 units/ml), streptomycin (50 µg/ml) and L-glutamine (2 mM). 100 TCID₅₀ units of live EBOV strain *Mayinga* (GenBank: NC_002549) were added to the serum or antibody dilutions. Following incubation at 37 °C for 1 hour, Vero C1008 cells (ATCC® CRL-1586™; 10⁴ cells/well) were added. Plates were then incubated at 37 °C with 5% CO₂ and cytopathic effects (CPE) were evaluated at day 7 post infection. Neutralization was defined as clear reduction of CPE in wells containing serum or antibody dilutions compared to positive controls. Neutralization titers were calculated from four replicates as geometric mean titers for sera (GMT; reciprocal value) or geometric mean concentrations in the case of monoclonal antibodies (GMC). The cut-off of the assay is determined by the first dilution of the respective serum or antibody.

2.2.5 Quantification and statistics

Flow cytometry analysis and quantifications were done by FlowJo10. EC₅₀ values, means and standard deviations of serum and antibody reactivities were calculated using GraphPad Prism (v7). Tests for significance were conducted using GraphPad Prism and R (R Core Team; 2018). The following statistical and bioinformatic calculations were performed by collaboration partners from the Pfeifer Lab at the University of Tübingen. Differences in survivor and rVSV-ZEBOV vaccinees (serum response and neutralization) were tested by unpaired t-tests.

Frequency increase of the 58 different V genes comparing EBOV GP Δ TM-specific B cell sequences and the IgG repertoire was analyzed by normalizing each data set (EBOV GP Δ TM-specific and IgG repertoire) on relative frequencies for each of the four vaccinees and computing the differences among relative frequencies. To test significance for the single V genes two data sets were generated: Set A including all four differences for the V gene of interest, and Set B including 57 differences, one for each other V gene, where the subject is chosen uniformly at random. On these two sets a one-sided Mann-Whitney U (rank sum) test was applied for determining whether set A is stochastically greater than set B. To account for the random sampling in the construction of set B, this setup was repeated 10³ times and the averaged resulting p values were used with $\alpha=0.05$ and Bonferroni correction for multiple testing. Frequency increase of V genes of EBOV neutralizing antibodies were tested for significance using a binomial test under the null hypothesis of equal V gene frequency, $\alpha=0.05$, and Bonferroni correction.

Sequence similarity of CDRH3 was determined by Geneious software using BLOSUM (BLOcks Substitution Matrix) with residue-specific and hydrophilic gap penalties (open gap penalty of 10,

extended gap penalty 0.2). The calculation of phylogenetic trees and sequence alignments were done with Geneious (v10). For comparing the heterogeneity of sequences within the same donor with that among different donors, pairwise alignment scores among all sequences were computed by needle (with default parameters) and grouped accordingly. The difference of both distribution of alignment scores was assessed with a Mann-Whitney-U test.

Sequence logo plots were generated with WebLogo3 (Crooks et al., 2004) followed by minor adjustments.

2.2.6 Sequence analyses

2.2.6.1 Ig heavy/light chain sequence analysis

A script for automated sequence quality check and generation of a table containing important sequence information was written by Christoph Kreer, Klein Lab. As a first step, sequencing chromatograms were filtered for a mean Phred score of 28 and a minimal length of 240 nt. Remaining sequences were annotated with IgBLAST (Ye et al., 2013) and trimmed to extract only the variable region from FWR1 to the end of the J gene. Base calls within the variable region with a Phred score below 16 were masked. The resulting table listed productivity information of resulting antibody chains (determined by presence or absence of stop codons and frameshifts), number of masked nucleotides and IgBLAST-extracted general information such as V, (D,) and J genes of heavy and light chains, CDR3 amino acid sequences and % germline identity and used for standardized evaluation of sequences. Script-detected stop codons and frameshifts were manually cross-validated by reviewing sequence chromatograms. Sequences for which no CDR3 amino acid hit was found in IgBLAST database, were manually forwarded to IMGT database and hits for CDR3 amino acid were entered into table. Following manual cross-validation, sequences with more than 15 masked nucleotides, stop codons, frameshifts, no hit in IgBLAST database or CDR3 amino acid hit were excluded from further analyses.

A second script written by Christoph Kreer, Klein Lab allowed automated identification of clonally related sequences that passed the quality check within single subjects. First, all productive heavy chain sequences of a particular subject were grouped by identical V_H genes. Next, the pairwise Levenshtein distance, which describes the minimal number of edits (deletions, insertions or exchanges) required to convert sequence A into sequence B, was determined for each CDRH3 pair. By dividing the Levenshtein distance by the total aa length of a CDRH3 (with respect to the shortest CDRH3 of the pair) multiplied by 100, a percentage could be calculated that describes the % identity of two CDRH3s A and B. Finally, an individual clone-number was assigned to sequence groups that matched the criteria of sharing the same V_H gene and having a minimal CDRH3 identity of 75%. 100 rounds of input sequence randomization and clonal assignment were performed and the result with the lowest number of remaining unassigned (non-

clonal) sequences was selected for downstream analyses. All clones were carefully cross-validated and, if suitable, clones were merged, split, and expanded or downsized by single sequences manually taking into account shared nucleotide mutations at same positions.

Following determination of clones within single subjects, sequences between individuals were compared using the same script with criteria as described above. Heavy chain sequences from distinct donors, that shared the same V_H gene and at least 75% CDRH3 identity (as determined by the Levenshtein distance divided by the length of the shorter CDR3Hs) were therefore assigned as clone by the script and were termed shared sequences. In the event that a shared sequence was additionally a member of a clone within its originating donor, all members from the respective intra-donor clone were assigned to the shared sequence group. Likewise, for the identification of the closest sequence pairs between different donors, pairwise Levenshtein distances for every shared sequence was calculated to all shared sequences from distinct donors and % identity calculated with respect to the shorter CDRH3 if applicable.

2.2.6.2 Unbiased B cell repertoire analyses

B cell receptor repertoire sequence data was generated by an unbiased template-switch-based NGS approach (Kreer, Doring, et al., 2020). In brief, 2.5×10^5 CD20⁺IgG⁺ B cells per donor were sorted and stored at -80 °C until further processing in a procedure comparable to sorts described in chapter 2.2.4.2.2 Isolation of CD20⁺IgG⁺GP⁺ B cells except cells were sorted in bulk and not stained with GP.

Lutz Gieselmann, Klein Lab isolated RNA with the RNeasy Micro Kit (Qiagen) using a QiaCube (Qiagen) instrument and generated cDNA by template-switch reverse transcription according to the SMARTer RACE 5'/3' manual (Takara/Clontech) with a self-designed template-switch oligo that includes an 18 nt unique molecular identifier (UMI). Heavy chain variable regions were amplified with an IgG-specific nested PCR and amplicons were used for library preparation and illumina MiSeq 2 x 300 bp sequencing.

2.2.6.2.1 NGS sequence processing

Raw read pre-processing was performed by Christoph Kreer, Klein Lab with an in-house pipeline primarily based on Python scripts, IgBLAST (Ye et al., 2013), Clustal Omega (Sievers et al., 2011), and the pRESTO toolkit (Vander Heiden et al., 2014). Raw reads were filtered for a mean Phred quality score of 25 and a mean read length of 250 bp. Unique molecular identifiers (UMIs) were extracted and IgBLAST was used to pre-annotate reads. Each read pair was annotated with its top V gene call, its UMI, and an additional 18 nt molecular identifier (MID) starting 12 nt after the framework region (FWR) 3. UMIs were grouped and sequences (referred to as „collisions“) were removed if they differed from the most abundant V gene call or had more than 1 nt difference to the remaining reads in their UMI group. We assumed that reads with the same V gene/MID and an UMI edit distance of 1 nt are more likely to represent RT, PCR, or sequencing errors within

the UMI than real different molecules. In order to rescue those erroneous UMIs, we re-grouped colliding reads and remaining single UMI reads by their MID and re-defined MID groups as the same UMI group, if they shared the same V gene and their UMI had no more than 1 nt difference. UMI groups were aligned with Clustal Omega and then collapsed to build consensus reads. Each base call was weighed by its quality (1 - error probability) and sums for different base calls were generated over each position to account for both, total abundance and the corresponding quality. The base with the highest sum was taken as the consensus base. Paired consensus reads were assembled to one sequence using pRESTOs AssemblePairs module with a minimal overlap of 6 nt. Assembled full-length sequences were annotated with IgBLAST and only productive sequences with full sequence annotation were kept for downstream analysis. V gene usage, CDR3 length and V gene germline identity distributions were determined from all final sequences without further collapsing.

2.3 List of contributions

Many people contributed to and co-worked with me on this project. Experiments I have not conducted alone or that were performed by others entirely are mentioned in the following: Invitations for participation in this project have been forwarded to rVSV-ZEBOV vaccinees by the Addo Lab and Saskia Borregaard from the Clinical Trial Center North, Eppendorf (see chapter 2.1.9). Medical consultations of study participants, blood draws and leukaphereses were conducted by Philipp Schommers and Henning Gruell. Human sample processing, i.e. PBMC, plasma and serum generation was executed together with Carola Ruping and Kanika Jain (see chapter 2.2.2.1). Single cell sorts and bulk sorting of B cells were assisted by M. Seda Ercanoglu or Kanika Jain (see chapters 2.2.4.2.2 and 2.2.6.2). Unbiased B cell repertoire analyses and NGS sequence processing were performed by Lutz Gieselmann and Christoph Kreer (see chapter 2.2.6.2). Statistical analyses were performed by the Pfeifer Lab, University of Tübingen and Christoph Kreer (see chapter 2.2.5). Sequences of single Ig heavy and light chains were analyzed in a standardized way using a computerized script developed by Christoph Kreer and manually checked and refined together with Matthias Zehner and Florian Klein (see chapter 2.2.6). Sequence logo plots and sequence similarity indexes were largely generated by Matthias Zehner (see chapter 2.2.5). For vaccinee EV03 and partially EV07, single cell PCR, sequencing, mini and midi preparation of plasmid DNA, Colony PCR and antibody production have been performed by Matthias Zehner. Glycoprotein cloning and production, flow cytometry HEK293T binding assays with EBOV GP-specific antibodies (see chapter 2.2.4.1) were performed together with Matthias Zehner. ELISAs were performed together with Matthias Zehner. Competition and peptide library ELISAs have been conducted by Matthias Zehner (see chapter 2.2.3.8.2). Throughout the project, Hanna Janicki supported DNA preparations, cell culture and protein production and purification. Neutralization assays have been performed by members of the Becker Lab, University of Marburg

(see 2.2.4.3). Cryo-EM methods have been conducted by the Diskin Lab, Weizmann Institute of Science (see chapter 2.2.3.8.2).

3 Results

The purpose of this doctoral thesis was to decipher the human antibody response to the rVSV-ZEBOV vaccination. As immunogenic component of this vaccine serves the Ebola virus glycoprotein (EBOV GP). Being the only molecule present on the viral surface, it is targeted by anti-Ebolavirus directed antibodies.

The first part of the results section describes the production and evaluation of GPs that were used for downstream experiments. The second part shows how the produced GPs were used to isolate EBOV GP-specific memory B cells from human peripheral blood mononuclear cells (PBMCs), which have been induced by rVSV-ZEBOV vaccination. Subsequently, it is described how heavy and light chain sequences of specific B cells have been identified, analyzed, cloned and produced as functional antibodies. Finally, binding and neutralization properties, target epitopes on the viral GP, autoreactivity and structural characteristics of these antibodies were comprehensively characterized.

3.1 Generation and validation of Ebola virus glycoprotein as a sorting bait

It has been found that a positive outcome of EVD is associated with the development of EBOV GP-specific antibodies (Baize et al., 1999; Maruyama et al., 1999). In order to identify such from human blood samples, we first sought to produce GP and ensure that it would closely recapitulate the structure and characteristics of native GP by several assays.

3.1.1 Glycoprotein cloning and production

To investigate the human B cell response to Ebolavirus glycoproteins, we first selected, cloned and produced Ebolavirus glycoproteins in a pCAGGS backbone as described in the methods section (chapter 2.2.1.12.1 Glycoprotein expression). Briefly, we amplified the EBOV GP ectodomain ($\Delta 651-676$), and introduced a GCN4 trimerization domain, to obtain GP in a formation as native as possible (**Figure 8A**). pCAGGS-EBOV GP Δ TM was transfected into HEK293F cells and protein production was monitored by Bis-Tris PAGE and silver staining (**Figure 8B**).

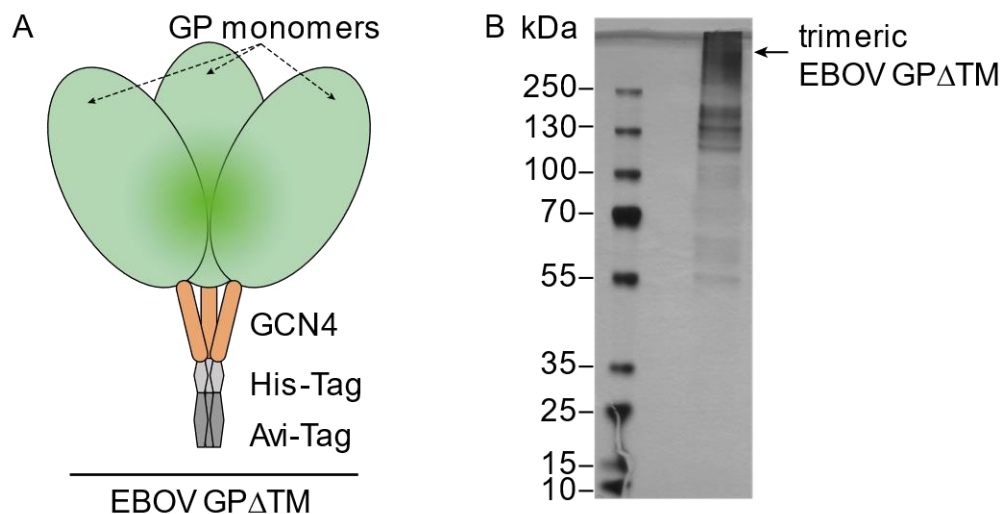


Figure 8. EBOV GP Δ TM scheme and silver staining of purified protein.

(A) Schematic representation of trimeric EBOV GP Δ TM. Three GP monomers (light green) are trimerized by GCN4 domain (orange) and carry C-terminal His-tags (light grey) and Avi-tags (grey). Protein is covalently conjugated to fluorophore DyLight 488 (green sphere). (B) Exemplary silver staining of purified protein. His-tagged protein was isolated from HEK293F cell culture supernatants using Ni-NTA affinity chromatography. Solvent of eluate was exchanged to PBS and the protein was separated by PAGE on native Bis-Tris gel and visualized via silver staining. The whole 350 kDa EBOV GP Δ TM trimer including glycans and MLD migrates at ~480 kDa (Beniac & Booth, 2017).

For later experiments characterizing cross-reactivity and target epitopes of antibodies, other GPs were cloned and produced (chapter 2.2.1.12.1 Glycoprotein expression and **Table 16**). Briefly, these were the dimeric EBOV *Makona* sGP and the trimeric EBOV *Makona* GP Δ MLD Δ TM originating from the same sequence as EBOV GP Δ TM, which is described in **Figure 8**. Binding to EBOV sGP or EBOV GP Δ MLD Δ TM served to identify mAbs that target the N-terminal part of GP1 or the MLD, respectively.

Additionally, we produced trimeric EBOV GP Δ TM of the closely related strain *Mayinga*, and trimeric GP Δ TM of the Ebolavirus species BDBV and SUDV, as well as trimeric GP Δ TM of the related Filovirus MARV.

3.1.2 Purified protein binds to previously reported anti-EBOV GP-specific antibodies in ELISA

Next, it should be verified that the His-tagged purified protein was in fact EBOV GP Δ TM. Therefore, we tested whether it binds to previously reported anti-EBOV GP antibodies with different target epitopes and affinities for GP. Six antibodies namely KZ52, mAb114, mAb100, ADI-15758, ADI-15999, and ADI-16037 were selected from publications (Bornholdt et al., 2016; Corti et al., 2016; Maruyama et al., 1999) and variable heavy (VH) and light chain (VL) regions were cloned into heavy (pIgH) and light chain expression vectors (pIgK and pIgL) harboring the

corresponding constant regions as described in the methods section (chapter 2.2.1.12.4 Cloning and production of EBOV-specific mAbs in plgH, plgK and plgL vectors). Pairs of expression vectors containing matching chains were co-transfected, antibodies were expressed and purified (chapter 2.2.3 Protein biology).

We coated the produced GP on ELISA plates and determined EBOV GP-specific antibody binding at 415 nm subtracted by background absorbance at 695 nm as described previously in the methods section (chapter 2.2.3.8.1 Enzyme-linked immunosorbent assay (ELISA)).

All antibodies tested here bound to the produced protein, verifying the presence of EBOV GP Δ TM (**Figure 9**). Importantly, the selected antibodies target different epitopes on GP (Bornholdt et al., 2016; Corti et al., 2016; Maruyama et al., 1999). The successful binding by all of them shows that epitopes of GP are structurally intact. Reference antibodies bound with varying potencies as evidenced by EC₅₀ values, with the most potent antibody being ADI-15758 with half-maximal binding at a concentration of 0.0118 μ g/mL. The obtained values correspond to those reported in original publications first describing these antibodies. The HIV-1-env-specific control antibody 3BNC117 was tested on initial assays and did not bind to EBOV GP Δ TM. The results were identical when binding of antibodies was tested against EBOV GP Δ TM labeled with DyLight 488, verifying that labeling did not influence availability of epitopes recognized by the tested antibodies (data not shown).

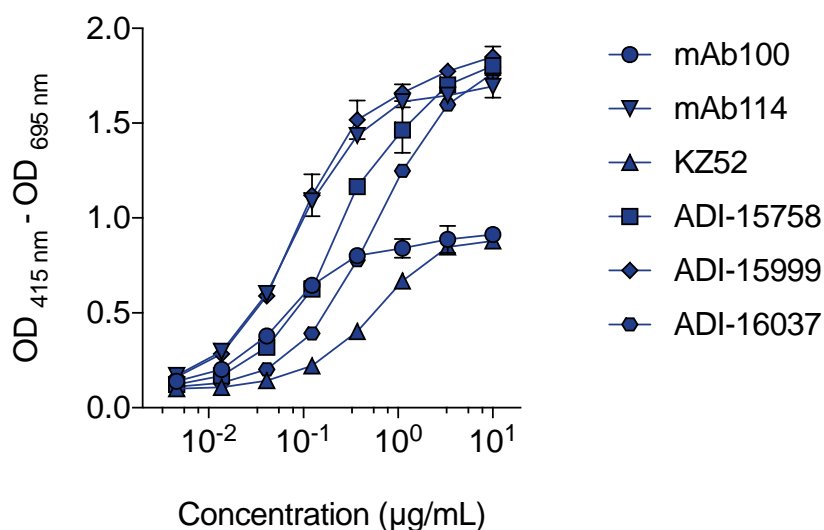


Figure 9. Reported EBOV GP-specific antibodies detect EBOV GP Δ TM in produced protein.

ELISA plates were coated with 2.5 μ g/mL of produced protein. Binding of reported anti-EBOV GP-specific antibodies was tested at starting concentrations of 10 μ g/mL in 1:3 dilutions. Shown are means and standard deviation of duplicates.

3.1.3 Produced GP is bound by HEK293T cells transiently expressing anti-EBOV GP-specific antibodies on their cell surface

In addition to ELISA assays, we tested the produced EBOV GP-DyLight 488 in a more advanced assay to ensure the presence of a variety of structural epitopes. This additional validation step minimized the risk of losing samples from vaccinated individuals. We established a flow cytometry-based assay as surrogate for GP-specific B cells as described in the methods section (chapter 2.2.1.12.2 Surface expression of Ebolavirus GP-specific antibodies). Briefly, sequences of six previously reported anti-EBOV GP-specific control antibodies KZ52, mAb100, mAb114, ADI-15758, ADI-15999 and ADI-16037 were cloned into pMX surface expression vectors and transiently transfected into HEK293T cells (**Figure 10A**). After expression, antibodies anchored within the cell membrane by a C-terminal PDGF receptor transmembrane domain and presented on the cell surface. The antibodies recognized diverse epitopes present on the native GPs. Precisely, these are i) a discontinuous epitope of base and internal fusion loop (IFL; mAb100), ii) a conformational epitope spanning GP1 and GP2 (KZ52), iii) the GP1 core (mAb114), iv) the GP2 stalk (ADI-15758, ADI-15999), v) and the glycan cap (ADI-16037), respectively. By flow cytometry, we examined whether the produced EBOV GP Δ TM bound to these EBOV GP-specific cells with distinct paratopes. The reporter protein mCherry served as a marker for successful transfection. A pMX-mCherry vector lacking an anti-EBOV GP antibody sequence served as a negative control for IgG expression and EBOV GP binding (**Figure 10**).

Morphological gates were set to define HEK293T cells in FSC-A vs. SSC-A dot plots (**Appendix Figure 2A**). Next, dead cells were excluded from further analysis by staining with 4',6-diamidino-2-phenylindole (DAPI) which can only migrate through damaged cell membranes (**Appendix Figure 2A**). Subsequently, viable mock-transfected HEK293T cells were visualized in an mCherry-reporting histogram in the PI (propidium iodide) fluorescence channel to define the PI signal threshold from untransfected mCherry-negative cells (**Appendix Figure 2**). Detection of an mCherry signal in the PI channel was indicative of a successful transfection. Percentages of mCherry-positive cells ranged from 46.6% to 60.9% in HEK293T cells transfected with antibody constructs (**Appendix Figure 2**). As positive transfection did not result in a separate population of mCherry-positive cells but rather a shift of the mCherry signal in mCherry histograms. To draw conclusions on the successful production of transfected antibodies and subsequent transport to cell membranes, we stained IgG on the surface of all mCherry-positive HEK293T cells transfected with one of the GP-specific antibodies by anti-IgG-APC staining, respectively (**Figure 10B** and **Appendix Figure 2B**). Finally, we analyzed binding of EBOV GP Δ TM-DyLight 488 to transfected cells by monitoring the FITC fluorescence channel (**Figure 10B**). The rightmost panel visualizes that the cells expressing anti-EBOV GP mAbs on their cell surface are binding to EBOV GP as evidenced by elevated FITC signals. In addition to EBOV GP Δ TM, for later experiments several additional GPs were produced and tested in this assay (**Appendix Figure 2**). These were EBOV

Mayinga GP Δ TM, EBOV *Makona* GP Δ MLD Δ TM, and EBOV *Makona* sGP. BDBV GP Δ TM, BDBV GP Δ TM, and BDBV GP Δ TM were also cloned and produced but their functionality could not be proven in this assay, as the available reference antibodies were not cross-reactive with these species.

We could show here that EBOV GP Δ TM is bound by cells transiently expressing anti-EBOV GP Δ TM-antibodies that recognize various epitopes. Therefore, we conclude that the produced GP is a suited to isolate EBOV GP-specific B cells with a broad range of epitopes and to study the total anti-EBOV GP B cell response in humans.

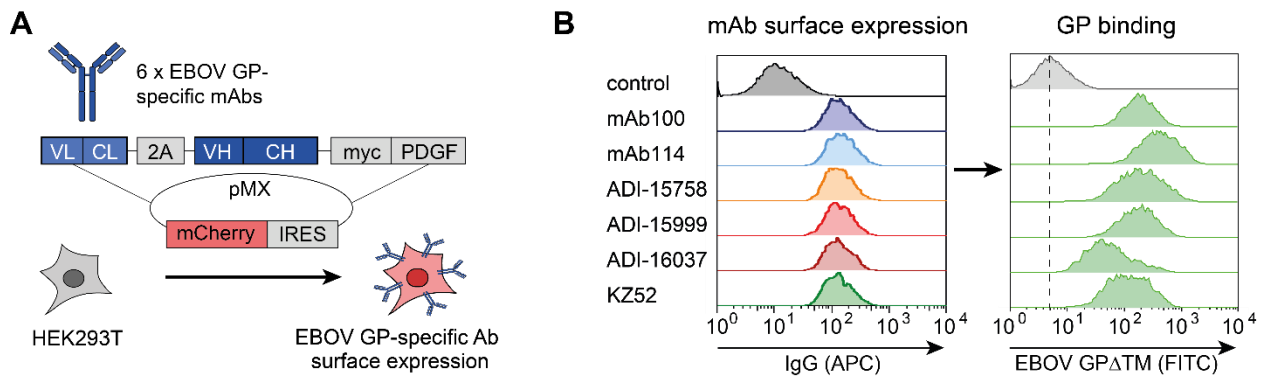


Figure 10. Test of EBOV GP constructs by surface expression of EBOV GP-specific antibodies.

(A) Generation of constructs for surface expression of EBOV-reactive antibodies (mAb100, mAb114, ADI-15758, ADI-15999, ADI-16037, and KZ52) on HEK293T cells. Variable and constant regions of immunoglobulin light (VL, CL) and heavy chains (VH, CH) were linked by a 2A self-processing signal sequence followed by a c-myc and a PDGF receptor-transmembrane domain. As control, an empty vector (pMX) containing an IRES-mCherry sequence was used. Plasmids were transiently transfected into HEK293T cells. (B) Flow cytometry analysis to evaluate EBOV GP Δ TM recognition by antibody-expressing HEK293T cells as a surrogate for anti-EBOV GP Δ TM-reactive B cells. Left: IgG expression evaluated by APC mean fluorescence intensity (MFI) of transfected cells. Right: EBOV GP Δ TM-DyLight 488 binding to surface expressed antibodies evaluated by FITC MFI. Dashed line indicates peak fluorescence intensity of no antibody vector control.

3.2 B cell immune response to rVSV-ZEBOV vaccination

After producing and testing different Ebolavirus GPs, we analyzed the rVSV-ZEBOV-induced antibody response in immunized subjects. Initially, we evaluated the total IgG response from serum against EBOV GP Δ TM. Hereafter, we used EBOV *Makona* GP Δ TM-DyLight488 to isolate EBOV GP-specific IgG-positive B cells on a single cell level and closely characterized these cells to decipher the rVSV-ZEBOV-induced B cell and monoclonal antibody response in humans for the first time.

3.2.1 Subjects and serum response

In order to analyze the sustainability of the human B cell response to rVSV-ZEBOV vaccination, we collected serum and PBMC samples from seven healthy individuals at 6 to 26 months after vaccination (**Figure 11A**). The age of participants ranged from 26 to 55 years (**Table 19**) and subjects were vaccinated with either 3×10^5 (EV01, EV02, EV04), 3×10^6 (EV03, EV05, EV06) plaque-forming units (pfu) of rVSV-ZEBOV (single intramuscular injection). Sera of all participants showed binding to EBOV glycoprotein (GP) in ELISAs, but with a significantly lower activity than serum samples of EVD survivors (**Figure 11B**).

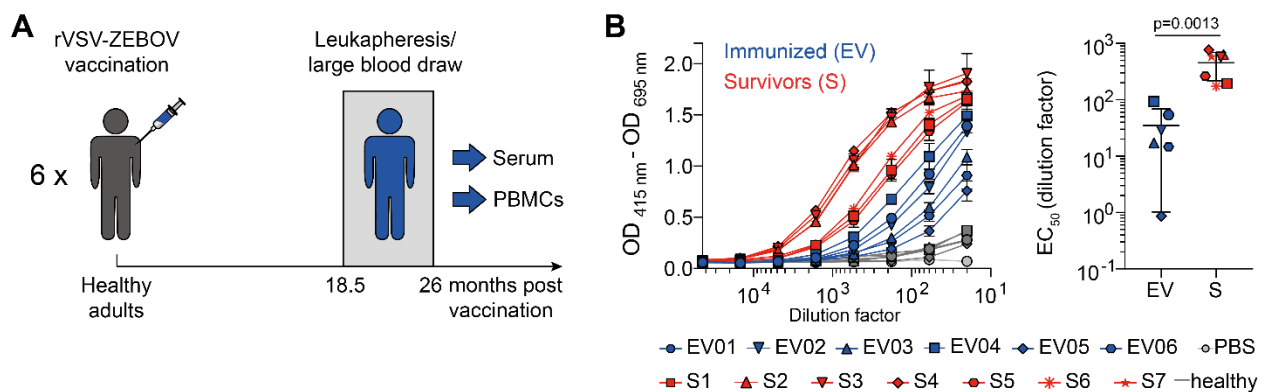


Figure 11. Sample collection of rVSV-ZEBOV-vaccinated individuals and serum reactivity to EBOV GP Δ TM (*Makona*).

(A) Sample collection from rVSV-ZEBOV-immunized donors (EV01-EV06) was performed between 18.5 to 26 months after single dose vaccination. Serum was collected and PBMC samples were obtained after leukapheresis or large blood draw. See also Table 19 for donor and vaccine dose information. (B) Serum reactivity to EBOV GP Δ TM (*Makona*) measured by ELISA in rVSV-ZEBOV-immunized subjects (blue) compared to EVD survivors (S1-S7, red, left panel). Mean dilution factors achieving EC₅₀ are 456 and 35 for vaccinees and survivors, respectively ($p=0.0013$, right panel). Error bars show standard deviation. PBS and healthy serum samples were used as negative controls. Significance was tested by an unpaired t-test.

Table 19. rVSV-ZEBOV-vaccinated subjects.

	EV01	EV02	EV03	EV04	EV05	EV06	EV07	Mean
Gender	female	female	male	male	male	male	male	71% male, 29% female
Age (years)	55	26	42	51	44	45	46	44
Sampling post immunization (months)	18.5	18.5	24	20.5	25	26	6	19.8
Vaccine dose (pfu)	3×10^5	3×10^5	3×10^6	3×10^5	3×10^6	3×10^5	2×10^7	n.a.
Sample type	PBMC, serum	PBMC, plasma	PBMC, serum	PBMC, serum	PBMC, serum	PBMC, serum	PBMC, serum, plasma	n.a.

EV = rVSV-ZEBOV-vaccinated subject; n.a. = not applicable; pfu = plaque forming units

3.2.2 Flow cytometric analysis and sort

After validating that the produced EBOV GP Δ TM-DyLight 488 is bound by anti-EBOV GP-specific expressing cells that recognize various epitopes, we set out to identify such cells in the aforementioned seven rVSV-ZEBOV-vaccinated subjects. CD19-enriched PBMCs were stained and incubated with EBOV GP Δ TM-DyLight 488 as described in the methods section (chapter 2.2.4.2.2 Isolation of CD20+IgG+GP+ B cells). The gating strategy for flow cytometric analysis of EV01-EV07 (in rows) is depicted in **Figure 12A**, with each column showing the following dot plot. For greater clarity, the number of depicted events in all pictograms was limited to 30,000.

Morphological gates were set to lymphocytes in an FSC-A vs. SSC-A dot plot. Next, we selected viable cells by gating DAPI-negative cells. Single cells were selected in an FSC-A vs. FSC-H dot plot. CD20- and IgG-positive cells were gated for final analysis of EBOV GP Δ TM-binding cells. Finally, viable, single CD20-, IgG- and EBOV GP Δ TM-positive cells were selected for single cell sorts. Between 0.25% and 0.65% of IgG-positive B cells in the different donors bound to EBOV GP Δ TM (**Figure 12A**, right column). A correlation between vaccine dose and frequency of EBOV GP-reactive B cells did not become apparent (**Figure 12** and **Table 19**).

Moreover, we cloned and produced an EBOV GP Δ TM that is also lacking the highly glycosylated mucin-like domain (EBOV GP Δ MLD Δ TM) and covalently labeled it with DyLight 488 (chapter 2.2.3.7.1 Conjugation to fluorophore). This protein should be tested as an alternative bait to isolate specific B cells from rVSV-ZEBOV-vaccinated donors (**Figure 8B**). The construct was designed for several reasons. Firstly, producing the highly glycosylated EBOV GP Δ TM was challenging, as the yields were low, while the production was costly. In contrast, the expression of EBOV GP Δ MLD Δ TM resulted in higher protein yield. Additionally, antibodies specifically

targeting the MLD portion of the EBOV GP are associated with poor antiviral effects. As assessed in a comprehensive study (Saphire, Schendel, Fusco, et al., 2018), MLD-targeting mAbs in general have poor neutralizing or protective characteristics. Finally, the highly glycosylated MLD is potentially shielding a large part of other GP-specific epitopes from the surface thereby escaping immune surveillance (Saphire, Schendel, Fusco, et al., 2018). Consequently, sorting EBOV GP-specific B cells from rVSV-ZEBOV-vaccinated individuals with a protein that comprises the MLD (i.e., EBOV GP Δ TM), could potentially influence the amount or the diversity of EBOV GP-specific antibodies that can be isolated. Producing a GP variant without the MLD domain might allow the isolation of a larger variety and higher percentage of effective antibodies. To test this, we decided to additionally isolate EBOV GP-specific B cells using EBOV GP Δ MLD Δ TM from one of the vaccinees. PBMCs of donor EV04 were selected as they had the highest frequency of EBOV GP-reactive B cells. The overall gating strategy can be seen in **Figure 12B**. After incubation with EBOV GP Δ MLD Δ TM, the frequency of EBOV GP-reactive IgG+ CD20+ B cells in EV04 was 0.57% and similar to the 0.62% detected after incubation with EBOV GP Δ TM. Therefore, from the sheer number of isolated cells it cannot be concluded that the presence of the MLD reduces the number of isolated antibodies.

To set the observations made for the vaccine-induced EBOV GP-specific B cells into a context, we compared the frequency of EBOV GP-reactive B cells in rVSV-ZEBOV-vaccinated individuals to those of a convalescent EVD survivor and donors that had never encountered EBOV GP antigen. These analyses served to set the frequency of EBOV GP-specific antibodies after rVSV-ZEBOV vaccination into a context between absent and prominent response.

PBMCs of a convalescent EVD survivor of the 2013-2016 West African epidemic were collected 51 days after disease onset. **Figure 12C** shows the last dot plot of the gating strategy with live, single, CD20+ IgG+ lymphocytes probed against EBOV GP Δ TM. In contrast to immunized donors, EBOV GP-reactive B cells were found more frequently in CD19-enriched PBMCs of the EVD survivor, that had 2.75% EBOV GP-reactive cells within the CD20+ IgG+ population. This is 4.4-fold to 11-fold higher compared to vaccinees. Of note, PBMCs of the survivor had been collected shortly after encountering EBOV, while PBMCs from vaccinees were obtained 2 years after immunization. These different time points of sample collection may have affected the observed frequencies of EBOV GP-specific B cells.

To determine the level of unspecific binding of EBOV GP Δ TM to CD20+ IgG+ cells, we moreover analyzed PBMCs of two donors, that had neither encountered EBOV GP by natural infection nor vaccination (**Figure 12D**). In such donors, in theory not a single IgG+ cell binding EBOV GP should be detected, as IgG+ B cells of a certain specificity can only be developed upon antigen recognition and isotype class switch from IgM/IgD constant regions. In the two non-immunized, non-EBOV-infected individuals, we observed 0.066% or 0.087% EBOV GP-specific CD20+ IgG+ cells. Precisely, 9 of 13721 or 39 of 44879 CD20+ IgG+ cells were EBOV GP-

reactive, respectively. These ratios define the background of unspecific EBOV GP-reactivity. These unspecific events make up for between 10.2% and 34.8% of the CD20+ IgG+ EBOV GP+ events from rVSV-ZEBOV vaccinees.

From the flow cytometric experiments, we conclude that rVSV-ZEBOV-induced B cells contain an EBOV GP-reactive population that is specific over background binding of EBOV GP to unspecific B cells. The frequency of this EBOV GP-specific B cell population, however, is lower in the here investigated single dose immunized donors than in a survivor of EVD.

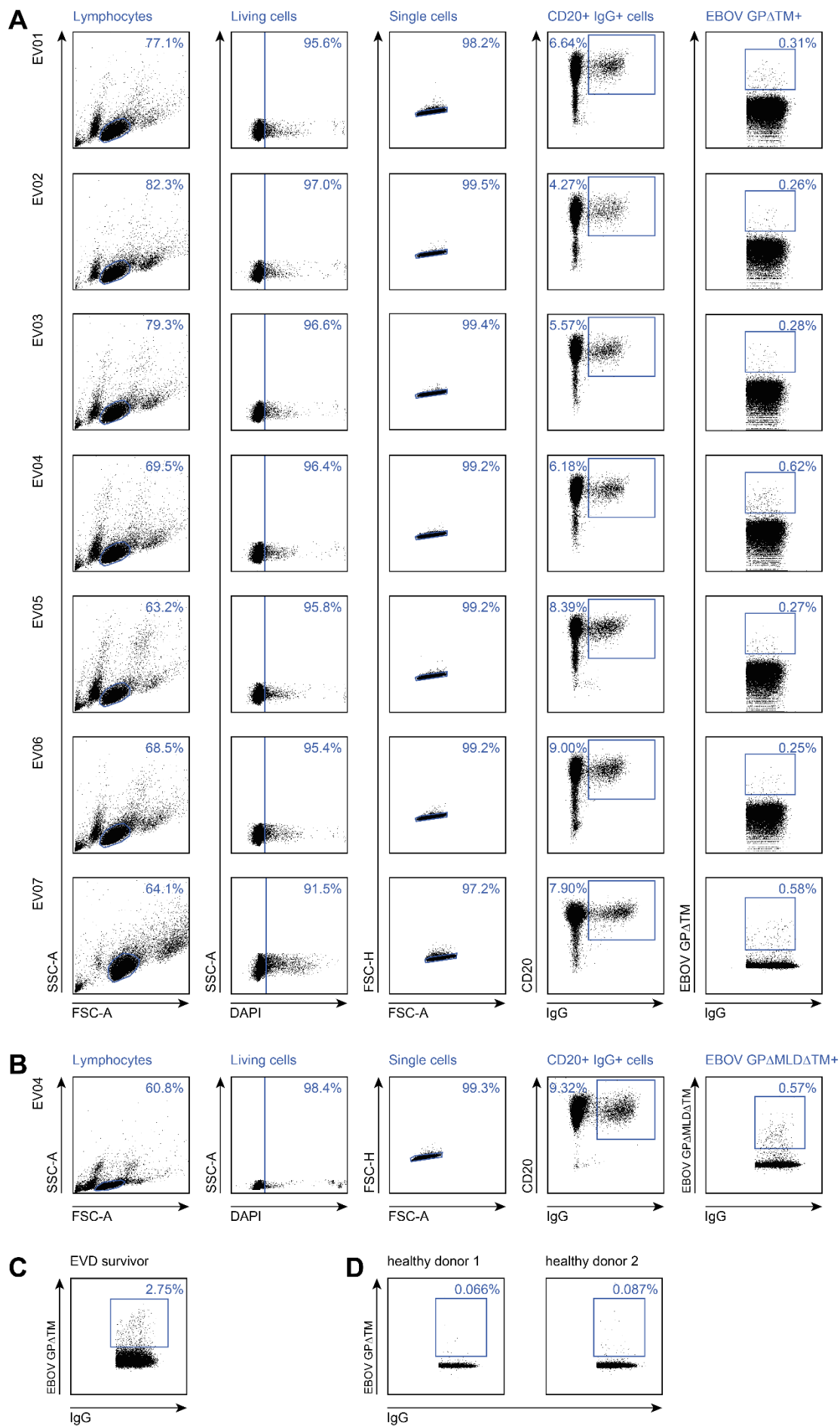


Figure 12. rVSV-ZEBOV vaccination induces EBOV GP-specific IgG+ B cells.

(A+B) Gating strategy for EBOV GP-specific B cells from rVSV-ZEBOV-vaccinated individuals. PBMCs of rVSV-ZEBOV-vaccinated donors (EV01-EV07; rows) were thawed, enriched for CD19+ cells by MACS, stained, and forwarded to flow cytometric analysis. Population of interest was determined by setting gates (across columns) for lymphocytes → live cells → single cells → CD20+ IgG+ cells. CD20+ IgG+ EBOV GP+ cells were selected for single cell sort. The EBOV GP used for sorts were (A) EBOV GP Δ TM comprising the MLD or (B) EBOV GP Δ MLD Δ TM lacking the MLD. (C+D) Frequency of EBOV GP-reactive B cells in a convalescent EVD survivor (C) and donors that did not encounter EBOV GP by infection or immunization (healthy donors; D). Dot plots show viable, single, CD20+, IgG+, lymphocytes and their reactivity to EBOV GP Δ TM. Sample preparation and gate setting as described for (A+B). Sample preparation and gating strategy were identical as for vaccinees.

3.2.3 Sequence analysis of EBOV GP-specific B cell receptors

For following in-depth single B cell and immunoglobulin (Ig) sequence analysis, we selected the isolated single cells of five subjects namely EV01, EV04 (vaccinated with 3×10^5 pfu), EV03, EV05 (vaccinated with 3×10^6 pfu), and EV07 (2×10^7 pfu rVSV-ZEBOV). We applied semi-nested PCR protocols using recently developed and highly effective multiplex primer sets (Kreer, Doring, et al., 2020) to amplify reverse transcribed cDNA of Ig heavy (V_H) and light chain variable ($V_{\kappa/\lambda}$) regions as described in the method section (chapter 2.2.4.2.3 Cell lysis and reverse transcription, 2.2.4.2.4 Semi-nested PCR of single cells). Of all five analyzed donors, in total 2735 B cells were processed and after a stringent quality check, 1,956 V_H and 269 $V_{\kappa/\lambda}$ remained. These sequences were closely evaluated for clonality, meaning that for every individual donor, we looked for pairs or groups of similar or identical sequences according to defined criteria (chapter 2.2.6.1 Ig heavy/light chain sequence analysis). If two or more individual B cells exhibited identical or similar BCRs, these cells are likely descendants of a common B cell progenitor and the result of clonal expansion after a B cell encountered their specific antigen, i.e. EBOV GP. Hence, the identification of clonal sequences in the here isolated cells is of high interest. Two or more sequences of the same donor were defined to be clonally related if they shared the V_H gene, if their CDRH3 identity was $\sim 75\%$ or higher, and CDRH3 length did not differ by more than 1 aa.

The analysis of V_H regions in the different donors revealed clonal origins for 25% to 46% of sequences (**Figure 13A**). Among the clonal sequences, we detected a highly polyclonal response in all subjects as all donors harbored many different clones. Precisely, we identified 49, 42, 51, 45, and 47 unique B cell clones for EV01, EV03, EV04, EV05, and EV07 respectively (**Figure 13B**). The size of pie chart slices is proportional to the number of members of a clone. Across donors, the majority of clones consisted of two or three members and expanded clones with more than ten members were rare. When comparing the distribution of sequenced heavy (IgH) and light chain (IgL) V gene families among all vaccinees, every identified clone was counted once, regardless of clone size (**Figure 13C**). Among vaccinees, we found comparable

distributions to different V genes. In heavy chains, genes of V gene family 3 were observed most frequently. In clonal EBOV GP-specific cells of all rVSV-ZEBOV-vaccinated individuals, the ratio of B cells using κ or λ light chains was between 1.35:1 and 1:3 in EBOV GP-specific B cell clones. The ratio is usually reported to be 2:1 in humans (Murphy, 2011), indicating a slight overrepresentation of λ light chains. The mean germline identity ranged from 90.5% to 93.7% for heavy and 94% to 95.9% for light chains (**Figure 13D**). In addition, only minor differences were detected for the average CDR3 length in amino acids (aa) of IgH (13 to 15 aa) and IgL (10 to 11 aa; **Figure 13D**).

As an alternative bait to EBOV GP Δ TM, the protein EBOV GP Δ MLD Δ TM was used to isolate EBOV GP-specific B cells from vaccinee EV04 (**Figure 13E-H**). While the frequency of EBOV GP Δ MLD Δ TM-specific IgG⁺ CD20⁺ B cells was similar as for EBOV GP Δ TM (**Figure 13A-D**), we now sought to take a closer look at the sequences isolated with this protein. Sequence analysis of obtained heavy and light chains revealed similar results as achieved with EBOV GP Δ TM. In 131 V_H regions that passed the quality control, we observed that 26% of sequences originated from clonally related B cells (**Figure 13E**). 71% of these clonal sequences had been identified in EBOV GP Δ TM-isolated sequences before and were therefore bait-independent clones (Clones GP Δ MLD Δ TM + GP Δ TM), and only 30% were exclusively identified after EBOV GP Δ MLD Δ TM sort (Clones GP Δ MLD only). Overall, the clonal sequences identified were also highly polyclonal (**Figure 13F**) and the distribution of V_H and V _{κ/λ} regions (**Figure 13G**), as well as germline identity and CDR3 lengths (**Figure 13H**) were comparable to those of clonal sequences obtained from the same donor by sorting with EBOV GP Δ TM. These results indicate that the majority of epitopes on GP is available to antibodies in the presence of the glycosylated MLD. Exemplary sequence information of identified sequences from EBOV GP Δ TM and EBOV GP Δ MLD Δ TM sorts of different donors are summarized in **Appendix Table 1** and **Appendix Table 2**, respectively. We conclude that rVSV-ZEBOV vaccination reproducibly elicits a highly polyclonal B cell response that shows convergent characteristics among vaccinees including V gene distribution, CDR3 lengths, and levels of somatic hypermutation (SHM).

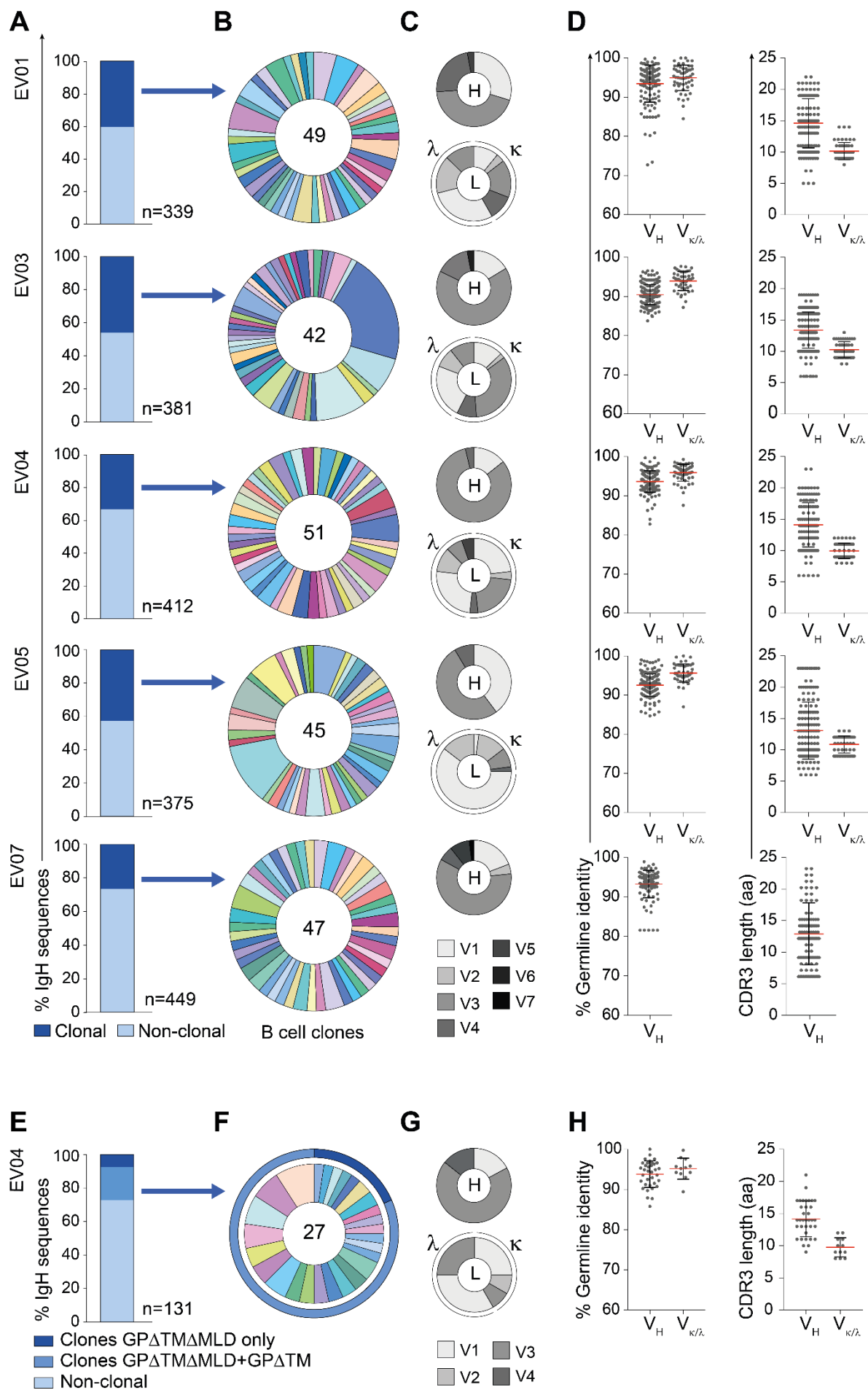


Figure 13. Deciphering the rVSV-ZEBOV-induced EBOV GP-specific B cell response.

(A-D) Sequence analysis of B cells isolated from rVSV-ZEBOV vaccinated individuals with EBOV GP Δ TM or (E-H) EBOV GP Δ MLD Δ TM. (A) Abundance of amplified high-quality clonal (dark blue) and non-clonal (light blue) immunoglobulin (Ig) sequences in sorted EBOV GP Δ TM-reactive IgG+/CD20+ B cells from rVSV-ZEBOV-vaccinated individuals (EV01, EV03-EV05, EV07). (B) Identified B cell clonotypes. Total number in the center of pie charts for each vaccinated individual. Each slice represents a unique B cell clone with the size proportional to the number of clonal members. (C) Distribution of V gene families in heavy (H, top) and light (L, κ/λ , bottom) chains of all unique clones. (D) Germline identity (left) and CDR3 aa lengths (right) of VH and V κ/λ of clonal sequences. Means are shown in red and SD in black. (E) Abundance of amplified high-quality clonal (Ig) sequences of clones exclusively identified by EBOV GP Δ MLD Δ TM (dark blue) or by both EBOV GP Δ MLD Δ TM and GP Δ TM (medium blue), and non-clonal (light blue) Ig sequences in sorted IgG+/CD20+ B cells from rVSV-ZEBOV-vaccinated individual EV04. (F) B cell clonotypes identified by sort with EBOV GP Δ MLD Δ TM. Total number in the center of pie chart. Each slice represents a unique B cell clone with the size proportional to the number of clonal members. The outer ring indicates, which clones were identified with only EBOV GP Δ MLD Δ TM (dark blue) or with both EBOV GP Δ MLD Δ TM and GP Δ TM (medium blue). (G) Distribution of V gene families in heavy (H, top) and light (L, κ/λ , bottom) chains of all unique clones. (H) Germline identity (left) and CDR3 aa lengths (right) of VH and V κ/λ of clonal sequences. Means are shown in red and SD in black.

3.2.4 Comparison of EBOV GP-specific population and total IgG B cell repertoire

The comparison of different sequence characteristics of EBOV GP-specific B cells revealed convergence in e.g., V gene distribution, CDRH3 aa length and V gene germline identity among the four different vaccinated individuals. Next, we wanted to examine whether the observed values can specifically be attributed to EBOV GP-specific B cells or are found generally in the B cell repertoire of the same donors. To answer this question, we isolated IgG-positive B cells from vaccinees without selecting for antigen-specificity and performed next generation sequencing analyses.

The gating strategy is depicted in **Figure 14**. Similarly to previously described sorts, we enriched CD19 cells from PBMCs of the four vaccinated individuals EV01, EV03, EV04 and EV05 and performed bulk sorts of total IgG-positive B cells in absence of EBOV GP (chapter Unbiased B cell repertoire analyses).

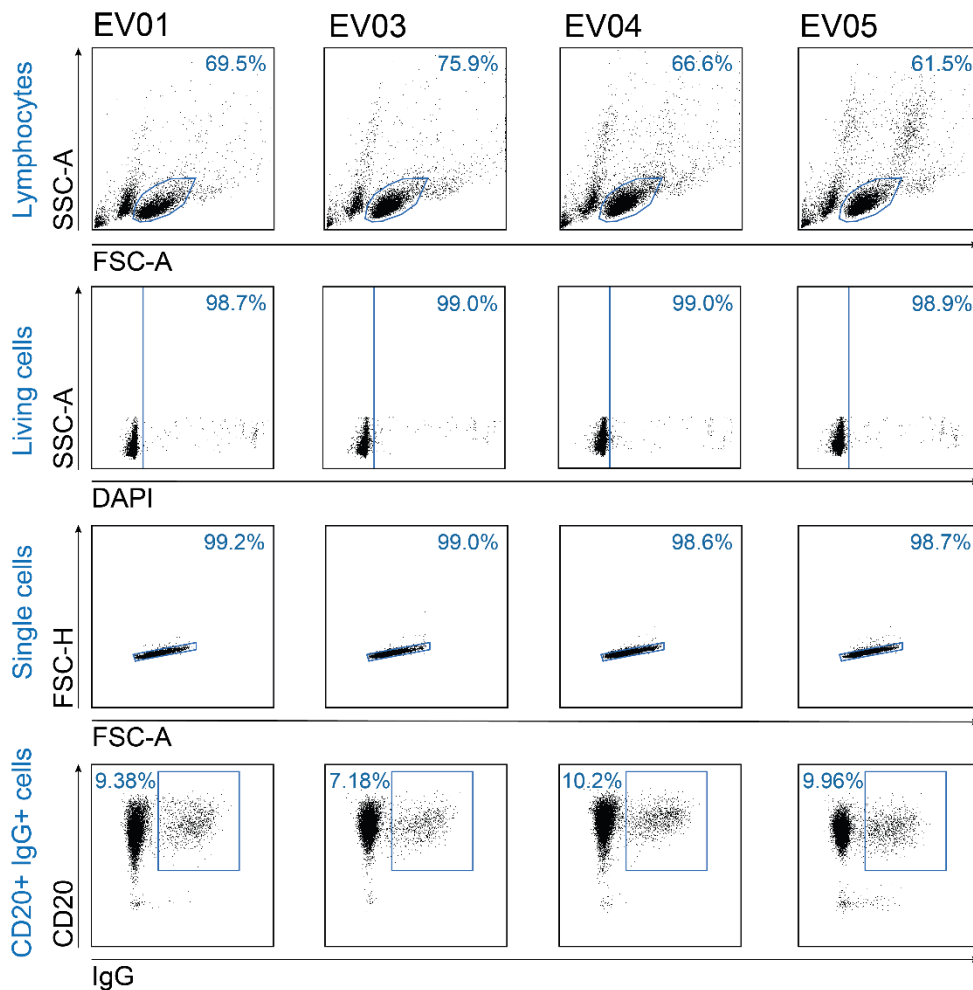


Figure 14. Gating strategy to select the memory B cell compartment from rVSV-ZEBOV-vaccinated individuals for B cell repertoire analyses by NGS.

PBMCs of rVSV-ZEBOV-vaccinated donors (EV01, EV03, EV04 and EV05; in columns) that were enriched for CD19 by MACS were morphologically gated for lymphocytes (top panel) → living cells (second panel) → single cells (third panel). CD20+ IgG+ B cells (bottom panel) were selected for bulk sort. In total, 250,000 memory B cells were sorted for each donor.

Unbiased next generation sequencing (NGS) analyses on the heavy chains of the memory B cell compartment were performed by Lutz Gieselmann and Christoph Kreer (chapter 2.2.6.1 Ig heavy/light chain sequence analysis). With the datasets provided by colleagues, sequence characteristics of interest of the total IgG-positive memory B cell compartment could be assessed and compared to the EBOV GP-specific IgG-positive memory B cell population of identical donors. Thereby, it was investigated whether the observed values for V gene germline identity were corresponding to values generally found in the memory B cell compartment of a certain donor, or whether they were deviating from the average and were specific for EBOV GP-reactive B cells. CDRH3 lengths (**Figure 15A** top) and V gene germline identity (**Figure 15A** bottom) of the total IgG memory B cell heavy chains are shown in grey. These values were compared to GP-reactive B cells (blue) of matching donors. Differences between repertoire and EBOV-specific

compartment were small. The mean CDRH3 lengths in the four donors were 0.8 to 1.3 aa longer in the complete B cell compartment compared to the EBOV-specific population and mean V gene germline identity was -0.9% to 1.0%. All individual numbers and frequencies comparing the EBOV-specific population and the total memory B cell repertoire of individual donors can be found in the Appendix: **Appendix Table 3** and **Appendix Table 4** list the absolute numbers of sequences found for every CDRH3 length and the relative frequency of sequences of every CDRH3 length, respectively. The absolute numbers and relative frequency of sequences found for every V gene germline identity percentage can be found in **Appendix Table 5** and **Appendix Table 6**.

Additionally, the absolute numbers and relative frequencies of individual V genes found in the IgG B cell repertoires and EBOV-specific population was determined and can be found in **Appendix Table 7** and **Appendix Table 8**. After pooling datasets of all vaccinated individuals, the frequency of individual V genes found in the IgG B cell repertoires (**Figure 15B** top) was also determined and compared to the distribution found in EBOV GP-specific IgG B cells (**Figure 15B** middle). To make differences in frequencies and potential preferences of certain V genes in the EBOV GP-specific population more visible, we calculated the relative difference of both V gene distributions (**Figure 15B** bottom). Quantification and significance were determined by members of the Pfeifer Lab, University of Tübingen (chapter 2.2.5 Quantification and statistics). The frequency of V genes 1-18, 1-24, 2-5, 3-9, 3-53, and 4-39 was reduced in the EBOV-specific memory B cell population in all individuals. On the other hand, several genes were observed with increased frequency in the EBOV-specific memory B cell population in all subjects analyzed. A not significant trend for higher abundance was observed for V genes 3-23, 3-74, and 4-4 (light green). IGHV3-15 (dark green) was detected significantly more frequently in the EBOV GP-specific B cell population. In the total memory B cell repertoire, IGHV3-15 was found on average in 1.84% of B cells compared to 12.5% in the EBOV-specific population. On a single donor level, it was observed 5.4-, 6.4, 4.8-, and 9.9-fold more frequently in EV01, EV03, EV04, EV05, respectively. Therefore, we conclude that while heavy chain CDR3 lengths and V gene identities are similar between the total memory B cell repertoire and the EBOV GP-specific population, differential V gene usage can be observed and IGHV3-15 expressing B cells are significantly increased in the EBOV GP-specific population.

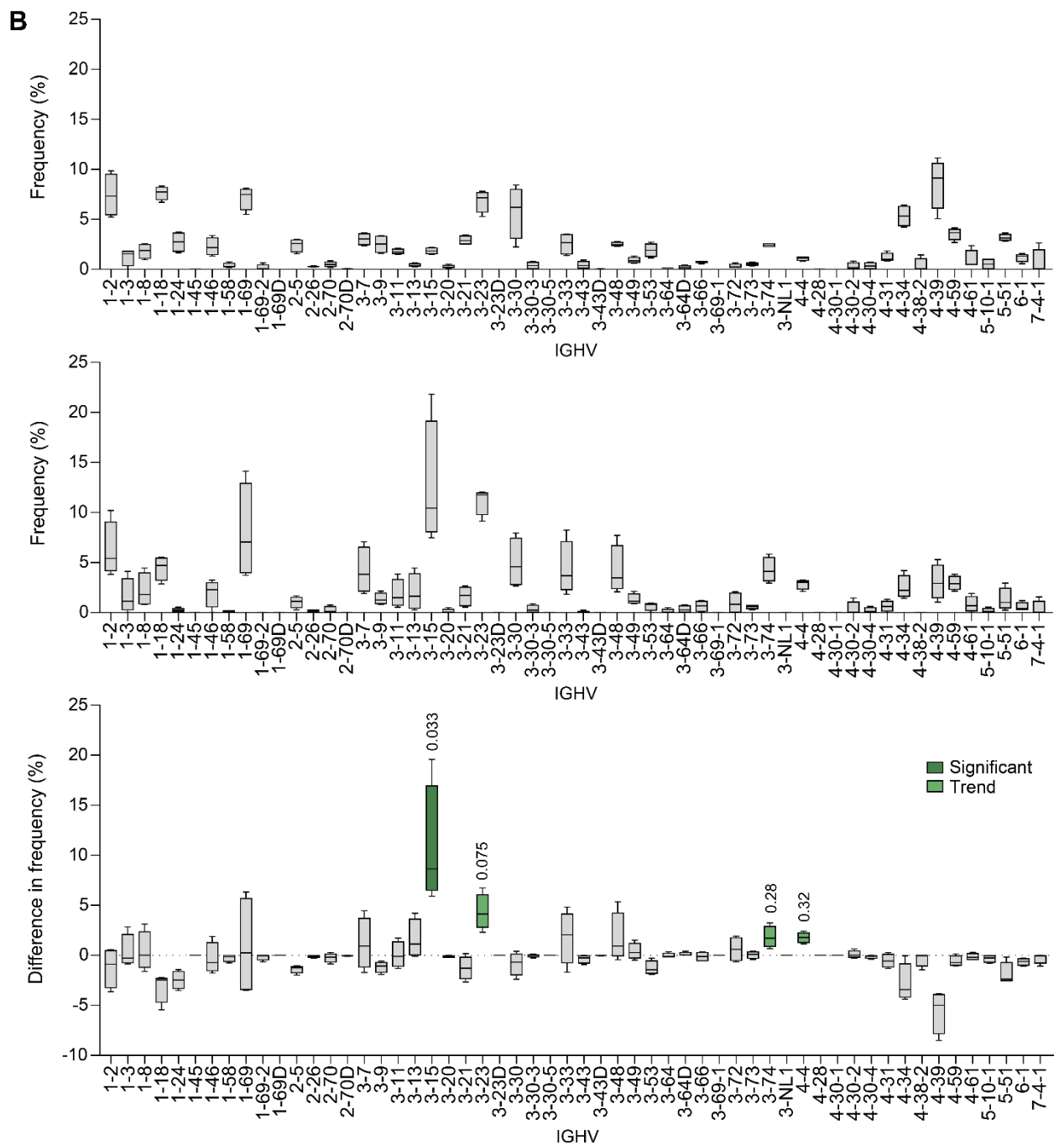
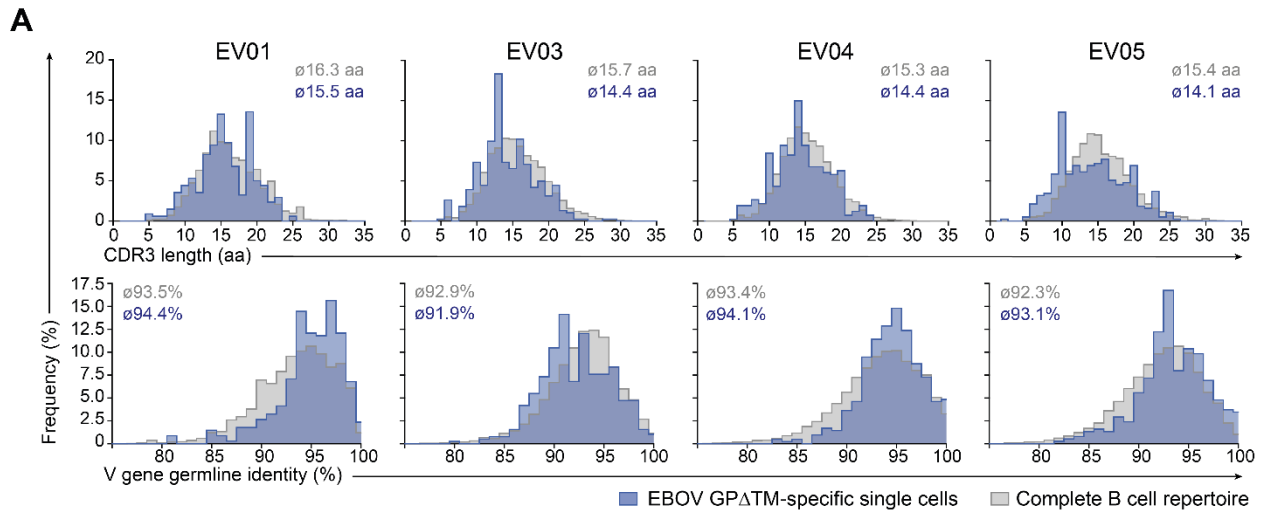


Figure 15. Comparing characteristics of the total IgG memory B cell compartment and the EBOV GP-specific IgG memory B cell population.

(A) Frequencies of heavy chains with certain CDR3 aa length (top panel) and % germline identity of V gene segments (bottom panel) found in the EBOV GP-specific IgG memory B cell population (blue) and the total IgG memory B cell repertoire (grey) of four rVSV-ZEBOV-vaccinated individuals (EV01, EV03, EV04 and EV05). (B) Relative frequencies (%) of heavy chain V gene segments utilized by total IgG memory B cell repertoire (top panel) and EBOV GP-specific memory IgG B cell population (middle panel) and differences in frequencies between the two groups (bottom panel) of data sets pooled from EV01, EV03, EV04 and EV05. Boxes contain 50% of available data points and indicate 75% of the difference between the highest or lowest value. Whiskers indicate min. and max. values. Lines within boxes display medians. Significance of frequency increase was tested by a re-sampling approach based on a one-sided Mann-Whitney U-test with $\alpha = 0.05$ and Bonferroni correction for multiple testing. Quantification and significance were determined by members of the Pfeifer Lab, University of Tübingen.

3.2.5 Convergent development of EBOV GP Δ TM-specific antibody sequences

3.2.5.1 Among rVSV-ZEBOV-vaccinated individuals

In order to further investigate the level of convergence in the rVSV-ZEBOV-induced B cell response, we compared heavy chain sequences across vaccinees. To do so, we extended the selection criteria that were used within individual donors to identify members of a clone. Precisely, we pooled data sets of all vaccinees and repeated the automated search for clones based on identical V gene, CDRH3 identity of at least 75%, difference in CDRH3 aa length of max. 1 aa. Thereby, we were able to identify 24 groups that comprised sequences from two or more distinct individuals and shared characteristics so that they were identified as clonally related although originating from different biological samples. Sequence information on members of these shared groups are summarized in **Appendix Table 9**.

For four individuals, the chemical properties of heavy and light chain CDR3s of 14 shared groups were closely analyzed (**Figure 16A**). We discriminated between identical (bold black), chemically related (black) or unrelated and chemically different (grey) amino acids. Notably, the abundance of identical or similar aa is high across different donors within shared groups. Moreover, in 11 of 14 shared groups heavy chains were also combined with light chains of the same chain type κ or λ . In 7 groups, even the V gene of the combined light chain was identical across donors and also the corresponding CDRL3 showed high convergence. In addition to comparing CDR3 characteristics, we compared full length heavy chain V genes within shared group members to each other and plotted the quantified % similarities in color-coded matrices (**Figure 16B**). A high degree of homology ranging from 74.8% to 95.0% average sequence concordance within groups could be observed. Finally, we plotted the % CDRH3 aa distance against the % V gene sequence nt distance for every EBOV GP-specific sequence of an individual

donor and the most similar sequence of every distinct donor (blue circles; **Figure 16C**). Antibody-shaped icons represent sequences that were assigned to shared groups and mostly cluster in the lower left part of the plot due to their low divergence. To investigate whether such convergent antibodies develop as a response also to other viruses, we performed the same analysis on six HIV-1-infected individuals (grey circles) and compared it to the EBOV GP-specific dataset of vaccinated individuals. It became apparent, that HIV-1-env-specific sequences show higher CDRH3 and V gene sequence divergence across donors. Notably, no groups sharing characteristics could be detected for the HIV-1-env-specific dataset (**Figure 16C**).

We therefore conclude that rVSV-ZEBOV vaccination induced the convergent development of similar EBOV GP-specific B cells across donors and that the presence of groups sharing characteristics is not commonly induced against all viruses.

Figure 16. Convergent development of EBOV GP Δ TM-specific antibody sequences in rVSV-ZEBOV-vaccinated individuals.

(A) Heavy chain sequences of all vaccinees with the same V gene were grouped and tested for their similarity on aa level by calculating the Levenshtein distance. Sequences from different donors with at least 75% CDRH3 homology were defined as shared group (s1-s16) and if available, clonal members were added to groups. Sequence origins are color-coded by orange, violet, green and yellow for EV01, EV03, EV04, and EV05, respectively. Bold letters indicate identical aa, black letters aa with similar chemical characteristics, and grey letters different aa. Chemical characteristics were defined by grouping aa into non-polar, polar, acidic, basic and aromatic aa. (B) Quantification of homology of CDRH3 sequences by pairwise comparison and determination of similarity index using BLOSUM (BLOcks SUBstitution Matrix) with Geneious software. (C) Percent distance of CDRH3 aa sequence (x-axis) and V gene nt sequence (y-axis) of each sequence to the most similar sequence identified in another donor as calculated by Levenshtein distance normalized on the shorter sequence, if applicable. EBOV GP-specific antibodies are shown as blue circles and shared groups with at least 75% CDRH3 homology as colored antibodies. The HIV-1 BG505.SOSIP-specific antibodies from six HIV-1-infected individuals are labeled as grey circles.

3.2.5.2 Among rVSV-ZEBOV-vaccinated individuals and EVD survivors

To investigate whether rVSV-ZEBOV vaccination credibly reproduces the antibody response of natural infections with positive outcome, we additionally integrated a set of sequences obtained from EVD survivors reported by Bornholdt and colleagues (Bornholdt et al., 2016).

By performing the same analyses as described for the comparison among rVSV-ZEBOV-vaccinated individuals, we identified five groups that shared characteristics and comprised at least one sequence of an EVD survivor and one sequence of a vaccinated individual each (**Figure 17A**). In four of five groups, the heavy chains were paired with light chains of the same chain type κ or λ . As for the groups shared between vaccinees, we also determined similarity indexes for groups shared between EV and survivors (**Figure 17B**). The average similarity indexes in these shared groups ranged from 73.8% to 100%.

We therefore conclude that the antibody response in rVSV-ZEBOV-vaccinated donors show similarities to the specific antibody response upon EBOV infection.

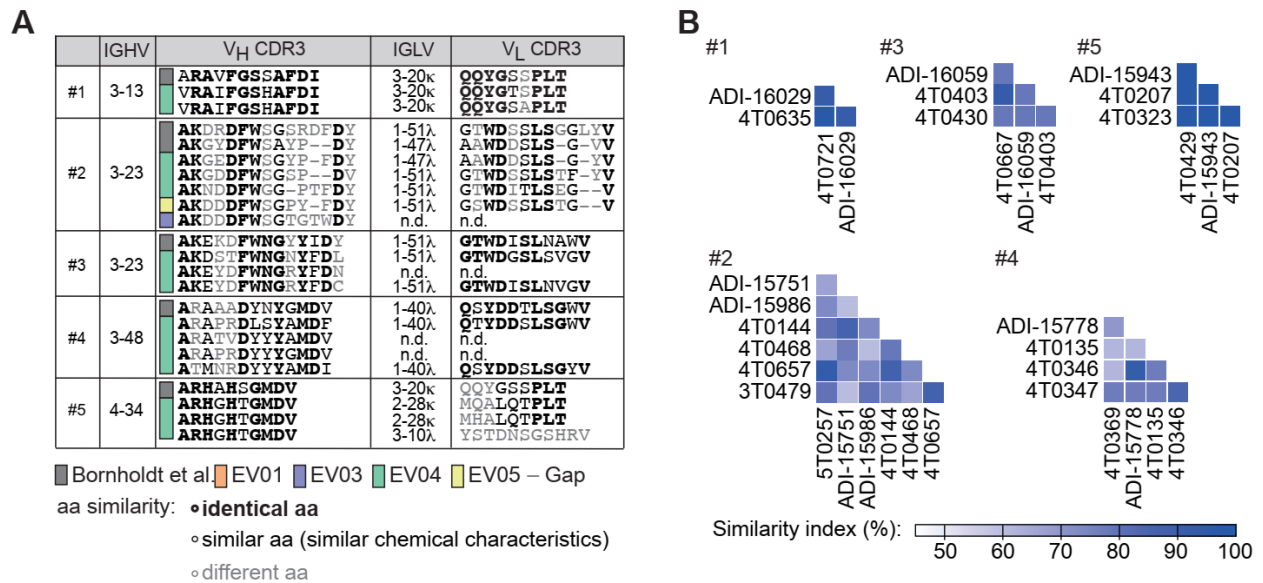


Figure 17. Convergent development of EBOV GP Δ TM-specific antibody sequences in rVSV-ZEBOV-vaccinated individuals and EVD survivors.

(A) Heavy chain sequences from rVSV-ZEBOV-vaccinated individuals (EV) and EVD survivors (Bornholdt et al., 2016) with the same V gene were grouped and tested for their similarity on aa level by calculating the Levenshtein distance. Sequences from different donors including at least one EVD survivor and a CDRH3 homology of at least 75% were defined as shared group (#1-#5) and if available, clonal members were added to groups. Sequence origins are color-coded by grey, orange, violet, green and yellow for EVD survivor, EV01, EV03, EV04, and EV05, respectively. Bold letters indicate identical aa, black letters aa with similar chemical characteristics, and grey letters different aa. Chemical characteristics were defined by grouping aa into non-polar, polar, acidic, basic and aromatic aa. (B) Quantification of homology of CDRH3 sequences by pairwise comparison and determination of similarity index using BLOSUM (BLOcks SUBstitution Matrix) with Geneious software.

3.2.6 rVSV-ZEBOV-induced antibodies bind to EBOV and are cross-reactive to other Filoviruses

Of all single B cells that were obtained, we cloned and produced 151 antibodies, of which 133 belonged to 122 individual B cell clones including the shared groups and 18 represented non-clonal (single) antibody sequences.

Initially, we confirmed antibody binding to EBOV *Makona* GP Δ TM via ELISA (**Figure 18A**). This step was necessary, because during single cell sorts of EBOV GP-specific B cells also B cells could have been isolated, which unspecifically bound to EBOV GP. Alternatively, errors during PCR and cloning steps could have been occurred that might abolish binding of antibodies to EBOV GP.

Of all antibodies tested, robust binding capacity against this protein was detected in 94 antibodies. This equaled 64%, 55%, 72%, and 55% of antibodies from EV01, EV03, EV04 and EV05, respectively, with similar ranges and geometric mean EC₅₀ values ranging from 0.14 to

0.24 µg/mL. All antibodies reactive against EBOV *Makona*, also bound to strain *Mayinga* (**Appendix Table 10**).

With regards to therapeutic approaches, antibodies that additionally detect GPs of other Filoviruses are of particular interest. Therefore, we next assessed the potential cross-reactivity of EBOV GP-reactive antibodies with GPs of BDBV and SUDV as well as the *Marburgvirus* MARV. On serum level, low reactivity was detected against BDBV GP Δ TM. In contrast to non-immunized serum samples, however, the response was stronger. Almost no reactivity could be observed for sera of rVSV-ZEBOV vaccinees against GPs from SUDV and Marburg virus (MARV), and it could hardly be discriminated from reactivity in sera of non-immunized subjects (**Figure 18B**).

Notably, we detected a high degree of cross-reactivity on the level of monoclonal antibodies (**Figure 18C**). In individual donors, 30 to 71% of antibodies showed cross-reactivity to GPs of BDBV, SUDV, MARV or several of them (**Figure 18C** left). In total, 53 of 94 tested antibodies were cross-reactive. 29 antibodies reacted with one more species in addition to EBOV (depicted in blue colors), while 24 reacted with EBOV and at least two more species (depicted in red colors). Of the bispecific antibodies, 19 reacted with BDBV (dark blue), nine with SUDV (medium blue) and one with MARV (light blue) apart from EBOV GP. In total, 21 antibodies reacted with EBOV, BDBV and SUDV GP (light red) and three with EBOV, BDBV, SUDV and MARV GP (dark red). The EC₅₀ values detected for each of the antibodies are displayed against all GPs, separately (**Figure 18C** right). Lines show the geometric means. It can be observed that concentrations for half-maximal binding values are higher compared to EBOV GP, and overall increase from BDBV, to SUDV, to MARV. Information regarding EBOV GP- or cross-specificity for every tested antibody are listed in **Appendix Table 10**.

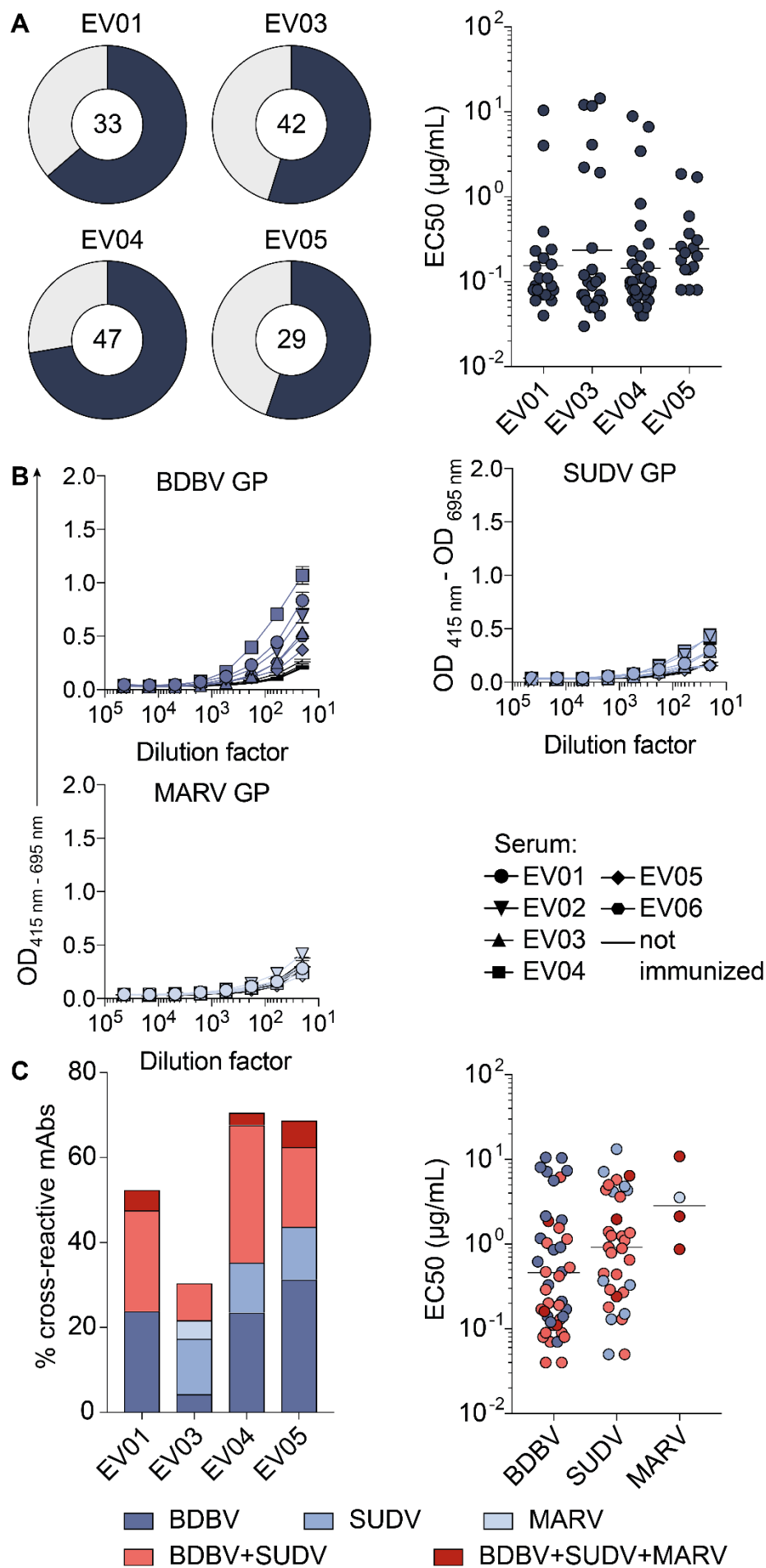


Figure 18. rVSV-ZEBOV-induced antibodies bind to EBOV GP and are cross-reactive to other Filoviruses.

(A) Binding analysis of mAbs isolated from vaccinated individuals (EV01, EV03, EV04 and EV05) against EBOV *Makona* GP Δ TM assessed by ELISA (total number in center of pie charts). Proportion of binding and non-binding mAbs (left) and individual EC₅₀ values of binding mAbs (right). Binding was defined as OD \geq 0.2 at 10 μ g/mL antibody concentration and an EC₅₀ \leq 15 μ g/mL. (B) Serum samples of rVSV-ZEBOV-vaccinated individuals (EV01-EV06; blue) were tested for cross-reactivity against the Filoviruses BDBV (dark), SUDV (medium), and Marburg virus (MARV; light blue). Serum samples of non-immunized subjects (black curves without symbols) were tested as controls. Sera were tested at starting dilutions of 1:20. Shown are means of duplicates. Error bars depict standard deviation. (C) Percentage (left) and EC₅₀ values (right) of EBOV GP Δ TM-specific mAbs with cross-reactivity against GPs from different Filoviruses determined by ELISA. Binding criteria were defined as in (A). mAbs specific for GPs of EBOV plus one other Filovirus species are shown in blue colors as in (B) and mAbs specific for GPs of EBOV plus 2 or 3 other Filovirus species are shown in light or dark red, respectively.

3.2.7 rVSV-ZEBOV-induced antibodies target a broad spectrum of epitopes

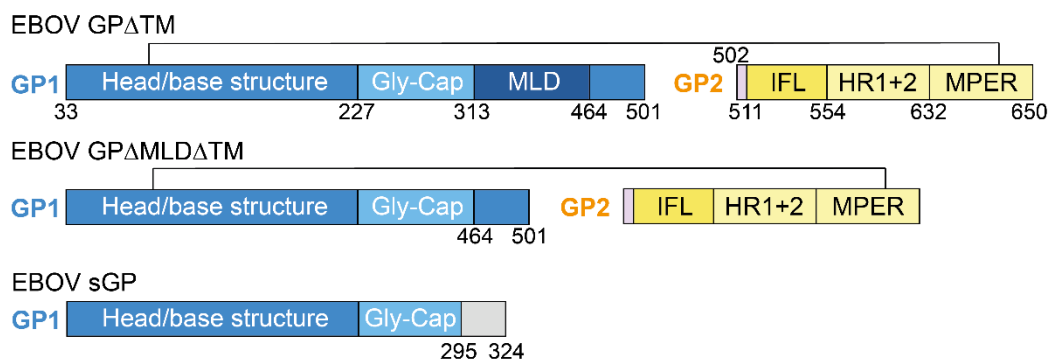
After determining the species-specificity and cross-reactivity of rVSV-ZEBOV-induced monoclonal antibodies, the binding regions and target epitopes of antibodies should be identified.

Therefore, we performed additional ELISAs with EBOV GP-reactive antibodies. First, we tested antibody binding capacity to different versions of the *Ebolavirus* GP, i.e., the trimeric EBOV GP Δ MLD Δ TM and the dimeric and structurally different secreted GP (sGP). Schemes of these GP versions with different domains can be seen (**Figure 19A**). In case antibodies fail to bind to GP Δ MLD Δ TM, although they react with EBOV GP Δ TM, the MLD is identified as binding region of an antibody. Vice versa, if antibodies bind both constructs GP Δ TM and GP Δ MLD Δ TM comprising or lacking the MLD, respectively, the target epitope is not located within this region. Additional information can be gained from ELISAs against sGP. If antibody binding is detected to sGP, the N-terminal part of GP1 that is shared by GP and sGP, is determined to be the binding region. If antibodies did not bind to sGP, further assays were necessary to identify the target region. Individual OD and EC₅₀ values for all antibodies can be seen in **Appendix Table 10**. The results for all antibodies of the different donors are summarized in **Figure 19B**. Between 28.6%, 47.8%, 38.2%, and 68.8% of antibodies from EV01, EV03, EV04 and EV05 bound to sGP, identifying the Head, Base or Glycan Cap within the N-terminal part of GP1 as binding region (**Figure 19B**). For a smaller fraction of 33.3%, 21.7%, 8.8%, and 6.3%, no binding was observed against EBOV GP Δ MLD Δ TM, identifying the MLD as binding region. In total, 41 of 94 antibodies bound to sGP and 16 antibodies to the MLD.

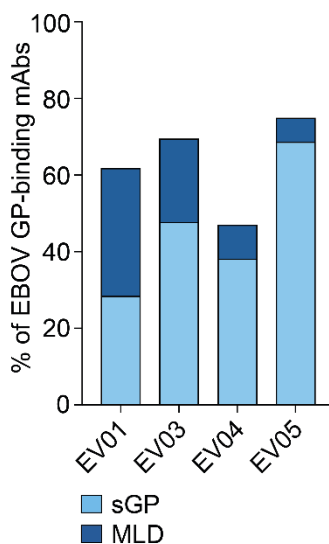
For the remaining 37 antibodies which did not bind to sGP, and binding was not dependent on the presence of the MLD, the epitope was either fully located in GP2 or partially dependent on GP2. To further unravel the epitopes, we secondly performed competition ELISAs with published

reference antibodies with epitopes fully or partially mapped to the GP2 domain. These were KZ52 and mAb100, which recognize epitopes within the GP1 glycan cap and GP2 internal fusion loop structure. Additionally, we tested competition with ADI-15758 and/or ADI-15999, which target the membrane proximal external region (MPER) of GP2. If ELISAs of rVSV-ZEBOV-induced antibodies to EBOV GP yielded reduced OD values in presence of a reference antibody, this was indicative of a reduced avidity because binding sites on the GP were occupied. Thereby, we could identify the epitopes of antibodies that bound to the same regions as reference antibodies. The results of these assays are listed in **Appendix Table 12** for individual antibodies and summarized per donor in **Figure 19C**. In EV05, no rVSV-ZEBOV-induced antibody was found to compete with ADI-15758 or ADI-15999. In the remaining subjects, one or two antibodies each competed with these two reference antibodies, mapping their target epitopes to the MPER. Two to four antibodies competed for EBOV GP binding regions with KZ52 and mAb100, which mapped their target epitopes to the GP1 glycan cap and GP2 internal fusion loop. The epitopes of the remaining 20 antibodies, however, remained unknown.

A



B



C

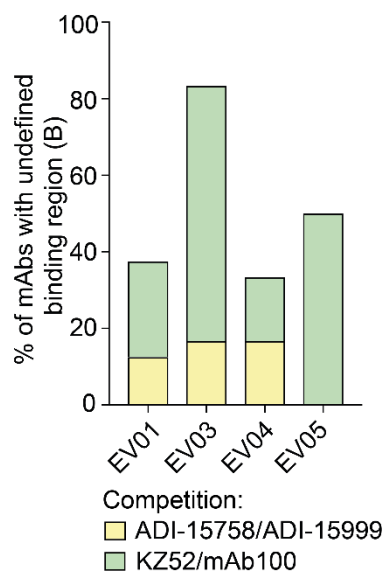


Figure 19. Epitope determination of rVSV-ZEBOV-induced antibodies.

(A) Schematic representation of EBOV GP constructs produced to determine target sites of EBOV-specific mAbs. EBOV GP Δ TM (top; lacking transmembrane domain residues 651-676), EBOV GP Δ MLD Δ TM (middle; lacking additionally the mucin-like domain [MLD] residues 313-163) and EBOV sGP (bottom; secreted GP) with C-terminal end structurally different from GP1 (light grey). GP1 and GP2 are shown in blue and yellow, respectively. GP1 contains the head/base structure, glycan cap (Gly-cap), MLD and the C-terminal end of GP1 (residues 464-501). GP2 contains the internal fusion loop (IFL), heptad repeats 1 and 2 (HR1+2), and the membrane-proximal external region (MPER). Lines represent disulfide bridges connecting GP subunits. (B) Percentage of EBOV GP Δ TM-specific antibodies reactive against sGP or MLD determined by ELISA using constructs described in (A). (C) Competition ELISA of EBOV GP Δ TM-reactive mAbs with target sites that had not been identified in (B). Antibodies for competition included KZ52 and mAb100 which target GP1, IFL and HR1, as well as ADI-15758 and ADI-15999 which target the MPER. Competition was defined as $\geq 25\%$ inhibition of binding.

To complement epitope mapping, we assessed binding to linear peptides of the EBOV GP Δ TM strain *Makona* for all EBOV GP-reactive antibodies. The peptide library consisted of eighty 18-mer peptides with 10 aa overlap and was validated using control antibodies including KZ52, mAb100, ADI-15758 and ADI-15999. Hits against peptides for individual antibodies can be seen in **Appendix Table 11**. Overall, 52 of the 94 antibodies bound to at least one linear peptide further confirming and refining epitope information gathered by previous ELISA analyses.

In total, we obtained epitope information for 80 of 94 antibodies and the combined results are shown in **Figure 20** in the left panel. The individual results of ELISAs against GP Δ TM, GP Δ MLD Δ TM and sGP, competition ELISAs, as well as peptide library ELISAs and the final assignment to an epitope for all tested antibodies are listed in **Appendix Table 10** and **Appendix Table 12**.

In summary, of all rVSV-ZEBOV-induced and EBOV GP-reactive antibodies, 48.9% bound to epitopes within the GP1 region, 14.9% bound the MLD, 8.5% bound to GP2, and 12.8% bound conformational epitopes including GP1 and GP2 parts. The target domains of the remaining 14.9% of antibodies could not be identified (**Figure 20** left panel).

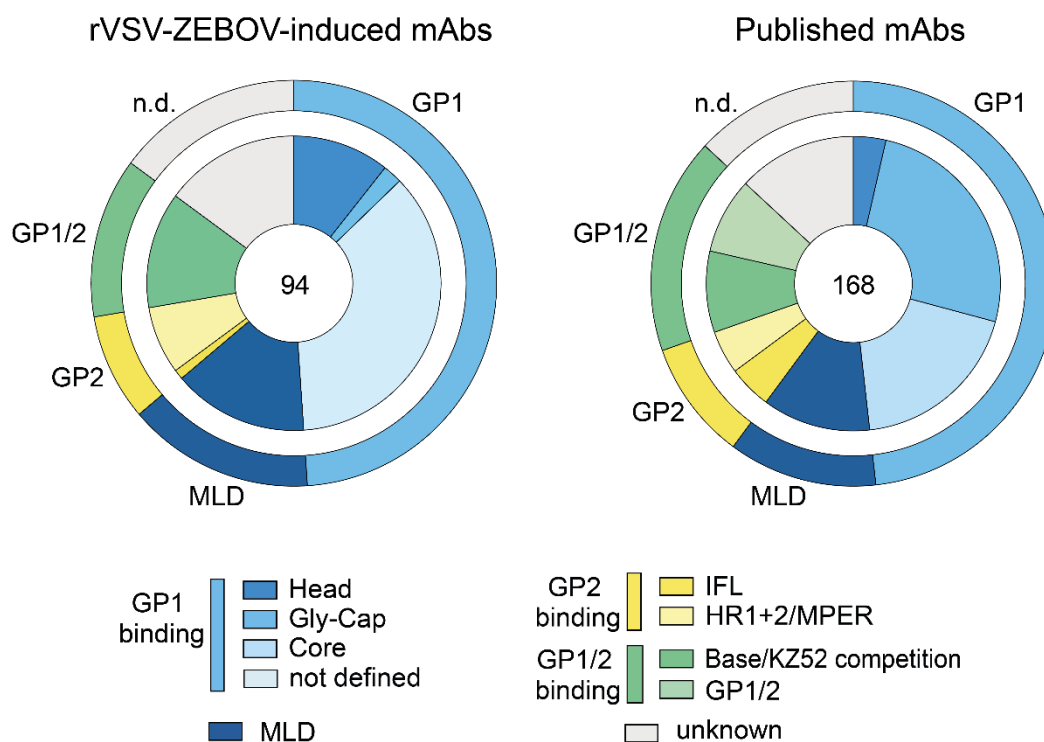


Figure 20. Epitope spectrum of rVSV-ZEBOV-induced antibodies and comparison to previously published antibodies.

(Left) Epitope spectrum of rVSV-ZEBOV-induced antibody repertoire. Target epitopes of 94 rVSV-ZEBOV-induced antibodies were determined in previous experiments and are summarized here. Target epitopes were elucidated by ELISA against EBOV sGP and GP Δ MLD Δ TM (**Figure 19B**), competition ELISAs against KZ52/mAb100 and ADI-15748/ADI-15999 (**Figure 19C**), and by peptide library screening (**Appendix Table 11**). See also **Appendix Table 10** and **Appendix Table 12** for individual antibody results. (Right) Epitope spectrum of antibodies obtained from animal models and EVD survivors (Saphire, Schendel, Fusco, et al., 2018). Total numbers are shown in the center of pie charts.

To draw conclusions on the question, whether rVSV-ZEBOV vaccination induces similar antibodies as natural infection, we compared our findings to results of a comprehensive study published recently by Saphire et al., which investigated the epitopes of 168 different antibodies from survivors or immunized animal models (**Figure 20** right panel) (Saphire, Schendel, Fusco, et al., 2018). These antibodies were obtained from numerous research groups. Interestingly, the overall distribution of antibodies to different epitopes was highly similar to rVSV-ZEBOV-induced antibodies (**Figure 20** left panel). We therefore conclude that rVSV-ZEBOV vaccination provides the full antigenic diversity of GP found in natural infection and thereby leads to the production of antibodies with a highly similar epitope spectrum.

3.2.7.1 Epitope distribution in cross-reactive or EBOV-specific antibodies

In an attempt to evaluate whether there is a link between target epitopes of rVSV-ZEBOV-induced antibodies to their ability to identify a single or several *Ebolavirus* species, we separately visualized epitope spectra of EBOV-restricted (**Figure 21A** left panel) and cross-reactive antibodies (**Figure 21A** right panel). In both groups, similarities could be observed. Approximately half of EBOV-specific as well as cross-reactive antibodies bind to the major subunit of the glycoprotein which is GP1. On the amino acid level, GP1 harbors conserved as well as disparate parts (**Figure 21B**), thereby explaining that EBOV-specific and cross-reactive antibodies likewise bind to GP1. 11% and 15% of cross-reactive and EBOV-specific antibodies, respectively, are competitors of the base-binding antibody KZ52 and target a conformational epitope spanning GP1 and GP2. Epitopes of the remaining antibodies, however, strongly vary between cross-reactive and EBOV-restricted antibodies. The proteinaceous part of the heavily glycosylated MLD is strongly varying between different *Ebolavirus* species (**Figure 21B**). As a result, antibodies binding in this region are likely to be species-specific. Indeed, the MLD is targeted by 27% of EBOV-restricted but only by 6% of cross-reactive antibodies. In contrast, we observed that epitopes of cross-reactive antibodies are located in the HR, MPER or IFL regions of GP2 (13%), which are domains that are conserved across *Ebolavirus* species. Additionally, cross-reactive antibodies target epitopes that remain unknown (23%), which is rarely the case for EBOV-specific antibodies.

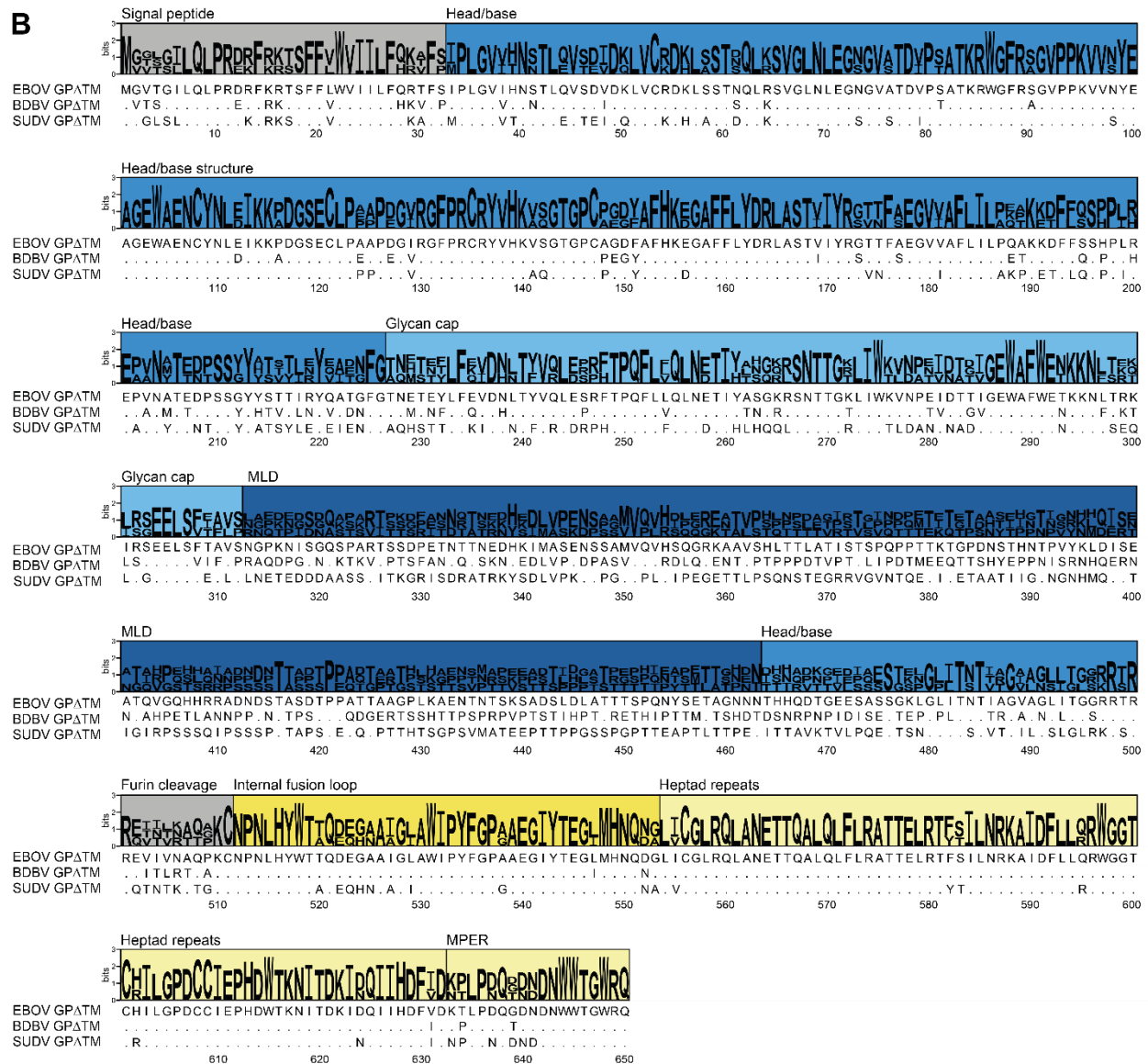
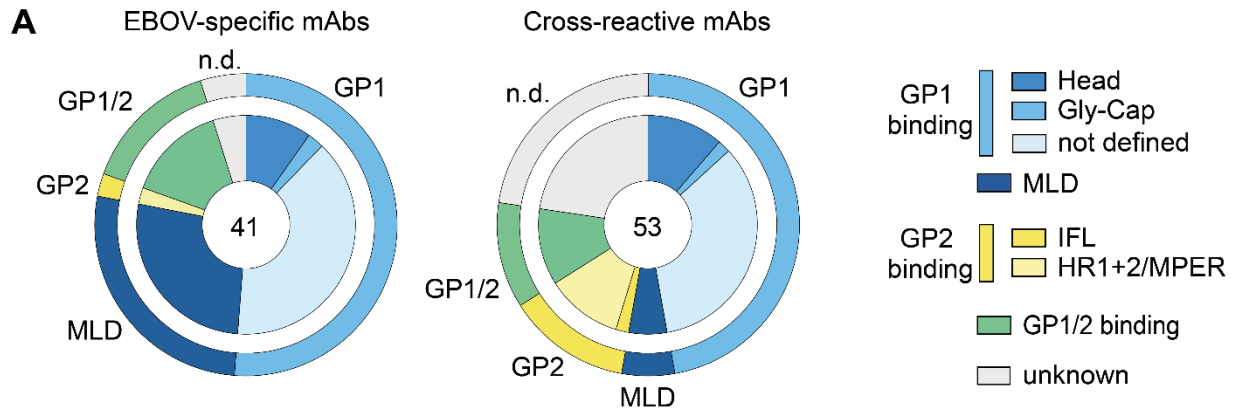


Figure 21. Epitope spectra of rVSV-ZEBOV-induced EBOV-specific versus cross-reactive antibodies.

(A) Summary of epitope analyses of rVSV-ZEBOV-induced antibodies determined by ELISA against EBOV sGP and GP Δ MLD Δ TM, competition ELISAs against KZ52/mAb100 and ADI-15748/ADI-15999, and by peptide library screening, identified for EBOV-specific antibodies (left) and those cross-reactive with BDBV, SUDV and/or MARV (right). Total numbers are in center of pie charts. (B) Alignment of amino acid sequences from GP Δ TM of the *Ebolavirus* species EBOV, BDBV and SUDV. Dots indicate identical amino acids in a certain position compared to the reference sequence of EBOV GP Δ TM. Sequence Logo plots above alignment were generated by WebLogo 3 with minor alterations. Layered letters show different amino acids found at a certain position. Total height of stacks symbolizes the degree of conservation of a certain position. Background colors of sequence logo as in (A).

3.2.8 rVSV-ZEBOV-induced antibodies neutralize EBOV

3.2.8.1 Neutralization by serum

Neutralization capacity is the most reliable predictor for *in vivo* protection against EVD. Therefore, we subsequently assessed whether serum samples of rVSV-ZEBOV-vaccinated individuals (EV; blue) have the ability to neutralize live EBOV *Mayinga* in an *in vitro* assay (**Figure 22**). As a control, sera from convalescent EVD patients were tested (red). Bars show the individual dilution factors of serum samples that still protect cells from infection. The individual dilution factors within the groups were highly varying. For survivor samples, sera could be diluted between 23- to 304-fold, and still achieve full neutralization. In EV sera, samples maintained neutralizing capacity when diluted up to 23- to 64-fold. Colored background areas depict the mean dilution factors at which sera of respective groups still exert full neutralization of live virus. The means were 104 for survivors and 30 for EV serum samples. Albeit not being significant, this difference suggested that the abundance of neutralizing antibodies in sera of vaccinees is lower compared to EVD survivors.

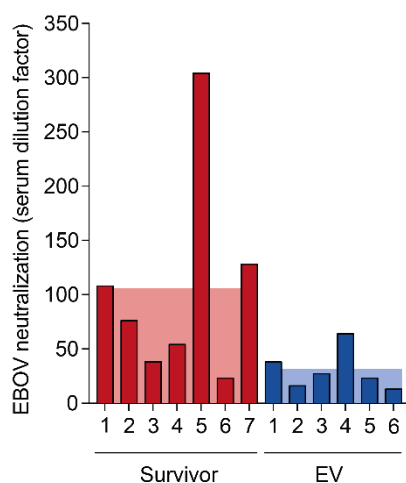


Figure 22. Serum neutralization activities after infection or vaccination.

Analysis of neutralization activity of serum samples from EVD survivors (red) and rVSV-ZEBOV-immunized donors (EV; blue). Shown are mean dilution factors yielding full neutralization of wildtype EBOV *Mayinga in vitro*. Colored background areas indicate mean of respective groups. Significance of difference between mean neutralization was tested by an unpaired t-test ($p=0.089$). Neutralization experiments were performed in quadruplicates.

3.2.8.2 Neutralization by monoclonal antibodies

Next, we wanted to elucidate whether the low neutralizing activity of sera from vaccinated individuals would also translate to low neutralizing activity of monoclonal antibodies. In all vaccinated subjects, we identified neutralizing antibodies (**Figure 23A**). In EV01, EV03, EV04, and EV05, respectively, 43%, 65%, 32%, and 56% of antibodies neutralized live EBOV *Mayinga* at a concentration of 100 $\mu\text{g/mL}$. Results for individual antibodies are listed in **Appendix Table 12**. In total, 44 of 94 antibodies neutralized at this concentration. 43 of the 44 neutralizing antibodies had previously been found to react with EBOV GP in ELISAs. Antibody 3T0209 was a weak neutralizer that did not bind to EBOV GP in ELISA and was not followed in subsequent analyses. The minimal concentrations yielding full neutralization were similar across vaccinated individuals (**Figure 23B**). The geometric means for neutralization activity were 2.22, 0.49, 0.99, and 2.21 $\mu\text{g/mL}$, for EV01, EV03, EV04, and EV05, respectively. Importantly, these concentrations were comparable to previously reported antibodies from survivors of EVD that have recently been approved for therapy (mAb114) (FDA, 2020a; Gaudinski et al., 2019) and/or protect non-human primates from infection (mAb100, ADI-15758, ADI-15999, ADI-16037) (Bornholdt et al., 2016; Corti et al., 2016). Neutralizing titers of these antibodies ranged from 0.055 to 2.5 $\mu\text{g/mL}$ as indicated by green background area. Nearly 70% of rVSV-ZEBOV-induced antibodies also neutralized within this range and some had even superior activity of 0.01 $\mu\text{g/mL}$ compared to previously reported antibodies. Notably, the majority of neutralizing antibodies were sGP binders, mapping their epitope to the N-terminal part of GP1 (**Figure 23C**). Surprisingly, four neutralizing antibodies target the highly varying MLD that is associated with low neutralization and protection capacity. Two antibodies competed for GP binding with ADI-15758 or ADI-15999 mapping their epitopes to GP2. Seven competed with KZ52 and mAb100, thereby identifying the GP1/2 interface as their target. The two most potent neutralizers 3T0331 and 4T0243 were competitors of KZ52 and mAb100, but with a 5- and 12-fold higher activity, respectively.

In addition to neutralizing EBOV, we assessed whether cross-reactive antibodies that bound to SUDV GP in ELISAs also cross-neutralized live SUDV *Boniface*. However, none of the antibodies led to a reduction of cytopathic effect (CPE) of SUDV see also **Appendix Table 12**.

We therefore conclude, that single dose rVSV-ZEBOV vaccination induces highly potent but EBOV-specific neutralizing antibodies in all individuals studied and that these antibodies are of comparable and even superior potency than previously reported ones.

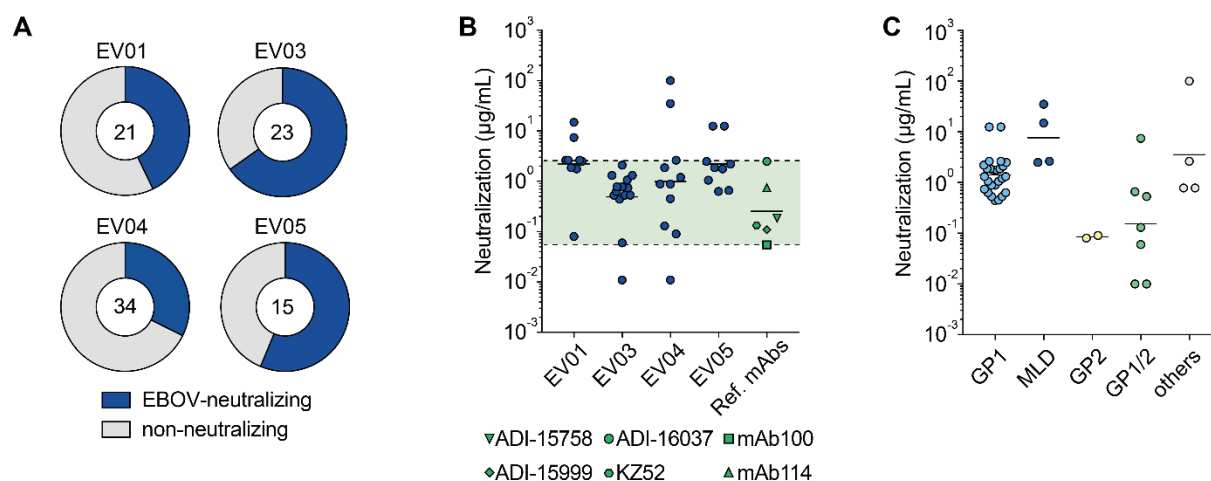


Figure 23. rVSV-ZEBOV vaccination induces potent neutralizing antibodies.

(A) Proportion of EBOV-reactive mAbs with neutralization activity (blue) and non-neutralizing mAbs (grey) from vaccinees (total number of tested antibodies in centers of pie charts). (B) Antibody concentrations ($\mu\text{g/mL}$) required to achieve full neutralization. mAbs obtained from rVSV-ZEBOV-immunized subjects (blue) compared to published reference antibodies KZ52, mAb114, mAb100, ADI-15758, ADI-15999, and ADI-16037 (green). The green background area illustrates the neutralization range of reference antibodies. Lines show geometric means. (C) Distribution of neutralizing antibodies according to their epitopes. Color scheme as in previous figures. All neutralization experiments were performed in quadruplicates.

3.2.8.3 Epitope spectrum of neutralizing antibodies and link to cross-reactivity

Subsequently, we sought to take a closer look on EBOV neutralizing antibodies in order to investigate whether they share characteristics. Such common features could serve as determinants of the development of neutralizing antibodies and vaccination success.

In order to identify such characteristics, we compared neutralizing antibodies with non-neutralizing antibodies. First, we compared the epitope spectra of both groups (**Figure 24A**). The most apparent difference between the two groups is that 62.8% (27 of 43) of neutralizing antibodies bound to epitopes of the GP1 domain, while this was the case for 37.3% (19 of 51) of non-neutralizing antibodies. In contrast, 19.6% non-neutralizing antibodies were directed against the MLD, while only 9.3% of neutralizing antibodies targeted this region. 4.7% of neutralizing antibodies targeted the HR1+2 and MPER, 16.3% bound structural epitopes involving GP1 and GP2 domain, and for 7% of antibodies the target epitope remained unknown. Notably, no neutralizing antibodies targeting the IFL were identified. Non-neutralizing antibodies targeted the GP2 regions IFL or HR1+2 and MPER, structural epitopes on GP1 and GP2 domains or unknown epitopes in 11.8%, 9.8%, and 21.6% of cases, respectively.

Next, we asked whether a link between neutralization capacity and cross-reactivity to other *Filovirus* species exists (**Figure 24B**). Therefore, we evaluated whether neutralizing or non-neutralizing antibodies exert cross-reactivity with GPs of other Filoviruses in ELISAs. All

antibodies from vaccinated individuals EV01, EV03, EV04 and EV05 were clustered into four different groups, i.e., neutralizing and cross-reactive with at least one more *Filovirus*, neutralizing and EBOV-specific, non-neutralizing and cross-reactive, or non-neutralizing and EBOV-specific. The largest group was made up by 35 antibodies that were not neutralizing but cross-reacted with other Filoviruses. Of those, 15 were cross-reactive with EBOV and one more Filovirus, and 20 were cross-reactive with at least two more Filoviruses. In contrast, 25 antibodies were neutralizing but not cross-reactive. 18 antibodies were both neutralizing and cross-reactive. Of those, 14 mAbs were cross-reactive with EBOV and one more Filovirus. Only four antibodies were broadly reactive and neutralizing. The remaining 16 antibodies were EBOV-specific and did not neutralize. Albeit being not significant, there seems to be mild trend for inverse correlation of breadth of recognized species and neutralizing capacity.

Additionally, we compared the epitope spectra of the four groups (**Figure 24C**). The epitopes of cross-reactive and EBOV-specific neutralizing antibodies did not vary much. The most apparent difference is that antibodies with target epitopes located on GP2 are cross-reactive, as already observed above. The spectrum of cross-reactive antibodies closely overlaps between neutralizing and non-neutralizing antibodies. The group of EBOV-specific and non-neutralizing antibodies is largely composed of antibodies targeting the MLD, thereby making MLD-directed antibodies less attractive for future studies. We conclude that there is no clear link between neutralization capacity, cross-reactivity and epitope spectra, which could serve for the early identification of promising antibodies in screens.

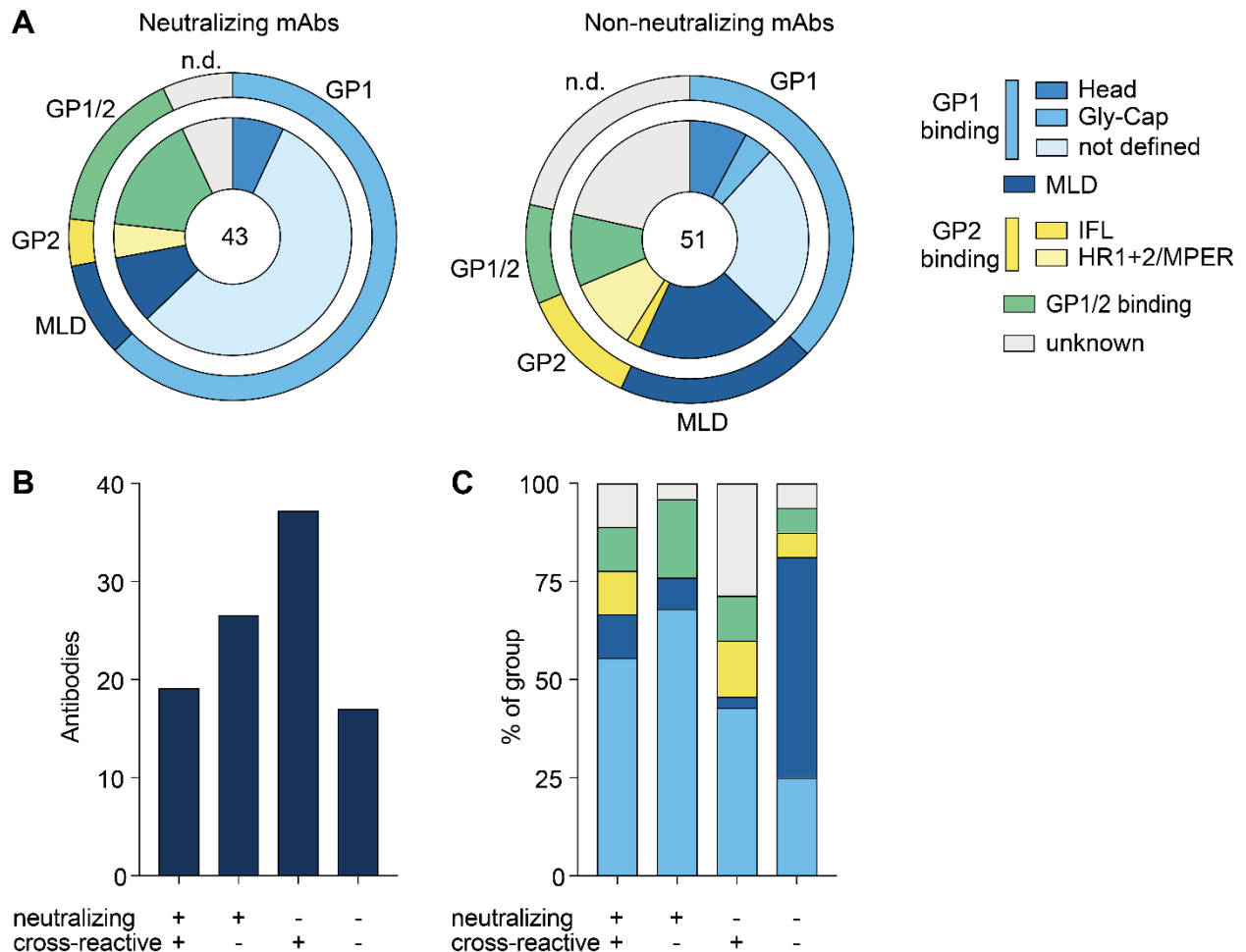


Figure 24. Epitope spectrum of rVSV-ZEBOV-induced neutralizing versus not neutralizing antibodies.

(A) Summary of epitope analyses of rVSV-ZEBOV-induced antibodies determined by ELISA against EBOV sGP and GP Δ MLD Δ TM, competition ELISAs against KZ52/mAb100 and ADI-15758/ADI-15999, and by peptide library screening, identified for EBOV-specific antibodies (left) and those cross-reactive with BDBV, SUDV and/or MARV (right). Total numbers of antibodies in center of pie charts. (B) Linking cross-reactivity to neutralizing capacity. (C) Proportional composition of target epitopes of antibodies clustered in (B). Color scheme as in (A).

3.2.8.4 Recurrent generation of an IGHV3-15/IGLV1-40 antibody class across donors

The most striking common feature among EBOV-neutralizing antibodies became apparent when comparing the V gene segments in these antibodies (Figure 25). Similar to the comparison of the B cell repertoire and the EBOV-specific B cell compartment before, we evaluated the frequency of all V gene segments that were identified in produced antibodies. V gene segments that did not give rise to binding or neutralizing antibodies were excluded for greater clarity. All heavy and light chain V gene segments that gave rise to at least one neutralizing antibody (dark blue) are depicted in Figure 25A. Additionally, the frequency for non-neutralizing but EBOV GP-binding antibodies

(light blue) and non-binding antibodies (grey) harboring these V gene segments are indicated. Although various V genes were observed in EBOV-neutralizing antibodies, we detected a significant preference for IGHV3-15 in heavy chains (**Figure 25A** left) and IGLV1-40 (**Figure 25A** right) in light chains of neutralizing antibodies. Of note, in all rVSV-ZEBOV-vaccinated individuals, neutralizing antibodies utilizing these genes were identified. 17 of 21 antibodies carrying IGHV3-15 neutralized EBOV (**Figure 25B** left). We next evaluated the light chain V gene segments, each of the IGHV3-15-expressing antibodies combined (**Figure 25B** right; light chain V gene segments indicated by outer ring). Interestingly, we found that all neutralizing IGHV3-15-carrying antibodies were exclusively paired with IGLV1-40-utilizing light chains and showed neutralization activity ranging from 0.44 to 12.5 µg/mL (for individual neutralization activities see **Appendix Table 12**). Vice versa, the remaining four non-neutralizing antibodies expressing IGHV3-15 were paired with different light chain V gene segments. No combination of IGHV3-15/IGLV1-40 was found in antibodies that did not neutralize or bind.

We conclude, that rVSV-ZEBOV can recurrently elicit a class of EBOV-neutralizing antibodies, which utilize the same V_H and V_λ gene segments. The development of these antibodies are correlates for *in vitro* protection and should be considered as candidates for future *in vivo* experiments.

To examine, whether common features in the amino acid sequence are present in IGHV3-15/IGLV1-40 antibodies, we aligned heavy (**Figure 25C** upper panel) and light chain (lower panel) V gene segments and compared them to the germline encoded V genes. On top of alignments, logo plots visualize amino acids at every position for which mutations occurred in one or more sequences. In all sequences, a high degree of overlapping mutations was observed indicating a strongly directed affinity maturation process upon rVSV-ZEBOV vaccination. For example, in heavy chains, various positions were consistently mutated. These include mutations rendering the Ser at position 40 to become an Asn or Thr in 88.2% of neutralizing antibodies. Similarly, within the CDRH1 and CDRH2 regions, Ser31, Lys59/Thr60, and Thr64/65 were mutated in over 50%. Due to different recombined D and J gene segments, the CDRH3 regions were highly diverse and did not reveal common features.

Interestingly, in IGLV1-40 light chains (**Figure 25C**, lower panel), Ser58 in the CDRL2 was replaced in 100% of sequences, mostly by Asn or Thr. Moreover, within the CDRL3, Ser110 and Ser112 were mutated to Arg in 82% and 65%, respectively. Notably, Gly113 was always mutated to Asp (17 of 17 sequences).

After determining that the class of IGHV3-15/IGLV1-40 antibodies were neutralizing and showed directed and common mutations within V gene segments, we further assessed, whether they targeted the same epitopes on the viral GP. Therefore, we performed competition ELISAs and tested antibodies belonging to this class against each other and published antibodies (**Figure 25D**). Antibodies belonging to this class showed high degrees of competition for binding to EBOV

GP against each other, suggesting similar or identical epitopes. They moreover competed for binding sites with the previously described and recently licensed mAb114. mAb114 was isolated from a survivor of EVD and is known to bind the GP1 core in a region responsible for mediating viral attachment to host cells (Corti et al., 2016; FDA, 2020a; Gaudinski et al., 2019; Misasi et al., 2016). In contrast, no competition could be detected for any of the IGHV3-15/IGLV1-40 antibodies against ADI-15999 (Bornholdt et al., 2016) which targets the MPER.

We further conclude that rVSV-ZEBOV-induces antibodies of the IGHV3-15/IGLV1-40 class target highly similar regions on the viral GP, and exhibit common mutations in their V gene segments, indicating a strongly directed affinity maturation in a reproducible pattern.

Figure 25. Recurrent development of a special EBOV-neutralizing antibody class.

(A) Frequency of heavy chain (left) and light chain (right) V gene segments in rVSV-ZEBOV-induced antibodies that neutralize EBOV *Mayinga* (dark blue), bind (light blue) or do not bind EBOV GPΔTM (grey; n=143). Shown are V genes with at least one neutralizing antibody. Significant changes in V gene frequency of neutralizing antibodies were tested using a binominal test under the null hypothesis of equal frequency, $\alpha=0.05$, and Bonferroni correction. Only IGHV3-15 and IGLV1-40 increases were highly significant with $p=2.2 \times 10^{-9}$. (B) Frequency of neutralizing IGHV3-15-carrying antibodies. Slices represent antibodies of unrelated clones from individual donors (left) and corresponding light chains (right). (C) Alignment of aa sequences of IGHV3-15 (top) and IGLV1-40-expressing (bottom) neutralizing antibodies to germline sequence. Identical aa are indicated by dots, aa at positions with $\geq 50\%$ mutations are bold. Sequence Logo plots were generated by WebLogo 3. (D) Percent competition between IGHV3-15/IGLV1-40 antibodies for binding to EBOV GPΔTM assessed by ELISA. Blue indicates competition, white displays simultaneous binding. Self-competition (in black contours) and competition with mAb114 were positive and ADI-15999 negative controls.

3.2.9 Structural analysis of rVSV-ZEBOV induced antibodies

Previous analyses and experiments had led to the identification of several antibodies with interesting characteristics. These were potent neutralizers of EBOV on the one hand, and members of the IGHV3-15/IGLV1-40 class antibodies on the other. Therefore, we aimed to elucidate the exact binding sites of selected candidates of these two groups. These were three IGHV3-15/IGLV1-40 class antibodies 1T0227, 3T0265 and 5T0180 from donors EV01, EV03 and EV05, respectively, as well as two potent neutralizers 3T0331 and 4m0368 from donors EV03 and EV04, respectively. Our collaborators Ron Diskin, Hadas Cohen-Dvashi and Nadav Elad at the Weizmann Institute of Science solved the structures of trimeric GPΔMLDΔTM with the Fabs.

3.2.9.1 IGHV3-15/IGLV1-40 antibody class

Previous experiments showed that all antibodies of the IGHV3-15/IGLV1-40 class bound to sGP, were mostly not cross-reactive (11/17), and all neutralized live EBOV. Competition ELISAs had further revealed similar epitopes for all antibodies belonging to the IGHV3-15/IGLV1-40 class. Moreover, all competed for binding on the GP with mAb114. This hinted at a target epitope within the GP1 core possibly participating in virus binding to host cells. To decipher the exact binding sites, three antibodies 1T0227, 3T0265 and 5T0180 were selected for structure analyses. They fully neutralized virus at concentrations of 1.86, 0.44 and 12.5 $\mu\text{g}/\text{mL}$, respectively (**Appendix Table 12**). Although derived from three independent vaccinated donors, we found that the selected antibodies overall target the same epitope on the trimeric EBOV GPΔMLDΔTM (**Figure 26A**), which becomes very clear in an overlay (**Figure 26B**). By their binding angle, which is antiparallel to the viral membrane, three mAbs can bind to each GP trimer simultaneously. Electron density maps of 1T0227 and 3T0265 suggest the location of the partial antibody Fc

fragment and it may be hypothesized that the Fc position may easily allow the recruitment of FcR-expressing cells (**Figure 26A** Insets Electron density maps). Previous competition ELISAs had revealed that IGHV3-15/IGLV1-40 class antibodies competed for GP binding with the survivor-derived mAb114. Therefore, we created an overlay of an EBOV GP in complex with an IGHV3-15/IGLV1-40 class antibody using 5T0180 as an example and included the published structure of mAb114 VH (blue) and VL (violet) (**Figure 26C**). Although not being completely convergent, the Fabs of mAb114 and 5T0180 partially overlap in the model, validating the observed competition. By approaching the GP in different angles, mainly the VH regions are located in nearby regions while VL are positioned further apart. IGHV3-15/IGLV1-40 antibodies avoid binding to the glycan cap (turquoise). mAb114 on the other hand interacts with the glycan cap. mAb114 is described to neutralize the virus via blocking the receptor-binding domain, thereby preventing virus binding to its host cell receptor Niemann-Pick C1 (NPC1) (Cohen-Dvashi et al., 2020). To evaluate, whether antibodies of the IGHV3-15/IGLV1-40 class occupy the same region on GP as NPC1, we superimposed the antibody 5T0180 as an example bound to EBOV GP and included the structure of NPC1 from a model showing binding to EBOV GP (**Figure 26D**). In fact, 5T0180 and NPC1 occupy the same epitope on the GP1 core as the two proteins clash in the overlay.

We therefore conclude that they cannot bind at the same time and that IGHV3-15/IGLV1-40 antibodies are likely to sterically prevent binding of GP to NPC1. Next, we wanted to identify the exact binding mode between antibodies 1T0227, 3T0265 and 5T0180 with GP and found that contacts can be mapped to three sites (**Figure 26E**). GP residues 114-119 form a loop (blue, termed 'Main I') consists of GP residues 144-146 which is buried in a groove between VH and VL domains. A second loop (green, termed 'Main II') consists of GP residues 144-146 and is located in the same burial but faced towards the VL. Two additional amino acids at positions 231 and 224 (black, termed 'Auxiliary' region) are also targeted by VL of antibodies. The heavy chain of Fab fragments was found to play a minor role in GP binding (**Figure 26F**). The CDRH1 and CDRH2 amino acids Trp33 and Asp56, respectively, interact with the Main region. Previous alignments had revealed a lack of convergence in CDRH3 regions (**Figure 25C** upper panel). In concordance, none of the highly diverse CDRH3 regions of 1T0227, 3T0265, or 5T0180 showed a common conformation like the rest of the heavy chain. Moreover, the CDRH3 regions barely interacted with GP. This finding was interesting, as the CDRH3 is often a key domain building the paratope. In contrast to heavy chains, and in particular to the CDRH3 domains, the number of contact sites between the light chains with GP seems to be less restricted (**Figure 26G**). The CDRL3 amino acid Tyr94 contacts Pro116 of the Main region by hydrophobic interaction. CDRL1-Tyr34 and CDRL3-Asp100 both contact residues of the Main II region (Pro146 and Thr144, respectively). Asp100 moreover forms a hydrogen bond to Gly224 belonging to the GP Auxiliary region.

Altogether, IGHV3-15/IGLV1-40 antibodies are of almost identical conformation and binding to the trimeric GP is mainly facilitated by light chains. They bind to the very apical part of the GP1 core, partly blocking the receptor binding domain.

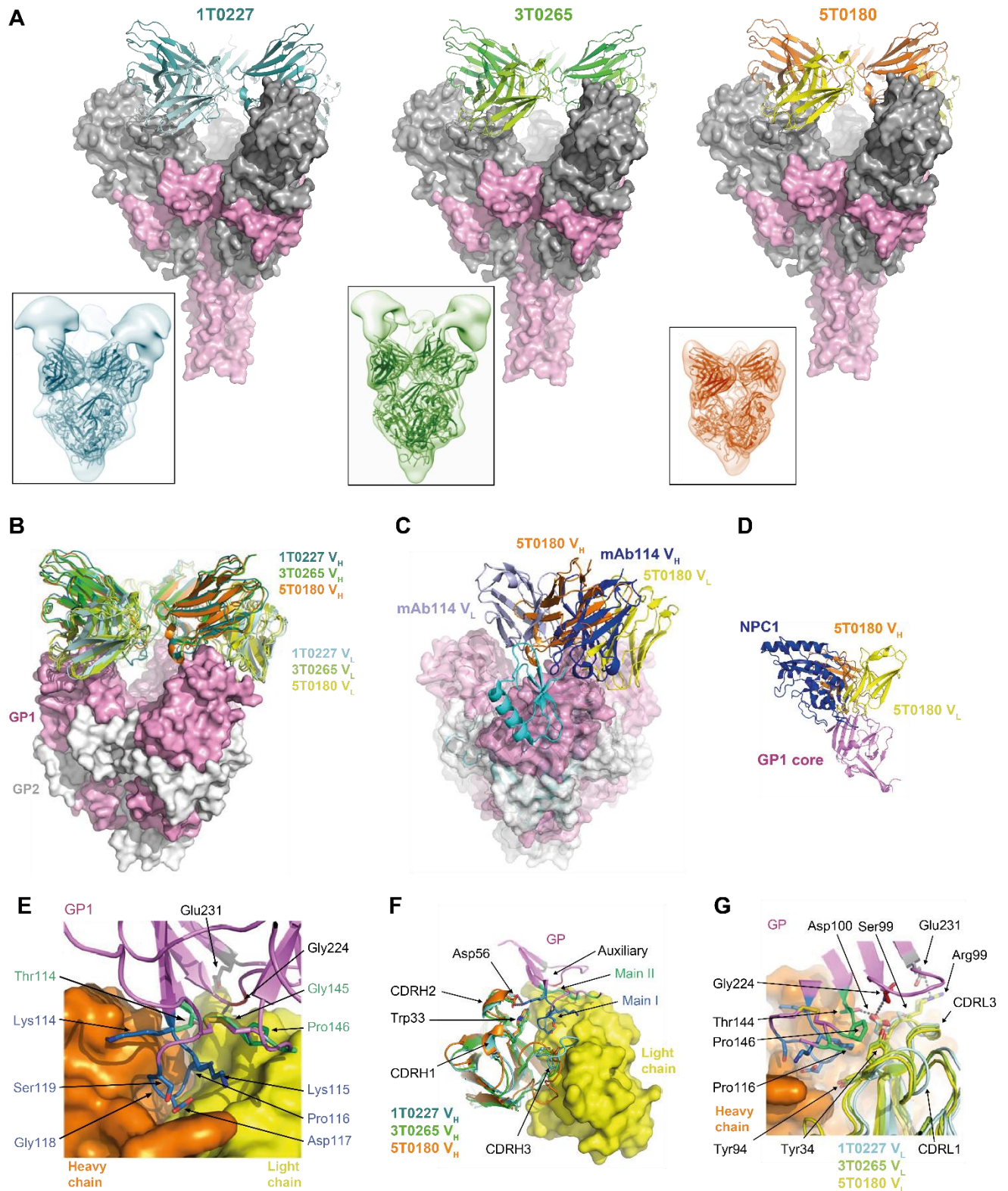


Figure 26. Antibodies of the IGHV3-15/IGLV1-40 class exhibit nearly identical binding mode and block receptor binding site.

(A) Antibody fractions for antigen binding (Fabs) of 1T0227 (left panel), 3T0265 (middle panel) and 5T0180 (right panel) in ribbon representation. Darker ribbons visualize V_H (cyan, green and orange, respectively), while V_L are depicted in brighter colors (light blue, light green and yellow, respectively). V_HV_L structures are represented in complex with the trimeric EBOV GP Δ MLD Δ TM, which is illustrated using surface representation, colored grey and pink for GP1 and GP2, respectively. Complexes are depicted in side views. Insets show the complete EBOV GP Δ MLD Δ TM/mAb model as ribbons inside semi-transparent and 15 Å low-pass-filtered, computed density maps. Density maps span the EBOV GP core and the V_HV_L regions of the Fabs and are mostly lacking density for the EBOV GP stalk and for the CH1CL regions of the Fabs. (B) Superimposition based on the three EBOV GP Δ MLD Δ TM/mAb models from (A). All mAbs recognize the same region of the GP1 core. GP1 and GP2 are colored pink and light grey, respectively. (C) VH3-15/V λ 1-40 mAbs use a different binding mode for targeting GP compared with mAb114. Superimposition of EBOV GP / 5T0180 with mAb114 bound to GP (PDB: 5FHC). The structures are shown from two different point of views for clarity. The glycan cap from the GP / mAb114 structure is indicated. mAb114 binds a similar region on the GP1 receptor binding site but with an opposite orientation that places its light chain at a distant location compared with mAb 5T0180. (D) IGHV3-15/IGLV1-40 class mAbs sterically block receptor binding site Niemann-Pick C1 (NPC1). Superimposition of a single EBOV GP/5T0180 protomer (colored as in (B)) with the model of NPC1 (blue) bound to EBOV GP (PDB: 5F1B, showing NPC1 only). (E) Close-up views of the main contacts between EBOV GP (in ribbon representation) and 5T0180 (in surface representation), using the same color scheme as in (B). (F) Contacts of 1T0227, 3T0265 and 5T0180 V_H (in ribbon representation) to GP1 (in ribbon representation) are limited for CDRH1 and CDRH2 and absent for CDRH3. 5T0180 light chain as representative light chain is displayed in ribbon representation. Color scheme as in (B). (G) 1T0227, 3T0265 and 5T0180 V_L (in ribbon representation) account for the main binding contacts to GP1 (in ribbon representation). 5T0180 heavy chain as representative heavy chain is displayed in ribbon representation. Color scheme as in (B).

3.2.9.2 Strong neutralizers 3T0331 and 4m0368

Apart from IGHV3-15/IGLV1-40 antibodies, we wanted to reveal structures of two exceptionally potent neutralizers from two donors with activities exceeding those of reference antibodies from EVD survivors. At the time structure analyses were initiated, the most potent rVSV-ZEBOV-induced antibodies identified here were 3T0331 and 4m0368, which fully neutralized live EBOV *Mayinga* at concentrations of 0.01 μ g/mL for and 0.13 μ g/mL, respectively (**Appendix Table 12**). These activities are comparable or superior to reference antibodies (**Figure 23**). 3T0331 did not bind sGP but competed with KZ52 and mAb100 for binding to GP. Additionally, the peptide library ELISAs revealed a hit contributing to the IFL region. Therefore, the target epitope of this antibody could roughly be mapped to GP2 with components of GP1. 4m0368 did not react with sGP either, and also competed with KZ52 and mAb100, albeit with lower affinity than 3T0331. Peptide library assays moreover revealed a hit located in the GP1, suggesting that also 4m0368 binds a

structural epitope composed of GP1 and GP2, but might include a larger fraction of GP1 than 3T0331.

In concordance with and further elucidating our previous results, structure analyses showed that 3T0331 binds to an epitope of the N-terminal region of GP1 and limited parts of GP1 at the side of the trimeric GP (**Figure 27A**). The binding angle likely positions the Fc part of 3T0331 close to the viral membrane and it can be speculated that this may cause limited accessibility to FcR-expressing cells (**Figure 27A** inset). The main contacts with EBOV GP are made by the burial of EBOV GP-Val505 in a hydrophobic pocket, and a series of polar contacts that include salt bridges between EBOV GP-Glu502 and two arginine residues from the heavy and the light chains (Arg101 & Arg91, respectively), a hydrogen bond between heavy chain Asn54 and a main chain carbonyl of EBOV, a salt-bridge between EBOV GP-Asp552 and heavy chain Lys65, and a hydrogen bond between EBOV GP-Arg54 and light chain Gln27 (**Figure 27B**).

Interestingly, the epitope of 3T0331 was found to partially overlap with the survivor-derived KZ52 (Lee et al., 2008; Maruyama et al., 1999) (**Figure 27E**, left). Moreover, the epitope was also partially shared with antibodies C2G4 and C4G7 of the ZMapp cocktail, which has been used therapeutically during the 2013-2016 epidemic in West Africa and in the current epidemic in the DRC (Group et al., 2016; Kupferschmidt, 2019; Pallesen et al., 2016; Qiu et al., 2011).

In slight deviation to results of the peptide library analysis, 4m0368 was found to bind an epitope, which is exclusively limited to residues from the GP2 portion, except of a glycan attached to EBOV GP1-Asn563 (**Figure 27C**). The angle by which 4m0368 approaches the side of the trimeric EBOV GP may position its Fc portion further away from the membrane, possibly making it more accessible to immune effector cells (**Figure 27C** inset). A central interaction is formed by the heavy chain Tyr102 that intercalates between the GP-Asn563-linked glycan and GP-Leu529 (**Figure 27D**). Additional interactions include the burial of GP-Ile527 in a hydrophobic pocket, a hydrogen bond between GP-Trp531 and heavy chain His101, a hydrogen bond between GP-Gln521 and light chain Tyr92, as well as a close contact salt-bridge and a hydrogen bond between GP-Glu564 and heavy chain Arg55 and Tyr54, respectively.

Of note, the epitope of 4m0368 was found to partially overlap with the one reported for the survivor-derived mAb100, which was shown to confer a certain degree of protection to challenged NHP (**Figure 27E**, right) (Corti et al., 2016; Misasi et al., 2016).

In summary, these structures showed that rVSV-ZEBOV vaccination leads to the development of antibodies targeting similar epitopes as antibodies obtained from EVD survivors (KZ52 and mAb100) or vaccinated animal models (C2G4 and C4G7), which are applied for therapy and/or clinically tested. In contrast to the chimeric ZMapp antibodies C2G4 and C4G7, 3T0331 and 4m0368 are entirely of human origin, which may have beneficial effects regarding efficacy, *in vivo* stability, and tolerability, thus making 3T0331 and 4m0368 interesting candidates for *in vivo* analyses.

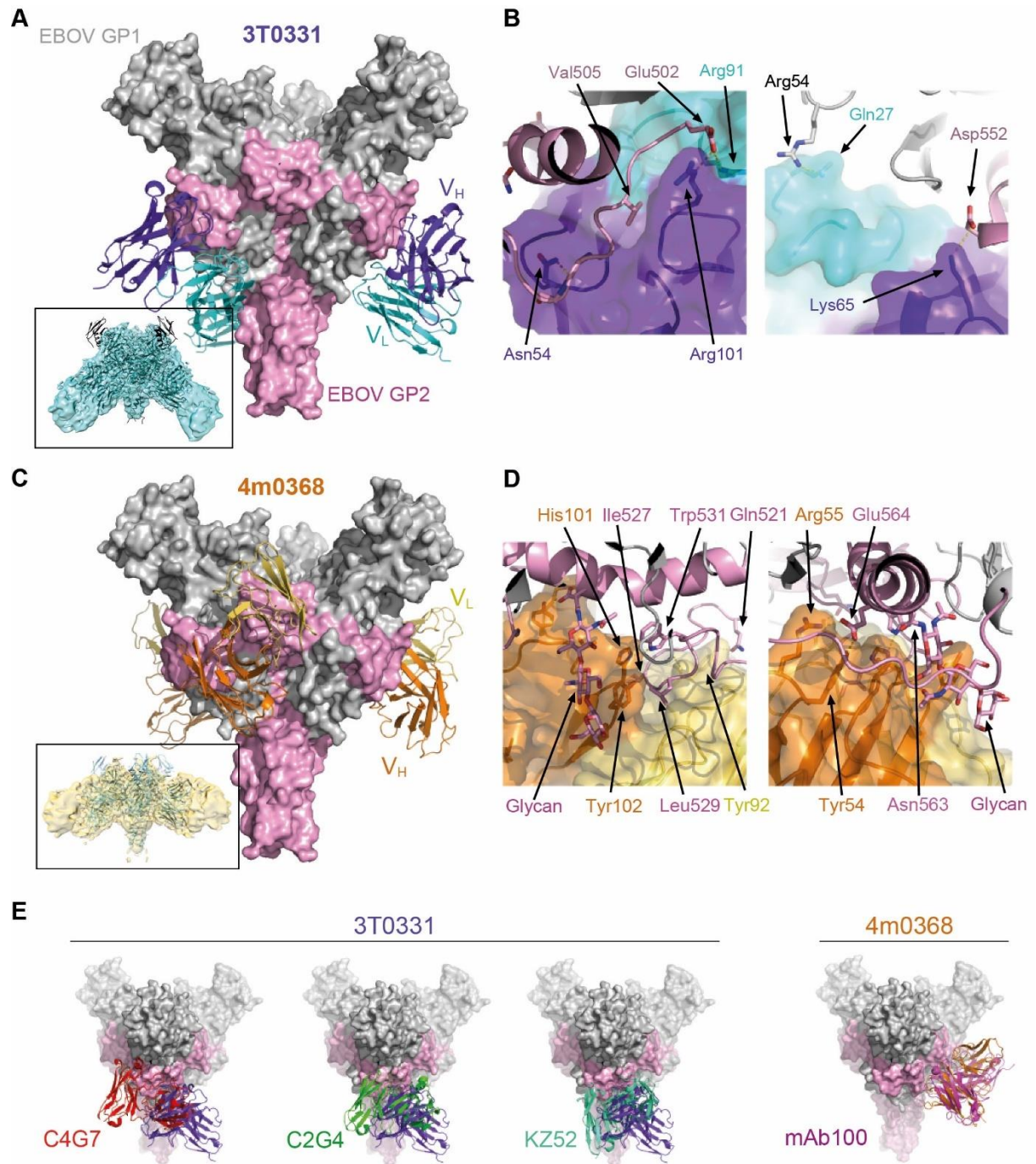


Figure 27. Neutralization determinants of mAbs 3T0331 and 4m0368.

(A) Structure of 3T0331 V_H (purple) and V_L (cyan) in ribbon representation bound to the trimeric EBOV GP, which is illustrated using surface representation, colored grey and pink for GP1 and GP2, respectively. Inset shows the complete EBOV GP/3T0331 model in the computed electron density (transparent cyan).

(B) Close-up views of the main contacts between 3T0331 and EBOV GP using the same color scheme as in (A). EBOV GP is shown in ribbon and 3T0331 is shown using semi-transparent surface representation. The main polar interactions are illustrated with a yellow dashed line.

(C) Structure of 4m0368 V_H (orange) and V_L (yellow) in ribbon representation bound to the trimeric EBOV GP represented using the same color scheme as in (A). Inset shows the complete EBOV GP/4m0368 model in the computed electron density (transparent yellow).

(D) Close-up views of the main contacts between 4m0368 and EBOV GP, using the same color scheme as in (C).

(E) Comparison EBOV GP recognitions sites of 3T0331 (left) with therapeutic antibodies C2G7 (PDB: 5KEN, left image, red), C2G4 (PDB: 5KEL, middle image, green) and KZ52 (right image, turquoise) as well as 4m0368 (right) to mAb100 (PDB: 5FHC, magenta).

4 Discussion

4.1 Analysis of the rVSV-ZEBOV antibody response

4.1.1 Objectives

In our study, we sought to perform in depth analyses on the human B cell and antibody response to rVSV-ZEBOV vaccination in humans (Agnandji et al., 2016). In this project, it was elucidated for the first time i) whether rVSV-ZEBOV vaccination induces clonal expansion and memory formation of EBOV GP-specific B cells; ii) which genetic and functional characteristics the vaccination-induced antibodies have and whether the response is reproducible among vaccinees; and iii) how vaccine-induced antibodies compare to those induced by EVD infection with regards to quantity, quality, durability, genetic as well as functional characteristics. These investigations should help to unravel the mode of action of rVSV-ZEBOV and evaluate its quality.

4.1.2 Considerations for characterizing the rVSV-ZEBOV-induced antibody response

A good vaccine should induce immune responses which closely resemble natural immune responses as observed in survivors of a disease. However, clear determinants of immunity to Ebola virus are not fully defined (Medaglini & Siegrist, 2017; Meyer, Malherbe, & Bukreyev, 2019; Rechten et al., 2017; Sapphire, Schendel, Fusco, et al., 2018), which made the evaluation of this vaccine challenging. In the past, a variety of analyses has been performed to evaluate the potential of vaccine-induced antibodies from animal models or from EVD survivors (Meyer et al., 2019; Sapphire, Schendel, Fusco, et al., 2018). These included binding assays, determination of target epitopes, various neutralization assays or different animal models. We therefore compared several characteristics and potential correlates of protection between EBOV GP-specific B cells identified in vaccinees to those reported in EVD survivors.

4.1.3 Analyzing the serum IgG response after vaccination is not a reliable determinant of immunity

First, we evaluated the EBOV binding and neutralization capacity of rVSV-ZEBOV vaccinee sera. Historically, EBOV-specific serum antibody titers or neutralizing capacity of convalescent patients have been evaluated and were considered a correlate of immunity (Meyer et al., 2019). Therefore, the assumption was made that the serum Ig titer could be consulted as a predictor of successful immunization (Marzi et al., 2013; McElroy et al., 2015). In all vaccinated donors, we observed higher EBOV-specific antibody serum titers compared to non-immunized donors (**Figure 11**). The

immunogenicity of rVSV-ZEBOV was therefore reliable. In order to set them into context with natural infection, next we compared antibody titers after vaccination across doses or to titers observed after overcoming infection. Although we observed 13-fold higher binding (**Figure 11**) and on average 3-fold more potent neutralization in survivors compared to vaccinee sera (**Figure 22**), these data only reflect single time points, which do not necessarily mirror the peak of antibody concentrations achieved after vaccination. Furthermore, sera of survivors have not been collected in the course of this study but have been provided by AG Becker. The time that had passed from infection until sample collection is concealed due to anonymization of the respective donors and samples. Others report an approximately 10-fold higher neutralization after natural infection than in vaccinees (Thom et al., 2021). Determining precise numbers is difficult, as different studies have used different assays, responses are highly variable and donor-dependent, various vaccine doses were administered, and sera were obtained at different times after infection or vaccination, respectively (Agnandji et al., 2016; Dahlke et al., 2017; Ehrhardt et al., 2019; Angela Huttner et al., 2018; A. Huttner et al., 2015; Khurana et al., 2016; Thom et al., 2021). Recently, a longitudinal analysis of EVD survivors showed that serum antibody levels are not constant but fluctuating after recovery and undergo periodic re-stimulation and increase of antibody levels, after a phase of decline (Adaken et al., 2021). Antibody levels neither in survivors nor vaccinees can therefore serve as a static mark for comparison. Moreover, vaccinees with lower antibody titers compared to EVD survivors were protected against EBOV infection as evidenced by tremendously decreased infection rates in rVSV-ZEBOV vaccinees during the West African EBOV outbreak (Ana Maria Henao-Restrepo et al., 2017). Heterogenous antibody responses have also been described for other vaccines (Antia et al., 2018). Thus, the question arose whether antibody titers after vaccination could really be consulted as correlates of protection (Meyer et al., 2019). We conclude from our results and findings of others that serum antibody responses after infection or vaccination are not suited as readout to monitor vaccination success or persistent immunity and therefore should not be considered as reliable determinants of protection. Instead, we propose that rather the antibody quality than quantity needs to be evaluated both in naturally acquired and vaccine-induced immunity against EBOV. Comprehensive analyses on a single cell level were necessary to inform on immunity, which are discussed in the following.

4.1.4 GP-specific memory B cells are less abundant after vaccination than after infection

On a cellular level, we compared the quantity of EBOV GP-specific memory B cells in immunized donors to an EVD survivor to set the frequency of EBOV GP-specific antibodies after rVSV-ZEBOV vaccination into a context between absent and prominent response. In flow cytometric analyses, we compared the frequency of EBOV GP-reactive B cells in rVSV-ZEBOV-vaccinated individuals, a re-convalescent EVD survivor and donors that had never encountered EBOV GP

antigen (**Figure 12**). It was observed that the survivor had 4.4 to 11-fold more EBOV GP-specific B cells than the vaccinated individuals. Importantly, PBMCs of vaccinees were obtained 2 years after immunization. This showed for the first time that EBOV-specific B cells can be detected in vaccinees years, while Khurana *et al.* reported that in rVSV-ZEBOV vaccinees the number of specific antibodies peaks at 3 months post immunization and rapidly declines in the following (Khurana *et al.*, 2016). PBMCs of the EVD survivor were obtained only 51 days after disease onset and it may be speculated that the population of specific B cells was still expanded. Therefore, it cannot be concluded that natural infection *per se* induces 4 to 11-fold higher numbers of specific B cells compared to rVSV-ZEBOV vaccination. It may only be speculated that natural infection and presence of viral antigen within the patient for months will foster the expansion of EBOV GP-specific B cells more pronounced than a single dose of vaccination.

4.1.5 rVSV-ZEBOV vaccination induces infrequent mutations in antibodies comparable to natural infection

We next evaluated the level of SHM of rVSV-ZEBOV-induced B cells by monitoring the % of germline identity on a single cell level (**Figure 13**). In many viral infections such as HIV, antibodies undergo several rounds of SHM to increase affinity and neutralizing potency against viruses – often by extensive mutations in the CDRH3 (Corti & Lanzavecchia, 2013). In case of EVD survivors, however, antibodies with a low number of germline mutations may already potently neutralize viruses (Bornholdt *et al.*, 2016; Corti *et al.*, 2016), and own unpublished observations). We found that a single dose of rVSV-ZEBOV vaccination resulted in similar mutation levels across vaccinees and comparable to survivors (own unpublished observations). Hence, a boost vaccination is not required in order to enhance SHM of EBOV-specific antibodies. Subsequently, we evaluated classical characteristics such as cross-reactivity, target epitopes and neutralization capacity of the rVSV-ZEBOV-induced monoclonal antibodies of vaccinees.

4.1.6 rVSV-ZEBOV vaccination induces cross-reactive neutralizing antibodies with a broad epitope spectrum comparable to natural infection

In order to identify target epitopes of individual antibodies, as well as unravel the total epitope spectrum of the rVSV-ZEBOV-induced antibody repertoire, we performed a range of binding and competition assays. Monoclonal antibodies were directed against all domains and regions of the EBOV GP, monitoring a diverse B cell response and target epitope spectrum. Remarkably, the frequency at which individual rVSV-ZEBOV-induced antibodies were directed to the different epitopes of GP closely resembled the pattern target epitopes of EVD survivor-derived antibodies (Ehrhardt *et al.*, 2019; Sapphire, Schendel, Fusco, *et al.*, 2018). Targeted epitopes were the Head, Glycan Cap, MLD and non-defined epitopes present on the GP1 domain of GP, as well as HR1/2 and MPER regions on the GP2 domain. Additionally, some antibodies recognized structural

epitopes spanning both the GP1 and GP2 domains (**Figure 19, Figure 20**). The neutralization capacity of rVSV-ZEBOV-induced antibodies was in the range of previously reported antibodies from human survivors and sometimes even exceeded their potency (**Figure 23**). In order to find correlations of antibody characteristics and neutralization capacity, which is the lead predictor to protection, we separately compared target epitopes of neutralizing and non-neutralizing antibodies (**Figure 24**). Epitopes of the GP1 domain are also present on the five-fold more abundant sGP, which has for a long time been hypothesized to serve as an immune evasion mechanism by preventing virus neutralization by capturing antibodies (Illykh et al., 2016; Mohan, Li, Ye, Compans, & Yang, 2012; Sanchez et al., 1996). However, we did not observe that sGP-reactivity diminished EBOV neutralization *in vivo* (**Appendix Table 10** and **Appendix Table 12**). On the contrary, we found that nearly two third of neutralizing antibodies were directed against epitopes present on the GP1 domain, while non-neutralizing antibodies were GP1-specific in one third of cases (**Figure 24**). Supportingly, several studies investigating numerous reported EBOV GP-specific antibodies including those of EVD survivors showed that sGP-directed antibodies confer protection *in vivo* and are not correlated with survival of NHPs (Bornholdt et al., 2016; Corti et al., 2016; Davis et al., 2019; Olinger et al., 2012; Sapphire, Schendel, Gunn, Milligan, & Alter, 2018). mAb114 (now referred to as Ansumimab and sold under the tradename Ebanga) – the only human monoclonal antibody licensed for therapy of EVD – is known to be sGP-reactive but protects humans (Corti et al., 2016; FDA, 2020a; Misasi et al., 2016; Mulangu et al., 2019). We found that MLD-binding antibodies were rarely neutralizing EBOV *in vitro* (**Figure 24**), which is concordant with other analyses (Davis et al., 2019; Sapphire, Schendel, Fusco, et al., 2018). We found that neutralizing antibodies were to a large proportion targeting the GP1 domain. This may be contributed to the exposed position of GP1 (Lee et al., 2008), making it easily accessible by antibodies. Others have found mixed results for neutralization capacities of GP1-directed antibodies; While Sapphire and colleagues found that only a low number of GP1 Glycan Cap- and Core-directed antibodies neutralized EBOV, they found nearly all Base- and Head-directed antibodies to be neutralizing (Sapphire, Schendel, Fusco, et al., 2018). On the other hand, KZ52 – an antibody targeting the GP1 base (Lee et al., 2008) – did not confer protection to NHPs (Qiu et al., 2014). We identified that a small proportion of the rVSV-ZEBOV-induced antibodies targeting GP2 were neutralizing (**Figure 24**). This was surprising, as Sapphire and colleagues saw a clear correlation of GP2 IFL and HR2-directed antibodies to neutralization and protection *in vivo* (Sapphire, Schendel, Fusco, et al., 2018). Findings for GP1 and GP2 thus remain inconclusive and a clear correlation of antibody target epitope and *in vivo* protection needs further investigation. Binding to the MLD is negatively correlating to neutralization and protection.

Another desired antibody feature is the ability to cross-neutralize other filoviruses. Therefore, we evaluated the cross-reactivity of rVSV-ZEBOV-induced antibodies to other Filovirus species, which might possibly indicate cross-neutralizing protective characteristics

against other filoviruses. We found that more than half of EBOV GP-binding antibodies were cross-reactive to one or more other species (**Figure 21**). This proportion was slightly higher than described in survivors and immunized animals (Saphire, Schendel, Fusco, et al., 2018). To elucidate whether we could identify link between target epitopes and cross-reactivity, we compared epitope spectra of species-specific or cross-reactive antibodies. Those that bound to the MLD, which is highly diverse across Ebolaviruses, were rarely cross-reactive (**Figure 21**). Others have not identified MLD-targeting cross-reactive mAbs (Saphire, Schendel, Fusco, et al., 2018). We and others found that antibodies, which bound to the rather conserved GP2 domain comprising the IFL and HR1/2 and MPER regions, were cross-reactive (**Figure 21** and (Saphire, Schendel, Fusco, et al., 2018)). rVSV-ZEBOV-induced antibodies directed to structural epitopes including GP1 and GP2 portions, did not show a tendency towards species-specificity or cross-reactivity. Neither was the case for sGP-directed antibodies. These findings are in line with results from others, further supporting that rVSV-ZEBOV vaccination leads to an authentic repertoire of Ebolavirus antibodies (Saphire, Schendel, Fusco, et al., 2018). However, their and our findings do not provide a clear conclusion on which epitopes are correlated to cross-reactivity. Moreover, none of the vaccine-induced antibodies that were cross-reactive with SUDV GP in a binding assay was able to neutralize the virus *in vivo* (**Appendix Table 10** and **Appendix Table 12**). Saphire and colleagues did not report whether they tested SUDV neutralization capacity, thus not allowing conclusions on cross-neutralization potential of survivor and animal-derived antibodies (Saphire, Schendel, Fusco, et al., 2018).

We could show in this project, that the vaccine-induced antibodies compare to those of EVD survivors by performing binding, competition, neutralization assays and structural analyses. This argues for a good vaccine design that provides the full antigenic diversity and induces antibody responses, which are resembling those of EVD survivors and comprises antibodies targeting the entire epitope spectrum of the EBOV GP. We conclude that MLD-reactivity of antibodies is negatively correlated with neutralizing potential and cross-reactivity to other filoviruses. Hence, specificity for this domain could serve as an exclusion criterium for closer evaluation of monoclonal antibodies as therapeutic candidates or determinants of immunity. Apart from this domain, we found no clear link between neutralization capacity, cross-reactivity and epitope spectra, which could serve for the early identification of promising antibodies in screens for cross-reactive, neutralizing and potentially protective antibodies.

Another hallmark of successful vaccination is the consistent immune response across vaccinees. Besides the comparison of the immune responses in a single vaccinee to those of survivors of natural infection, it is therefore important to perform comparisons between several vaccinated individuals. This provides insights on the fidelity of the immunization success. Therefore, we next closely evaluated the sequences of rVSV-ZEBOV-induced antibodies in individual vaccinees and compared them to each other.

4.2 Analysis of sequence convergence in antibodies

4.2.1 IGHV3-15/IGLV1-40 class antibodies are recurrently induced by rVSV-ZEBOV vaccination

In order to do so, we compared the total memory B cell repertoire of individual donors to their EBOV GP specific memory B cell compartment. We found that IGHV3-15 and IGLV1-40 were significantly increased in the EBOV specific population. Similarly, others have reported that antigen-experienced repertoires showed significant enrichments or depletions of some V and J gene segment families compared to naïve B cell repertoires (Wu et al., 2010). The identification of a shift in VH gene frequency in naïve vs. antigen-experienced BCR repertoires shows that for counteracting pathogens certain combinations of gene segments are preferred over others (DeKosky et al., 2016; Wu et al., 2010). Further resolution to particular VH gene segments and VL gene segment pairings was provided by several reports on viral infections and vaccinations. Elsewhere, preferred VH combinations across donors have also been referred to as convergent, recurrent, public or multi-donor antibodies or clonotypes. Of note, these terms are frequently also used for analyses merely focusing on the VH gene segments without considering the paired VL gene segments (Davis et al., 2019; Godoy-Lozano et al., 2016; Jackson et al., 2014; Nielsen, Yang, Jackson, Hoh, Roltgen, Jean, et al., 2020; Tian et al., 2008; Zhou et al., 2015). A consistent and distinguishing terminology and analysis approach within the scientific community would simplify review of available data and the evaluation of their impact.

Several groups have reported preferred VH/VL gene segment pairings in antigen-specific antibodies of convalescent patients. For example, in Zika virus patients, expanded B cell clones specifically pairing IGHV3-23 and IGKV1-5 chains have been reported. These additionally cross-reacted with Dengue virus (Robbiani et al., 2017). Convergent antibodies have also been identified in West Nile Virus survivors (Throsby et al., 2006). In Lassa virus survivors, pairing of IGHV3-21 with IGLV2-14 was described (Hastie et al., 2019). A combination of IGHV3-30/IGKV3-11 was frequent in antibodies neutralizing human cytomegalovirus (Thomson et al., 2008). In Hepatitis B virus-associated acute liver failure, IGHV1-3 was preferred across donors and almost exclusively paired with IGKV1 family genes (Farci et al., 2010). For HIV-1, preferred usage of IGHV1-69 has been reported in gp41-directed mAbs amongst infected individuals (Setliff et al., 2018). Additionally, antibodies with similar characteristics have been described convergently evolving from similar IGHV gene segments IGHV2 or IGHV1-46 paired with likewise similar LC V gene segments IGKV3-11, IGKVID-33 and IGLV1-47 (Scheid et al., 2011). In several reports on EVD survivors, antibodies utilizing IGHV3-13 including mAb114 have been described (Bornholdt et al., 2016; Corti et al., 2016; Davis et al., 2019) but no preferred VL gene segments are reported. Less is known about convergent antibodies in vaccinated individuals. In infants vaccinated against the bacterium *Haemophilus influenzae* type b, IGHV3-23/IGKV2D-29 antibodies are

reported (Lucas et al., 2003). Upon Influenza A vaccination, IGHV6-1/IGKV3-1 combining neutralizing antibodies were detected across vaccinees (Joyce et al., 2016). A recent study reported preferred VH gene segments as a response to vaccination against SARS-CoV-2. Both, the BioNTech-Pfizer as well as the Moderna mRNA vaccines triggered a significant increase in IGHV3-53 and IGHV3-30 across vaccinees (Z. Wang et al., 2021). Several VL gene segments were increased significantly, with IGKV1-39, IGKV1-33, IGLV3-21 being found in 50% of reported sequences. Sequences sharing identical combinations of VH/JH and VL/JL gene segments were identified across Moderna and BioNTech-Pfizer vaccinees, and, moreover, in convalescent COVID-19 patients (Z. Wang et al., 2021).

Here, we showed that in all four investigated subjects vaccinated with rVSV-ZEBOV, several V gene segments of HC were increased in the EBOV GP-specific repertoire of memory B cells compared to their total memory BCR repertoire (**Figure 15, Appendix Table 5, Appendix Table 6, Appendix Table 7, and Appendix Table 8**). Particularly IGHV3-15 was significantly preferred in every individual. Antibodies utilizing IGHV3-15 were paired with IGLV1-40 in 80% of analyzed monoclonal antibodies (**Figure 25**). In the dataset of Bornholdt and colleagues, an IGHV3-15/IGLV1-40 class antibody could also be identified in a survivor of the 2014 West African epidemic (Bornholdt et al., 2016). Interestingly, another group has also identified IGHV3-15/IGLV1-40 class antibodies after vaccination against EBOV (Rijal et al., 2019). These were found in six individuals after immunization with a recombinant chimpanzee adenovirus 3 (ChAd3-EBOZ) and boost vaccination with modified vaccinia Ankara exposing GPs from the filoviruses EBOV strain *Mayinga*, SUDV strain *Gulu*, MARV strain *Musoke* and the TAFV nucleoprotein (MVA-BN Filo) (Rijal et al., 2019). In addition to their identical genetic composition and shared mutations, IGHV3-15/IGLV1-40 class antibodies exhibited same functional characteristics (**Appendix Table 10 and Appendix Table 12**). They bound to EBOV GP but showed low cross-reactivity with other Filovirus GPs (Ehrhardt et al., 2019; Rijal et al., 2019). They targeted the same epitopes on GP and competed for binding with each other (Cohen-Dvashi et al., 2020; Ehrhardt et al., 2019; Rijal et al., 2019). All rVSV-ZEBOV-induced IGHV3-15/IGLV1-40 class antibodies neutralized EBOV *in vitro* (Ehrhardt et al., 2019), which remains the most reliable predictor for *in vivo* protection (Saphire, Schendel, Fusco, et al., 2018). Finally, structural analyses verified identical epitopes and binding angles within the group. Importantly, the binding approach of IGHV3-15/IGLV1-40 class antibodies to EBOV GP closely resembled binding of the survivor-derived mAb114 (Cohen-Dvashi et al., 2020) (**Figure 26**). mAb114 neutralizes the virus by blocking the NPC1, thereby inhibiting the first step of virus entry to target cells (Carette et al., 2011). In a clinical trial, mAb114 reduced case fatality from 67% to 32% (Kupferschmidt, 2019). It is the first monoclonal antibody with approved licensure as treatment against EBOV (FDA, 2020a). Due to a similar binding approach, it may be hypothesized that antibodies of the IGHV3-15/IGLV1-40 class are of efficacy and are thus promising candidates

for future analyses. More importantly, these results show that a single dose vaccination reproducibly facilitates the induction of a class of antibodies that compares to the therapeutically and protective mAb114. Finally, it highlights the opportunity to identify efficacious therapeutic candidates from vaccinated individuals additionally to conventional studies of disease survivors.

The independent identification of the same combination of two preferred VH and VL gene segments after vaccination with two distinct Ebolavirus vaccines (Ehrhardt et al., 2019; Rijal et al., 2019) strongly argues for a convergent immune response to EBOV-vaccination. Moreover, it indicates a predominant role in EBOV-specific immunity including natural infection. The identification of IGHV3-15/IGLV1-40 class antibodies in two cohorts immunized with vaccines utilizing distinct backbones suggests that their generation is not an artefact induced by influence of the vaccination approach. Their identification in both vaccinee populations thus gives the first evidence that their development in humans was independent of the vaccine backbone, thus supporting the reliability and relevance of such analyses. Both studies analyzed immune responses of participants of phase I clinical studies. These findings should trigger a new awareness to evaluate early clinical studies. They offer the early possibility to isolate a wide range of human antibodies that could greatly improve the knowledge on the particular infectious disease and identify candidates for antibody therapy and prophylaxis that are in no way inferior to antibodies isolated from survivors.

4.2.2 Shared antibodies with nearly identical HC and LC sequences occur across donors after rVSV-ZEBOV vaccination

In addition to the IGHV3-15/IGLV1-40 class antibodies, we described here the identification of several groups of antibodies in distinct vaccinated individuals which we termed shared antibodies (**Figure 16**). These antibodies exhibited a high degree of genetic identity of up to 95% within a group (**Appendix Table 9**). Not only did they share their VH and VL gene segments. Moreover, they exhibited nearly identical CDR3 length and identity in both chains, which is extremely rare and commonly only seen in clonally related cells derived from a mutual B cell ancestor (Glanville et al., 2011). The human immune system is able to generate a sheer endless number of different BCRs and antibodies. The mechanisms of VDJ recombination, NHEJ and pairing of HC with LC stochastically generates 10^{12} BCRs in the naïve repertoire (Sethna, Elhanati, Callan, Walczak, & Mora, 2019). Due to remaining challenges in BCR repertoire analyses, the overall number of clones within an individual has not been fully elucidated. Also, the abundance of nearly identical naïve and antigen-experienced BCR across donors remains the topic of discussion (Briney, Inderbitzin, Joyce, & Burton, 2019; Glanville et al., 2011; Kreer, Gruell, Mora, Walczak, & Klein, 2020; Soto et al., 2019). In addition to their genetically remarkable similarity, antibodies within a shared group also exhibited shared characteristics as specificity for the same target epitopes, cross-reactivity with other filoviruses and neutralization capacity (**Appendix Table 10** and

Appendix Table 12). Some shared groups comprised a small number of sequences and/or spanned sequences from two vaccinees (**Appendix Table 9**). Others were more frequent and comprised sequences of 4 out of 5 investigated subjects. The antibodies within these groups were potent neutralizers or cross-reacted with other Ebolavirus species. Thus, the here identified shared clones are remarkable and should be further investigated to elucidate their potential role in the antiviral response.

In order to evaluate the uniqueness of their identification, we performed identical analyses with HIV-1 envelope-reactive antibodies but were not able to identify similar groups of shared antibodies (**Figure 16**). The emergence of the novel SARS-CoV-2 prompted such comprehensive analyses also in convalescent COVID-19 patients and vaccinated individuals. Convergent antibodies utilizing IGHV1-58/IGKV3-20 and IGHV3-30-3/IGKV1-39 have been observed in several convalescent patients of COVID-19 and their amino acid sequences were over 92% identical across individuals (Robbiani et al., 2020). Likewise, in individuals vaccinated with the Moderna or BioNTech/Pfizer mRNA vaccines, shared antibodies were detected. Importantly, among the preferred VH gene segments was IGHV3-30, which was also found in convalescent COVID-19 patients (Z. Wang et al., 2021). It remains to be clarified why Ju and colleagues did not detect shared antibodies or inter-donor V gene preferences in SARS-CoV-2 patients (Ju et al., 2020). In Dengue survivors, two shared antibody groups with HC and LC sequences of high similarity including identical CDRH3 aa sequence are described. However, their analyses do not reveal whether the two groups originated from distinct donors and is therefore not possible to evaluate their uniqueness (Throsby et al., 2006). Finally, in a very recent publication both convergent antibodies and groups of shared antibodies were identified after administration of a vaccine containing four distinct influenza strains. Antibodies combining IGHV3-9/D2-15/J6 HC with IGLV1-40/J3 LC and >75% CDRH3 aa identity were identified. Moreover, pairings of IGHV3-7/IGHD4-17/IGHJ6 with IGLV3-21/IGLJ1 and highly similar CDRH3 and CDRL3 aa sequences were observed. As only one representative mAb per group was further characterized, it cannot be concluded with certainty whether the remarkable sequence identity is mirrored in similar patterns of binding and neutralizing breadth and potency, target epitopes and other functional and structural characteristics (Forgacs et al., 2021).

In the course of this work, we identified five groups of shared antibodies that were shared between independent rVSV-ZEBOV vaccinated individuals and a survivor of EVD (**Figure 17**). One of them utilizing IGHV3-13 and IGKV3-20. This V gene segment is also part of the therapeutically used mAb114 (Ebanga) and was also frequent in mAbs of other EVD survivors (Corti et al., 2016; Davis et al., 2019). The finding that rVSV-ZEBOV vaccination specifically induced affinity maturation and isotype class switch in naïve B cells, which are nearly identical to those of convalescent survivors and therapeutically effective antibodies, can be considered as an indicator for protective capacity of vaccine-induced antibodies.

B cells of clonal origin from an individual donor share their genetic composition as well as characteristics such as and target epitope specificity (Burnet, 1959). What has been known for clones of an individual donor, could also be shown to be true for shared clones of independent donors in rVSV-ZEBOV vaccination in this project. The characterization of vaccine-induced donor-independent shared and convergent antibody classes strongly indicates that genetic convergence translates to functional similarity. To my knowledge a direct link between shared HC and LC sequences and identical binding approach by structure analysis has not been shown by others before, as publications on shared antibodies are rare. However, the potential was also mentioned in a recent paper investigating the antibody response to SARS-CoV-2 and comprehensively analyzing the antibody HCs (Nielsen, Yang, Jackson, Hoh, Roltgen, Stevens, et al., 2020). This knowledge could be used to expand current antibody databases and libraries by their functionalities. Further, it offers the possibility to evaluate the quality of antibody repertoires already from the sequence before performing binding, neutralization, and challenge assays. Moreover, it offers the possibility for straightforward designing antibodies for therapy *in silico* without the need for elaborate approaches requiring sample material from human donors and subsequent isolation, sequencing, cloning and characterization setups. Finally, the convergent identification of particular antibodies across vaccinated individuals, which are protective in infected individuals, could be considered a novel and true determinant of immunity and an indicator of effective vaccination. Such analyses could help to identify a lead vaccine from several candidates. This could not only be considered for the evaluation of vaccination strategies against EBOV, SUDV and MARV, but also other viral infections.

We and others (Bornholdt et al., 2016; Cohen-Dvashi et al., 2020; Corti et al., 2016; Davis et al., 2019; Ehrhardt et al., 2019; Farci et al., 2010; Hastie et al., 2019; Joyce et al., 2016; Lucas et al., 2003; Rijal et al., 2019; Robbiani et al., 2017; Scheid et al., 2011; Setliff et al., 2018; Thomson et al., 2008; Throsby et al., 2006; Z. Wang et al., 2021) have reported V gene preferences in the development of virus-specific antibodies upon natural infection and vaccination. These preferred convergent antibody responses showed effective and protective characteristics against viruses. Importantly, convergent antibodies could be observed across individuals and, therefore, the development of such antibodies should be considered as determinants of immunity and an indicator of effective vaccination. Our findings have strong implications for the progress of other Filovirus vaccine developments. The antibody responses in individuals vaccinated with the experimental SUDV and MARV vaccines should be comprehensively analyzed to inform on and to compare the quality of the different vaccine candidates and choose a lead candidate for future outbreaks. Moreover, the identified antibodies could serve to confirm known and to identify novel epitopes of vulnerability on the viral GP.

4.3 Achieving cross-protection – the holy grail?

A high percentage of the here described rVSV-ZEBOV-induced antibodies showed cross-reactivity to other Ebolavirus species and rarely even to MARV, but neither sera nor individual mAbs neutralized SUDV *in vitro* (**Appendix Table 12**). We are not aware of any publication to report on SUDV or MARV cross-neutralizing mAbs that were detected in Ebolavirus-vaccinated humans. This is in line with studies in EVD survivors, which show that the specificity of the induced antibody response is largely limited to the species that has caused the infection (Bornholdt et al., 2016; L. B. King et al., 2019). Natural human cross-reactive antibodies are reported, but cross-neutralizing antibodies are generated scarcely (A. I. Flyak et al., 2018; A. I. Flyak et al., 2016; P. Gilchuk et al., 2018; Pavlo Gilchuk et al., 2021; P. Gilchuk et al., 2020; Wec et al., 2017). Likely, convalescent survivors of an EBOV outbreak might not be protected against BDBV, SUDV and MARV. In rVSV-ZEBOV immunized NHPs, a partial protection against BDBV has been reported but animals succumbed when challenged with SUDV (Falzarano et al., 2011; Geisbert et al., 2009). Importantly, the simultaneous immunization of NHP with EBOV, SUDV and MARV GPs elicited a monoclonal antibody neutralizing EBOV, SUDV, BDBV, and RESTV (X. Zhao et al., 2017). Pan-neutralizing antibodies were also reported in mice vaccinated with a combination of EBOV, SUDV, and MARV GPs (Holtzberg et al., 2016). Additionally, immunization with the HR2-MPER region produced neutralizing antibodies in rabbits (A. I. Flyak et al., 2018). These findings prove that the vaccine-induced generation of cross-neutralizing and protective mAbs is in principle possible. The current evidence suggests that this will require immunization with several *Filovirus* GPs. Therefore, designated vaccines against other filoviruses will be necessary in addition to EBOV vaccinations.

Numerous candidates have been developed against BDBV, SUDV and MARV and shown efficacy in non-human primate models, which is considered the gold standard to predict efficacy in humans (Garbutt et al., 2004; Geisbert et al., 2009; S. M. Jones et al., 2005; Reynolds & Marzi, 2017; Suschak & Schmaljohn, 2019; Wolfe, Taylor, & Zarrabian, 2020). Cross-protection against different filoviruses could be achieved by blending different vaccine candidates against pathogenic *Filovirus* species (Geisbert & Feldmann, 2011; Geisbert et al., 2009; Matassov et al., 2018; Suschak & Schmaljohn, 2019), by vaccination platforms utilizing hybrid GP trimers consisting of EBOV-SUDV GP1 domains and MARV GP2 domains (Martins et al., 2015), or by sequentially vaccinating against one species and boosting against one or several other species. It is likely that also for humans, designated vaccinations for the other filoviruses will be needed to confer immunity. As of May 2021, the SUDV vaccine candidate cAd3-EBO-S, was clinically evaluated alone (NCT04041570, NCT04723602) and as bivalent vaccine together with EBOV GP (NCT02368119). Furthermore, a DNA vaccine comprising two plasmids, one encoding EBOV GP and the other encoding SUDV GP (NCT00605514) (<https://clinicaltrials.gov/search?term=sudan+virus>). A DNA plasmid (NCT00605514) and a cAd3-

Marburg vaccine candidate have been tested in clinical trials, too (<https://clinicaltrials.gov/search?term=marburg+virus>) (Suschak & Schmaljohn, 2019). Additionally, the vaccine candidates Ad26-Filo and MVA-BN-Filo, comprising proteinaceous parts of EBOV, SUDV and MARV GP, respectively, have been tested either alone or in with boost vaccination in different order in a clinical trial. To my knowledge, no comprehensive analyses on the molecular B cell response of vaccinees has been performed for any of the trials.

The different approaches have distinct advantages and pitfalls: Blending independent Filovirus vaccines, multivalent vaccines, as well as a vaccination comprising hybrid GPs can be administered in a single dose. In contrast, sequential vaccinations require several doses, which could be difficult to realize in regions of political unrest. It could be argued that sequential vaccinations might increase the quality and quantity of the antibody response due to repeated antigen encountering. However, our results showed that merely a single dose generated potent antibodies comparable to antibodies induced by natural infection in their level of germline sequence mutation, epitope spectrum and neutralizing efficiency (**Figure 13**, **Figure 15**, **Figure 20**, and **Figure 23**). Also others found that a boost vaccination only transiently increases the quantity of specific antibodies but has no permanent effect on antibody quantity or characteristics (NCT02280408) (Regules et al., 2017; Rijal et al., 2019; Suschak & Schmaljohn, 2019). It should be considered, though, that thousands of individuals in the DRC and neighboring countries have received the rVSV-ZEBOV vaccination already. This population will most likely be the ones at risk of Sudan and Marburg virus infections due to partially overlapping endemicity zones. Different vaccination strategies might be required for individuals who have received one of the EBOV-specific regimens and those who have not. VSV-directed immune responses have been observed after rVSV-ZEBOV vaccination (Poetsch et al., 2018). Thus, boost vaccinations utilizing other platforms might be preferable. Additionally, it remains to be elucidated, whether a boost vaccination to those who have received an EBOV GP encoding vaccine before, with a blend or hybrid vaccination of EBOV, SUDV and MARV specific GPs would be the vaccine of choice. Antibodies generated by vaccinees receiving the ChAd3-EBOZ and MVA-BN-Filo boost vaccination were broadly reactive with EBOV, BDBV and SUDV in 20 of 84 cases (Rijal et al., 2019). In vaccinees who received the rVSV-ZEBOV vaccine, we detected antibodies reactive with EBOV, BDBV and SUDV in 24 of 94 mAbs studied (**Figure 18**). This observation indicates that the ChAd3-EBOZ and MVA-BN-Filo boost in comparison to the species-specific rVSV-ZEBOV does not elevate the generation of highly desired cross-reactive antibodies. It is conceivable that a preexisting immunity to EBOV might limit the development of a protective antibody response against other filoviruses. Experiments in animal models should be performed to investigate these questions, to shape the design of future clinical trials in humans. When analyzing and evaluating clinical studies of individuals to receive (boost) vaccinations against SUDV and/or MARV,

longitudinal studies searching for cross-neutralizing antibodies against other EBOV, BDBV, SUDV and MARV in vaccinees should be strived for.

To ultimately prove vaccine efficacy, candidates have to be tested *in vivo* and provide efficacy data in human patients. The unpredictable outbreak nature of Marburg- and Ebolaviruses complicates this requirement. Furthermore, this procedure necessitates the onset of a novel outbreak in order to proceed with vaccine development and licensure. Likely, it will not be possible to test several candidates. Therefore, lead candidates should be defined for each Filovirus already before phase III trials can be performed. Based on the findings of this thesis, I propose that comprehensive molecular analyses comparable to the analyses of this work should be performed for the available SUDV and MARV vaccine candidates and vaccination approaches among the tested options. Comprehensive memory B cell and antibody analyses on the induced SUDV and MARV-specific memory B cell repertoire will help to answer important questions regarding the quantity, polyclonality, convergence, specificity, neutralization and protective capacity, and durability of the vaccine-induced B cell repertoire of the vaccinees. Comparing the findings of vaccinated cohorts enrolled in the different trials to each other and to survivors of SUDV and MARV infections, could identify the vaccination approach that induces the most promising antibody response. The most promising vaccine candidates should therefore be provided for compassionate use upon the next SUDV and MARV outbreaks and be prioritized as the lead candidate for clinical trial studies.

In addition to their implications on vaccine development, the here identified antibodies should be evaluated as therapeutics and post-exposure prophylaxis in infection. Vaccine-induced antibodies can complement the rarely identified pan-neutralizing antibodies or antibody cocktails providing protection against different filoviruses (A. I. Flyak et al., 2018; A. I. Flyak et al., 2016; P. Gilchuk et al., 2018; Pavlo Gilchuk et al., 2021; Wec et al., 2017). This should be of utmost importance, as no therapies to treat MVD or EVD caused by SUDV have been licensed so far. This may have additional implications for other viruses and diseases (Z. Wang et al., 2021). In general, our findings highlight that the analysis of vaccinated individuals can provide chances to identify and isolate antibodies that can serve as therapeutics against viruses.

4.4 Conclusions

In this work, the rVSV-ZEBOV-induced memory B cell and antibody immune response in human vaccinees was analyzed on a single cell level for the first time. Albeit lower than after infection, it could be shown that the vaccine-induced antibody response was durable for more than two years across doses. It was found to be a polyclonal yet convergent antibody response in all vaccinees. This convergence was found on a genetic and functional level. We identified and structurally explained the preference and privileged role of IGHV3-15/IGLV1-40 class antibodies that were present in all donors. Moreover, the quality of rVSV-ZEBOV-induced antibody response was

comparable to that of EVD survivors, which is demonstrated by a nearly identical repertoire of target epitopes, structural analyses and comparable, even exceeding neutralization capacities. These findings also evaluate potential determinants of protection and have implications for future strategies on vaccine design and the identification of therapeutics in viral infections.

5 References

- Adaken, C., Scott, J. T., Sharma, R., Gopal, R., Dicks, S., Niazi, S., . . . Pollakis, G. (2021). Ebola virus antibody decay-stimulation in a high proportion of survivors. *Nature*, *590*(7846), 468-472. doi:10.1038/s41586-020-03146-y
- Adams, P. D., Afonine, P. V., Bunkoczi, G., Chen, V. B., Davis, I. W., Echols, N., . . . Zwart, P. H. (2010). PHENIX: a comprehensive Python-based system for macromolecular structure solution. *Acta Crystallogr D Biol Crystallogr*, *66*(Pt 2), 213-221. doi:10.1107/S09074444909052925
- Agnandji, S. T., Fernandes, J. F., Bache, E. B., Obiang Mba, R. M., Brosnahan, J. S., Kabwende, L., . . . Kremsner, P. G. (2017). Safety and immunogenicity of rVSVDeltaG-ZEBOV-GP Ebola vaccine in adults and children in Lambarene, Gabon: A phase I randomised trial. *PLoS Med*, *14*(10), e1002402. doi:10.1371/journal.pmed.1002402
- Agnandji, S. T., Huttner, A., Zinser, M. E., Njuguna, P., Dahlke, C., Fernandes, J. F., . . . Siegrist, C. A. (2016). Phase 1 Trials of rVSV Ebola Vaccine in Africa and Europe. *N Engl J Med*, *374*(17), 1647-1660. doi:10.1056/NEJMoa1502924
- Alt, F. W., Bothwell, A. L., Knapp, M., Siden, E., Mather, E., Koshland, M., & Baltimore, D. (1980). Synthesis of secreted and membrane-bound immunoglobulin mu heavy chains is directed by mRNAs that differ at their 3' ends. *Cell*, *20*(2), 293-301. doi:10.1016/0092-8674(80)90615-7
- Alt, F. W., Zhang, Y., Meng, F. L., Guo, C., & Schwer, B. (2013). Mechanisms of programmed DNA lesions and genomic instability in the immune system. *Cell*, *152*(3), 417-429. doi:10.1016/j.cell.2013.01.007
- Alvarez, C. P., Lasala, F., Carrillo, J., Muniz, O., Corbi, A. L., & Delgado, R. (2002). C-type lectins DC-SIGN and L-SIGN mediate cellular entry by Ebola virus in cis and in trans. *J Virol*, *76*(13), 6841-6844. doi:10.1128/jvi.76.13.6841-6844.2002
- Antia, A., Ahmed, H., Handel, A., Carlson, N. E., Amanna, I. J., Antia, R., & Slifka, M. (2018). Heterogeneity and longevity of antibody memory to viruses and vaccines. *PLoS Biol*, *16*(8), e2006601. doi:10.1371/journal.pbio.2006601
- Asma, G. E., Langlois van den Bergh, R., & Vossen, J. M. (1984). Development of pre-B and B lymphocytes in the human fetus. *Clin Exp Immunol*, *56*(2), 407-414. Retrieved from <https://www.ncbi.nlm.nih.gov/pubmed/6610515>
<https://www.ncbi.nlm.nih.gov/pmc/articles/PMC1536228/pdf/clinexpimmunol00146-0187.pdf>
- Bah, E. I., Lamah, M. C., Fletcher, T., Jacob, S. T., Brett-Major, D. M., Sall, A. A., . . . Fowler, R. A. (2015). Clinical presentation of patients with Ebola virus disease in Conakry, Guinea. *N Engl J Med*, *372*(1), 40-47. doi:10.1056/NEJMoa1411249
- Baize, S., Leroy, E. M., Georges-Courbot, M. C., Capron, M., Lansoud-Soukate, J., Debre, P., . . . Georges, A. J. (1999). Defective humoral responses and extensive intravascular apoptosis are associated with fatal outcome in Ebola virus-infected patients. *Nature Medicine*, *5*(4), 423-426. doi:Doi 10.1038/7422
- Baize, S., Pannetier, D., Oestereich, L., Rieger, T., Koivogui, L., Magassouba, N. F., . . . Günther, S. (2014). Emergence of Zaire Ebola Virus Disease in Guinea. *New England Journal of Medicine*, *371*(15), 1418-1425. doi:10.1056/NEJMoa1404505
- Barrette, R. W., Metwally, S. A., Rowland, J. M., Xu, L., Zaki, S. R., Nichol, S. T., . . . McIntosh, M. T. (2009). Discovery of swine as a host for the Reston ebolavirus. *Science*, *325*(5937), 204-206. doi:10.1126/science.1172705
- Behring, E. v. (1890, 1890). Untersuchungen über das Zustandekommen Der Diphtherie-Immunität Bei Thieren. *Deutsche Medicinische Wochenschrift*, *5*(50). Retrieved from <https://archiv.ub.uni-marburg.de/ubfind/Record/urn:nbn:de:hebis:04-eb2013-0165/View>
<http://archiv.ub.uni-marburg.de/eb/2013/0165>
- Behring, E. v. B., Oscar; Kossel, Albrecht. (1893, 1893). Zur Behandlung diphtheriekranker Menschen mit Diphtherieheilserum. *Deutsche Medicinische Wochenschrift*, *17 u. 18*(49), 1-24. Retrieved from <https://archiv.ub.uni-marburg.de/ubfind/Record/urn:nbn:de:hebis:04-eb2013-0236>
<http://archiv.ub.uni-marburg.de/eb/2013/0236>

- Behring, E. v. K., Shibasaburo. (1890, 1890). Ueber das Zustandekommen Der Diphtherie-Immunität Und der Tetanus-Immunität Bei Thieren. *Deutsche Medicinische Wochenschrift*, 16(49), 1113–1114. Retrieved from <http://archiv.ub.uni-marburg.de/ubfind/Record/urn:nbn:de:hebis:04-eb2013-0164/View>
<http://archiv.ub.uni-marburg.de/eb/2013/0164>
- Beigel, J. H., Tomashek, K. M., Dodd, L. E., Mehta, A. K., Zingman, B. S., Kalil, A. C., . . . Members, A.-S. G. (2020). Remdesivir for the Treatment of Covid-19 - Final Report. *N Engl J Med*, 383(19), 1813-1826. doi:10.1056/NEJMoa2007764
- Beniac, D. R., & Booth, T. F. (2017). Structure of the Ebola virus glycoprotein spike within the virion envelope at 11 Å resolution. *Sci Rep*, 7, 46374. doi:10.1038/srep46374
- Bernasconi, N. L., Traggiai, E., & Lanzavecchia, A. (2002). Maintenance of serological memory by polyclonal activation of human memory B cells. *Science*, 298(5601), 2199-2202. doi:10.1126/science.1076071
- Bornholdt, Z. A., Herbert, A. S., Mire, C. E., He, S., Cross, R. W., Wec, A. Z., . . . Dye, J. M. (2019). A Two-Antibody Pan-Ebolavirus Cocktail Confers Broad Therapeutic Protection in Ferrets and Nonhuman Primates. *Cell Host Microbe*, 25(1), 49-58 e45. doi:10.1016/j.chom.2018.12.005
- Bornholdt, Z. A., Turner, H. L., Murin, C. D., Li, W., Sok, D., Souders, C. A., . . . Walker, L. M. (2016). Isolation of potent neutralizing antibodies from a survivor of the 2014 Ebola virus outbreak. *Science*, 351(6277), 1078-1083. doi:10.1126/science.aad5788
- Briney, B., Inderbitzin, A., Joyce, C., & Burton, D. R. (2019). Commonality despite exceptional diversity in the baseline human antibody repertoire. *Nature*, 566(7744), 393-397. doi:10.1038/s41586-019-0879-y
- Bukreyev, A., Volchkov, V. E., Blinov, V. M., & Netesov, S. V. (1993). The GP-protein of Marburg virus contains the region similar to the 'immunosuppressive domain' of oncogenic retrovirus P15E proteins. *FEBS Lett*, 323(1-2), 183-187. doi:10.1016/0014-5793(93)81476-g
- Burnet, F. M. (1959). *The clonal selection theory of acquired immunity*. Nashville,: Vanderbilt University Press.
- Burnet, F. M. (1976). A modification of Jerne's theory of antibody production using the concept of clonal selection. *CA Cancer J Clin*, 26(2), 119-121. doi:10.3322/canjclin.26.2.119
- Carette, J. E., Raaben, M., Wong, A. C., Herbert, A. S., Obernosterer, G., Mulherkar, N., . . . Brummelkamp, T. R. (2011). Ebola virus entry requires the cholesterol transporter Niemann-Pick C1. *Nature*, 477(7364), 340-343. doi:10.1038/nature10348
- CDC. (1990). Epidemiologic Notes and Reports Update: Filovirus Infection in Animal Handlers. *MMWR - Morbidity and Mortality Weekly Report*, 39(13), 221. Retrieved from <https://www.cdc.gov/mmwr/preview/mmwrhtml/00001593.htm>
- CDC. (2021a, 03/15). Ebola Outbreaks - 2021 Democratic Republic of the Congo, North Kivu Province. Retrieved from <https://www.cdc.gov/vhf/ebola/outbreaks/drc/2021-february.html>
- CDC. (2021b, 03/15). Ebola Outbreaks - 2021 Guinea, N'Zérékoré Prefecture. Retrieved from <https://www.cdc.gov/vhf/ebola/outbreaks/guinea/2021-february.html>
- CDC. (2021c, 01/22). History of Ebola Virus Disease (EVD) Outbreaks. Retrieved from <https://www.cdc.gov/vhf/ebola/history/chronology.html>
- CDC. (2021d, 03/24). Outbreak Brief 5: Ebola virus disease (EVD) Outbreak. Retrieved from <https://africacdc.org/disease-outbreak/outbreak-brief-5-ebola-virus-disease-evd-outbreak/>
https://africacdc.org/wp-content/uploads/2021/03/AfricaCDC_EbolaBrief_24Mar21_EN.pdf
- Chandran, K., Sullivan, N. J., Felbor, U., Whelan, S. P., & Cunningham, J. M. (2005). Endosomal proteolysis of the Ebola virus glycoprotein is necessary for infection. *Science*, 308(5728), 1643-1645. doi:10.1126/science.1110656
- Cohen-Dvashi, H., Zehner, M., Ehrhardt, S., Katz, M., Elad, N., Klein, F., & Diskin, R. (2020). Structural Basis for a Convergent Immune Response against Ebola Virus. *Cell Host Microbe*, 27(3), 418-427 e414. doi:10.1016/j.chom.2020.01.007
- Cooper, M. D., Peterson, R. D., & Good, R. A. (1965). Delineation of the Thymic and Bursal Lymphoid Systems in the Chicken. *Nature*, 205, 143-146. doi:10.1038/205143a0
- Corti, D., & Lanzavecchia, A. (2013). Broadly neutralizing antiviral antibodies. *Annu Rev Immunol*, 31, 705-742. doi:10.1146/annurev-immunol-032712-095916

- Corti, D., Misasi, J., Mulangu, S., Stanley, D. A., Kanekiyo, M., Wollen, S., . . . Sullivan, N. J. (2016). Protective monotherapy against lethal Ebola virus infection by a potentially neutralizing antibody. *Science*, *351*(6279), 1339-1342. doi:10.1126/science.aad5224
- Cote, M., Misasi, J., Ren, T., Bruchez, A., Lee, K., Filone, C. M., . . . Cunningham, J. (2011). Small molecule inhibitors reveal Niemann-Pick C1 is essential for Ebola virus infection. *Nature*, *477*(7364), 344-348. doi:10.1038/nature10380
- Crooks, G. E., Hon, G., Chandonia, J. M., & Brenner, S. E. (2004). WebLogo: a sequence logo generator. *Genome Res*, *14*(6), 1188-1190. doi:10.1101/gr.849004
- Dahlke, C., Kasonta, R., Lunemann, S., Krahling, V., Zinser, M. E., Biedenkopf, N., . . . Consortium, V. (2017). Dose-dependent T-cell Dynamics and Cytokine Cascade Following rVSV-ZEBOV Immunization. *EBioMedicine*, *19*, 107-118. doi:10.1016/j.ebiom.2017.03.045
- Damon, I. (2018). New Tools in the Ebola Arsenal. *N Engl J Med*, *21*(379), 1981-1982.
- Davis, C. W., Jackson, K. J. L., McElroy, A. K., Halfmann, P., Huang, J., Chennareddy, C., . . . Ahmed, R. (2019). Longitudinal Analysis of the Human B Cell Response to Ebola Virus Infection. *Cell*, *177*(6), 1566-1582 e1517. doi:10.1016/j.cell.2019.04.036
- de La Vega, M. A., Wong, G., Kobinger, G. P., & Qiu, X. (2015). The multiple roles of sGP in Ebola pathogenesis. *Viral Immunol*, *28*(1), 3-9. doi:10.1089/vim.2014.0068
- Deen, G. F., Broutet, N., Xu, W., Knust, B., Sesay, F. R., McDonald, S. L. R., . . . Sahr, F. (2017). Ebola RNA Persistence in Semen of Ebola Virus Disease Survivors — Final Report. *New England Journal of Medicine*, *377*(15), 1428-1437. doi:10.1056/NEJMoa1511410
- DeKosky, B. J., Lungu, O. I., Park, D., Johnson, E. L., Charab, W., Chrysostomou, C., . . . Georgiou, G. (2016). Large-scale sequence and structural comparisons of human naive and antigen-experienced antibody repertoires. *Proc Natl Acad Sci U S A*, *113*(19), E2636-2645. doi:10.1073/pnas.1525510113
- Di Noia, J. M., & Neuberger, M. S. (2007). Molecular mechanisms of antibody somatic hypermutation. *Annu Rev Biochem*, *76*, 1-22. doi:10.1146/annurev.biochem.76.061705.090740
- Diallo, B., Sissoko, D., Loman, N. J., Bah, H. A., Bah, H., Worrell, M. C., . . . Duraffour, S. (2016). Resurgence of Ebola Virus Disease in Guinea Linked to a Survivor With Virus Persistence in Seminal Fluid for More Than 500 Days. *Clin Infect Dis*, *63*(10), 1353-1356. doi:10.1093/cid/ciw601
- Dominguez-Soto, A., Aragonese-Fenoll, L., Martin-Gayo, E., Martinez-Prats, L., Colmenares, M., Naranjo-Gomez, M., . . . Corbi, A. L. (2007). The DC-SIGN-related lectin LSECtin mediates antigen capture and pathogen binding by human myeloid cells. *Blood*, *109*(12), 5337-5345. doi:10.1182/blood-2006-09-048058
- Edelman, G. M., & Poulik, M. D. (1961). Studies on structural units of the gamma-globulins. *J Exp Med*, *113*, 861-884. doi:10.1084/jem.113.5.861
- Ehrhardt, S. A., Zehner, M., Krahling, V., Cohen-Dvashi, H., Kreer, C., Elad, N., . . . Klein, F. (2019). Polyclonal and convergent antibody response to Ebola virus vaccine rVSV-ZEBOV. *Nat Med*, *25*(10), 1589-1600. doi:10.1038/s41591-019-0602-4
- Ehrlich, P. (1900). *Croonian Lecture - On Immunity with Special Reference to Cell Life*. Retrieved from <https://royalsocietypublishing.org/doi/pdf/10.1098/rspl.1899.0121>
https://www.pei.de/SharedDocs/Downloads/DE/institut/veroeffentlichungen-von-paul-ehrich/1897-1905/1900-croonian-lecture-on-immunity-reference-cell-life.pdf?__blob=publicationFile&v=2
- Ehrlich, P. (1908). Über Partialfunktionen der Zelle. In *Nobel Lecture, December 11, 1908. Nobel lectures, Physiology or Medicine* (pp. 203-247): Beiträge zur experimentellen Pathologie und Chemotherapie.
- Ehrlich, P. K., Hermann; von Wassermann, August Paul. (1894, April 19). Ueber die Gewinnung und Verwendung des Diphtherieheilserums. *Deutsche Medicinische Wochenschrift*, *20*(18), 353-355. Retrieved from https://www.pei.de/SharedDocs/Downloads/DE/institut/veroeffentlichungen-von-paul-ehrich/1886-1896/1894-gewinnung-verwendung-diphtherieheilserums.pdf?__blob=publicationFile&v=2
- Emsley, P., Lohkamp, B., Scott, W. G., & Cowtan, K. (2010). Features and development of Coot. *Acta Crystallogr D Biol Crystallogr*, *66*(Pt 4), 486-501. doi:10.1107/S0907444910007493

- Evans, P. R., & Murshudov, G. N. (2013a). How good are my data and what is the resolution? *Acta Crystallographica Section D-Biological Crystallography*, 69, 1204-1214. doi:10.1107/S0907444913000061
- Evans, P. R., & Murshudov, G. N. (2013b). How good are my data and what is the resolution? *Acta Crystallogr D Biol Crystallogr*, 69(Pt 7), 1204-1214. doi:10.1107/S0907444913000061
- Falzarano, D., Feldmann, F., Grolla, A., Leung, A., Ebihara, H., Strong, J. E., . . . Feldmann, H. (2011). Single immunization with a monovalent vesicular stomatitis virus-based vaccine protects nonhuman primates against heterologous challenge with Bundibugyo ebolavirus. *J Infect Dis*, 204 Suppl 3, S1082-1089. doi:10.1093/infdis/jir350
- Farci, P., Diaz, G., Chen, Z., Govindarajan, S., Tice, A., Agulto, L., . . . Zamboni, F. (2010). B cell gene signature with massive intrahepatic production of antibodies to hepatitis B core antigen in hepatitis B virus-associated acute liver failure. *Proc Natl Acad Sci U S A*, 107(19), 8766-8771. doi:10.1073/pnas.1003854107
- FDA. (2019). *Approval Letter for Ervebo (Ebola Zaire Vaccine, Live)*. Sponsor: Merck Sharp & Dohme Corp. Retrieved from <https://www.fda.gov/media/133757/download>
- FDA. (2020a). *Approval Letter for Ebanga (Ansuvimab-zyk)*. Sponsor: Ridgeback Biotherapeutics, LP Retrieved from https://www.accessdata.fda.gov/drugsatfda_docs/nda/2020/761172Orig1s000Approv.pdf
- FDA. (2020b). *Approval Letter for Inmazeb (ATOLTIVIMAB; ODESIVIMAB; MAFTIVIMAB)*. Sponsor: REGENERON PHARMACEUTICALS Retrieved from https://www.accessdata.fda.gov/drugsatfda_docs/applletter/2020/761169Orig1s000ltr.pdf
- Flyak, Andrew I., Ilinykh, Philipp A., Murin, Charles D., Garron, T., Shen, X., Fusco, Marnie L., . . . Crowe, James E. (2015). Mechanism of Human Antibody-Mediated Neutralization of Marburg Virus. *Cell*, 160(5), 893-903. doi:10.1016/j.cell.2015.01.031
- Flyak, A. I., Kuzmina, N., Murin, C. D., Bryan, C., Davidson, E., Gilchuk, P., . . . Crowe, J. E., Jr. (2018). Broadly neutralizing antibodies from human survivors target a conserved site in the Ebola virus glycoprotein HR2-MPER region. *Nat Microbiol*, 3(6), 670-677. doi:10.1038/s41564-018-0157-z
- Flyak, A. I., Shen, X., Murin, C. D., Turner, H. L., David, J. A., Fusco, M. L., . . . Crowe, J. E., Jr. (2016). Cross-Reactive and Potent Neutralizing Antibody Responses in Human Survivors of Natural Ebolavirus Infection. *Cell*, 164(3), 392-405. doi:10.1016/j.cell.2015.12.022
- Forbes, K. M., Webala, P. W., Jaaskelainen, A. J., Abdurahman, S., Ogola, J., Masika, M. M., . . . Sironen, T. (2019). Bombali Virus in Mops condylurus Bat, Kenya. *Emerg Infect Dis*, 25(5). doi:10.3201/eid2505.181666
- Forgacs, D., Abreu, R. B., Sautto, G. A., Kirchenbaum, G. A., Drabek, E., Williamson, K. S., . . . Ross, T. M. (2021). Convergent antibody evolution and clonotype expansion following influenza virus vaccination. *PLoS One*, 16(2), e0247253. doi:10.1371/journal.pone.0247253
- Gaebler, C., Gruell, H., Velinzon, K., Scheid, J. F., Nussenzweig, M. C., & Klein, F. (2013). Isolation of HIV-1-reactive antibodies using cell surface-expressed gp160Deltac(BaL.). *J Immunol Methods*, 397(1-2), 47-54. doi:10.1016/j.jim.2013.09.003
- Garbutt, M., Liebscher, R., Wahl-Jensen, V., Jones, S., Moller, P., Wagner, R., . . . Stroher, U. (2004). Properties of replication-competent vesicular stomatitis virus vectors expressing glycoproteins of filoviruses and arenaviruses. *J Virol*, 78(10), 5458-5465. doi:10.1128/jvi.78.10.5458-5465.2004
- Gaudinski, M. R., Coates, E. E., Novik, L., Widge, A., Houser, K. V., Burch, E., . . . Beresnev, T. (2019). Safety, tolerability, pharmacokinetics, and immunogenicity of the therapeutic monoclonal antibody mAb114 targeting Ebola virus glycoprotein (VRC 608): an open-label phase 1 study. *The Lancet*, 393(10174), 889-898. doi:10.1016/s0140-6736(19)30036-4
- Geisbert, T. W., & Feldmann, H. (2011). Recombinant vesicular stomatitis virus-based vaccines against Ebola and Marburg virus infections. *J Infect Dis*, 204 Suppl 3, S1075-1081. doi:10.1093/infdis/jir349
- Geisbert, T. W., Geisbert, J. B., Leung, A., Daddario-DiCaprio, K. M., Hensley, L. E., Grolla, A., & Feldmann, H. (2009). Single-injection vaccine protects nonhuman primates against infection with marburg virus and three species of ebola virus. *J Virol*, 83(14), 7296-7304. doi:10.1128/JVI.00561-09

- Geisbert, T. W., & Jahrling, P. B. (1995). Differentiation of filoviruses by electron microscopy. *Virus Res*, 39(2-3), 129-150. doi:10.1016/0168-1702(95)00080-1
- Gilchuk, P., Kuzmina, N., Ilinykh, P. A., Huang, K., Gunn, B. M., Bryan, A., . . . Crowe, J. E., Jr. (2018). Multifunctional Pan-ebolavirus Antibody Recognizes a Site of Broad Vulnerability on the Ebolavirus Glycoprotein. *Immunity*, 49(2), 363-374 e310. doi:10.1016/j.immuni.2018.06.018
- Gilchuk, P., Murin, C. D., Cross, R. W., Ilinykh, P. A., Huang, K., Kuzmina, N., . . . Crowe, J. E. (2021). Protective pan-ebolavirus combination therapy by two multifunctional human antibodies. *bioRxiv*, 2021.2005.2002.442324. doi:10.1101/2021.05.02.442324
- Gilchuk, P., Murin, C. D., Milligan, J. C., Cross, R. W., Mire, C. E., Ilinykh, P. A., . . . Crowe, J. E., Jr. (2020). Analysis of a Therapeutic Antibody Cocktail Reveals Determinants for Cooperative and Broad Ebolavirus Neutralization. *Immunity*, 52(2), 388-403 e312. doi:10.1016/j.immuni.2020.01.001
- Glanville, J., Kuo, T. C., von Budingen, H. C., Guey, L., Berka, J., Sundar, P. D., . . . Pons, J. (2011). Naive antibody gene-segment frequencies are heritable and unaltered by chronic lymphocyte ablation. *Proc Natl Acad Sci U S A*, 108(50), 20066-20071. doi:10.1073/pnas.1107498108
- Godoy-Lozano, E. E., Tellez-Sosa, J., Sanchez-Gonzalez, G., Samano-Sanchez, H., Aguilar-Salgado, A., Salinas-Rodriguez, A., . . . Martinez-Barnette, J. (2016). Lower IgG somatic hypermutation rates during acute dengue virus infection is compatible with a germinal center-independent B cell response. *Genome Med*, 8(1), 23. doi:10.1186/s13073-016-0276-1
- Goldstein, T., Anthony, S. J., Gbakima, A., Bird, B. H., Bangura, J., Tremeau-Bravard, A., . . . Mazet, J. A. K. (2018). The discovery of Bombali virus adds further support for bats as hosts of ebolaviruses. *Nat Microbiol*, 3(10), 1084-1089. doi:10.1038/s41564-018-0227-2
- Gramberg, T., Soilleux, E., Fisch, T., Lator, P. F., Hofmann, H., Wheeldon, S., . . . Pohlmann, S. (2008). Interactions of LSECtin and DC-SIGN/DC-SIGNR with viral ligands: Differential pH dependence, internalization and virion binding. *Virology*, 373(1), 189-201. doi:10.1016/j.virol.2007.11.001
- Group, P. I. W., Multi-National, P. I. I. S. T., Davey, R. T., Jr., Dodd, L., Proschan, M. A., Neaton, J., . . . Malvy, D. (2016). A Randomized, Controlled Trial of ZMapp for Ebola Virus Infection. *N Engl J Med*, 375(15), 1448-1456. doi:10.1056/NEJMoa1604330
- Gupta, M., Mahanty, S., Greer, P., Towner, J. S., Shieh, W. J., Zaki, S. R., . . . Rollin, P. E. (2004). Persistent infection with ebola virus under conditions of partial immunity. *J Virol*, 78(2), 958-967. doi:10.1128/jvi.78.2.958-967.2004
- Han, B. A., Kramer, A. M., & Drake, J. M. (2016). Global Patterns of Zoonotic Disease in Mammals. *Trends Parasitol*, 32(7), 565-577. doi:10.1016/j.pt.2016.04.007
- Hansen, F., Feldmann, H., & Jarvis, M. A. (2021). Targeting Ebola virus replication through pharmaceutical intervention. *Expert Opin Investig Drugs*, 30(3), 201-226. doi:10.1080/13543784.2021.1881061
- Hastie, K. M., Cross, R. W., Harkins, S. S., Zandonatti, M. A., Koval, A. P., Heinrich, M. L., . . . Saphire, E. O. (2019). Convergent Structures Illuminate Features for Germline Antibody Binding and Pan-Lassa Virus Neutralization. *Cell*, 178(4), 1004-1015 e1014. doi:10.1016/j.cell.2019.07.020
- Henao-Restrepo, A. M., Camacho, A., Longini, I. M., Watson, C. H., Edmunds, W. J., Egger, M., . . . Kieny, M.-P. (2017). Efficacy and effectiveness of an rVSV-vectored vaccine in preventing Ebola virus disease: final results from the Guinea ring vaccination, open-label, cluster-randomised trial (Ebola Ça Suffit!). *The Lancet*, 389(10068), 505-518. doi:10.1016/s0140-6736(16)32621-6
- Henao-Restrepo, A. M., Longini, I. M., Egger, M., Dean, N. E., Edmunds, W. J., Camacho, A., . . . Rottingen, J. A. (2015). Efficacy and effectiveness of an rVSV-vectored vaccine expressing Ebola surface glycoprotein: interim results from the Guinea ring vaccination cluster-randomised trial. *Lancet*, 386(9996), 857-866. doi:10.1016/S0140-6736(15)61117-5
- Holtsberg, F. W., Shulenin, S., Vu, H., Howell, K. A., Patel, S. J., Gunn, B., . . . Aman, M. J. (2016). Pan-ebolavirus and Pan-filovirus Mouse Monoclonal Antibodies: Protection against Ebola and Sudan Viruses. *J Virol*, 90(1), 266-278. doi:10.1128/JVI.02171-15
- Huttner, A. (2017). A dose-dependent plasma signature of the safety and immunogenicity of the rVSV-Ebola vaccine in Europe and Africa. *Science Transl Med*.

- Huttner, A., Agnandji, S. T., Combescure, C., Fernandes, J. F., Bache, E. B., Kabwende, L., . . . Rothenberger, S. (2018). Determinants of antibody persistence across doses and continents after single-dose rVSV-ZEBOV vaccination for Ebola virus disease: an observational cohort study. *The Lancet Infectious Diseases*, *18*(7), 738-748. doi:10.1016/s1473-3099(18)30165-8
- Huttner, A., Dayer, J. A., Yerly, S., Combescure, C., Auderset, F., Desmeules, J., . . . Consortium, V. S.-E. (2015). The effect of dose on the safety and immunogenicity of the VSV Ebola candidate vaccine: a randomised double-blind, placebo-controlled phase 1/2 trial. *Lancet Infect Dis*, *15*(10), 1156-1166. doi:10.1016/S1473-3099(15)00154-1
- Hystad, M. E., Myklebust, J. H., Bo, T. H., Sivertsen, E. A., Rian, E., Forfang, L., . . . Smeland, E. B. (2007). Characterization of early stages of human B cell development by gene expression profiling. *J Immunol*, *179*(6), 3662-3671. doi:10.4049/jimmunol.179.6.3662
- Ilinykh, P. A., Shen, X., Flyak, A. I., Kuzmina, N., Ksiazek, T. G., Crowe, J. E., Jr., & Bukreyev, A. (2016). Chimeric Filoviruses for Identification and Characterization of Monoclonal Antibodies. *J Virol*, *90*(8), 3890-3901. doi:10.1128/JVI.00101-16
- Imai, K., Slupphaug, G., Lee, W. I., Revy, P., Nonoyama, S., Catalan, N., . . . Durandy, A. (2003). Human uracil-DNA glycosylase deficiency associated with profoundly impaired immunoglobulin class-switch recombination. *Nat Immunol*, *4*(10), 1023-1028. doi:10.1038/ni974
- Jackson, K. J., Liu, Y., Roskin, K. M., Glanville, J., Hoh, R. A., Seo, K., . . . Boyd, S. D. (2014). Human responses to influenza vaccination show seroconversion signatures and convergent antibody rearrangements. *Cell Host Microbe*, *16*(1), 105-114. doi:10.1016/j.chom.2014.05.013
- Jacob, J., Kelsoe, G., Rajewsky, K., & Weiss, U. (1991). Intracloonal generation of antibody mutants in germinal centres. *Nature*, *354*(6352), 389-392. doi:10.1038/354389a0
- Jahrling, P. B., Geisbert, J., Swearingen, J. R., Jaax, G. P., Lewis, T., Huggins, J. W., . . . Peters, C. J. (1996). Passive immunization of Ebola virus-infected cynomolgus monkeys with immunoglobulin from hyperimmune horses. *Arch Virol Suppl*, *11*, 135-140. doi:10.1007/978-3-7091-7482-1_12
- Jahrling, P. B., Geisbert, T. W., Dalgard, D. W., Johnson, E. D., Ksiazek, T. G., Hall, W. C., & Peters, C. J. (1990). Preliminary report: isolation of Ebola virus from monkeys imported to USA. *Lancet*, *335*(8688), 502-505. doi:10.1016/0140-6736(90)90737-p
- Jerne, N. K. (1955). The Natural-Selection Theory of Antibody Formation. *Proc Natl Acad Sci U S A*, *41*(11), 849-857. doi:10.1073/pnas.41.11.849
- Johnson, E. D., Johnson, B. K., Silverstein, D., Tukei, P., Geisbert, T. W., Sanchez, A. N., & Jahrling, P. B. (1996). Characterization of a new Marburg virus isolated from a 1987 fatal case in Kenya. *Arch Virol Suppl*, *11*, 101-114. doi:10.1007/978-3-7091-7482-1_10
- Johnson, K. M., Lange, J. V., Webb, P. A., & Murphy, F. A. (1977). Isolation and partial characterisation of a new virus causing acute haemorrhagic fever in Zaire. *Lancet*, *1*(8011), 569-571. doi:10.1016/s0140-6736(77)92000-1
- Jones, K. E., Patel, N. G., Levy, M. A., Storeygard, A., Balk, D., Gittleman, J. L., & Daszak, P. (2008). Global trends in emerging infectious diseases. *Nature*, *451*(7181), 990-993. doi:10.1038/nature06536
- Jones, S. M., Feldmann, H., Stroher, U., Geisbert, J. B., Fernando, L., Grolla, A., . . . Geisbert, T. W. (2005). Live attenuated recombinant vaccine protects nonhuman primates against Ebola and Marburg viruses. *Nat Med*, *11*(7), 786-790. doi:10.1038/nm1258
- Joyce, M. G., Wheatley, A. K., Thomas, P. V., Chuang, G. Y., Soto, C., Bailer, R. T., . . . McDermott, A. B. (2016). Vaccine-Induced Antibodies that Neutralize Group 1 and Group 2 Influenza A Viruses. *Cell*, *166*(3), 609-623. doi:10.1016/j.cell.2016.06.043
- Ju, B., Zhang, Q., Ge, J., Wang, R., Sun, J., Ge, X., . . . Zhang, L. (2020). Human neutralizing antibodies elicited by SARS-CoV-2 infection. *Nature*, *584*(7819), 115-119. doi:10.1038/s41586-020-2380-z
- Khurana, S., Fuentes, S., Coyle, E. M., Ravichandran, S., Davey, R. T., & Beigel, J. H. (2016). Human antibody repertoire after VSV-Ebola vaccination identifies novel targets and virus-neutralizing IgM antibodies. *Nature Medicine*, *22*(12), 1439-1447. doi:10.1038/nm.4201

- King, A. M. Q. A., M. J.; Carstens, E. B.; Lefkowitz E. J. . (2011). *Virus Taxonomy - Ninth Report of the International Committee on Taxonomy of Viruses* (M. J. A. Andrew M.Q. King, Eric B. Carstens, Elliot J. Lefkowitz Ed.): Elsevier.
- King, L. B., West, B. R., Moyer, C. L., Gilchuk, P., Flyak, A., Ilinykh, P. A., . . . Saphire, E. O. (2019). Cross-reactive neutralizing human survivor monoclonal antibody BDBV223 targets the ebolavirus stalk. *Nat Commun*, *10*(1), 1788. doi:10.1038/s41467-019-09732-7
- Komori, T., Okada, A., Stewart, V., & Alt, F. W. (1993). Lack of N regions in antigen receptor variable region genes of TdT-deficient lymphocytes. *Science*, *261*(5125), 1171-1175. doi:10.1126/science.8356451
- Kreer, C., Doring, M., Lehnen, N., Ercanoglu, M. S., Gieselmann, L., Luca, D., . . . Klein, F. (2020). openPrimeR for multiplex amplification of highly diverse templates. *J Immunol Methods*, *112752*. doi:10.1016/j.jim.2020.112752
- Kreer, C., Gruell, H., Mora, T., Walczak, A. M., & Klein, F. (2020). Exploiting B Cell Receptor Analyses to Inform on HIV-1 Vaccination Strategies. *Vaccines (Basel)*, *8*(1). doi:10.3390/vaccines8010013
- Kuhn, J. H., Becker, S., Ebihara, H., Geisbert, T. W., Johnson, K. M., Kawaoka, Y., . . . Jahrling, P. B. (2010). Proposal for a revised taxonomy of the family Filoviridae: classification, names of taxa and viruses, and virus abbreviations. *Arch Virol*, *155*(12), 2083-2103. doi:10.1007/s00705-010-0814-x
- Kupferschmidt, K. (2019). Finally, some good news about Ebola: Two new treatments dramatically lower the death rate in a trial. *Science, Latest News*. doi:10.1126/science.aaz1032
- Kupferschmidt, K. (2021). New Ebola outbreak likely sparked by a person infected 5 years ago. *Science, Latest News*. doi:10.1126/science.abi4876
- Lafaille, J. J., Decloux, A., Bonneville, M., Takagaki, Y., & Tonegawa, S. (1989). Junctional Sequences of T-Cell Receptor Gamma-Delta-Genes - Implications for Gamma-Delta-T-Cell Lineages and for a Novel Intermediate of V-(D)-J Joining. *Cell*, *59*(5), 859-870. doi:10.1016/0092-8674(89)90609-0
- Le Guenno, B., Formenty, P., Wyers, M., Gounon, P., Walker, F., & Boesch, C. (1995). Isolation and partial characterisation of a new strain of Ebola virus. *Lancet*, *345*(8960), 1271-1274. doi:10.1016/s0140-6736(95)90925-7
- Ledgerwood, J. E., DeZure, A. D., Stanley, D. A., Coates, E. E., Novik, L., Enama, M. E., . . . Team, V. R. C. S. (2017). Chimpanzee Adenovirus Vector Ebola Vaccine. *N Engl J Med*, *376*(10), 928-938. doi:10.1056/NEJMoa1410863
- Lee, J. E., Fusco, M. L., Hessell, A. J., Oswald, W. B., Burton, D. R., & Saphire, E. O. (2008). Structure of the Ebola virus glycoprotein bound to an antibody from a human survivor. *Nature*, *454*(7201), 177-182. doi:10.1038/nature07082
- Lee, J. E., & Saphire, E. O. (2009). Ebolavirus glycoprotein structure and mechanism of entry. *Future Virol*, *4*(6), 621-635. doi:10.2217/fvl.09.56
- Lefranc, M.-P. (2011). IMGT, the International ImMunoGeneTics Information System. *Cold Spring Harbor (CSH) Protocols*. doi:DOI:10.1101/pdb.top115
- Lefranc, M. P., Giudicelli, V., Ginestoux, C., Bodmer, J., Muller, W., Bontrop, R., . . . Chaume, D. (1999). IMGT, the international ImMunoGeneTics database. *Nucleic Acids Res*, *27*(1), 209-212. doi:10.1093/nar/27.1.209
- Leroy, E. M., Kumulungui, B., Pourrut, X., Rouquet, P., Hassanin, A., Yaba, P., . . . Swanepoel, R. (2005). Fruit bats as reservoirs of Ebola virus. *Nature*, *438*(7068), 575-576. doi:10.1038/438575a
- Lucas, A. H., McLean, G. R., Reason, D. C., O'Connor, A. P., Felton, M. C., & Moulton, K. D. (2003). Molecular ontogeny of the human antibody repertoire to the Haemophilus influenzae type B polysaccharide: expression of canonical variable regions and their variants in vaccinated infants. *Clin Immunol*, *108*(2), 119-127. doi:10.1016/s1521-6616(03)00094-9
- Ma, Y., Pannicke, U., Schwarz, K., & Lieber, M. R. (2002). Hairpin opening and overhang processing by an Artemis/DNA-dependent protein kinase complex in nonhomologous end joining and V(D)J recombination. *Cell*, *108*(6), 781-794. doi:10.1016/s0092-8674(02)00671-2
- Madej, T., Lanczycki, C. J., Zhang, D., Thiessen, P. A., Geer, R. C., Marchler-Bauer, A., & Bryant, S. H. (2014). MMDB and VAST+: tracking structural similarities between macromolecular complexes. *Nucleic Acids Res*, *42*(Database issue), D297-303. doi:10.1093/nar/gkt1208

- Manz, R. A., Thiel, A., & Radbruch, A. (1997). Lifetime of plasma cells in the bone marrow. *Nature*, 388(6638), 133-134. doi:10.1038/40540
- Martins, K., Carra, J. H., Cooper, C. L., Kwilas, S. A., Robinson, C. G., Shurtleff, A. C., . . . Bavari, S. (2015). Cross-protection conferred by filovirus virus-like particles containing trimeric hybrid glycoprotein. *Viral Immunol*, 28(1), 62-70. doi:10.1089/vim.2014.0071
- Maruyama, T., Rodriguez, L. L., Jahrling, P. B., Sanchez, A., Khan, A. S., Nichol, S. T., . . . Burton, D. R. (1999). Ebola Virus can be effectively neutralized by antibody produced in natural human infection. *J Virol*.
- Marzi, A., Engelmann, F., Feldmann, F., Haberthur, K., Shupert, W. L., Brining, D., . . . Messaoudi, I. (2013). Antibodies are necessary for rVSV/ZEBOV-GP-mediated protection against lethal Ebola virus challenge in nonhuman primates. *Proc Natl Acad Sci U S A*, 110(5), 1893-1898. doi:10.1073/pnas.1209591110
- Marzi, A., Halfmann, P., Hill-Batorski, L., Feldmann, F., Shupert, W. L., Neumann, G., . . . Kawaoka, Y. (2015). Vaccines. An Ebola whole-virus vaccine is protective in nonhuman primates. *Science*, 348(6233), 439-442. doi:10.1126/science.aaa4919
- Matassov, D., Mire, C. E., Latham, T., Geisbert, J. B., Xu, R., Ota-Setlik, A., . . . Eldridge, J. H. (2018). Single-Dose Trivalent VesiculoVax Vaccine Protects Macaques from Lethal Ebolavirus and Marburgvirus Challenge. *J Virol*, 92(3). doi:10.1128/JVI.01190-17
- Maul, R. W., & Gearhart, P. J. (2010). AID and somatic hypermutation. *Adv Immunol*, 105, 159-191. doi:10.1016/S0065-2776(10)05006-6
- Maxmen, A. (2018). Experimental Ebola drugs face tough test in war zone. *Nature*, 561(7721), 14. doi:10.1038/d41586-018-06132-7
- McCoy, A. J., Grosse-Kunstleve, R. W., Adams, P. D., Winn, M. D., Storoni, L. C., & Read, R. J. (2007). Phaser crystallographic software. *J Appl Crystallogr*, 40(Pt 4), 658-674. doi:10.1107/S0021889807021206
- McElroy, A. K., Akondy, R. S., Davis, C. W., Ellebedy, A. H., Mehta, A. K., Kraft, C. S., . . . Ahmed, R. (2015). Human Ebola virus infection results in substantial immune activation. *Proc Natl Acad Sci U S A*, 112(15), 4719-4724. doi:10.1073/pnas.1502619112
- Medaglini, D., & Siegrist, C. A. (2017). Immunomonitoring of human responses to the rVSV-ZEBOV Ebola vaccine. *Curr Opin Virol*, 23, 88-94. doi:10.1016/j.coviro.2017.03.008
- Meyer, M., Malherbe, D. C., & Bukreyev, A. (2019). Can Ebola Virus Vaccines Have Universal Immune Correlates of protection? *Trends Microbiol*, 27(1), 8-16. doi:10.1016/j.tim.2018.08.008
- Miranda, M. E. G., White, M. E., Dayrit, M. M., Hayes, C. G., Ksiazek, T. G., & Burans, J. P. (1991). Seroepidemiological Study of Filovirus Related to Ebola in the Philippines. *Lancet*, 337(8738), 425-426. doi:10.1016/0140-6736(91)91199-5
- Misasi, J., Gilman, M. S., Kanekiyo, M., Gui, M., Cagigi, A., Mulangu, S., . . . McLellan, J. S. (2016). Structural and molecular basis for Ebola virus neutralization by protective human antibodies. *Science*, 351(6279), 1343-1346. doi:10.1126/science.aad6117
- Mohan, G. S., Li, W., Ye, L., Compans, R. W., & Yang, C. (2012). Antigenic subversion: a novel mechanism of host immune evasion by Ebola virus. *PLoS Pathog*, 8(12), e1003065. doi:10.1371/journal.ppat.1003065
- MSF. (2020). Eleventh outbreak declared over in Équateur province. Retrieved from <https://www.msf.org/drc-ebola-outbreak-crisis-update>
- Muhlberger, E. (2007). Filovirus replication and transcription. *Future Virol*, 2(2), 205-215. doi:10.2217/17460794.2.2.205
- Mulangu, S., Dodd, L. E., Davey, R. T., Jr., Tshiani Mbaya, O., Proschan, M., Mukadi, D., . . . Team, P. C. S. (2019). A Randomized, Controlled Trial of Ebola Virus Disease Therapeutics. *N Engl J Med*, 381(24), 2293-2303. doi:10.1056/NEJMoa1910993
- Muramatsu, M., Kinoshita, K., Fagarasan, S., Yamada, S., Shinkai, Y., & Honjo, T. (2000). Class switch recombination and hypermutation require activation-induced cytidine deaminase (AID), a potential RNA editing enzyme. *Cell*, 102(5), 553-563. doi:10.1016/S0092-8674(00)00078-7
- Murin, C. D., Fusco, M. L., Bornholdt, Z. A., Qiu, X., Olinger, G. G., Zeitlin, L., . . . Saphire, E. O. (2014). Structures of protective antibodies reveal sites of vulnerability on Ebola virus. *Proc Natl Acad Sci U S A*, 111(48), 17182-17187. doi:10.1073/pnas.1414164111

- Murphy, K. E. (2011). Janeway's Immunobiology. In *Janeway's Immunobiology* (8th edition ed., pp. 888): Taylor & Francis Ltd.
- Nanbo, A., Imai, M., Watanabe, S., Noda, T., Takahashi, K., Neumann, G., . . . Kawaoka, Y. (2010). Ebola virus is internalized into host cells via macropinocytosis in a viral glycoprotein-dependent manner. *PLoS Pathog*, *6*(9), e1001121. doi:10.1371/journal.ppat.1001121
- Negredo, A., Palacios, G., Vazquez-Moron, S., Gonzalez, F., Dopazo, H., Molero, F., . . . Tenorio, A. (2011). Discovery of an ebolavirus-like filovirus in Europe. *PLoS Pathog*, *7*(10), e1002304. doi:10.1371/journal.ppat.1002304
- Nielsen, S. C. A., Yang, F., Jackson, K. J. L., Hoh, R. A., Roltgen, K., Jean, G. H., . . . Boyd, S. D. (2020). Human B Cell Clonal Expansion and Convergent Antibody Responses to SARS-CoV-2. *Cell Host Microbe*, *28*(4), 516-525 e515. doi:10.1016/j.chom.2020.09.002
- Nielsen, S. C. A., Yang, F., Jackson, K. J. L., Hoh, R. A., Roltgen, K., Stevens, B., . . . Boyd, S. D. (2020). Human B cell clonal expansion and convergent antibody responses to SARS-CoV-2. *bioRxiv*. doi:10.1101/2020.07.08.194456
- Nimmerjahn, F., & Ravetch, J. V. (2010). Antibody-mediated modulation of immune responses. *Immunity*, *32*(6), 265-275. doi:10.1016/j.imm.2010.09.010
- Norn, C. H., Lapidus, G., & Fleishman, S. J. (2017). High-accuracy modeling of antibody structures by a search for minimum-energy recombination of backbone fragments. *Proteins*, *85*(1), 30-38. doi:10.1002/prot.25185
- Nossal, G. J., & Lederberg, J. (1958). Antibody production by single cells. *Nature*, *181*(4620), 1419-1420. doi:10.1038/1811419a0
- Oettinger, M. A., Schatz, D. G., Gorka, C., & Baltimore, D. (1990). RAG-1 and RAG-2, adjacent genes that synergistically activate V(D)J recombination. *Science*, *248*(4962), 1517-1523. doi:10.1126/science.2360047
- Olinger, G. G., Jr., Pettitt, J., Kim, D., Working, C., Bohorov, O., Bratcher, B., . . . Zeitlin, L. (2012). Delayed treatment of Ebola virus infection with plant-derived monoclonal antibodies provides protection in rhesus macaques. *Proc Natl Acad Sci U S A*, *109*(44), 18030-18035. doi:10.1073/pnas.1213709109
- Ozawa, T., Kishi, H., & Muraguchi, A. (2006). Amplification and analysis of cDNA generated from a single cell by 5'-RACE: application to isolation of antibody heavy and light chain variable gene sequences from single B cells. *Biotechniques*, *40*(4), 469-470, 472, 474 passim. doi:10.2144/000112123
- Pallesen, J., Murin, C. D., de Val, N., Cottrell, C. A., Hastie, K. M., Turner, H. L., . . . Ward, A. B. (2016). Structures of Ebola virus GP and sGP in complex with therapeutic antibodies. *Nat Microbiol*, *1*(9), 16128. doi:10.1038/nmicrobiol.2016.128
- Pascal, K. E., Dudgeon, D., Trefry, J. C., Anantpadma, M., Sakurai, Y., Murin, C. D., . . . Kyrtatsos, C. A. (2018). Development of Clinical-Stage Human Monoclonal Antibodies That Treat Advanced Ebola Virus Disease in Nonhuman Primates. *J Infect Dis*, *218*(suppl_5), S612-S626. doi:10.1093/infdis/jiy285
- Pettersen, E. F., Goddard, T. D., Huang, C. C., Couch, G. S., Greenblatt, D. M., Meng, E. C., & Ferrin, T. E. (2004). UCSF Chimera--a visualization system for exploratory research and analysis. *J Comput Chem*, *25*(13), 1605-1612. doi:10.1002/jcc.20084
- Philippe Le Mercier, C. H., Patrick Masson; Edouard de Castro; Swiss Institute of Bioinformatics. (2014 and 2017, 02/26). Ebola virus. Retrieved from <https://viralzone.expasy.org/207>
- Pinto, D., Park, Y. J., Beltramello, M., Walls, A. C., Tortorici, M. A., Bianchi, S., . . . Corti, D. (2020). Cross-neutralization of SARS-CoV-2 by a human monoclonal SARS-CoV antibody. *Nature*, *583*(7815), 290-295. doi:10.1038/s41586-020-2349-y
- Poetsch, J. H., Dahlke, C., Zinser, M. E., Kasonta, R., Lunemann, S., Rechten, A., . . . Addo, M. M. (2018). Detectable Vesicular Stomatitis Virus (VSV)-Specific Humoral and Cellular Immune Responses Following VSV-Ebola Virus Vaccination in Humans. *J Infect Dis*. doi:10.1093/infdis/jiy565
- Punjani, A., Rubinstein, J. L., Fleet, D. J., & Brubaker, M. A. (2017). cryoSPARC: algorithms for rapid unsupervised cryo-EM structure determination. *Nat Methods*, *14*(3), 290-296. doi:10.1038/nmeth.4169

- Qiu, X., Alimonti, J. B., Melito, P. L., Fernando, L., Stroher, U., & Jones, S. M. (2011). Characterization of Zaire ebolavirus glycoprotein-specific monoclonal antibodies. *Clin Immunol*, *141*(2), 218-227. doi:10.1016/j.clim.2011.08.008
- Qiu, X., Wong, G., Audet, J., Bello, A., Fernando, L., Alimonti, J. B., . . . Kobinger, G. P. (2014). Reversion of advanced Ebola virus disease in nonhuman primates with ZMapp. *Nature*, *514*(7520), 47-53. doi:10.1038/nature13777
- Radoshitzky, S. R., Warfield, K. L., Chi, X., Dong, L., Kota, K., Bradfute, S. B., . . . Kuhn, J. H. (2011). Ebolavirus delta-peptide immunoadhesins inhibit marburgvirus and ebolavirus cell entry. *J Virol*, *85*(17), 8502-8513. doi:10.1128/JVI.02600-10
- Rahlf, T. S., Reinhard. (2015). Deutschland in Daten. In T. Rahlf (Ed.), *Zeitreihen zur Historischen Statistik* (pp. 74-87): Bundeszentrale für politische Bildung, Bonn.
- Rajewsky, K. (1996). Clonal selection and learning in the antibody system. *Nature*, *381*(6585), 751-758. doi:10.1038/381751a0
- Rechtien, A., Richert, L., Lorenzo, H., Martrus, G., Hejblum, B., Dahlke, C., . . . Addo, M. M. (2017). Systems Vaccinology Identifies an Early Innate Immune Signature as a Correlate of Antibody Responses to the Ebola Vaccine rVSV-ZEBOV. *Cell Rep*, *20*(9), 2251-2261. doi:10.1016/j.celrep.2017.08.023
- Regules, J. A., Beigel, J. H., Paolino, K. M., Voell, J., Castellano, A. R., Hu, Z., . . . r, V.-Z.-G. P. S. G. (2017). A Recombinant Vesicular Stomatitis Virus Ebola Vaccine. *N Engl J Med*, *376*(4), 330-341. doi:10.1056/NEJMoa1414216
- Reynolds, P., & Marzi, A. (2017). Ebola and Marburg virus vaccines. *Virus Genes*, *53*(4), 501-515. doi:10.1007/s11262-017-1455-x
- Rijal, P., Elias, S. C., Machado, S. R., Xiao, J., Schimanski, L., O'Dowd, V., . . . Townsend, A. R. (2019). Therapeutic Monoclonal Antibodies for Ebola Virus Infection Derived from Vaccinated Humans. *Cell Rep*, *27*(1), 172-186 e177. doi:10.1016/j.celrep.2019.03.020
- Robbiani, D. F., Bozzacco, L., Keeffe, J. R., Khouri, R., Olsen, P. C., Gazumyan, A., . . . Nussenzweig, M. C. (2017). Recurrent Potent Human Neutralizing Antibodies to Zika Virus in Brazil and Mexico. *Cell*, *169*(4), 597-609 e511. doi:10.1016/j.cell.2017.04.024
- Robbiani, D. F., Gaebler, C., Muecksch, F., Lorenzi, J. C. C., Wang, Z., Cho, A., . . . Nussenzweig, M. C. (2020). Convergent antibody responses to SARS-CoV-2 in convalescent individuals. *Nature*, *584*(7821), 437-442. doi:10.1038/s41586-020-2456-9
- Rohou, A., & Grigorieff, N. (2015). CTFFIND4: Fast and accurate defocus estimation from electron micrographs. *J Struct Biol*, *192*(2), 216-221. doi:10.1016/j.jsb.2015.08.008
- Ruprecht, C. R., & Lanzavecchia, A. (2006). Toll-like receptor stimulation as a third signal required for activation of human naive B cells. *Eur J Immunol*, *36*(4), 810-816. doi:10.1002/eji.200535744
- Sanchez, A., & Rollin, P. E. (2005). Complete genome sequence of an Ebola virus (Sudan species) responsible for a 2000 outbreak of human disease in Uganda. *Virus Res*, *113*(1), 16-25. doi:10.1016/j.virusres.2005.03.028
- Sanchez, A., Trappier, S. G., Mahy, B. W., Peters, C. J., & Nichol, S. T. (1996). The virion glycoproteins of Ebola viruses are encoded in two reading frames and are expressed through transcriptional editing. *Proc Natl Acad Sci U S A*, *93*(8), 3602-3607. doi:10.1073/pnas.93.8.3602
- Sanchez, A., Yang, Z. Y., Xu, L., Nabel, G. J., Crews, T., & Peters, C. J. (1998). Biochemical analysis of the secreted and virion glycoproteins of Ebola virus. *J Virol*, *72*(8), 6442-6447. Retrieved from <https://www.ncbi.nlm.nih.gov/pubmed/9658086>
<https://www.ncbi.nlm.nih.gov/pmc/articles/PMC109803/pdf/jv006442.pdf>
- Saphire, E. O., Schendel, S. L., Fusco, M. L., Gangavarapu, K., Gunn, B. M., Wec, A. Z., . . . Viral Hemorrhagic Fever Immunotherapeutic, C. (2018). Systematic Analysis of Monoclonal Antibodies against Ebola Virus GP Defines Features that Contribute to Protection. *Cell*, *174*(4), 938-952 e913. doi:10.1016/j.cell.2018.07.033
- Saphire, E. O., Schendel, S. L., Gunn, B. M., Milligan, J. C., & Alter, G. (2018). Antibody-mediated protection against Ebola virus. *Nat Immunol*, *19*(11), 1169-1178. doi:10.1038/s41590-018-0233-9
- Schatz, D. G., & Ji, Y. (2011). Recombination centres and the orchestration of V(D)J recombination. *Nat Rev Immunol*, *11*(4), 251-263. doi:10.1038/nri2941

- Scheid, J. F., Mouquet, H., Feldhahn, N., Seaman, M. S., Velinzon, K., Pietzsch, J., . . . Nussenzweig, M. C. (2009). Broad diversity of neutralizing antibodies isolated from memory B cells in HIV-infected individuals. *Nature*, *458*(7238), 636-640. doi:10.1038/nature07930
- Scheid, J. F., Mouquet, H., Ueberheide, B., Diskin, R., Klein, F., Oliveira, T. Y., . . . Nussenzweig, M. C. (2011). Sequence and structural convergence of broad and potent HIV antibodies that mimic CD4 binding. *Science*, *333*(6049), 1633-1637. doi:10.1126/science.1207227
- Schnell, M. J., Buonocore, L., Kretzschmar, E., Johnson, E., & Rose, J. K. (1996). Foreign glycoproteins expressed from recombinant vesicular stomatitis viruses are incorporated efficiently into virus particles. *Proc Natl Acad Sci U S A*, *93*(21), 11359-11365. doi:10.1073/pnas.93.21.11359
- Schrader, C. E., Linehan, E. K., Mochevova, S. N., Woodland, R. T., & Stavnezer, J. (2005). Inducible DNA breaks in Ig S regions are dependent on AID and UNG. *J Exp Med*, *202*(4), 561-568. doi:10.1084/jem.20050872
- Schroeder, H. W., Jr., & Cavacini, L. (2010). Structure and function of immunoglobulins. *J Allergy Clin Immunol*, *125*(2 Suppl 2), S41-52. doi:10.1016/j.jaci.2009.09.046
- Sethna, Z., Elhanati, Y., Callan, C. G., Walczak, A. M., & Mora, T. (2019). OLGA: fast computation of generation probabilities of B- and T-cell receptor amino acid sequences and motifs. *Bioinformatics*, *35*(17), 2974-2981. doi:10.1093/bioinformatics/btz035
- Setliff, I., McDonnell, W. J., Raju, N., Bombardi, R. G., Murji, A. A., Scheepers, C., . . . Georgiev, I. S. (2018). Multi-Donor Longitudinal Antibody Repertoire Sequencing Reveals the Existence of Public Antibody Clonotypes in HIV-1 Infection. *Cell Host Microbe*, *23*(6), 845-854 e846. doi:10.1016/j.chom.2018.05.001
- Siegert, R., Shu, H. L., Slenczka, W., Peters, D., & Muller, G. (1967). [On the etiology of an unknown human infection originating from monkeys]. *Dtsch Med Wochenschr*, *92*(51), 2341-2343. doi:10.1055/s-0028-1106144
- Sievers, F., Wilm, A., Dineen, D., Gibson, T. J., Karplus, K., Li, W., . . . Higgins, D. G. (2011). Fast, scalable generation of high-quality protein multiple sequence alignments using Clustal Omega. *Mol Syst Biol*, *7*, 539. doi:10.1038/msb.2011.75
- Silverstein, A. M. (1999). Paul Ehrlich's passion: the origins of his receptor immunology. *Cell Immunol*, *194*(2), 213-221. doi:10.1006/cimm.1999.1505
- Simmons, G., Reeves, J. D., Grogan, C. C., Vandenberghe, L. H., Baribaud, F., Whitbeck, J. C., . . . Pohlmann, S. (2003). DC-SIGN and DC-SIGNR bind ebola glycoproteins and enhance infection of macrophages and endothelial cells. *Virology*, *305*(1), 115-123. doi:10.1006/viro.2002.1730
- Sivapalasingam, S., Kamal, M., Slim, R., Hosain, R., Shao, W., Stoltz, R., . . . Lipsich, L. (2018). Safety, pharmacokinetics, and immunogenicity of a co-formulated cocktail of three human monoclonal antibodies targeting Ebola virus glycoprotein in healthy adults: a randomised, first-in-human phase 1 study. *The Lancet Infectious Diseases*, *18*(8), 884-893. doi:10.1016/s1473-3099(18)30397-9
- Soto, C., Bombardi, R. G., Branchizio, A., Kose, N., Matta, P., Sevy, A. M., . . . Crowe, J. E., Jr. (2019). High frequency of shared clonotypes in human B cell receptor repertoires. *Nature*, *566*(7744), 398-402. doi:10.1038/s41586-019-0934-8
- Stavnezer, J., Guikema, J. E., & Schrader, C. E. (2008). Mechanism and regulation of class switch recombination. *Annu Rev Immunol*, *26*, 261-292. doi:10.1146/annurev.immunol.26.021607.090248
- Suder, E., Furuyama, W., Feldmann, H., Marzi, A., & de Wit, E. (2018). The vesicular stomatitis virus-based Ebola virus vaccine: From concept to clinical trials. *Hum Vaccin Immunother*, *14*(9), 2107-2113. doi:10.1080/21645515.2018.1473698
- Suschak, J. J., & Schmaljohn, C. S. (2019). Vaccines against Ebola virus and Marburg virus: recent advances and promising candidates. *Hum Vaccin Immunother*, *15*(10), 2359-2377. doi:10.1080/21645515.2019.1651140
- Takada, A., Ebihara, H., Jones, S., Feldmann, H., & Kawaoka, Y. (2007). Protective efficacy of neutralizing antibodies against Ebola virus infection. *Vaccine*, *25*(6), 993-999. doi:10.1016/j.vaccine.2006.09.076

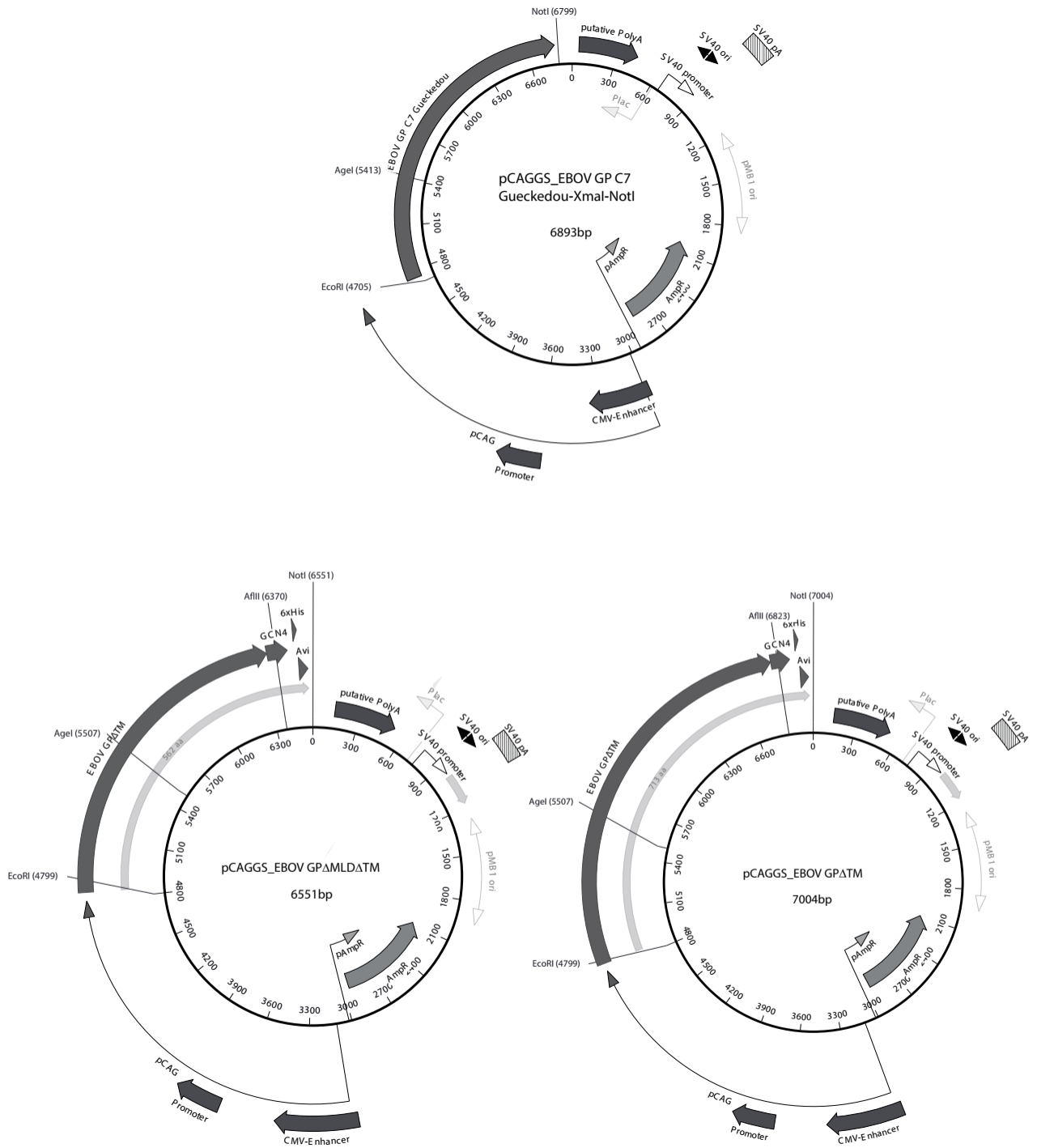
- Talmage, D. W. (1959). Immunological specificity, unique combinations of selected natural globulins provide an alternative to the classical concept. *Science*, *129*(3364), 1643-1648. doi:10.1126/science.129.3364.1643
- Thom, R., Tipton, T., Strecker, T., Hall, Y., Akoi Bore, J., Maes, P., . . . Carroll, M. W. (2021). Longitudinal antibody and T cell responses in Ebola virus disease survivors and contacts: an observational cohort study. *Lancet Infect Dis*, *21*(4), 507-516. doi:10.1016/S1473-3099(20)30736-2
- Thomson, C. A., Bryson, S., McLean, G. R., Creagh, A. L., Pai, E. F., & Schrader, J. W. (2008). Germline V-genes sculpt the binding site of a family of antibodies neutralizing human cytomegalovirus. *EMBO J*, *27*(19), 2592-2602. doi:10.1038/emboj.2008.179
- Throsby, M., Geuijen, C., Goudsmit, J., Bakker, A. Q., Korimbocus, J., Kramer, R. A., . . . de Kruif, J. (2006). Isolation and characterization of human monoclonal antibodies from individuals infected with West Nile Virus. *J Virol*, *80*(14), 6982-6992. doi:10.1128/JVI.00551-06
- Tian, C., Luskin, G. K., Dischert, K. M., Higginbotham, J. N., Shepherd, B. E., & Crowe, J. E., Jr. (2008). Immunodominance of the VH1-46 antibody gene segment in the primary repertoire of human rotavirus-specific B cells is reduced in the memory compartment through somatic mutation of nondominant clones. *J Immunol*, *180*(5), 3279-3288. doi:10.4049/jimmunol.180.5.3279
- Tiller, T., Meffre, E., Yurasov, S., Tsuiji, M., Nussenzweig, M. C., & Wardemann, H. (2008). Efficient generation of monoclonal antibodies from single human B cells by single cell RT-PCR and expression vector cloning. *Journal of Immunological Methods*, *329*(1-2), 112-124. doi:10.1016/j.jim.2007.09.017
- Tiller, T., Meffre, E., Yurasov, S., Tsuiji, M., Nussenzweig, M. C., & Wardemann, H. (2008). Efficient generation of monoclonal antibodies from single human B cells by single cell RT-PCR and expression vector cloning. *J Immunol Methods*, *329*(1-2), 112-124. doi:10.1016/j.jim.2007.09.017
- Tonegawa, S. (1976). Reiteration frequency of immunoglobulin light chain genes: further evidence for somatic generation of antibody diversity. *Proc Natl Acad Sci U S A*, *73*(1), 203-207. doi:10.1073/pnas.73.1.203
- Tonegawa, S. (1983). Somatic generation of antibody diversity. *Nature*, *302*(5909), 575-581. doi:10.1038/302575a0
- Towner, J. S., Sealy, T. K., Khristova, M. L., Albarino, C. G., Conlan, S., Reeder, S. A., . . . Nichol, S. T. (2008). Newly discovered ebola virus associated with hemorrhagic fever outbreak in Uganda. *PLoS Pathog*, *4*(11), e1000212. doi:10.1371/journal.ppat.1000212
- Vander Heiden, J. A., Yaari, G., Uduman, M., Stern, J. N., O'Connor, K. C., Hafler, D. A., . . . Kleinstein, S. H. (2014). pRESTO: a toolkit for processing high-throughput sequencing raw reads of lymphocyte receptor repertoires. *Bioinformatics*, *30*(13), 1930-1932. doi:10.1093/bioinformatics/btu138
- Volchkov, V. E., Becker, S., Volchkova, V. A., Ternovoj, V. A., Kotov, A. N., Netesov, S. V., & Klenk, H. D. (1995). GP mRNA of Ebola virus is edited by the Ebola virus polymerase and by T7 and vaccinia virus polymerases. *Virology*, *214*(2), 421-430. doi:10.1006/viro.1995.0052
- Volchkova, V. A., Feldmann, H., Klenk, H. D., & Volchkov, V. E. (1998). The nonstructural small glycoprotein sGP of Ebola virus is secreted as an antiparallel-orientated homodimer. *Virology*, *250*(2), 408-414. doi:10.1006/viro.1998.9389
- Volchkova, V. A., Klenk, H. D., & Volchkov, V. E. (1999). Delta-peptide is the carboxy-terminal cleavage fragment of the nonstructural small glycoprotein sGP of Ebola virus. *Virology*, *265*(1), 164-171. doi:10.1006/viro.1999.0034
- von Boehmer, L., Liu, C., Ackerman, S., Gitlin, A. D., Wang, Q., Gazumyan, A., & Nussenzweig, M. C. (2016). Sequencing and cloning of antigen-specific antibodies from mouse memory B cells. *Nat Protoc*, *11*(10), 1908-1923. doi:10.1038/nprot.2016.102
- Wang, H., Shi, Y., Song, J., Qi, J., Lu, G., Yan, J., & Gao, G. F. (2016). Ebola Viral Glycoprotein Bound to Its Endosomal Receptor Niemann-Pick C1. *Cell*, *164*(1-2), 258-268. doi:10.1016/j.cell.2015.12.044
- Wang, Z., Schmidt, F., Weisblum, Y., Muecksch, F., Barnes, C. O., Finkin, S., . . . Nussenzweig, M. C. (2021). mRNA vaccine-elicited antibodies to SARS-CoV-2 and circulating variants. *Nature*. doi:10.1038/s41586-021-03324-6

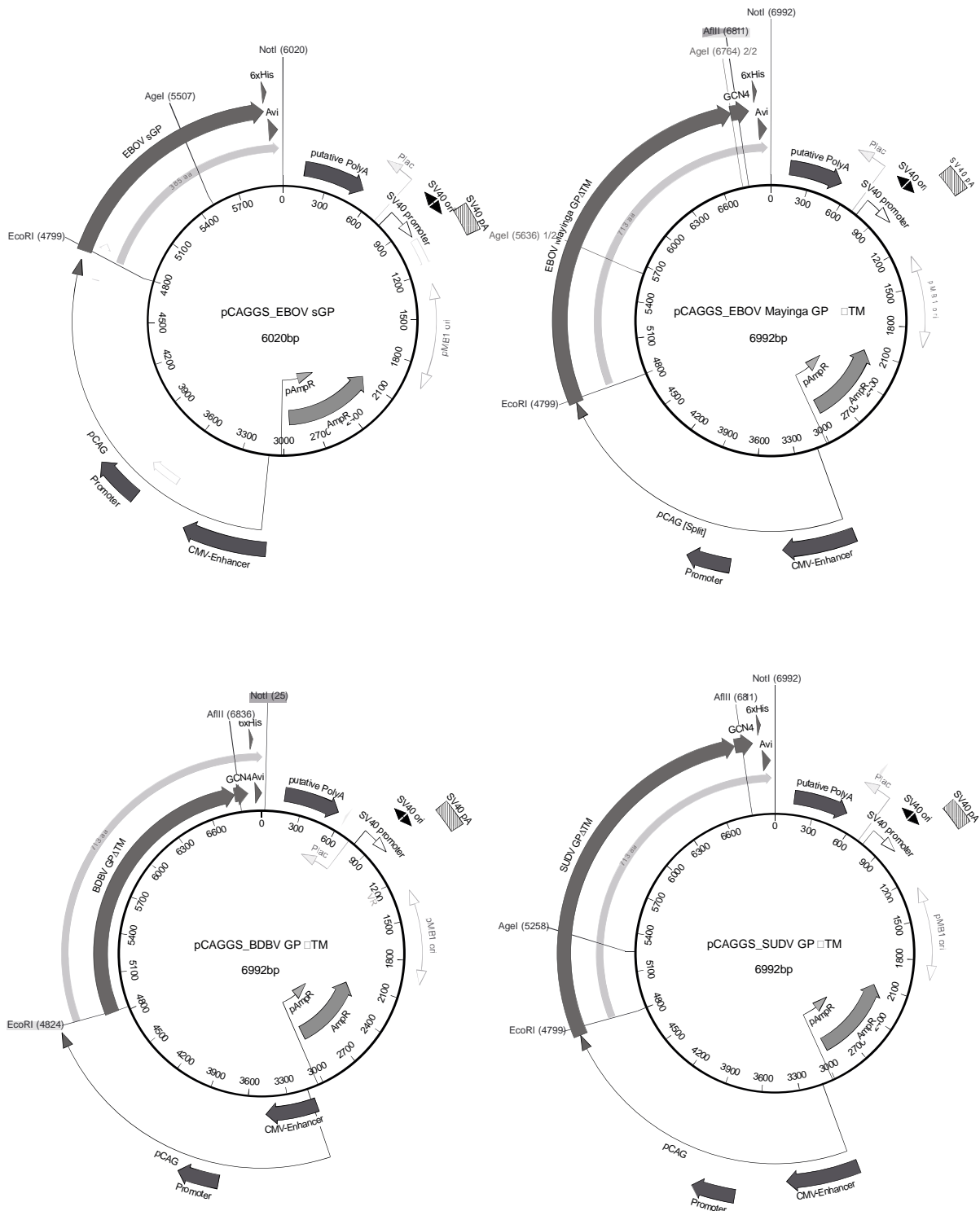
- Warfield, K. L., Howell, K. A., Vu, H., Geisbert, J., Wong, G., Shulenin, S., . . . Aman, M. J. (2018). Role of Antibodies in Protection Against Ebola Virus in Nonhuman Primates Immunized With Three Vaccine Platforms. *J Infect Dis*, 218(suppl_5), S553-S564. doi:10.1093/infdis/jiy316
- Warren, T. K., Jordan, R., Lo, M. K., Ray, A. S., Mackman, R. L., Soloveva, V., . . . Bavari, S. (2016). Therapeutic efficacy of the small molecule GS-5734 against Ebola virus in rhesus monkeys. *Nature*, 531(7594), 381-385. doi:10.1038/nature17180
- Wec, A. Z., Herbert, A. S., Murin, C. D., Nyakatura, E. K., Abelson, D. M., Fels, J. M., . . . Bornholdt, Z. A. (2017). Antibodies from a Human Survivor Define Sites of Vulnerability for Broad Protection against Ebolaviruses. *Cell*, 169(5), 878-890 e815. doi:10.1016/j.cell.2017.04.037
- Weigert, M. G., Cesari, I. M., Yonkovich, S. J., & Cohn, M. (1970). Variability in the lambda light chain sequences of mouse antibody. *Nature*, 228(5276), 1045-1047. doi:10.1038/2281045a0
- White, J. M., & Schornberg, K. L. (2012). A new player in the puzzle of filovirus entry. *Nat Rev Microbiol*, 10(5), 317-322. doi:10.1038/nrmicro2764
- WHO. (1978a). Ebola haemorrhagic fever in Sudan, 1976. Report of a WHO/International Study Team. *Bull World Health Organ*, 56(2), 247-270. Retrieved from <https://www.ncbi.nlm.nih.gov/pubmed/307455>
- WHO. (1978b). Ebola haemorrhagic fever in Zaire, 1976. *Bull World Health Organ*, 56(2), 271-293. Retrieved from <https://www.ncbi.nlm.nih.gov/pubmed/307456>
- WHO. (2018a). Compassionate use of Ebola vaccine in the context of the Ebola outbreak in North Kivu, Democratic Republic of the Congo. Retrieved from <https://www.who.int/ebola/drc-2018/faq-vaccine/en/>
- <https://www.afro.who.int/sites/default/files/2018-11/Frequently%20Asked%20Questions-%20Compassionate%20Use%20of%20Ebola%20Vaccine%20in%20the%20context%20of%20the%20Ebola%20outbreak%20in%20North%20Kivu%2C%20Democratic%20Republic%20of%20Congo.pdf>
- WHO. (2018b). Ebola Haemorrhagic Fever. <http://www.who.int/mediacentre/factsheets/fs103/en/>. Retrieved from <http://www.who.int/mediacentre/factsheets/fs103/en/>
- WHO. (2018c). Ebola vaccines – Background paper for SAGE (Strategic Advisory Group of Experts) deliberations. https://www.who.int/immunization/sage/meetings/2018/october/2_Ebola_SAGE2018Oct_BgDoc_20180919.pdf. Retrieved from https://www.who.int/immunization/sage/meetings/2018/october/2_Ebola_SAGE2018Oct_BgDoc_20180919.pdf
- WHO. (2019). Preliminary results on the efficacy of rVSV-ZEBOV-GP Ebola vaccine using the ring vaccination strategy in the control of an Ebola outbreak in the Democratic Republic of the Congo: an example of integration of research into epidemic response. <https://www.who.int/csr/resources/publications/ebola/ebola-ring-vaccination-results-12-april-2019.pdf>, 1-4.
- WHO. (2020a). 10th Ebola outbreak in the Democratic Republic of the Congo declared over; vigilance against flare-ups and support for survivors must continue. Retrieved from <https://www.who.int/news/item/25-06-2020-10th-ebola-outbreak-in-the-democratic-republic-of-the-congo-declared-over-vigilance-against-flare-ups-and-support-for-survivors-must-continue>
- WHO. (2020b). New Ebola outbreak detected in northwest Democratic Republic of the Congo; WHO surge team supporting the response. Retrieved from <https://www.who.int/news/item/01-06-2020-new-ebola-outbreak-detected-in-northwest-democratic-republic-of-the-congo-who-surge-team-supporting-the-response>
- WHO. (2021a, 02/23). Ebola virus disease. Retrieved from <https://www.who.int/news-room/factsheets/detail/ebola-virus-disease>
- WHO. (2021b, 02/19). Ebola virus disease - Disease outbreak news. Retrieved from <https://www.who.int/csr/don/archive/disease/ebola/en/>
- Wilson, P. C., & Donald Capra, J. (1998). The super-information age of immunoglobulin genetics. *J Exp Med*, 188(11), 1973-1975. doi:10.1084/jem.188.11.1973
- Winter, G. (2010). xia2: an expert system for macromolecular crystallography data reduction. *Journal of Applied Crystallography*, 43, 186-190. doi:10.1107/S0021889809045701

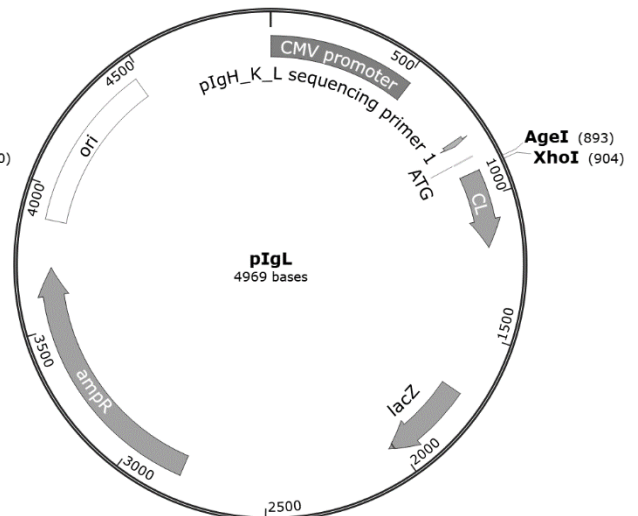
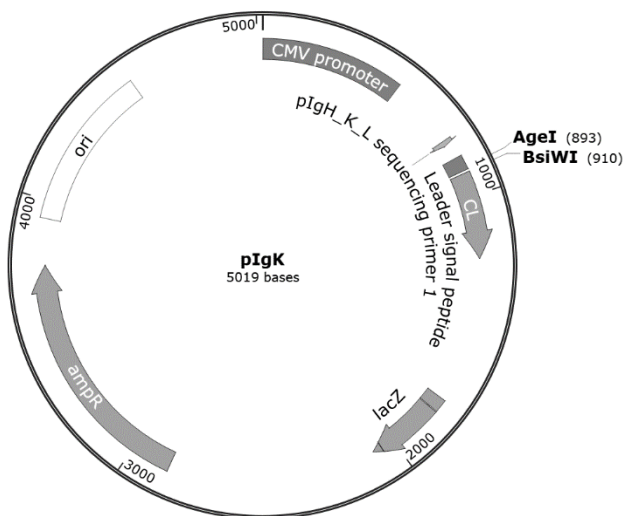
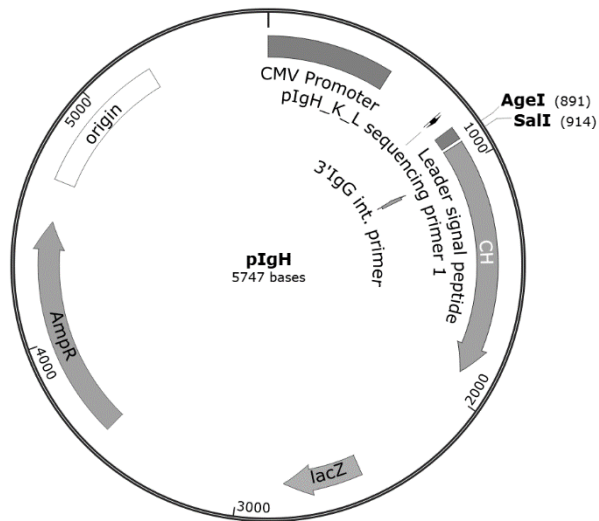
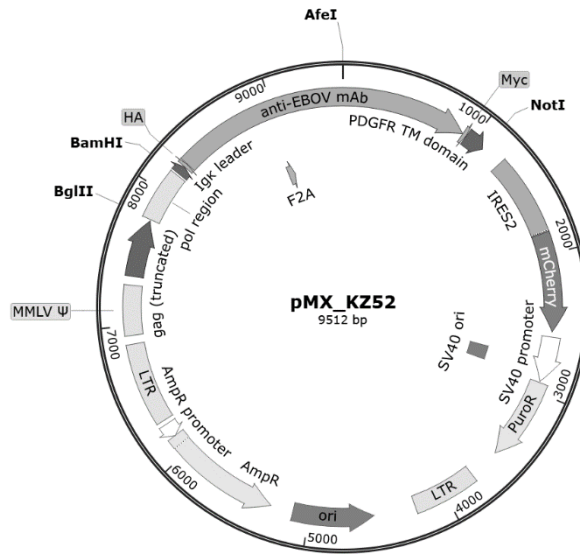
- Wolf, T., Kann, G., Becker, S., Stephan, C., Brodt, H. R., de Leuw, P., . . . Zacharowski, K. (2015). Severe Ebola virus disease with vascular leakage and multiorgan failure: treatment of a patient in intensive care. *Lancet*, *385*(9976), 1428-1435. doi:10.1016/S0140-6736(14)62384-9
- Wolfe, D. N., Taylor, M. J., & Zarrabian, A. G. (2020). Lessons learned from Zaire ebolavirus to help address urgent needs for vaccines against Sudan ebolavirus and Marburg virus. *Hum Vaccin Immunother*, *16*(11), 2855-2860. doi:10.1080/21645515.2020.1741313
- Wong, G., Audet, J., Fernando, L., Fausther-Bovendo, H., Alimonti, J. B., Kobinger, G. P., & Qiu, X. (2014). Immunization with vesicular stomatitis virus vaccine expressing the Ebola glycoprotein provides sustained long-term protection in rodents. *Vaccine*, *32*(43), 5722-5729. doi:10.1016/j.vaccine.2014.08.028
- Wong, G., Mendoza, E. J., Plummer, F. A., Gao, G. F., Kobinger, G. P., & Qiu, X. (2018). From bench to almost bedside: the long road to a licensed Ebola virus vaccine. *Expert Opin Biol Ther*, *18*(2), 159-173. doi:10.1080/14712598.2018.1404572
- Wu, Y. C., Kipling, D., Leong, H. S., Martin, V., Ademokun, A. A., & Dunn-Walters, D. K. (2010). High-throughput immunoglobulin repertoire analysis distinguishes between human IgM memory and switched memory B-cell populations. *Blood*, *116*(7), 1070-1078. doi:10.1182/blood-2010-03-275859
- Ye, J., Ma, N., Madden, T. L., & Ostell, J. M. (2013). IgBLAST: an immunoglobulin variable domain sequence analysis tool. *Nucleic Acids Res*, *41*(Web Server issue), W34-40. doi:10.1093/nar/gkt382
- Zhao, X., Howell, K. A., He, S., Brannan, J. M., Wec, A. Z., Davidson, E., . . . Aman, M. J. (2017). Immunization-Elicited Broadly Protective Antibody Reveals Ebolavirus Fusion Loop as a Site of Vulnerability. *Cell*, *169*(5), 891-904 e815. doi:10.1016/j.cell.2017.04.038
- Zhao, Y., Ren, J., Harlos, K., Jones, D. M., Zeltina, A., Bowden, T. A., . . . Stuart, D. I. (2016). Toremfene interacts with and destabilizes the Ebola virus glycoprotein. *Nature*, *535*(7610), 169-172. doi:10.1038/nature18615
- Zhou, T., Lynch, R. M., Chen, L., Acharya, P., Wu, X., Doria-Rose, N. A., . . . Kwong, P. D. (2015). Structural Repertoire of HIV-1-Neutralizing Antibodies Targeting the CD4 Supersite in 14 Donors. *Cell*, *161*(6), 1280-1292. doi:10.1016/j.cell.2015.05.007
- Zhu, W., Banadyga, L., Emeterio, K., Wong, G., & Qiu, X. (2019). The Roles of Ebola Virus Soluble Glycoprotein in Replication, Pathogenesis, and Countermeasure Development. *Viruses*, *11*(11). doi:10.3390/v111110999

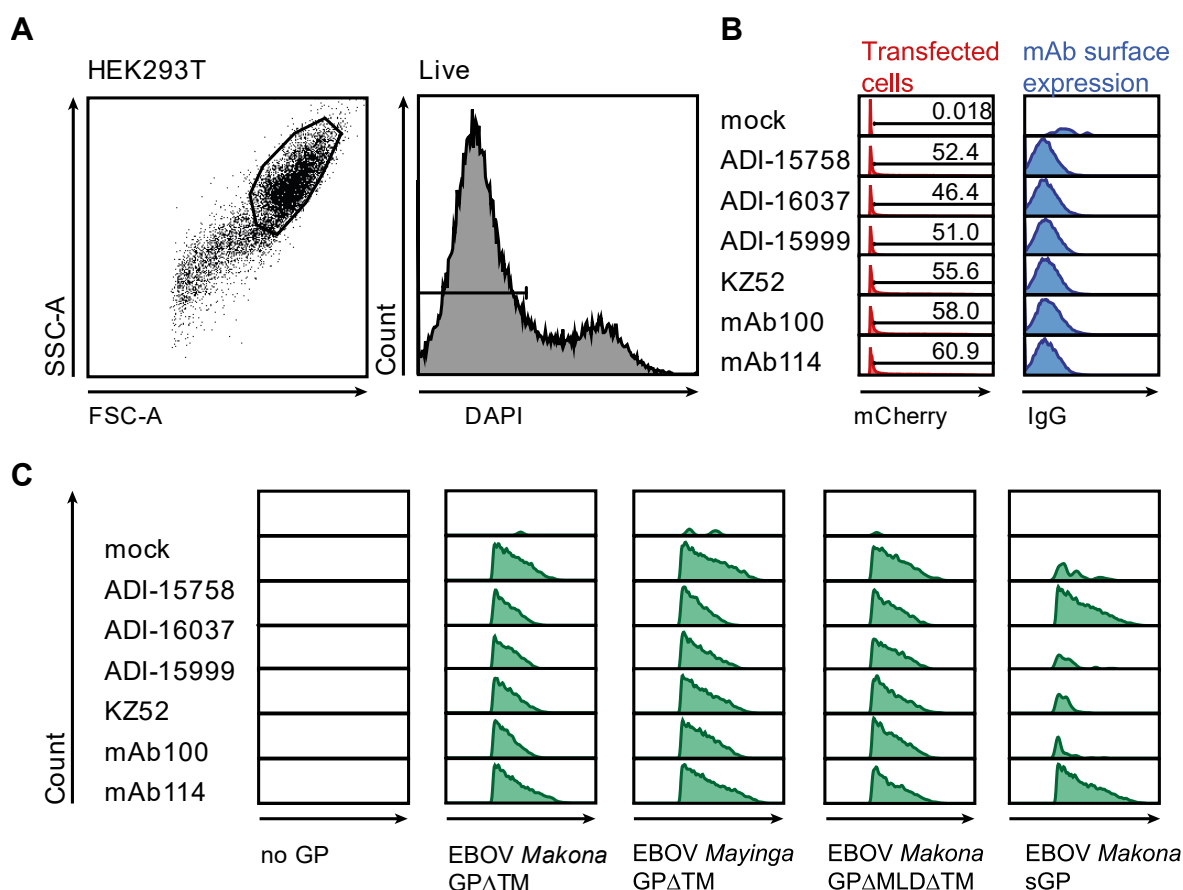
6 Appendix

Appendix Figure 1. Vector maps.









Appendix Figure 2. Gating strategy of testing of different GP constructs by binding to surface expressed of EBOV GP-specific antibodies.

Generation of constructs for surface expression of EBOV-reactive antibodies (mAb100, mAb114, ADI-15758, ADI-15999, ADI-16037, and KZ52) on HEK293T cells (**Figure 10**). Variable and constant regions of immunoglobulin light (VL, CL) and heavy chains (VH, CH) were linked by a 2A self-processing signal sequence followed by a c-myc and a PDGF receptor-transmembrane domain. As control, an empty vector (pMX) containing an IRES-mCherry sequence was used. Plasmids were transiently transfected into HEK293T cells. (A) Flow cytometry analysis to evaluate EBOV GP Δ TM recognition by antibody-expressing HEK293T cells as a surrogate for anti-EBOV GP Δ TM-reactive B cells. Left: Dot plot showing FSC-A vs. SSC-A served to morphologically gate HEK293T cells. Right: Histogram to select live and DAPI-negative cells. Representative dot plots of one sample. (B) Left: Transfection efficiency was monitored by reporter protein mCherry detected in the PI channel (red). Right: Cells expressing transfected EBOV GP-specific IgG antibodies on their cell surface were labeled with anti-IgG antibody and APC MFI was monitored (blue). (C) Binding of different GP constructs to surface expressed antibodies was evaluated by FITC MFI. FITC detection was monitored by adding no GP, EBOV *Makona* GP Δ TM, EBOV *Mayinga* GP Δ TM, EBOV *Makona* GP Δ MLD Δ TM, and EBOV *Makona* sGP (from left to right).

Appendix Table 1. Information on clonal and/or produced antibody sequences.

EV01.

Antibody	Clone #	# of clonal members	Pro-duced	IGHV	IGHD	IGHJ	IGH Identity (%)	V _H CDR3 (aa)	V _H CDR3 length (aa)	Light chain	IGKV/ IGLV	IGKJ/ IGLJ	IGK/IGL Identity (%)	V _L CDR3 (aa)	V _L CDR3 length (aa)
1T0114	1-26	2	yes	3-23*01	3-9*01	4*02	95.9	AKDNSYNEILTSGHGPPDY	19	κ	3-11*01	4*01	97.2	QQRSQWEPPLT	10
1T0116	1-31	2	yes	3-33*01	3-22*01	4*02	96.9	ARSHNSGYRYRYFDY	15	κ	3-15*01	3*01	99.3	QQYNNWPPIT	10
1T0121	1-51	2	no	4-59*08	3-3*01	6*02	92.8	ARAPRHYDFWGSYYNGMDV	21	n.d.	n.d.	n.d.	n.d.	n.d.	n.d.
1T0125	1-52	2	no	5-51*03	2-15*01	5*01	97.3	AKREGHCSDLCYSWFDS	19	n.d.	n.d.	n.d.	n.d.	n.d.	n.d.
1T0126	1-34	2	no	3-7*01	3-10*01	4*02	97	TREVRGSAY	9	n.d.	n.d.	n.d.	n.d.	n.d.	n.d.
1T0129	1-4	6	yes	1-2*02	1-1*01	4*02	84.9	GTEGIPSDIDY	10	κ	4-1*01	2*01	84.5	QQYNTTPRT	9
1T0130	1-9	2	yes	1-46*01	3-22*01	3*02	99	ARHDSGGYDAFDI	13	λ	3-25*02	2*01	94.8	QSSDSSSTYVV	11
1T0139	1-46	3	yes	4-4*07	5-12*01	4*02	95.9	ARESYRYNAYDIHPPDY	17	λ	3-1*01	2*01	93.6	QAWASNTVV	9
1T0144	1-43	2	no	4-39*01	3-10*01	6*02	97.3	ARPIYMRVGTSMVD	15	n.d.	n.d.	n.d.	n.d.	n.d.	n.d.
1T0148	1-44	5	no	4-4*07	6-25*01	3*02	94.9	ARGVYRWAAFSAADNFD	19	λ	3-1*01	2*01	95	QAWDSGTYYV	10
1T0161	1-13	2	no	1-69*04	2-2*01	6*02	97	ARDRYSAEIVVAGDYGMVD	21	λ	2-23*02	1*01	98	YSYAGSSTYV	10
1T0162	1-8	2	no	1-3*01	6-6*01	6*02	97.2	ASAAARRGYYTILDV	14	n.d.	n.d.	n.d.	n.d.	n.d.	n.d.
1T0177	1-20	2	no	3-21*01	2-15*01	5*02	93.2	ARVVCGECSGGYCYSAWLDP	20	n.d.	n.d.	n.d.	n.d.	n.d.	n.d.
1T0201	1-18	2	yes	3-15*01	3-3*01	6*02	95.3	TTRVDMWCKYGTDV	15	λ	1-40*01	3*02	96.6	QSYDSRLSDSWV	12
1T0211	1-50	2	no	5-51*01	3-3*01	4*02	94.2	AKLQGFWMAYLYFDF	15	λ	1-51*01	3*02	94.3	GTWDTSLSTGLYMW	14
1T0221	1-1	7	yes	1-18*01	3-22*01	5*02	95.6	ARHVTMILDGWFD	14	κ	3-20*01	4*01	98.6	QQYGSSPLT	9
1T0222	1-38	2	yes	3-7*01	6-13*01	4*02	98.6	AVGAAAAGRY	9	κ	1-17*01	1*01	100	LQHNSYPQT	9
1T0225	1-40	2	yes	4-30-2*01	3-16*01	4*02	95	ARDFGGPFDDH	10	λ	2-14*01	2*01	95.1	SSYTSNFSV	10
1T0227	1-15	3	yes	3-15*01	6-19*01	4*02	96.7	TTHVPDYNASYYWVY	15	λ	1-40*01	1*01	96.6	QSYDIRLSDNYV	12
1T0242	1-39	5	yes	3-74*01	3-16*01	4*02	94.3	ARDLSWVLFDS	11	λ	2-8*01	1*01	93.6	CSYTGKPSFV	10
1T0248	1-25	2	yes	3-23*01	1-26*01	4*02	93.6	AKDKGPRATLGAILDS	16	κ	4-1*01	3*01	95	QQYFGTPLT	9
1T0264	1-22	3	yes	3-23*01	1-26*01	4*02	93.9	AKDNVRPSGYSVWLDY	17	λ	1-47*01	2*01	94.8	AAWDDSLSNQGV	12
1T0265	1-48	5	no	4-59*08	5-12*01	5*02	80.5	ARHPSGYGYDWMGYNWFEP	19	λ	1-47*01	1*01	87.7	ASWDASVSAYV	11
1T0267	1-45	2	no	4-4*07	4-17*01	4*02	92.2	ASTRPYGDYGGYFAN	15	n.d.	n.d.	n.d.	n.d.	n.d.	n.d.
1T0301	1-41	2	yes	4-34*12	3-10*01	6*02	95.2	ARSGVLGYGMVD	13	λ	1-47*01	1*01	97.3	AAWDDSLSDYV	11

Appendix Table 1. Information on clonal and/or produced antibody sequences.

EV01 (continued).

Antibody	Clone #	# of clonal members	Pro-duced	IGHV	IGHD	IGHJ	IGH Identity (%)	V _H CDR3 (aa)	V _H CDR3 length (aa)	Light chain	IGKV/IGLV	IGKJ/IGLJ	IGK/IGL Identity (%)	V _L CDR3 (aa)	V _L CDR3 length (aa)
1T0321	1-Single01	1	yes	1-2*02	4-17*01	6*02	94.5	ATPTMTTRSYHHMDV	16	κ	2-28*01	1*01	98.7	MHALQTFWT	9
1T0322	1-19	2	no	3-15*01	1-26*01	2*01	90.6	TTGPGDF	7	n.d.	n.d.	n.d.	n.d.	n.d.	n.d.
1T0325	1-23	2	yes	3-23*01	2-2*01	4*02	92.9	AKEREVAVFPGAVFNY	16	κ	4-1*01	4*01	98	QYYISLPLT	9
1T0344	1-30	2	no	3-30-3*01	2-2*01	6*02	91.2	TRGGDIVVPADSLDIYGMVDV	20	κ	1-17*01	2*01	96.9	LQCNSYPRT	9
1T0351	1-37	2	yes	3-7*01	4-11*01	4*02	96.6	ARTVRFVDY	9	κ	2-30*01	1*01	98	MQGTHWFPPT	9
1T0361	1-21	2	no	3-21*01	6-19*01	4*02	96.2	ARPGISVAGDATNFDS	16	n.d.	n.d.	n.d.	n.d.	n.d.	n.d.
1T0371	1-12	3	yes	1-69*09	5-24*01	5*02	94.9	ATLEMATLFA	10	κ	1-16*02	4*01	98.6	QQYNSYPFT	9
1T0402	1-27	2	no	3-30*03	n.m.	6*02	98	AIGGSRVPMADV	13	n.d.	n.d.	n.d.	n.d.	n.d.	n.d.
1T0404	1-49	2	no	4-59*01	3-22*01	4*02	95.5	ARAPRWYDRSGYISLPPDF	19	n.d.	n.d.	n.d.	n.d.	n.d.	n.d.
1T0451	1-7	3	yes	1-3*01	3-16*01	6*02	89.1	ARGRGTSYIAFDV	14	κ	1-39*01	2*01	93	QQTYRSPLYT	10
1T0455	1-16	3	yes	3-15*01	3-22*01	4*02	94	TTLVH	5	λ	1-40*01	2*01	97.3	QSYDSRSLSDHVV	12
1T0456	1-17	2	yes	3-15*01	3-10*01	4*02	96	IATPFTLILPESG	13	λ	1-51*01	3*02	97	GTWDSLSLSTGLYVV	14
1T0473	1-14	5	yes	1-8*01	3-10*01	6*02	94.9	ARGNQFGEILLSSYYGLDV	19	κ	3-20*01	3*01	95.4	QQYSSLLIT	9
1T0474	1-29	2	no	3-30*04	2-2*01	6*02	96.3	ARDFAYGRSSYALRVGVDGMDV	22	n.d.	n.d.	n.d.	n.d.	n.d.	n.d.
1T0476	1-33	2	no	3-53*02	3-9*01	2*01	94.5	ARWSKDFHDIITGPPYFDL	20	n.d.	n.d.	n.d.	n.d.	n.d.	n.d.
1T0480	1-42	7	yes	4-39*01	4-11*01	4*02	87.9	ARSWRXYRRYSRNFDY	15	λ	1-40*01	2*01	89.5	QSYDTNLLGDVI	11
1T0546	1-32	2	yes	3-33*01	6-19*01	4*02	93.2	ARAGAAAGIDV	11	κ	4-1*01	4*01	96.1	QQYDSIPLT	9
1T0552	1-24	2	yes	3-23*01	3-16*01	3*02	89.5	AKFSQLFGYAFDI	13	κ	3-20*01	1*01	93.4	QQYGNPFWT	9
1T0554	1-5	2	yes	1-3*01	2-15*01	6*02	98	ASSGGRYYYVMDV	13	κ	3-20*01	4*01	100	QQYSSSPLT	9
1T0565	1-28	5	yes	3-30*03	1-14*01	6*02	90.2	AIGGSTVTPGLDV	13	κ	1D-12*01	4*01	90.9	QQAKSPPLT	9
1T0582	1-6	5	yes*	1-3*01	6-6*01	6*02	98.6	ASTSRRRGYYYVMDV	14	κ	3-20*01	4*01	99.3	QQYSSSPLT	9
1T0614	1-36	3	yes	3-7*01	6-13*01	4*02	94.2	ARSPAAAAGTY	11	κ	2-30*02	1*01	97.7	MQGSHWFPWT	9
1T0623	1-11	2	yes	1-69*09	2-21*02	3*01	87.2	ATENCGGDCQRPDPVFDV	19	κ	4-1*01	2*01	93.1	QQYYSTPRT	9
1T0653	1-Single02	1	yes	3-7*01	3-16*01	4*02	96.2	AKSPLISNAY	10	κ	2-30*01	1*01	97	MQGTHWFPWT	9
1T0655	1-10	2	yes	1-46*01	6-19*01	6*02	93.9	ARDRQWLPINGYSYFNMGMDV	21	κ	1-39*01	1*01	91.6	QQSFSSPRT	9
1T0665	1-35	3	yes	3-7*01	6-13*01	6*02	98.6	ARGRQLIVL	9	λ	2-14*01	2*01	98	SSYTSRSTLV	10

Appendix Table 1. Information on clonal and/or produced antibody sequences.

EV03.

Antibody	Clone #	# of clonal members	Pro-duced	IGHV	IGHD	IGHJ Identity (%)	IGH Identity (%)	V _H CDR3 (aa)	V _H CDR3 length chain (aa)	Light chain	IGKV/ IGLV	IGKJ/ IGLJ	IGK/IGL Identity (%)	V _L CDR3 (aa)	V _L CDR3 length (aa)
3T0103	3-5	2	no	1-2*02	3-16*02	4*02	93.6	VRGGLSGDRSELFFKY	16	n.d.	n.d.	n.d.	n.d.	n.d.	n.d.
3T0123	3-2	2	yes	1-18*01	6-13*01	4*02	87.1	ARGLGDSYSNAMFVYVFDY	19	κ	3-15*01	2*01	88.7	QQYSQRPT	8
3T0134	3-27	3	no	3-23*01	6-6*01	4*02	91.1	ARGAAARFSPFDF	13	n.d.	n.d.	n.d.	n.d.	n.d.	n.d.
3T0135	3-42	2	yes	3-74*01	1-26*01	4*02	94.2	ARGGNYILDY	10	λ	2-18*02	1*01	96.9	SSYTSSATYV	10
3T0147	3-46	2	yes	4-4*02	7-27*01	4*02	93.4	ARSPLGKRGFDF	12	λ	1-40*01	3*02	93.9	QSYDSRLRDNWV	12
3T0150	3-25	7	no	3-23*01	2-2*01	4*02	90	AILGNCRSTSYARGY	16	n.d.	n.d.	n.d.	n.d.	n.d.	n.d.
3T0159	3-44	2	yes	4-34*01	3-16*01	3*02	84.9	AKSAGWAIYAFDM	13	κ	3-20*01	2*01	87.2	QLYGRSPIMYA	11
3T0166	3-31	2	no	3-23*01	6-13*01	4*01	87.5	AKGPAARFSPFDV	13	n.d.	n.d.	n.d.	n.d.	n.d.	n.d.
3T0182	3-37	2	no	3-49*04	3-16*01	2*01	96	SRKGEDYHWYFDL	13	n.d.	n.d.	n.d.	n.d.	n.d.	n.d.
3T0183	3-6	37	yes*	1-69*06	3-16*01	6*02	90.1	ARQVRRRLGYGMDV	13	κ	3-15*01	2*01	92.7	QQYSDWPPYT	10
3T0202	3-12	17	yes*	3-13*01	3-10*01	4*02	94.2	ARAAFGAVFFDY	12	κ	3-20*01	5*01	96.5	QQYGNSPIT	9
3T0204	3-33	2	no	3-23*01	6-19*01	4*02	90.9	AKDFVQWLALFDY	13	n.d.	n.d.	n.d.	n.d.	n.d.	n.d.
3T0209	3-7	12	yes*	1-8*01	3-16*02	6*02	88.2	ARGAIIIGGVIALFGMDV	17	κ	1-27*01	1*01	93	QKYSSGGPRT	9
3T0213	3-4	6	yes	1-2*02	2-8*02	4*02	92.9	ARGRTTAGATGPLYDN	16	λ	2-23*02	3*02	93.9	CSLAGRGNWV	10
3T0215	3-35	2	yes	3-48*04	6-13*01	4*01	89.9	ARDTLEAGSWYPPFDK	15	λ	3-10*01	3*02	96.6	YSTDSSSGTQRV	11
3T0216	3-48	2	yes	4-4*02	3-10*01	6*01	88.2	VKIPFGISGMDV	12	κ	3-20*01	2*01	91.4	QLYTRPPPPRYT	11
3T0245	3-22	3	yes	3-15*01	6-6*01	6*02	89	ATRVHNGMDV	11	λ	1-40*01	3*02	95.6	QSYDSSLRDACV	12
3T0253	3-24	3	yes	3-15*01	1-14*01	6*02	93	TTRHRGMDV	10	λ	1-40*01	2*01	97.3	QSYDSSLSDAVV	12
3T0258	3-1	3	yes	1-18*01	6-13*01	3*01	87.6	AWRRSSWFAFDV	12	κ	3-20*01	2*01	94.1	QQYVSSPYT	9
3T0265	3-19	2	yes	3-15*01	n.m.	4*02	89.7	LTTPPPRY	8	λ	1-40*01	3*02	93.9	QSYDARLRDGEV	12
3T0303	3-10	4	yes	3-11*01	5-24*01	5*01	89.4	ASGTLKGDGYLFEES	16	κ	1-5*03	1*01	90.7	HQYKTWPWA	9
3T0325	3-41	2	yes	3-74*01	3-3*01	6*02	93.9	ARAAVDFRSASYIFGLDV	18	λ	2-18*02	1*01	97.3	SSFTSSTYF	10
3T0331	3-26	4	yes	3-23*01	6-25*01	4*02	90.1	AKSVRLSRPSPFDL	14	κ	3-11*01	4*01	94.4	QQRASWPLT	9
3T0338	3-Single02	1	yes	3-15*02	2-21*01	6*02	90.6	TTLNLGGGFPGEWRSV	16	λ	1-40*01	3*02	95	QSYDSRLRDSWV	12
3T0350	3-28	3	yes	3-23*01	1-1*01	4*02	90.2	AKDLKGNWNDGPPFDY	15	λ	1-51*01	3*02	95.2	GTWGNLSLGPFWV	13

Appendix Table 1. Information on clonal and/or produced antibody sequences.

EV03 (continued).

Antibody	Clone #	# of clonal members	Pro-duced	IGHV	IGHD	IGHJ	IGH identity (%)	V _H CDR3 (aa)	V _H CDR3 length (aa)	Light chain	IGKV/IGLV	IGKJ/IGLJ	IGK/IGL identity (%)	V _L CDR3 (aa)	V _L CDR3 length (aa)
3T0353	3-45	3	yes	4-34*01	3-16*01	3*02	85.1	ARTAGWGIYGFDI	13	κ	3-20*01	2*01	90.3	QLYGRSPIVYT	11
3T0368	3-49	4	yes	1-2*02	6-13*01	4*02	92.8	AAGLGH	6	λ	3-25*02	3*02	95.8	QSVDSGAWV	10
3T0405	3-34	2	yes	3-30*03	4-17*01	4*02	95.5	AANYRSELE	10	κ	2-30*02	1*01	96.3	MQATLMPWT	9
3T0409	3-43	4	yes	4-34*01	7-27*01	3*01	90	ARTGGWGIYAFDV	13	κ	3-20*01	2*01	93.1	QQYGRSPLIMYT	12
3T0411	3-23	2	yes	3-15*01	1-7*01	4*02	94.4	TTGHITGTLF	10	κ	4-1*01	4*01	97.7	QQYYSMMIT	9
3T0415	3-30	4	yes	3-23*01	2-8*01	6*02	92.5	AINGGV	6	κ	4-1*01	4*01	93.7	QQHYATRVT	9
3T0420	3-29	2	yes	3-23*01	3-9*01	4*02	89.5	ARDPRVATTGTVYFDS	16	λ	3-25*02	2*01	92.6	QSADTSGTLVV	11
3T0427	3-38	2	yes	3-64D*06	3-3*01	4*02	86.5	TKDHHWSGQYTDY	13	κ	3-11*01	1*01	95.1	QQRSSWRT	8
3T0442	3-32	2	yes	3-23*01	4-17*01	4*02	90.4	AMGYGIYNS	9	κ	3-15*01	1*01	94.4	QQYINWPPWT	10
3T0458	3-8	2	yes	1-8*01	3-9*01	3*01	85.8	ARGFEWRSGNRRADFV	17	κ	1-5*03	1*01	89.9	QHYSYGSPWT	10
3T0465	3-50	2	no	3-33*01	2-15*01	4*02	93.9	ARESCYGGSCFFDH	14	n.d.	n.d.	n.d.	n.d.	n.d.	n.d.
3T0478	3-47	2	yes	4-59*01	3-22*01	4*02	94.2	ARDKRYDSSGYSHFYD	17	λ	1-47*01	3*02	97.6	AAWDGSLSGPV	11
3T0506	3-39	7	yes	3-72*01	3-22*01	3*02	92.7	VRVADYFDSGGYSLDAFDI	19	λ	1-51*01	3*02	94.6	ETWDTGLRGVV	11
3T0527	3-40	2	yes	3-74*03	1-26*01	1*01	90.7	AVVFLGAVR	9	κ	4-1*01	1*01	94.7	HQYDIPWT	9
3T0553	3-Single01	1	yes	3-33*01	2-8*02	6*02	94.9	ARGGDLLEVBSTDIYGLDV	20	κ	1-17*03	1*01	97.9	LQHNRYPWT	9
3T0611	3-36	2	yes	3-48*01	4-17*01	4*02	93.1	AGILDDYRDYGYDY	14	λ	3-25*02	3*02	94.8	QSSDNNNGSYRVM	12
3T0650	3-20	2	yes	3-15*01	3-3*02	5*02	92.9	VATPHWSVA	10	λ	1-40*01	3*02	96.6	QSYDSSLRDQWV	12
3T0662	3-3	2	yes	1-2*02	5-12*01	5*02	93.5	ASPGYCSTSNCPSP	14	λ	3-25*03	2*01	92.2	QSADSAGGSLI	11
3T0673	3-21	4	yes	3-15*01	3-22*01	5*02	87.3	TTYYYDNGGGSYSNP	14	λ	1-40*01	2*01	94.3	QSYDSRLRDFGI	12

Appendix Table 1. Information on clonal and/or produced antibody sequences.

EV04.

Antibody	Clone #	# of clonal members	Pro-duced	IGHV	IGHD	IGHJ	IGH Identity (%)	V _H CDR3 (aa)	V _H CDR3 length (aa)	Light chain	IGKV/IGLV	IGKJ/IGLJ	IGK/IGL Identity (%)	V _L CDR3 (aa)	V _L CDR3 length (aa)
4T0115	4-46	2	yes	3-9*01	5-24*01	6*02	94.6	AREGRDYNLPYYAMDV	17	κ	1-9*01	3*01	96.5	QRFNSYPIFT	10
4T0136	4-22	5	no	3-23*01	2-2*01	6*02	94.2	AKGMDCSSTTAPFCFYGMDV	20	λ	5-45*02	3*02	96.5	MIWHNLAW	9
4T0140	4-35	2	no	3-48*01	1-26*01	4*02	92.1	AKLGGSGHFHDS	12	λ	2-23*01	3*02	97.6	CSYAGTSAWM	10
4T0145	4-12	5	no	3-11*01	2-2*01	6*02	94.9	ARGERRHQPLFGLDV	15	κ	3-15*01	4*01	95.7	QQCNDWPLT	9
4T0149	4-13	2	no	3-11*01	2-8*01	4*02	97.3	ARDGMVYSMILLEHYFDS	18	n.d.	n.d.	n.d.	n.d.	n.d.	n.d.
4T0154	4-10	2	yes	1-69*02	5-24*01	4*02	89.7	AVEMATPSDT	10	κ	1-16*02	2*01	95.8	LQYSTYPT	9
4T0159	4-49	3	yes*	4-39*01	n.m.	4*01	93.3	ARRFDS	6	κ	3-15*01	1*01	96.8	QQYNDWFWT	9
4T0162	4-37	2	no	3-48*01	5-18*01	4*02	92.5	ARVPLRQYSLDF	12	n.d.	n.d.	n.d.	n.d.	n.d.	n.d.
4T0165	4-5	2	no	1-2*02	4-11*01	5*02	93.6	ATVPTVTMFGWFD	14	n.d.	n.d.	n.d.	n.d.	n.d.	n.d.
4T0168	4-Single01	1	yes	3-30*18	6-13*01	4*02	94.2	AKGATAAVFDS	12	κ	4-1*01	1*01	94.4	QQYINPPWT	9
4T0171	4-39	3	yes	3-72*01	3-22*01	3*02	91	VRVADVFDSSGYSVDAFEM	19	λ	1-51*01	2*01	93.9	GTWDTSLRGVI	11
4T0182	4-6	2	yes	1-2*02	3-10*01	6*02	95.9	AAPGETIVRGVIHYHGMGV	20	κ	2-28*01	2*01	97.7	MQALQTP	8
4T0201	4-23	2	no	3-23*01	3-3*01	6*02	92.6	AKDLGNFWSGYDGMVD	17	n.d.	n.d.	n.d.	n.d.	n.d.	n.d.
4T0202	4-45	2	no	3-74*01	3-3*01	5*02	94.9	VRDIGLIYGAWFDP	14	n.d.	n.d.	n.d.	n.d.	n.d.	n.d.
4T0219	4-29	3	no	3-33*01	2-15*01	4*02	96.3	AREFCFGGSCYFDY	14	n.d.	n.d.	n.d.	n.d.	n.d.	n.d.
4T0238	4-Single02	1	yes	1-3*01	3-3*02	5*02	92.9	ARDISLFPKGFDP	14	κ	4-1*01	4*01	94.7	QQYSSTPLT	9
4T0243	4-57	3	yes	4-59*01	5-18*01	6*02	92.8	ARAPRGYSSGKYNYYGLDV	19	λ	3-25*02	1*01	93.1	QSADSSGGYYV	11
4T0251	4-36	4	no	3-48*01	6-19*01	4*02	96.2	ARGQLVEDY	10	κ	3-15*01	1*01	95.9	QQYDNNWFPQT	9
4T0258	4-1	2	no	1-18*04	3-22*01	3*02	94.5	ARSISMILVGFPI	14	n.d.	n.d.	n.d.	n.d.	n.d.	n.d.
4T0262	4-8	2	yes	1-46*01	3-10*01	5*02	91.5	ARGITMIRDGFWDH	14	κ	1-5*01	2*03	95.1	LQYSSSSPYS	10
4T0269	4-Single03	1	yes	3-30*02	3-22*01	3*01	88.8	AKLPTHYRDDNEEVFDV	17	κ	1-5*01	2*01	92.2	QQYRNYFRT	9
4T0284	4-2	4	yes	1-18*04	3-10*01	5*02	96.3	ARGITMVRGLDWFD	15	κ	3-15*01	4*01	97.2	QQYKNWPLT	9
4T0306	4-55	4	yes	6-1*01	3-3*01	6*02	90.5	VREYDILWNGFYPPGGAMDV	19	κ	1-33*01	2*01	93	QQYDDLPR	9
4T0312	4-19	2	no	3-15*01	3-22*01	5*02	99.7	TTDWLRISMT	10	λ	1-40*01	3*02	97.6	QSYDSRLSDLWV	12
4T0337	4-42	2	yes	3-74*01	5-18*01	4*02	91.5	ARGGSDRAMAHDH	13	κ	3-20*01	2*01	95.5	QQYGSAPFT	9

Appendix Table 1. Information on clonal and/or produced antibody sequences.

EV04 (continued).

Antibody	Clone #	# of clonal members	Pro-duced	IGHV	IGHD	IGHJ Identity (%)	IGH Identity (%)	V _H CDR3 (aa)	V _H CDR3 length (aa)	Light chain	IGKV/IGLV	IGKJ/IGLJ	IGK/IGL Identity (%)	V _L CDR3 (aa)	V _L CDR3 length (aa)
4T0341	4-11	2	yes	1-69*01	3-22*01	6*02	94.9	ARDYRPYYDGGSYYSYYALDV	23	κ	1-5*03	2*01	98.2	QQYNTYST	8
4T0344	4-24	2	yes	3-23*01	4-11*01	4*02	93.6	VKGSWPRTVLSTYYFDY	18	κ	1-27*01	1*01	96.1	QKYNAPWR	9
4T0350	4-41	2	yes	3-72*01	n.m.	6*02	92	VRTMDV	6	κ	1-5*01	4*01	96.1	QHNSYPLT	9
4T0351	4-28	2	no	3-30*02	3-22*01	2*01	82.8	AKESRQDTSGRHTYFDL	18	n.d.	n.d.	n.d.	n.d.	n.d.	n.d.
4T0365	4-50	2	yes	4-39*01	3-10*01	4*02	91.9	ATSSRGSVSYRSRY	14	λ	1-51*01	3*02	92.9	SVWDSLSGSRV	11
4T0369	4-34	4	no	3-48*02	3-10*01	6*02	92.5	ARAPRDLSYAMDF	13	λ	1-40*01	3*02	95.6	QTYDDSLSGWV	11
4T0412	4-Single04	1	yes	3-33*01	1-14*01	2*01	92.2	VRETFQPGGEVPLWYFDV	19	κ	1-39*01	1*01	95.1	QQSYGTPRT	9
4T0417	4-31	3	yes	3-33*01	6-13*01	4*02	93.6	ARDAHNSRLDY	11	κ	3-20*01	3*01	92.1	QQYGYSPPRIT	11
4T0418	4-56	2	no	3-23*01	2-15*01	4*02	99.7	AKRVVLDY	8	n.d.	n.d.	n.d.	n.d.	n.d.	n.d.
4T0421	4-21	2	yes	3-15*01	2-21*01	6*02	91.7	TTGDFVWRQYHQYQYGMVDV	18	λ	2-14*01	1*01	94.6	NSYTSGSI PFV	11
4T0423	4-47	3	yes	3-9*01	1-26*01	6*02	93.6	AKENRIELLPGWGMVDV	16	λ	2-23*02	3*02	95.6	CSYAGTSAFVWV	12
4T0427	4-38	3	yes	3-53*01	6-19*01	6*02	93.9	ARDEEWLFSYGGMVDV	15	λ	1-47*01	1*01	98.3	AAWDDSLSAYI	11
4T0429	4-48	3	yes	4-34*01	n.m.	6*02	89	ARHGHGTGMVDV	10	κ	2-28*01	4*01	96.3	MQALQTPLT	9
4T0430	4-25	3	no	3-23*01	3-3*01	2*01	93.2	AKDSTFWNGNYFDL	14	λ	1-51*01	3*02	98.3	GTWDGSLSVGV	11
4T0433	4-52	2	no	4-4*02	3-16*01	4*02	94.9	ARLSHYGGD	9	n.d.	n.d.	n.d.	n.d.	n.d.	n.d.
4T0434	4-44	2	yes	3-74*01	6-19*01	4*02	95.3	ARDVGLYNTGWIDY	14	κ	4-1*01	4*01	97.7	QQFYSTPLT	9
4T0437	4-Single05	1	yes	3-23*01	2-2*01	6*02	93.8	ASGVDCSSGRPFPCFYGMVDV	20	λ	5-45*02	3*02	95.2	MTWHNLVWV	9
4T0444	4-15	7	yes*	3-13*01	3-10*01	4*02	92.5	ARAPFGDLALDY	12	κ	3-20*01	4*01	95.5	HQYSSSPILT	9
4T0452	4-20	3	yes	3-15*06	3-16*01	4*02	88.7	ATEPRGYDWG	10	λ	1-40*01	3*02	95.2	QSYDSRLRDNWV	12
4T0460	4-30	2	no	3-33*01	6-13*01	4*02	94.2	ARQSIASNTYYFDD	14	n.d.	n.d.	n.d.	n.d.	n.d.	n.d.
4T0478	4-54	3	no	4-61*02	7-27*01	6*02	91.3	ARESRGTGQGGYNGMVDV	17	n.d.	n.d.	n.d.	n.d.	n.d.	n.d.
4T0479	4-27	2	no	3-23*01	3-10*01	4*02	94.9	AKDVWFGPRGNLDY	14	n.d.	n.d.	n.d.	n.d.	n.d.	n.d.
4T0484	4-43	2	no	3-74*01	6-13*01	4*02	91.5	ARGPSSNWYGLDY	13	n.d.	n.d.	n.d.	n.d.	n.d.	n.d.
4T0520	4-32	4	yes	3-33*01	5-12*01	4*02	95.2	ARQATISDFYYLDS	14	κ	1-39*01	4*01	94.4	QQTYSRPL	8
4T0525	4-Single06	1	yes	1-69*08	3-16*01	4*02	93.8	AGGDTGLFDS	10	κ	1-16*02	4*01	96.1	QQYNTLPFT	9

Appendix Table 1. Information on clonal and/or produced antibody sequences.

EV04 (continued).

Antibody	Clone #	# of clonal members	Pro-duced	IGHV	IGHD	IGHJ Identity (%)	IGH	V _H CDR3 (aa)	V _H CDR3 length chain (aa)	Light chain	IGKV/ IGLV	IGKJ/ IGLJ	IGK/IGL Identity (%)	V _L CDR3 (aa)	V _L CDR3 length (aa)
4T0541	4-Single10	1	yes	3-23*01	3-16*02	4*02	91.5	AKVSDYLWGSHRVFDY	16	κ	1-5*01	1*01	96.2	QQYNSYSPT	9
4T0551	4-3	2	no	1-18*04	3-9*01	4*02	84	ARGIGQGTGYHY	12	n.d.	n.d.	n.d.	n.d.	n.d.	n.d.
4T0563	4-51	2	yes	4-39*01	6-19*01	4*02	97.7	ARRRSSGRFPFDY	14	κ	3-20*01	5*01	98.6	QQYGSSPLT	9
4T0570	4-7	2	yes	1-46*01	2-21*02	3*02	91.5	ARALFFRVTGARDVFDI	17	κ	1-16*02	4*01	95.8	QQYYTYPLT	9
4T0577	4-9	2	no	1-69*01	2-21*01	4*02	94.9	ARSEGGDSYFDY	12	n.d.	n.d.	n.d.	n.d.	n.d.	n.d.
4T0635	4-16	2	no	3-13*01	3-10*02	3*02	94.5	VRAIFGSHAFDI	12	n.d.	n.d.	n.d.	n.d.	n.d.	n.d.
4T0657	4-58	3	yes	3-23*01	3-3*01	4*02	92.2	AKNDDFWGGTFDY	14	λ	1-51*01	3*02	97.3	GTWDITLSEGV	11
4T0675	4-53	2	no	4-61*02	5-18*01	6*02	93	ARDGGYTHAYAMDV	14	n.d.	n.d.	n.d.	n.d.	n.d.	n.d.
4T0764	4-Single07	1	yes	4-59*01	3-10*01	4*02	92.8	ARLLGSQDS	10	λ	2-14*01	2*01	96.3	SSYRTRNTHVI	11
4T0770	4-Single08	1	yes	3-74*01	3-22*01	4*02	91.2	ARGGNYNDY	10	λ	2-18*02	1*01	96.6	SSFSSNTYV	10
4T0784	4-Single09	1	yes	3-33*01	2-2*01	6*02	96.9	VRGGDLLLPDSIDYGMVDV	20	κ	1-17*01	3*01	94.7	LQHNTYPFS	9

Appendix Table 1. Information on clonal and/or produced antibody sequences.

EV05.

Antibody	Clone #	# of clonal members	Pro-duced	IGHV	IGHD	IGHJ Identity (%)	IGH Identity (%)	V _H CDR3 (aa)	V _H CDR3 length (aa)	Light chain	IGKV/IGLV	IGKJ/IGLJ	IGK/IGL Identity (%)	V _L CDR3 (aa)	V _L CDR3 length (aa)
5T0101	5-36	19	yes	3-33*01	3-16*01	4*02	92.9	ARDTLGVFDY	10	κ	2-24*01	2*01	95.7	VQSTQFPSP	9
5T0104	5-1	10	yes	1-18*01	3-22*01	6*02	91.5	ARISPSYDRSGDFYNYQSMVDV	23	κ	4-1*01	2*01	97.7	QQYNSPYT	9
5T0106	5-20	2	no	3-15*01	3-22*01	4*02	94.9	FYMMVGA	7	n.d.	n.d.	n.d.	n.d.	n.d.	n.d.
5T0107	5-35	2	yes	3-30*18	6-13*01	4*02	88.9	AKDRYCDAGTCSSGLDY	17	κ	2-28*01	1*01	93.4	MQSLAARPT	9
5T0119	5-38	3	no	3-33*01	1-14*01	4*02	91.9	ARDQFHHE	8	n.d.	n.d.	n.d.	n.d.	n.d.	n.d.
5T0122	5-31	2	no	3-23*04	3-3*01	3*01	95.6	AKGVDFWSPYSFALDL	16	n.d.	n.d.	n.d.	n.d.	n.d.	n.d.
5T0124	5-49	2	yes	4-4*07	2-8*01	6*02	90.8	ARESCNIECYSIHYGMDV	20	λ	1-47*01	3*02	93.8	ASWDDRLSARL	11
5T0139	5-28	2	yes	3-23*01	3-3*01	4*02	92.9	VKWKGFHN	9	κ	3-20*01	2*01	96.9	QQYGGPPT	9
5T0140	5-32	2	no	3-23*04	2-15*01	4*02	85.8	AKVLHPVGKKAAPSFND	17	n.d.	n.d.	n.d.	n.d.	n.d.	n.d.
5T0147	5-39	5	yes	3-49*04	5-12*01	4*02	85.4	TRSGRYEY	9	κ	2-24*01	5*01	87	FQATEFPPT	9
5T0149	5-29	6	no	3-23*04	1-1*01	4*02	92.2	ARGSAITSYFFDF	13	n.d.	n.d.	n.d.	n.d.	n.d.	n.d.
5T0160	5-2	2	no	1-18*01	3-9*01	5*02	98.6	ARDITIFSGWFDP	14	n.d.	n.d.	n.d.	n.d.	n.d.	n.d.
5T0165	5-10	2	no	3-15*01	4-11*01	4*02	94.7	ATDTVAIVRVLTTSG	15	n.d.	n.d.	n.d.	n.d.	n.d.	n.d.
5T0180	5-17	2	yes	3-15*01	3-22*01	4*02	94.7	VRGPFYCDTCGPNDY	15	λ	1-40*01	2*01	96.6	QTYDSRLRDQWV	12
5T0181	5-47	4	yes	3-74*01	3-10*02	4*02	93.5	VRTRYVASSADY	12	κ	2-28*01	3*01	97.7	MQALQVPPL	9
5T0202	5-18	3	yes	3-15*01	3-16*02	4*02	89.7	TTSLNIWGTYRDC	13	λ	1-40*01	3*02	94.9	QSYDSRLRDSWV	12
5T0209	5-13	3	yes	3-15*01	3-22*01	4*02	94.4	ADYIYESRGY	10	λ	1-40*01	3*02	97.3	QSYDSRLSDHWV	12
5T0223	5-16	6	yes	3-15*01	2-8*02	5*02	90.4	TKGGFGAHS	9	λ	1-40*01	3*02	93.9	QTYDSRLSDHWV	12
5T0246	5-0	1	yes	3-15*01	3-10*01	4*02	95	TTVMDFDSSG	10	λ	8-61*01	3*02	96.3	LLYMGSGISV	10
5T0256	5-24	2	no	3-15*01	3-22*01	4*02	96.7	TTYIYASRGY	10	λ	1-40*01	3*02	97.7	QSYDSRLSDSWV	12
5T0257	5-0	1	yes	3-23*01	3-3*01	4*02	98.6	AKDDDFWMSGPYFDY	14	λ	1-51*02	3*02	98.6	GSWSSSLSTGV	11
5T0259	5-15	4	yes	3-15*01	3-16*01	6*02	90.5	TVVLMSEFGYGYGMGV	16	κ	2-28*01	5*01	98	MQALETSMT	9
5T0278	5-23	2	yes	3-15*01	3-9*01	5*02	91.2	YTLRFFPGNS	11	λ	1-40*01	2*01	94.5	QSYDARLRDQWV	12
5T0305	5-34	3	no	3-30*18	3-3*01	6*01	94.6	AQDGGGPTYFFYGMAV	16	n.d.	n.d.	n.d.	n.d.	n.d.	n.d.
5T0322	5-41	10	yes	3-7*03	2-15*01	6*03	88.4	ARRSCAAPCFFASNHCMDA	20	λ	2-11*01	2*01	92	SSITDFNKLIV	10

Appendix Table 1. Information on clonal and/or produced antibody sequences.

EV05 (continued).

Antibody	Clone #	# of clonal members	Pro-duced	IGHV	IGHD	IGHJ	IGH Identity (%)	V _H CDR3 (aa)	V _H CDR3 length chain (aa)	Light chain	IGKV/IGLV	IGKJ/IGLJ	IGK/IGL Identity (%)	V _L CDR3 (aa)	V _L CDR3 length (aa)
5T0337	5-25	2	yes	3-15*01	3-16*01	2*01	92.7	MTGFEHTYSYFDL	13	λ	1-40*01	3*02	95.9	QSYDSRLRDAMV	12
5T0347	5-19	4	no	3-15*01	n.m.	6*02	93.3	TTRYSGMDV	10	λ	1-40*01	2*01	97.6	QSYDSRLRDHVV	12
5T0376	5-0	1	yes	4-59*01	2-21*02	4*02	93.8	ARGLLGPGDS	10	λ	2-14*01	2*01	96.2	SSYKTGSTPVV	11
5T0377	5-50	2	yes	4-59*01	3-9*01	4*02	96.2	ARMSRYFDWLSQQWSPFLVLD	21	λ	2-14*01	1*01	94.9	SSYTRTTTF	9
5T0378	5-48	2	yes	4-39*01	n.m.	4*02	98.7	ARRFDY	6	κ	3-15*01	1*01	100	QQYNNWPWT	9
5T0404	5-7	3	yes	1-69*09	2-2*01	6*03	90.1	ARLYCSSSSCSIYNYMDV	18	κ	1-33*01	2*03	95.8	QQYDSL PYS	9
5T0406	5-8	3	yes	1-69*01	3-3*01	6*02	91	ARFRFQGGGSFYYYGLDL	19	λ	1-44*01	1*01	98	AAWDDRLNGPGYV	13
5T0409	5-14	2	no	3-15*01	3-22*01	4*02	95.7	TRGPYDSDGPHDY	14	λ	1-40*01	3*02	95.6	QSYDSRLRDQWV	12
5T0425	5-9	3	no	3-15*01	3-22*01	4*02	95.9	LYMIVGT	7	n.d.	n.d.	n.d.	n.d.	n.d.	n.d.
5T0429	5-21	4	no	3-15*01	3-16*01	4*02	94.4	NRGPFDDHQS GPHDY	14	λ	1-40*01	3*02	94.9	QSYDSRLRDQWV	12
5T0431	5-40	2	no	3-66*01	5-12*01	3*02	95.9	ARGATPDAFDI	11	n.d.	n.d.	n.d.	n.d.	n.d.	n.d.
5T0432	5-44	2	no	3-73*02	3-10*01	4*02	96.4	SRHGI	6	n.d.	n.d.	n.d.	n.d.	n.d.	n.d.
5T0435	5-37	2	no	3-33*01	6-19*01	4*02	99	ARDLMLVRYFDH	13	n.d.	n.d.	n.d.	n.d.	n.d.	n.d.
5T0436	5-5	2	no	1-2*02	1-1*01	3*02	92.5	ARPSRYNNWDFAFEI	15	n.d.	n.d.	n.d.	n.d.	n.d.	n.d.
5T0438	5-45	9	yes	3-74*01	4-17*01	4*02	89.9	VRDFTGERDF	10	λ	1-47*01	1*01	95.2	VAMDDRLSGYV	11
5T0440	5-12	2	no	3-15*05	3-22*01	5*02	94.4	TKGGSSGHS	9	λ	1-40*01	3*02	95.9	QTYDSRLSDHVV	12
5T0451	5-11	3	yes	3-15*01	3-9*01	4*02	89.7	TRGPYDNFSGWRDY	14	λ	1-40*01	3*02	94.6	QSYDARLRDSDWV	12
5T0459	5-46	2	yes	3-74*03	1-26*01	4*02	91	AQSGNYRFDY	10	λ	2-14*01	1*01	93.5	TSYTPINTFV	10
5T0464	5-6	3	yes	1-46*01	3-22*01	6*02	88.1	ARSGYPRGMDV	12	λ	2-14*01	1*01	94.2	TSEFASTSYV	10
5T0465	5-0	1	yes	4-59*01	6-19*01	6*02	95.9	ARAPRGYSSGWYYYGMDV	19	λ	3-1*01	2*01	96.8	QAWDSSSTAVV	10
5T0474	5-27	3	yes	3-23*01	1-1*01	4*02	90.8	AKTGQFDY	8	κ	2-30*01	1*01	97.7	MQGMNWPRT	9
5T0544	5-26	3	no	3-15*01	2-15*01	3*02	95.7	TTRKGGFDI	9	n.d.	n.d.	n.d.	n.d.	n.d.	n.d.
5T0584	5-30	3	no	3-23*01	1-7*01	4*02	90.4	ARGENGNVEY	10	n.d.	n.d.	n.d.	n.d.	n.d.	n.d.
5T0623	5-33	2	no	3-23*03	3-22*01	4*02	98	ANSPYYDSSGGYGSFDY	18	λ	1-44*01	3*02	99.7	AAWDDSLNGWV	11

Appendix Table 1. Information on clonal and/or produced antibody sequences.

EV07.

Antibody	Clone #	# of clonal members	Pro-duced	IGHV	IGHD	IGHJ Identity (%)	IGH Identity (%)	V _H CDR3 (aa)	V _H CDR3 length chain (aa)	IGKV/ IGLV	IGKJ/ IGLJ	IGK/IGL Identity (%)	V _L CDR3 (aa)	V _L CDR3 length (aa)
7T0107	7-19	2	no	3-13*04	4-17*01	4*02	93.2	ARASFGDLYFDF	12	v.δ.	n.d.	n.d.	n.d.	n.d.
7T0108	7-13	2	no	3-13*04	3-10*01	4*02	97.9	ARAGFELYFDS	12	v.δ.	n.d.	n.d.	n.d.	n.d.
7T0118	7-10	2	no	2-5*02	3-16*01	4*02	96.3	AHIQGLREPWGAQKAYYFDF	20	v.δ.	n.d.	n.d.	n.d.	n.d.
7T0123	7-14	3	no	3-13*04	3-16*01	4*01	92.5	ARARFGDVFFDL	12	v.δ.	n.d.	n.d.	n.d.	n.d.
7T0124	7-33	2	no	3-23*01	2-21*01	6*02	86.1	ARDCRPHMTSWGGDV	16	v.δ.	n.d.	n.d.	n.d.	n.d.
7T0128	7-24	2	no	3-15*01	3-22*01	4*02	93.9	MTYYSDSSGYNVY	14	v.δ.	n.d.	n.d.	n.d.	n.d.
7T0138	7-8	3	no	1-69*04	1-20*01	4*02	94.9	ARDLGRAIIGSVDDY	15	v.δ.	n.d.	n.d.	n.d.	n.d.
7T0146	7-15	2	no	3-13*04	3-9*01	4*02	93.2	ARAFGKLFYDY	12	v.δ.	n.d.	n.d.	n.d.	n.d.
7T0154	7-38	5	no	3-73*01	6-19*01	4*02	81.5	TTGIIDVAGTNIDF	14	λ	4-69*01	2*01	91.3	QTWGAGFHVV 10
7T0172	7-47	2	no	7-4-1*02	3-10*01	6*02	97.3	ARVLDGEYYGSGSHDNTSGIPYYGMDV	30	v.δ.	n.d.	n.d.	n.d.	n.d.
7T0183	7-31	3	no	3-20*01	2-2*01	4*02	97.3	ARDLRGPAIYYFDY	15	v.δ.	n.d.	n.d.	n.d.	n.d.
7T0188	7-39	3	no	3-74*01	2-15*01	4*02	94.6	ARGGNSPEGYCY	13	v.δ.	n.d.	n.d.	n.d.	n.d.
7T0191	7-43	2	no	5-10-1*01	n.m.	4*02	95.6	VRRSDY	6	v.δ.	n.d.	n.d.	n.d.	n.d.
7T0193	7-1	3	no	1-18*01	2-8*02	4*02	94.2	ARVFSMIVAHFDY	14	v.δ.	n.d.	n.d.	n.d.	n.d.
7T0208	7-12	2	no	3-13*01	3-10*01	4*02	93.2	ARAWFEGVFFDY	12	v.δ.	n.d.	n.d.	n.d.	n.d.
7T0211	7-34	2	no	3-48*04	3-10*01	4*02	95.9	ARVTMATIFYFGL	12	v.δ.	n.d.	n.d.	n.d.	n.d.
7T0230	7-3	2	no	1-3*01	3-10*01	3*02	91.5	SRGRGIPYGFAFDI	14	v.δ.	n.d.	n.d.	n.d.	n.d.
7T0235	7-18	2	no	3-13*01	3-10*02	3*02	94.9	ARALFGSHVFDI	12	v.δ.	n.d.	n.d.	n.d.	n.d.
7T0238	7-44	2	no	5-10-1*01	n.m.	4*02	95.6	ARRFDY	6	v.δ.	n.d.	n.d.	n.d.	n.d.
7T0239	7-9	2	no	1-69*08	2-15*01	4*02	95.6	ARDLPGVIVDASAANDDY	18	v.δ.	n.d.	n.d.	n.d.	n.d.
7T0246	7-4	2	no	1-3*01	5-18*01	4*02	93.2	ATVLLLLDSGFDY	13	v.δ.	n.d.	n.d.	n.d.	n.d.
7T0250	7-36	2	no	3-48*03	3-9*01	6*02	92.9	ARSGYFDGLLSPSDYYVLDV	21	v.δ.	n.d.	n.d.	n.d.	n.d.
7T0258	7-16	2	no	3-13*04	2-21*01	4*02	92.8	TRATFGETYPDY	12	v.δ.	n.d.	n.d.	n.d.	n.d.
7T0265	7-5	3	no	1-46*01	5-24*01	3*01	90.8	ARLGTVATIPAVFDL	15	v.δ.	n.d.	n.d.	n.d.	n.d.
7T0275	7-46	2	no	5-51*01	3-10*01	6*02	92.5	ARLNVWFGDLLAVDEAARGGIDV	23	v.δ.	n.d.	n.d.	n.d.	n.d.

Appendix Table 1. Information on clonal and/or produced antibody sequences.

EV07 (continued).

Antibody	Clone #	# of clonal members	IGHV	IGHD	IGHJ Identity (%)	IGH	V _H CDR3 (aa)	V _H CDR3 length (aa)	Light chain	IGKV/IGLV	IGKJ/IGLJ	IGK/IGL Identity (%)	V _L CDR3 (aa)	V _L CDR3 length (aa)
7T0281	7-40	2	no	4-39*07	n.m.	4*02	ARRFDS	6	n.d.	n.d.	n.d.	n.d.	n.d.	n.d.
7T0286	7-45	2	no	5-10-1*01	n.m.	4*02	VRRSDY	6	n.d.	n.d.	n.d.	n.d.	n.d.	n.d.
7T0291	7-30	3	no	3-15*01	3-3*01	4*02	TTSGYD	6	n.d.	n.d.	n.d.	n.d.	n.d.	n.d.
7T0303	7-7	2	no	1-69*04	1-26*01	4*02	ARDLGSFDGN	10	n.d.	n.d.	n.d.	n.d.	n.d.	n.d.
7T0307	7-11	3	no	2-5*02	4-17*01	4*02	VHSYGRN	7	n.d.	n.d.	n.d.	n.d.	n.d.	n.d.
7T0310	7-2	4	no	1-3*01	5-24*01	4*02	ARGRGTIYGYSFDY	14	n.d.	n.d.	n.d.	n.d.	n.d.	n.d.
7T0313	7-20	2	no	3-15*01	3-22*01	4*02	TTKHTIITLRSDY	13	n.d.	n.d.	n.d.	n.d.	n.d.	n.d.
7T0340	7-37	3	no	3-7*03	6-13*01	4*02	GAGRQLVPY	9	n.d.	n.d.	n.d.	n.d.	n.d.	n.d.
7T0350	7-23	2	no	3-15*01	2-15*01	4*02	TTSNMGAY	8	n.d.	n.d.	n.d.	n.d.	n.d.	n.d.
7T0356	7-25	3	no	3-15*01	3-3*01	4*02	TTSGYD	6	κ	1-12*01	1*01	99.7	QQANSFPRT	9
7T0357	7-26	2	no	3-15*01	n.m.	6*02	TTRVYNGMDL	11	n.d.	n.d.	n.d.	n.d.	n.d.	n.d.
7T0386	7-29	2	no	3-15*01	4-17*01	4*02	VLQYRDYHY	9	n.d.	n.d.	n.d.	n.d.	n.d.	n.d.
7T0413	7-32	2	no	3-21*01	3-22*01	3*02	ARDSRDPNEMLVLYKEGDAFDI	22	n.d.	n.d.	n.d.	n.d.	n.d.	n.d.
7T0416	7-42	2	no	4-59*01	5-18*01	6*02	ARVPRGYNALKYGLDV	18	n.d.	n.d.	n.d.	n.d.	n.d.	n.d.
7T0434	7-17	2	no	3-13*04	3-10*01	4*02	ARAWFGGVFYDS	12	n.d.	n.d.	n.d.	n.d.	n.d.	n.d.
7T0436	7-35	2	no	3-48*04	3-10*01	3*01	ASLGLWLGELLYDPTFDL	19	n.d.	n.d.	n.d.	n.d.	n.d.	n.d.
7T0512	7-22	4	no	3-15*01	1-1*01	4*02	SRDLAAVRQ	9	λ	1-40*01	3*02	94.6	QSYDSRLXDSW	12
7T0522	7-6	2	no	1-46*01	1-7*01	6*02	GRHRGTTDYGTD	13	n.d.	n.d.	n.d.	n.d.	n.d.	n.d.
7T0551	7-41	2	no	4-59*08	1-26*01	4*02	ATHGCVRRRSGICGNAYFDS	20	n.d.	n.d.	n.d.	n.d.	n.d.	n.d.
7T0575	7-28	2	no	3-15*01	3-16*01	4*02	STVRSGEDY	9	n.d.	n.d.	n.d.	n.d.	n.d.	n.d.
7T0581	7-21	2	no	3-15*01	2-8*01	4*02	TSERMVSH	8	λ	1-40*01	3*02	94.2	QSYDSRLRDSW	12
7T0686	7-27	2	no	3-15*01	4-17*01	1*01	VLHYRDLHH	9	λ	1-40*01	3*02	95.6	QSYDSSIRDSW	12

Addition to **Appendix Table 1:**

Shown are exemplary sequences of every identified clone.

single = non-clonal sequence that was produced as monoclonal antibody

n.m. = no match

n.d. = not determined

* = additional member/s of clone was/were produced as antibody

Appendix Table 2. Information on clonal and/or produced antibody sequences obtained with alternative sorting bait EBOV GP Δ MLD Δ TM.

Antibody	Clone #	# of GP Δ MLD members	# of GP Δ TM members	Pro-duced	IGHV	IGHD	IGHJ	IGH Identity (%)	VH CDR3 (aa)	VH CDR3 length (aa)	IGHV/IGLV	IGKJ/IGLJ	IGK/IGL Identity (%)	VL CDR3 (aa)	VL CDR3 length (aa)
4m0302	4-44	1	2	no*	3-74*016-19*01	4*02	4*02	96.3	ARDVGLYNI ^W IGWIDY	14	n.d.	n.d.	n.d.	n.d.	n.d.
4m0314	4-69	2	0	yes	1-2*02	1-1*01	6*02	89.7	ASPPQNNRLYFYGM ^D V	17	λ	1-51*01	2*01	94.2	GTWDTSLR ^G VI
4m0331	4-65	2	0	no	3-21*013-10*01	3*02	3*02	93.6	AREGARSNYFLGDATDI	17	n.d.	n.d.	n.d.	n.d.	n.d.
4m0333	4-58	2	3	yes*	3-23*01	3-3*01	6*02	94.9	AKGDDFWSGSPDV	13	λ	1-51*01	1*01	97.6	GTWDSLSLSTFYV
4m0334	4-42	2	2	no*	3-74*015-18*01	4*02	4*02	87.9	ARGGSDTAMAHDY	13	n.d.	n.d.	n.d.	n.d.	n.d.
4m0342	4-60	2	1	no	3-21*024-11*01	6*02	6*02	90.2	ARDNDYHDDSSAGGM ^D V	16	n.d.	n.d.	n.d.	n.d.	n.d.
4m0344	4-71	1	1	no*	3-74*013-22*01	4*02	4*02	92.2	ARGGNYNDY	10	n.d.	n.d.	n.d.	n.d.	n.d.
4m0349	4-64	2	0	no	3-30*183-22*01	6*02	6*02	96.6	AKDRARGYGYGM ^D V	16	n.d.	n.d.	n.d.	n.d.	n.d.
4m0354	4-27	1	2	no*	3-23*013-16*01	4*02	4*02	90.2	AKDVWFGPRGSLDW	14	n.d.	n.d.	n.d.	n.d.	n.d.
4m0357	4-63	2	0	yes	3-7*01	3-10*01	4*02	93.6	ARGGSGIVPAIFF	13	λ	3-10*01	3*02	97.9	YSTDSSGYHFMV
4m0361	4-59	2	1	yes	4-39*014-17*01	4*02	4*02	85.8	ARVTMKNFFDS	11	λ	3-21*02	1*01	94.2	QVWNTYIV
4m0365	4-62	1	1	yes	3-74*012-21*02	5*02	5*02	100	ARAVLGVVTRYNWFDP	17	κ	1-39*01	1*01	99.7	QQSYSTPRT
4m0367	4-66	1	1	no	3-15*05	2-8*01	4*02	87.7	ITEMVFPPTGY	10	n.d.	n.d.	n.d.	n.d.	n.d.
4m0368	4-52	1	2	yes	4-4*02	3-16*01	5*02	92.5	LRLSHYGGA	9	κ	1-39*01	1*01	95.8	QQTYNTPRT
4m0373	4-12	1	5	yes	3-11*01	2-2*01	6*02	94.6	ARGERRHQVLSGM ^D V	15	n.d.	n.d.	n.d.	n.d.	n.d.
4m0387	4-68	1	1	yes	1-2*02	2-21*02	3*02	95.2	ARLTVVTAISAFDI	14	κ	1-5*01	1*01	95.4	QHYFDYYIGA
4m0394	4-39	1	3	no*	3-72*013-22*01	3*02	3*02	91	VRVADVFDSSGYSVDAFEM	19	λ	1-51*01	2*01	93.9	GTWDTSLR ^G VI
4m0401	4-1	1	2	no	1-18*013-22*01	4*02	4*02	97.6	ARVISMLVGF ^D N	14	n.d.	n.d.	n.d.	n.d.	n.d.
4m0407	4-2	1	4	no*	1-18*043-22*01	5*02	5*02	97.6	ARTITMIFLGF ^D P	14	n.d.	n.d.	n.d.	n.d.	n.d.
4m0410	4-46	1	2	no*	3-9*01	5-24*01	6*02	95.6	TREGRDGNLPLYYAM ^D V	17	n.d.	n.d.	n.d.	n.d.	n.d.
4m0422	4-67	2	0	no	3-11*013-22*01	4*02	4*02	96.6	ARKSGIYDSPY	11	n.d.	n.d.	n.d.	n.d.	n.d.
4m0437	4-61	1	1	no	4-59*016-13*01	4*02	4*02	92.1	ARGRSSNWYE ^G TFEY	15	n.d.	n.d.	n.d.	n.d.	n.d.
4m0443	4-15	1	7	no*	3-13*013-10*01	4*02	4*02	95.9	ARARFGDLAFDY	12	n.d.	n.d.	n.d.	n.d.	n.d.
4m0447	4-31	1	3	no*	3-33*016-13*01	4*02	4*02	92.9	ARDAHNSRLDY	11	n.d.	n.d.	n.d.	n.d.	n.d.
4m0450	4-70	1	1	no*	1-3*01	3-3*02	5*02	98.6	ARDISL ^F NPGWF ^D P	14	n.d.	n.d.	n.d.	n.d.	n.d.
4m0492	4-57	1	3	no*	4-59*01	3-3*01	6*02	96.6	ARAPRGYSFWSGQYY ^G YGV ^D V	21	n.d.	n.d.	n.d.	n.d.	n.d.

Addition to **Appendix Table 2:**

Shown are exemplary sequences of every identified clone.

GP Δ MLD members = sequences obtained by sorting with construct EBOV GP Δ MLD Δ TM as alternative bait

GP Δ TM members = sequences obtained by sorting with construct EBOV GP Δ TM as bait

* = clonal member obtained with EBOV GP Δ TM construct was produced as antibody

Appendix Table 3. Absolute numbers of sequences for CDRH3 amino acid length for EBOV-specific and IgG memory B cell population in individual rVSV-ZEBOV vaccinees EV01, EV03, EV04 and EV05.

% V gene identity	EV01		EV03		EV04		EV05	
	IgG repertoire	EBOV-reactive IgG	IgG repertoire	EBOV-reactive IgG	IgG repertoire	EBOV-reactive IgG	IgG repertoire	EBOV-reactive IgG
1	0	0	0	0	0	0	0	0
2	0	0	0	0	0	0	0	1
3	0	0	0	0	0	0	0	0
4	2	0	0	0	1	0	1	0
5	15	3	51	1	52	1	55	2
6	31	2	131	10	214	8	125	8
7	38	2	105	0	139	8	155	12
8	116	5	298	7	265	11	267	13
9	286	12	521	15	611	9	685	22
10	511	15	881	28	1005	35	1061	51
11	771	18	1516	17	1693	18	1539	22
12	1027	12	2109	38	2339	39	1973	26
13	1372	28	2287	70	3001	34	2379	23
14	1817	32	2587	28	3398	62	2685	26
15	1600	45	2563	25	3185	39	2648	27
16	1561	33	2336	39	2893	27	2060	29
17	1278	23	2042	27	2709	28	1991	19
18	1228	11	1889	16	2139	25	1928	17
19	987	46	1681	19	1683	23	1410	18
20	1044	17	1234	12	1229	26	1083	26
21	657	15	880	17	795	3	832	7
22	805	8	642	5	698	5	526	6
23	341	10	395	4	394	8	392	14
24	202	0	307	1	215	3	294	2
25	159	2	241	1	136	0	165	4
26	287	0	139	0	69	0	145	1
27	39	0	79	0	53	0	122	0
28	23	0	65	1	26	0	37	0
29	18	0	48	1	19	0	32	0
30	16	0	29	0	12	0	69	0
31	9	0	11	0	6	0	14	0
32	14	0	6	0	9	0	10	0
33	4	0	6	0	2	0	2	0
34	3	0	4	0	3	0	5	0
35	3	0	4	0	2	0	4	0
36	0	0	0	0	5	0	2	0
37	0	0	1	0	1	0	3	0
38	2	0	0	0	1	0	2	0
39	0	0	1	0	0	0	1	0
Total	16266	339	25089	382	29002	412	24702	376

Appendix Table 4. Relative frequency of sequences for CDRH3 amino acid length for EBOV-specific and IgG memory B cell population in individual rVSV-ZEBOV vaccinees EV01, EV03, EV04 and EV05.

% V gene identity	EV01		EV03		EV04		EV05	
	IgG repertoire	EBOV-reactive IgG	IgG repertoire	EBOV-reactive IgG	IgG repertoire	EBOV-reactive IgG	IgG repertoire	EBOV-reactive IgG
1	0,00000	0,00000	0,00000	0,00000	0,00000	0,00000	0,00000	0,00000
2	0,00000	0,00000	0,00000	0,00000	0,00000	0,00000	0,00000	0,00266
3	0,00000	0,00000	0,00000	0,00000	0,00000	0,00000	0,00000	0,00000
4	0,00012	0,00000	0,00000	0,00000	0,00003	0,00000	0,00004	0,00000
5	0,00092	0,00885	0,00203	0,00262	0,00179	0,00243	0,00223	0,00532
6	0,00191	0,00590	0,00522	0,02618	0,00738	0,01942	0,00506	0,02128
7	0,00234	0,00590	0,00419	0,00000	0,00479	0,01942	0,00627	0,03191
8	0,00713	0,01475	0,01188	0,01832	0,00914	0,02670	0,01081	0,03457
9	0,01758	0,03540	0,02077	0,03927	0,02107	0,02184	0,02773	0,05851
10	0,03142	0,04425	0,03511	0,07330	0,03465	0,08495	0,04295	0,13564
11	0,04740	0,05310	0,06042	0,04450	0,05838	0,04369	0,06230	0,05851
12	0,06314	0,03540	0,08406	0,09948	0,08065	0,09466	0,07987	0,06915
13	0,08435	0,08260	0,09116	0,18325	0,10348	0,08252	0,09631	0,06117
14	0,11171	0,09440	0,10311	0,07330	0,11716	0,15049	0,10870	0,06915
15	0,09836	0,13274	0,10216	0,06545	0,10982	0,09466	0,10720	0,07181
16	0,09597	0,09735	0,09311	0,10209	0,09975	0,06553	0,08339	0,07713
17	0,07857	0,06785	0,08139	0,07068	0,09341	0,06796	0,08060	0,05053
18	0,07549	0,03245	0,07529	0,04188	0,07375	0,06068	0,07805	0,04521
19	0,06068	0,13569	0,06700	0,04974	0,05803	0,05583	0,05708	0,04787
20	0,06418	0,05015	0,04918	0,03141	0,04238	0,06311	0,04384	0,06915
21	0,04039	0,04425	0,03508	0,04450	0,02741	0,00728	0,03368	0,01862
22	0,04949	0,02360	0,02559	0,01309	0,02407	0,01214	0,02129	0,01596
23	0,02096	0,02950	0,01574	0,01047	0,01359	0,01942	0,01587	0,03723
24	0,01242	0,00000	0,01224	0,00262	0,00741	0,00728	0,01190	0,00532
25	0,00977	0,00590	0,00961	0,00262	0,00469	0,00000	0,00668	0,01064
26	0,01764	0,00000	0,00554	0,00000	0,00238	0,00000	0,00587	0,00266
27	0,00240	0,00000	0,00315	0,00000	0,00183	0,00000	0,00494	0,00000
28	0,00141	0,00000	0,00259	0,00262	0,00090	0,00000	0,00150	0,00000
29	0,00111	0,00000	0,00191	0,00262	0,00066	0,00000	0,00130	0,00000
30	0,00098	0,00000	0,00116	0,00000	0,00041	0,00000	0,00279	0,00000
31	0,00055	0,00000	0,00044	0,00000	0,00021	0,00000	0,00057	0,00000
32	0,00086	0,00000	0,00024	0,00000	0,00031	0,00000	0,00040	0,00000
33	0,00025	0,00000	0,00024	0,00000	0,00007	0,00000	0,00008	0,00000
34	0,00018	0,00000	0,00016	0,00000	0,00010	0,00000	0,00020	0,00000
35	0,00018	0,00000	0,00016	0,00000	0,00007	0,00000	0,00016	0,00000
36	0,00000	0,00000	0,00000	0,00000	0,00017	0,00000	0,00008	0,00000
37	0,00000	0,00000	0,00004	0,00000	0,00003	0,00000	0,00012	0,00000
38	0,00012	0,00000	0,00000	0,00000	0,00003	0,00000	0,00008	0,00000
39	0,00000	0,00000	0,00004	0,00000	0,00000	0,00000	0,00004	0,00000
Total	1	1	1	1	1	1	1	1

Appendix Table 5. Absolute numbers of sequences for every % V gene germline identity for EBOV-specific and IgG memory B cell population in individual rVSV-ZEBOV vaccinees EV01, EV03, EV04 and EV05.

% V gene identity	EV01		EV03		EV04		EV05	
	IgG repertoire	EBOV-reactive IgG	IgG repertoire	EBOV-reactive IgG	IgG repertoire	EBOV-reactive IgG	IgG repertoire	EBOV-reactive IgG
65	0	0	0	0	1	0	0	0
66	0	0	0	0	0	0	0	0
67	0	0	0	0	1	0	0	0
68	0	0	0	0	2	0	0	0
69	0	0	0	0	2	0	0	0
70	1	0	0	0	4	0	0	0
71	1	0	2	0	2	0	0	0
72	1	0	0	0	6	0	0	0
73	1	1	0	0	7	0	3	0
74	0	1	2	0	5	0	2	0
75	1	0	3	0	6	0	4	0
76	0	0	1	0	11	0	7	0
77	7	0	12	0	17	0	21	0
78	14	0	14	0	31	0	29	0
79	63	0	24	0	48	0	47	0
80	17	0	31	1	55	0	54	0
81	34	3	51	0	103	0	103	0
82	37	0	82	0	115	0	153	1
83	59	0	170	2	171	2	210	2
84	99	0	144	3	256	1	305	3
85	195	5	287	3	339	2	417	5
86	217	3	356	6	551	0	561	6
87	422	1	541	16	705	4	890	5
88	482	6	806	21	980	7	1141	11
89	619	6	1208	28	1275	6	1490	9
90	1133	9	1679	40	1634	15	1801	21
91	1070	11	2163	54	2106	19	2135	27
92	1285	14	2626	26	2399	39	2426	46
93	1554	24	3077	46	2755	47	2590	63
94	1647	49	3113	29	2929	53	2633	30
95	1733	41	2923	29	2950	61	2447	39
96	1597	40	2096	32	2613	51	1931	37
97	1363	53	1507	18	2323	36	1390	26
98	1428	41	1207	18	2180	30	1096	18
99	991	23	676	6	1469	19	559	14
100	195	8	288	4	951	20	257	13
Total	16266	339	25089	382	29002	412	24702	376

Appendix Table 6. Relative frequencies of sequences for every % V gene germline identity for EBOV-specific and IgG memory B cell population in individual rVSV-ZEBOV vaccinees EV01, EV03, EV04 and EV05.

% V gene identity	EV01		EV03		EV04		EV05	
	IgG repertoire	EBOV-reactive IgG	IgG repertoire	EBOV-reactive IgG	IgG repertoire	EBOV-reactive IgG	IgG repertoire	EBOV-reactive IgG
65	0,00000	0,00000	0,00000	0,00000	0,00003	0,00000	0,00000	0,00000
66	0,00000	0,00000	0,00000	0,00000	0,00000	0,00000	0,00000	0,00000
67	0,00000	0,00000	0,00000	0,00000	0,00003	0,00000	0,00000	0,00000
68	0,00000	0,00000	0,00000	0,00000	0,00007	0,00000	0,00000	0,00000
69	0,00000	0,00000	0,00000	0,00000	0,00007	0,00000	0,00000	0,00000
70	0,00006	0,00000	0,00000	0,00000	0,00014	0,00000	0,00000	0,00000
71	0,00006	0,00000	0,00008	0,00000	0,00007	0,00000	0,00000	0,00000
72	0,00006	0,00000	0,00000	0,00000	0,00021	0,00000	0,00000	0,00000
73	0,00006	0,00295	0,00000	0,00000	0,00024	0,00000	0,00012	0,00000
74	0,00000	0,00295	0,00008	0,00000	0,00017	0,00000	0,00008	0,00000
75	0,00006	0,00000	0,00012	0,00000	0,00021	0,00000	0,00016	0,00000
76	0,00000	0,00000	0,00004	0,00000	0,00038	0,00000	0,00028	0,00000
77	0,00043	0,00000	0,00048	0,00000	0,00059	0,00000	0,00085	0,00000
78	0,00086	0,00000	0,00056	0,00000	0,00107	0,00000	0,00117	0,00000
79	0,00387	0,00000	0,00096	0,00000	0,00166	0,00000	0,00190	0,00000
80	0,00105	0,00000	0,00124	0,00262	0,00190	0,00000	0,00219	0,00000
81	0,00209	0,00885	0,00203	0,00000	0,00355	0,00000	0,00417	0,00000
82	0,00227	0,00000	0,00327	0,00000	0,00397	0,00000	0,00619	0,00266
83	0,00363	0,00000	0,00678	0,00524	0,00590	0,00485	0,00850	0,00532
84	0,00609	0,00000	0,00574	0,00785	0,00883	0,00243	0,01235	0,00798
85	0,01199	0,01475	0,01144	0,00785	0,01169	0,00485	0,01688	0,01330
86	0,01334	0,00885	0,01419	0,01571	0,01900	0,00000	0,02271	0,01596
87	0,02594	0,00295	0,02156	0,04188	0,02431	0,00971	0,03603	0,01330
88	0,02963	0,01770	0,03213	0,05497	0,03379	0,01699	0,04619	0,02926
89	0,03805	0,01770	0,04815	0,07330	0,04396	0,01456	0,06032	0,02394
90	0,06965	0,02655	0,06692	0,10471	0,05634	0,03641	0,07291	0,05585
91	0,06578	0,03245	0,08621	0,14136	0,07262	0,04612	0,08643	0,07181
92	0,07900	0,04130	0,10467	0,06806	0,08272	0,09466	0,09821	0,12234
93	0,09554	0,07080	0,12264	0,12042	0,09499	0,11408	0,10485	0,16755
94	0,10125	0,14454	0,12408	0,07592	0,10099	0,12864	0,10659	0,07979
95	0,10654	0,12094	0,11651	0,07592	0,10172	0,14806	0,09906	0,10372
96	0,09818	0,11799	0,08354	0,08377	0,09010	0,12379	0,07817	0,09840
97	0,08379	0,15634	0,06007	0,04712	0,08010	0,08738	0,05627	0,06915
98	0,08779	0,12094	0,04811	0,04712	0,07517	0,07282	0,04437	0,04787
99	0,06092	0,06785	0,02694	0,01571	0,05065	0,04612	0,02263	0,03723
100	0,01199	0,02360	0,01148	0,01047	0,03279	0,04854	0,01040	0,03457
Total	1	1	1	1	1	1	1	1

Appendix Table 7. Absolute frequency of V gene segments used in identified IgG memory B cell repertoire and IgG memory B cell population in individual rVSV-ZEBOV vaccinees EV01, EV03, EV04 and EV05.

IGHV	EV01		EV03		EV04		EV05	
	IgG repertoire	EBOV-reactive IgG	IgG repertoire	EBOV-reactive IgG	IgG repertoire	EBOV-reactive IgG	IgG repertoire	EBOV-reactive IgG
1-2	972	13	2470	39	1516	24	2150	19
1-3	210	14	462	5	532	4	5	0
1-8	400	9	331	17	740	4	242	3
1-18	1089	14	2088	11	2303	23	1860	20
1-24	337	0	943	1	483	1	839	2
1-45	1	0	4	0	13	0	7	0
1-46	218	11	442	0	759	9	835	9
1-58	123	0	52	1	70	1	68	0
1-69	1321	16	1957	54	1595	39	1776	14
1-69-2	104	0	0	0	0	0	0	0
1-69D	0	0	0	0	0	0	0	0
2-5	360	4	756	4	852	7	382	1
2-26	47	1	90	1	81	0	56	1
2-70	141	0	126	3	50	0	114	1
2-70D	16	0	0	0	2	0	2	0
3-7	425	24	590	10	1057	8	853	19
3-9	552	5	403	4	955	9	443	3
3-11	277	4	373	7	621	16	455	2
3-13	105	3	61	17	124	10	86	1
3-15	341	38	379	37	457	31	547	82
3-20	36	0	127	2	72	0	28	0
3-21	406	9	645	4	1002	10	786	2
3-23	1110	31	1329	46	2174	48	1928	45
3-23D	0	0	0	0	0	0	0	0
3-30	1373	27	1387	12	2001	25	557	10
3-30-3	120	3	193	2	0	0	4	0
3-30-5	0	0	0	0	0	0	0	0
3-33	224	12	885	7	551	16	843	31
3-43	153	0	5	0	90	1	118	0
3-43D	0	0	18	0	0	0	0	0
3-48	374	11	636	8	683	32	691	14
3-49	219	3	230	5	225	4	151	8
3-53	188	3	402	0	652	4	670	3
3-64	22	0	40	2	33	0	53	0
3-64D	0	0	96	3	0	0	99	2
3-66	135	4	146	0	238	1	183	4
3-69-1	3	0	4	0	3	0	5	0
3-72	30	0	45	8	94	7	160	0
3-73	117	1	87	3	148	3	141	2
3-74	369	10	563	14	750	19	645	22
3-NL1	0	0	0	0	0	0	0	0
4-4	134	11	305	12	368	12	244	8

4-28	4	0	3	0	8	0	6	0
4-30-1	0	0	0	0	0	0	0	0
4-30-2	134	5	74	0	0	0	0	0
4-30-4	118	2	161	1	6	0	1	0
4-31	136	0	463	2	291	3	263	5
4-34	1046	7	1064	16	1324	6	1517	9
4-38-2	0	0	364	0	0	0	1	0
4-39	1486	18	1273	4	3236	11	2257	12
4-59	599	13	919	10	782	9	1025	12
4-61	92	2	117	0	684	8	121	3
5-10-1	0	0	267	1	0	0	251	2
5-51	506	10	706	1	918	4	902	4
6-1	92	1	342	2	455	5	332	1
7-4-1	1	0	666	6	3	0	0	0
Total	16266	339	25089	382	29001	414	24702	376

Appendix Table 8. Relative frequency of V gene segments used in identified IgG memory B cell repertoire and IgG memory B cell population in individual rVSV-ZEBOV vaccinees EV01, EV03, EV04 and EV05.

IGHV	EV01		EV03		EV04		EV05	
	IgG repertoire	EBOV-reactive IgG	IgG repertoire	EBOV-reactive IgG	IgG repertoire	EBOV-reactive IgG	IgG repertoire	EBOV-reactive IgG
1-2	0,0598	0,0383	0,0984	0,1021	0,0523	0,0580	0,0870	0,0505
1-3	0,0129	0,0413	0,0184	0,0131	0,0183	0,0097	0,0002	0,0000
1-8	0,0246	0,0265	0,0132	0,0445	0,0255	0,0097	0,0098	0,0080
1-18	0,0669	0,0413	0,0832	0,0288	0,0794	0,0556	0,0753	0,0532
1-24	0,0207	0,0000	0,0376	0,0026	0,0167	0,0024	0,0340	0,0053
1-45	0,0001	0,0000	0,0002	0,0000	0,0004	0,0000	0,0003	0,0000
1-46	0,0134	0,0324	0,0176	0,0000	0,0262	0,0217	0,0338	0,0239
1-58	0,0076	0,0000	0,0021	0,0026	0,0024	0,0024	0,0028	0,0000
1-69	0,0812	0,0472	0,0780	0,1414	0,0550	0,0942	0,0719	0,0372
1-69-2	0,0064	0,0000	0,0000	0,0000	0,0000	0,0000	0,0000	0,0000
1-69D	0,0000	0,0000	0,0000	0,0000	0,0000	0,0000	0,0000	0,0000
2-5	0,0221	0,0118	0,0301	0,0105	0,0294	0,0169	0,0155	0,0027
2-26	0,0029	0,0029	0,0036	0,0026	0,0028	0,0000	0,0023	0,0027
2-70	0,0087	0,0000	0,0050	0,0079	0,0017	0,0000	0,0046	0,0027
2-70D	0,0010	0,0000	0,0000	0,0000	0,0001	0,0000	0,0001	0,0000
3-7	0,0261	0,0708	0,0235	0,0262	0,0364	0,0193	0,0345	0,0505
3-9	0,0339	0,0147	0,0161	0,0105	0,0329	0,0217	0,0179	0,0080
3-11	0,0170	0,0118	0,0149	0,0183	0,0214	0,0386	0,0184	0,0053
3-13	0,0065	0,0088	0,0024	0,0445	0,0043	0,0242	0,0035	0,0027
3-15	0,0210	0,1121	0,0151	0,0969	0,0158	0,0749	0,0221	0,2181
3-20	0,0022	0,0000	0,0051	0,0052	0,0025	0,0000	0,0011	0,0000
3-21	0,0250	0,0265	0,0257	0,0105	0,0346	0,0242	0,0318	0,0053
3-23	0,0682	0,0914	0,0530	0,1204	0,0750	0,1159	0,0781	0,1197

3-23D	0,0000	0,0000	0,0000	0,0000	0,0000	0,0000	0,0000	0,0000
3-30	0,0844	0,0796	0,0553	0,0314	0,0690	0,0604	0,0225	0,0266
3-30-3	0,0074	0,0088	0,0077	0,0052	0,0000	0,0000	0,0002	0,0000
3-30-5	0,0000	0,0000	0,0000	0,0000	0,0000	0,0000	0,0000	0,0000
3-33	0,0138	0,0354	0,0353	0,0183	0,0190	0,0386	0,0341	0,0824
3-43	0,0094	0,0000	0,0002	0,0000	0,0031	0,0024	0,0048	0,0000
3-43D	0,0000	0,0000	0,0007	0,0000	0,0000	0,0000	0,0000	0,0000
3-48	0,0230	0,0324	0,0253	0,0209	0,0236	0,0773	0,0280	0,0372
3-49	0,0135	0,0088	0,0092	0,0131	0,0078	0,0097	0,0061	0,0213
3-53	0,0116	0,0088	0,0160	0,0000	0,0225	0,0097	0,0271	0,0080
3-64	0,0014	0,0000	0,0016	0,0052	0,0011	0,0000	0,0021	0,0000
3-64D	0,0000	0,0000	0,0038	0,0079	0,0000	0,0000	0,0040	0,0053
3-66	0,0083	0,0118	0,0058	0,0000	0,0082	0,0024	0,0074	0,0106
3-69-1	0,0002	0,0000	0,0002	0,0000	0,0001	0,0000	0,0002	0,0000
3-72	0,0018	0,0000	0,0018	0,0209	0,0032	0,0169	0,0065	0,0000
3-73	0,0072	0,0029	0,0035	0,0079	0,0051	0,0072	0,0057	0,0053
3-74	0,0227	0,0295	0,0224	0,0366	0,0259	0,0459	0,0261	0,0585
3-NL1	0,0000	0,0000	0,0000	0,0000	0,0000	0,0000	0,0000	0,0000
4-4	0,0082	0,0324	0,0122	0,0314	0,0127	0,0290	0,0099	0,0213
4-28	0,0002	0,0000	0,0001	0,0000	0,0003	0,0000	0,0002	0,0000
4-30-1	0,0000	0,0000	0,0000	0,0000	0,0000	0,0000	0,0000	0,0000
4-30-2	0,0082	0,0147	0,0029	0,0000	0,0000	0,0000	0,0000	0,0000
4-30-4	0,0073	0,0059	0,0064	0,0026	0,0002	0,0000	0,0000	0,0000
4-31	0,0084	0,0000	0,0185	0,0052	0,0100	0,0072	0,0106	0,0133
4-34	0,0643	0,0206	0,0424	0,0419	0,0457	0,0145	0,0614	0,0239
4-38-2	0,0000	0,0000	0,0145	0,0000	0,0000	0,0000	0,0000	0,0000
4-39	0,0914	0,0531	0,0507	0,0105	0,1116	0,0266	0,0914	0,0319
4-59	0,0368	0,0383	0,0366	0,0262	0,0270	0,0217	0,0415	0,0319
4-61	0,0057	0,0059	0,0047	0,0000	0,0236	0,0193	0,0049	0,0080
5-10-1	0,0000	0,0000	0,0106	0,0026	0,0000	0,0000	0,0102	0,0053
5-51	0,0311	0,0295	0,0281	0,0026	0,0317	0,0097	0,0365	0,0106
6-1	0,0057	0,0029	0,0136	0,0052	0,0157	0,0121	0,0134	0,0027
7-4-1	0,0001	0,0000	0,0265	0,0157	0,0001	0,0000	0,0000	0,0000
Total	1,0000	1,0000	1,0000	1,0000	1,0000	1,0000	1,0000	1,0000

Appendix Table 9. Information on sequences sharing characteristics between donors.

Shared #	Donor	Antibody #	Clone #	Pro-duced	IGHV	IGHD	IGHJ Identity (%)	IGH Identity (%)	V _H CDR3 (aa)	V _H CDR3 length (aa)	Light chain	IGKV/ IGLV	IGKJ/ IGLJ	IGK/IGL Identity (%)	V _L CDR3 (aa)	V _L CDR3 length (aa)
s1	EV01	1T0221	1-1	yes	1-18*01	3-22*01	5*02	95.6	ARHVTMILDGWFDP	14	κ	3-20*01	4*01	98.6	QQYGSSPLT	9
		1T0281	1-1	no	1-18*01	3-10*01	4*02	95.3	AREITMVRGGWLDY	14	κ	3-15*01	2*01	99.3	QQYNNWAT	8
		1T0465	1-1	yes	1-18*01	3-10*01	4*02	95.6	ARDITMVRGGWLDY	14	κ	3-15*01	2*01	96.1	QQYNTWAT	8
		1T0478	1-1	no	1-18*01	3-10*01	5*02	96.3	ARGITMVRGEHWLDP	15	κ	4-1*01	4*01	94.9	QQFYSTPLT	9
		1T0527	1-1	no	1-18*01	3-10*01	4*02	94.3	ARDIVMVRGVGYFDY	15	κ	3-20*01	1*01	91.9	HQYGSSGPFST	10
	1T0645	1-1	no	1-18*01	3-10*01	4*02	95.9	ARDITMVRGGWLDY	14	n.d.	n.d.	n.d.	n.d.	n.d.	n.d.	n.d.
	1T0676	1-1	no	1-18*01	3-10*01	4*02	97	AREITMVRGGWLDY	14	n.d.	n.d.	n.d.	n.d.	n.d.	n.d.	n.d.
	4T0173	4-2	no	1-18*04	3-10*01	5*02	91.2	ARSITMIRGGWFDP	14	κ	1-5*01	1*01	96.4	QDYNGPT	7	
	4T0284	4-2	yes	1-18*04	3-10*01	5*02	96.3	ARGITMVRGLDWFDP	15	κ	3-15*01	4*01	97.2	QQYKNWPLT	9	
	4T0510	4-2	no	1-18*01	3-10*01	5*01	96.9	ARGVTMRELNWFDS	15	n.d.	n.d.	n.d.	n.d.	n.d.	n.d.	n.d.
EV04	4T0726	4-2	yes	1-18*04	3-22*01	5*02	93.5	ARTITMILLGWFDP	14	κ	3-20*01	3*01	96.9	QQYGTSPIT	9	
	5T0160	5-2	no	1-18*01	3-9*01	5*02	98.6	ARDITIFSGGWFDP	14	κ	3-20*01	1*01	100	QQYGSSPRT	9	
EV05	5T0605	5-2	no	1-18*01	3-9*01	5*02	98.6	ARDITIFSGGWFDP	14	κ	3-20*01	1*01	100	QQYGSSPRT	9	

Appendix Table 9. Information on sequences sharing characteristics between donors (continued).

Shared #	Donor	Antibody #	Clone #	Pro-duced	IGHV	IGHD	IGHJ	IGH Identity (%)	V _H CDR3 (aa)	V _H CDR3 length (aa)	Light chain	IGKV/IGLV	IGKJ/IGLJ	IGK/IGL Identity (%)	V _L CDR3 (aa)	V _L CDR3 length (aa)
		1T0241	1-0	no	3-13*01	3-10*01	4*02	97.9	ARAFSGQVFFDY	12	n.d.	n.d.	n.d.	n.d.	n.d.	n.d.
		3T0128	3-12	no	3-13*01	3-10*01	5*02	92.1	ARAFGAVYYDL	12	n.d.	n.d.	n.d.	n.d.	n.d.	n.d.
		3T0158	3-12	no	3-13*01	2-8*01	4*02	90.8	ARAFGAVYFDL	12	κ	1-39*01	4*01	99.6	QQSYSTLT	8
		3T0202	3-12	yes	3-13*01	3-10*01	4*02	94.2	ARAFGAVFFDY	12	κ	3-20*01	5*01	96.5	QQYGNSPIT	9
		3T0226	3-12	no	3-13*01	2-8*01	4*02	92.8	ARAFGAVYFDY	12	n.d.	n.d.	n.d.	n.d.	n.d.	n.d.
		3T0277	3-12	no	3-13*01	3-16*01	4*02	92.1	ARAFGHIFYDI	12	n.d.	n.d.	n.d.	n.d.	n.d.	n.d.
		3T0344	3-12	no	3-13*01	4-17*01	4*02	95.5	ARAFGDVFDN	12	n.d.	n.d.	n.d.	n.d.	n.d.	n.d.
		3T0351	3-12	no	3-13*01	2-8*01	4*01	90.1	VRAAFGAVYFDL	12	n.d.	n.d.	n.d.	n.d.	n.d.	n.d.
		3T0360	3-12	no	3-13*01	3-16*01	4*02	89	VRAAFGHVFDI	12	κ	3-15*01	2*01	99.3	QQYNNWAT	8
		3T0370	3-12	no	3-13*01	3-10*01	5*02	94.4	VRAAFGEIYYDL	12	κ	3-20*01	5*01	94.4	QQYGNSPIT	9
		3T0375	3-12	no	3-13*04	2-21*01	4*02	95.5	VRAAFGAVYDF	12	n.d.	n.d.	n.d.	n.d.	n.d.	n.d.
		3T0460	3-12	no	3-13*01	2-15*01	4*02	89.7	VRAAFGHVFFDS	12	n.d.	n.d.	n.d.	n.d.	n.d.	n.d.
		3T0468	3-12	yes	3-13*01	2-21*01	4*02	91.1	ARAFGAVYFDN	12	κ	3-20*01	5*01	92.3	QQYGRSPIT	9
		3T0517	3-12	no	3-13*01	3-10*01	4*02	90.8	VRAAFGHVFFDV	12	n.d.	n.d.	n.d.	n.d.	n.d.	n.d.
		3T0533	3-12	no	3-13*01	3-10*01	4*02	95.2	ARAFGHVFFDS	12	κ	3-20*01	5*01	94.4	QQYGNSPIT	9
		3T0641	3-12	no	3-13*01	2-8*01	4*02	92.8	ARAFGAVYFDQ	12	κ	3-20*01	5*01	96.9	QHYHNSPIT	9
		3T0674	3-12	no	3-13*01	2-8*01	4*02	89.4	VRAAFGAVYDS	12	n.d.	n.d.	n.d.	n.d.	n.d.	n.d.
		3T0681	3-12	no	3-13*01	4-17*01	4*02	96.6	ARAFGDVYFDS	12	κ	3-20*01	5*01	99	QQYGNSPIT	9

Appendix Table 9. Information on sequences sharing characteristics between donors (continued).

Shared #	Donor	Antibody #	Clone #	Pro-duced	IGHV	IGHD	IGHJ Identity (%)	IGH Identity (%)	V _H CDR3 (aa)	V _H CDR3 length (aa)	Light chain	IGKV/ IGLV	IGKJ/ IGLJ	IGK/IGL Identity (%)	V _L CDR3 (aa)	V _L CDR3 length (aa)
		4T0134	4-15	no	3-13*01	2-21*02	4*02	95.5	ARASFGDLYFDY	12	n.d.	n.d.	n.d.	n.d.	n.d.	n.d.
		4T0357	4-15	no	3-13*01	3-10*01	4*02	93.2	ARASFGDLFFDY	12	n.d.	n.d.	n.d.	n.d.	n.d.	n.d.
		4T0371	4-15	no	3-13*01	3-10*01	4*02	94.5	ARARFGDLALDY	12	κ	3-20*01	4*01	96.9	HOYGSSPLT	9
		4T0444	4-15	yes	3-13*01	3-10*01	4*02	92.5	ARARFGDLALDY	12	κ	3-20*01	4*01	95.5	HOYSSSPLT	9
		4T0501	4-15	no	3-13*01	3-10*01	4*02	98.3	ARARFGDLVFDY	12	n.d.	n.d.	n.d.	n.d.	n.d.	n.d.
		4T0578	4-15	yes	3-13*01	2-21*02	2*01	95.5	ARASFGDLYFDL	12	κ	4-1*01	3*01	95.4	QQYNSPLT	9
		4T0766	4-15	no	3-13*01	3-10*01	3*01	92.1	APARFGDLVYDV	12	κ	3-20*01	5*01	96.5	QQYGSSPIT	9
		7T0107	7-19	no	3-13*04	4-17*01	4*02	93.2	ARASFGDLYFDF	12	n.d.	n.d.	n.d.	n.d.	n.d.	n.d.
		7T0127	7-19	no	3-13*01	3-10*01	4*02	95.2	ARAWFGDTLDFE	12	n.d.	n.d.	n.d.	n.d.	n.d.	n.d.
		7T0108	7-13	no	3-13*04	3-10*01	4*02	97.9	ARAGFGELEYFDS	12	n.d.	n.d.	n.d.	n.d.	n.d.	n.d.
		7T0123	7-14	no	3-13*04	3-16*01	4*01	92.5	ARARFGDVFFDL	12	n.d.	n.d.	n.d.	n.d.	n.d.	n.d.
		7T0146	7-15	no	3-13*04	3-9*01	4*02	93.2	APADFGLKIFYDY	12	n.d.	n.d.	n.d.	n.d.	n.d.	n.d.
		7T0208	7-12	no	3-13*01	3-10*01	4*02	93.2	ARAWFGGVFYDY	12	n.d.	n.d.	n.d.	n.d.	n.d.	n.d.
		7T0448	7-12	no	3-13*01	3-10*01	4*02	95.5	VRAWFGEVYDY	12	n.d.	n.d.	n.d.	n.d.	n.d.	n.d.
		7T0264	7-0	no	3-13*04	3-10*01	4*02	92.8	ARAAFGELEFWDSD	12	n.d.	n.d.	n.d.	n.d.	n.d.	n.d.
		7T0270	7-0	no	3-13*01	4-17*01	4*02	94.5	ARVFHGDLYFDY	12	n.d.	n.d.	n.d.	n.d.	n.d.	n.d.
		7T0321	7-16	no	3-13*04	3-16*01	4*02	88.7	ARAAFGETYPPDY	12	n.d.	n.d.	n.d.	n.d.	n.d.	n.d.
		7T0258	7-16	no	3-13*04	2-21*01	4*02	92.8	TRATFGETYPPDY	12	n.d.	n.d.	n.d.	n.d.	n.d.	n.d.
		7T0334	7-15	no	3-13*04	3-10*01	4*02	95.5	ARADFGEVYDY	12	n.d.	n.d.	n.d.	n.d.	n.d.	n.d.
		7T0379	7-13	no	3-13*04	3-10*01	4*02	94.9	ARASFGDLYFDN	12	n.d.	n.d.	n.d.	n.d.	n.d.	n.d.
		7T0384	7-14	no	3-13*04	3-10*01	4*02	94.9	ARARFGNLFFDC	12	n.d.	n.d.	n.d.	n.d.	n.d.	n.d.
		7T0434	7-17	no	3-13*04	3-10*01	4*02	93.5	ARAWFGGVFYDS	12	n.d.	n.d.	n.d.	n.d.	n.d.	n.d.
		7T0503	7-14	no	3-13*04	3-10*01	4*02	96.2	ARARFGDLFFDL	12	n.d.	n.d.	n.d.	n.d.	n.d.	n.d.
		7T0218	7-0	no	3-13*04	3-16*01	4*02	96.6	VRADFGNVFFYDF	12	n.d.	n.d.	n.d.	n.d.	n.d.	n.d.
		7T0615	7-17	no	3-13*04	4-23*01	4*02	92.5	ARARFGGVFFDX	12	n.d.	n.d.	n.d.	n.d.	n.d.	n.d.

s3

Appendix Table 9. Information on sequences sharing characteristics between donors (continued).

Shared #	Donor	Antibody #	Clone #	Pro-duced	IGHV	IGHD	IGHJ	IGH Identity (%)	V _H CDR3 (aa)	V _H CDR3 length chain (aa)	IGK/IgL-Identity (%)	IGK/IgJ/IGLJ	V _L CDR3 (aa)	V _L CDR3 length (aa)
s4	EV03	3T0155	3-22	no	3-15*01	n.m.	6*02	91.3	ATRYYYNGMDV	11	λ	1-40*01 3*02	QSYDSSLRDSTV	12
		3T0236	3-22	no	3-15*01	2-2*01	6*02	88.3	TTRYQYNGMDV	11	λ	1-40*01 2*01	QSYDSRLRDSAV	12
		3T0245	3-22	yes	3-15*01	6-6*01	6*02	89	ATRVHYNMGMDV	11	λ	1-40*01 3*02	QSYDSSLRDACV	12
	EV05	5T0347	5-19	no	3-15*01	n.m.	6*02	93.3	TTRYYSGMDV	10	λ	1-40*01 2*01	QSYDSSLRDHVV	12
		5T0477	5-19	no	3-15*01	3-9*01	6*02	96.7	TTRYYYNGMDV	11	λ	1-40*01 2*01	QSYDSRLRDHVV	12
		5T0604	5-19	no	3-15*01	n.m.	6*02	97	TSRYYYNGMDV	11	λ	1-40*01 2*01	QSYDSRLSDLVV	12
		5T0680	5-19	no	3-15*01	n.m.	6*02	93	TTRYSYNGMDV	11	n.d.	n.d.	n.d.	n.d.
EV07	7T0357	7-26	no	3-15*01	n.m.	6*02	93	TTRVYYNGMDL	11	n.d.	n.d.	n.d.	n.d.	
	7T0537	7-26	no	3-15*01	n.m.	6*02	95.3	TTRIYYNGMDV	11	n.d.	n.d.	n.d.	n.d.	
s5	EV03	3T0479	3-0	no	3-23*01	3-3*01	4*02	95.6	AKDDDFWSGTGTWDY	15	n.d.	n.d.	n.d.	n.d.
		4T0144	4-58	no	3-23*01	3-3*01	4*02	95.6	AKGEDFWSGYPFDY	14	λ	1-47*01 1*01	AAWDDSLSGYV	11
	EV04	4T0468	4-58	no	3-23*01	3-3*01	6*02	94.5	AKGDDFWGSPDV	13	λ	1-51*01 1*01	GTWDSLSLTFYV	12
		4T0657	4-58	yes	3-23*01	3-3*01	4*02	92.2	AKNDDFWGGPTFDY	14	λ	1-51*01 3*02	GTWDTLSEGV	11
	EV05	5T0257	5-0	yes	3-23*01	3-3*01	4*02	98.6	AKDDDFWSGYPFDY	14	λ	1-51*02 3*02	GSWDSLSLSTGV	11
		7T0529	7-0	no	3-23*01	3-3*01	4*02	95.6	AKNDDFWSGHYFDH	14	n.d.	n.d.	n.d.	n.d.
	EV07	7T0682	7-0	no	3-23*01	3-3*01	4*02	96.9	AKNADFWSGYPDY	13	n.d.	n.d.	n.d.	n.d.
4T0636		4-0	no	3-23*03	3-22*01	4*02	97.6	ANSPYYGSSGNYGSFDY	18	κ	4-1*01 1*01	QQYYTPT	9	
s6	EV05	5T0623	5-33	no	3-23*03	3-22*01	4*02	98	ANSPYYDSSGYYGSFDY	18	λ	1-44*01 3*02	AAWDDSLNGWV	11
		5T0693	5-33	no	3-23*03	3-22*01	4*02	97.6	ANSPYYDSSGYYGSFDY	18	λ	1-44*01 3*02	AAWDDSLNGWV	11
s8	EV01	1T0218	1-30	no	3-30-3*01	2-2*01	6*02	95.2	ARGGDIVFAGSLDYYGMDV	20	κ	1-17*01 2*01	LQHNSYPRT	9
		1T0344	1-30	no	3-30-3*01	2-2*01	6*02	91.2	TRGGDIVVPADSLDYYGMDV	20	κ	1-17*01 2*01	LQCNLYPRT	9
	EV03	3T0131	3-0	no	3-30-3*01	2-15*01	6*02	96.6	ARGGDIVVEVGARPDYYGMDV	21	κ	1-17*03 1*01	LQHNRYPWT	9

Appendix Table 9. Information on sequences sharing characteristics between donors (continued).

Shared #	Donor	Antibody	Clone #	Pro-duced	IGHV	IGHD	IGHJ	IGH Identity (%)	V _H CDR3 (aa)	V _H CDR3 length (aa)	Light chain	IGHV/IGLV	IGKJ/IGLJ	IGK/IGL Identity (%)	V _L CDR3 (aa)	V _L CDR3 length (aa)
s9	EV01	1T0616	1-0	no	3-33*01	2-2*01	6*02	97.6	ARGGDLILLDPANDYGM DV	20	n.d.	n.d.	n.d.	n.d.	n.d.	n.d.
	EV04	4T0784	4-0	yes	3-33*01	2-2*01	6*02	96.9	VRGGDLLLPDSIDYGM DV	20	κ	1-17*01	3*01	94.7	LQHNTYFFS	9
s10	EV03	3T0465	3-50	no	3-33*01	2-15*01	4*02	93.9	ARESCYGGSCFFDH	14	λ	3-1*01	2*01	95.8	QAWDSRTVV	9
		3T0680	3-50	no	3-33*01	2-21*02	4*02	89.9	AREFCGGDCSLDY	14	n.d.	n.d.	n.d.	n.d.	n.d.	n.d.
	EV04	4T0219	4-29	no	3-33*01	2-15*01	4*02	96.3	AREFCFGGSCYFDY	14	n.d.	n.d.	n.d.	n.d.	n.d.	n.d.
		4T0611	4-29	no	3-33*01	2-15*01	4*02	98	AREYCSGGSCVFDY	15	n.d.	n.d.	n.d.	n.d.	n.d.	n.d.
		4T0639	4-29	no	3-33*01	2-15*01	4*02	95.6	AREYCSGGTCYCDY	14	λ	3-1*01	2*01	95.8	QTWDSRTVV	9
EV05	5T0682	5-0	no	3-33*01	1-26*01	4*02	97.6	AREEAFGGSYIIDY	14	n.d.	n.d.	n.d.	n.d.	n.d.	n.d.	
s11	EV03	3T0319	3-39	no	3-72*01	3-22*01	3*02	93.4	VRVGDYWDSSGYSLD AFDI	19	λ	1-51*01	3*02	94.9	ETWDTSLRGVV	11
		3T0417	3-39	no	3-72*01	3-22*01	3*02	90	VRVGDYWDSSGYSLD AFDI	19	λ	1-51*01	3*02	93.2	ETWDTSLRGVV	11
		3T0454	3-39	no	3-72*01	3-22*01	3*02	90.7	VRVGDYWDSSGYSLD AFDI	19	λ	1-51*01	3*02	92.9	ETWDTSLRGVV	11
	EV03	3T0506	3-39	yes	3-72*01	3-22*01	3*02	92.7	VRVADYFDSSGYSLD AFDI	19	λ	1-51*01	3*02	94.6	ETWDTGLRGVV	11
		3T0557	3-39	no	3-72*01	3-22*01	3*02	90	VRVGDYWDSSGYSLD AFDI	19	λ	1-51*01	3*02	95.6	ETWDTSLRGVV	11
		3T0561	3-39	no	3-72*01	3-22*01	3*02	90	VRVGDYWDSSGYSLD AFDI	19	λ	1-51*01	3*02	92.9	ETWDTSLRGVV	11
	EV04	3T0652	3-39	no	3-72*01	3-22*01	3*02	92.7	VRVGDYFDNSGYSLD AFDI	19	λ	1-51*01	3*02	95.6	ETWDTSLRGVV	11
		4T0171	4-39	yes	3-72*01	3-22*01	3*02	91	VRVADVFDSGYSVDAFEM	19	λ	1-51*01	2*01	93.9	GTWDTSLRGVI	11
EV04	4T0324	4-39	no	3-72*01	3-22*01	3*02	91	VRVADVFDSGYSVDAFEM	19	n.d.	n.d.	n.d.	n.d.	n.d.	n.d.	
	4T0545	4-39	no	3-72*01	3-22*01	3*02	91	VRVADVFDSGYSVDAFEM	19	n.d.	n.d.	n.d.	n.d.	n.d.	n.d.	
		4-39	no	3-72*01	3-22*01	3*02	91	VRVADVFDSGYSVDAFEM	19	n.d.	n.d.	n.d.	n.d.	n.d.	n.d.	

Appendix Table 9. Information on sequences sharing characteristics between donors (continued).

Shared #	Donor	Antibody #	Clone #	Pro-duced	IGHV	IGHD	IGHJ Identity (%)	IGH Identity (%)	V _H CDR3 (aa)	V _H CDR3 length (aa)	Light chain	IGKV/ IGLV	IGKJ/ IGLJ	IGK/IGL Identity (%)	V _L CDR3 (aa)	V _L CDR3 length (aa)
s14	EV04	4T0133	4-49	no	4-39*01	n.m.	4*02	92.6	ARRFDL	6	n.d.	n.d.	n.d.	n.d.	n.d.	n.d.
		4T0159	4-49	yes	4-39*01	n.m.	4*01	93.3	ARRFDS	6	κ	3-15*01	1*01	96.8	QQYNDWFPWT	9
		4T0176	4-49	yes	4-39*02	n.m.	4*02	96.6	VRRFDY	6	κ	3-15*01	1*01	96.8	QQYNKWFPWT	9
	EV05	5T0378	5-48	yes	4-39*01	n.m.	4*02	98.7	ARRFDY	6	κ	3-15*01	1*01	100	QQYNNWFPWT	9
		5T0420	5-48	yes	4-39*02	n.m.	4*02	93.6	ARRFDL	6	κ	3-15*01	1*01	94.7	QQYNIWFPWT	9
	EV07	7T0263	7-40	no	4-39*01	n.m.	6*02	95	ARRMDV	6	n.d.	n.d.	n.d.	n.d.	n.d.	n.d.
		7T0281	7-40	no	4-39*07	n.m.	4*02	92.9	ARRFDS	6	n.d.	n.d.	n.d.	n.d.	n.d.	n.d.
s15	EV04	4T0764	4-0	yes	4-59*01	3-10*01	4*02	92.8	ARGLLGSQDS	10	λ	2-14*01	2*01	96.3	SSYRTRNTHVI	11
	EV05	5T0376	5-0	yes	4-59*01	2-21*02	4*02	93.8	ARGLLGPGDS	10	λ	2-14*01	2*01	96.2	SSYKTGSTPVP	11
s16	EV04	4T0243	4-57	yes	4-59*01	5-18*01	6*02	92.8	ARAPRGYSSGKYNYYGLDV	19	λ	3-25*02	1*01	93.1	QADSSGGYYV	11
		4T0511	4-57	no	4-59*01	3-10*01	6*02	96.2	ARAPRSYGRGSYYYGIDV	19	λ	3-1*01	2*01	96.8	QAWDSSTFQVV	11
	EV05	4T0571	4-57	no	4-59*01	5-18*01	6*02	95.9	ARAPRGYNNYNNYYSHIDV	19	n.d.	n.d.	n.d.	n.d.	n.d.	n.d.
		5T0465	5-0	yes	4-59*01	6-19*01	6*02	95.9	ARAPRGYSSGMYYYGMDV	19	λ	3-1*01	2*01	96.8	QAWDSSTAVV	10
EV07	7T0545	7-0	no	4-59*01	3-10*01	6*02	96.9	ARGIRGVSRRGHYYGMDV	19	n.d.	n.d.	n.d.	n.d.	n.d.	n.d.	
s17	EV04	4T0258	4-1	no	1-18*04	3-22*01	3*02	94.5	ARSISMLVGPFDI	14	n.d.	n.d.	n.d.	n.d.	n.d.	n.d.
		4T0552	4-1	no	1-18*04	3-22*01	4*02	96.3	ARFISMIIVGHFDY	14	n.d.	n.d.	n.d.	n.d.	n.d.	n.d.
	EV07	7T0130	7-0	no	1-18*04	3-22*01	4*02	93.6	ARVISMIIVGALDY	14	n.d.	n.d.	n.d.	n.d.	n.d.	n.d.

Appendix Table 9. Information on sequences sharing characteristics between donors (continued).

Shared #	Donor	Antibody	Clone #	Pro-duced	IGHV	IGHD	IGHJ Identity (%)	IGH Identity (%)	V _H CDR3 (aa)	V _H CDR3 length (aa)	Light chain	IGKV/IGLV	IGKJ/IGLJ	IGK/IGL Identity (%)	V _L CDR3 (aa)	V _L CDR3 length (aa)	
																	IGHV
s18	EV01	1T0374	1-7	no	1-3*01	1-26*01	6*02	96.6	ARGRGTYYYAMDV	14	n.d.	n.d.	n.d.	n.d.	n.d.	n.d.	
		1T0451	1-7	yes	1-3*01	3-16*01	6*02	89.1	ARGRGTSYYAFDV	14	κ	1-39*01	2*01	93	QQTYRSPLYT	10	
		1T0603	1-7	no	1-3*01	1-26*01	6*02	91.5	ARGRGTSYYAFDV	14	n.d.	n.d.	n.d.	n.d.	n.d.	n.d.	
	EV07	7T0310	7-2	no	1-3*01	5-24*01	4*02	92.2	ARGRGTIYGSFDY	14	n.d.	n.d.	n.d.	n.d.	n.d.	n.d.	n.d.
		7T0341	7-2	no	1-3*01	5-18*01	4*02	96.6	ARGRGDTYGFSDY	14	n.d.	n.d.	n.d.	n.d.	n.d.	n.d.	n.d.
		7T0360	7-2	no	1-3*01	3-10*01	4*02	93.5	ARGRGIVYGFSDY	14	n.d.	n.d.	n.d.	n.d.	n.d.	n.d.	n.d.
		7T0630	7-2	no	1-3*01	5-18*01	4*02	92.9	ARGRGYSYGFSDY	14	n.d.	n.d.	n.d.	n.d.	n.d.	n.d.	n.d.
s19	EV03	3T0146	3-0	no	1-3*01	1-26*01	6*02	90.6	ARGPIVGATYYYYGLDV	17	n.d.	n.d.	n.d.	n.d.	n.d.	n.d.	
	EV07	7T0663	7-0	no	1-3*01	1-26*01	6*02	94.9	ARGPMVGATYYYYGMDV	17	n.d.	n.d.	n.d.	n.d.	n.d.	n.d.	
s20	EV04	4T0467	4-0	no	1-69*08	1-26*01	4*02	90.5	ARGVGATSDY	10	n.d.	n.d.	n.d.	n.d.	n.d.	n.d.	
	EV07	7T0149	7-0	no	1-69*08	1-26*01	4*02	93.2	ARGVGATSEE	10	n.d.	n.d.	n.d.	n.d.	n.d.	n.d.	
s21	EV04	4T0616	4-0	no	2-5*02	4-17*01	4*02	93.3	VHRYGQN	7	n.d.	n.d.	n.d.	n.d.	n.d.	n.d.	
		7T0307	7-11	no	2-5*02	4-17*01	4*02	92.6	VHSYGRN	7	n.d.	n.d.	n.d.	n.d.	n.d.	n.d.	
	EV07	7T0477	7-11	no	2-5*02	4-17*01	4*02	94	VHSYGRN	7	n.d.	n.d.	n.d.	n.d.	n.d.	n.d.	
		7T0621	7-11	no	2-5*02	3-16*01	4*02	94	VHSYGRN	7	n.d.	n.d.	n.d.	n.d.	n.d.	n.d.	
s22	EV04	4T0635	4-16	no	3-13*01	3-10*02	3*02	94.5	VRAIFGSHAFDI	12	n.d.	n.d.	n.d.	n.d.	n.d.	n.d.	
		4T0721	4-16	no	3-13*01	3-10*02	3*02	93.1	VRAIFGSHAFDI	12	n.d.	n.d.	n.d.	n.d.	n.d.	n.d.	
	EV07	7T0235	7-18	no	3-13*01	3-10*02	3*02	94.9	ARALFGSHVFDI	12	n.d.	n.d.	n.d.	n.d.	n.d.	n.d.	
		7T0354	7-18	no	3-13*04	3-10*02	3*02	94.5	ARALFGGHAFDI	12	n.d.	n.d.	n.d.	n.d.	n.d.	n.d.	

Appendix Table 9. Information on sequences sharing characteristics between donors (continued).

Shared #	Donor	Antibody #	Clone #	Pro-duced	IGHV	IGHD	IGHJ	IGH Identity (%)	V _H CDR3 (aa)	V _H CDR3 length (aa)	Light chain	IGKV/IGLV	IGKJ/IGLJ	IGK/IGL Identity (%)	V _L CDR3 (aa)	V _L CDR3 length (aa)
s23	EV01	1T0322	1-19	no	3-15*01	1-26*01	2*01	90.6	TTGPGDF	7	n.d.	n.d.	n.d.	n.d.	n.d.	n.d.
		1T0570	1-19	no	3-15*01	5-24*01	4*02	89	TTGRTDF	7	n.d.	n.d.	n.d.	n.d.	n.d.	n.d.
	EV05	5T0555	5-0	no	3-15*01	n.m.	4*02	82.8	TTDPRE	6	n.d.	n.d.	n.d.	n.d.	n.d.	n.d.
		7T0153	7-0	no	3-15*01	n.m.	4*02	93.4	TTGPRD	6	n.d.	n.d.	n.d.	n.d.	n.d.	n.d.
s24	EV01	1T0368	1-0	no	3-30*04	5-18*01	4*02	92.9	AREGGSISYGFY	12	n.d.	n.d.	n.d.	n.d.	n.d.	n.d.
		7T0254	7-0	no	3-30*04	5-18*01	4*02	93.6	AREGSSYSYGFY	12	n.d.	n.d.	n.d.	n.d.	n.d.	n.d.
s25	EV03	3T0224	3-0	no	3-30*04	3-3*02	6*02	93.2	ARGDLVLVLEDSTDYYGMDV	20	n.d.	n.d.	n.d.	n.d.	n.d.	n.d.
		7T0121	7-0	no	3-30*04	2-2*01	6*02	95.3	ARGDIVVLQSEDIYGLDV	20	n.d.	n.d.	n.d.	n.d.	n.d.	n.d.
	EV07	7T0383	7-0	no	3-30*04	6-13*01	6*02	92.5	SRGGDLVLTSTIDYGMVDV	20	n.d.	n.d.	n.d.	n.d.	n.d.	n.d.
		7T0533	7-0	no	3-30*04	2-15*01	6*02	91.9	VRGGDIIVLVSVDYHGMDV	20	n.d.	n.d.	n.d.	n.d.	n.d.	n.d.
s26	EV04	4T0693	4-0	no	3-48*01	1-1*01	4*02	90.8	ARLEQRSFYFDY	12	n.d.	n.d.	n.d.	n.d.	n.d.	n.d.
		7T0229	7-0	no	3-48*04	3-10*01	4*02	94.5	ARVRQRSFYFDS	12	n.d.	n.d.	n.d.	n.d.	n.d.	n.d.
s27		5T0138	5-38	no	3-49*04	5-12*01	4*02	91.4	TRGSGRYEY	9	n.d.	n.d.	n.d.	n.d.	n.d.	n.d.
		5T0147	5-38	yes	3-49*04	5-12*01	4*02	85.4	TRGSGRYEY	9	κ	2-24*01	J5*01	87	FQATEFFRT	9
	EV05	5T0263	5-38	no	3-49*04	5-12*01	4*02	85	TRGSGRYEY	9	n.d.	n.d.	n.d.	n.d.	n.d.	n.d.
		5T0545	5-38	no	3-49*04	5-12*01	4*02	85.7	TRGSGRYEY	9	n.d.	n.d.	n.d.	n.d.	n.d.	n.d.
		5T0606	5-38	no	3-49*04	5-12*01	4*02	84.7	TRGSGRYEY	9	n.d.	n.d.	n.d.	n.d.	n.d.	n.d.
EV07	7T0240	7-0	no	3-49*04	1-26*01	4*02	89.2	TRGSGRYEY	9	n.d.	n.d.	n.d.	n.d.	n.d.	n.d.	
s28	EV05	5T0103	5-0	no	3-74*01	1-1*01	3*02	90.4	ARGSTANKRRRAFDI	15	n.d.	n.d.	n.d.	n.d.	n.d.	n.d.
		7T0228	7-0	no	3-74*01	1-1*01	3*02	90.1	ARGSTANKRRRAFDI	15	n.d.	n.d.	n.d.	n.d.	n.d.	n.d.

Addition to **Appendix Table 9:**

n.m. = no match

n.d. = not determined

X = aa not identified

Appendix Table 10. Summary of rVSV-ZEBOV-induced antibody binding to Filovirus GPs.

Antibody				GP binding ¹										Binding region ¹					
Name	Clone #	Shared sequence	Number of clonal members	EBOV (Makona)		EBOV (Mayinga)		BDBV		SUDV		MARV		sGP		EBOV ΔMLD		ctrl.	
				EC ₅₀	OD	EC ₅₀	OD	EC ₅₀	OD	EC ₅₀	OD	EC ₅₀	OD	EC ₅₀	OD	EC ₅₀	OD	EC ₅₀	OD
1T0114	1-26		2	--	<0.2	N/A	N/A	N/A	N/A	N/A	N/A	N/A	N/A	N/A	N/A	N/A	N/A	N/A	N/A
1T0116	1-31		2	--	<0.2	N/A	N/A	N/A	N/A	N/A	N/A	N/A	N/A	N/A	N/A	N/A	N/A	N/A	N/A
1T0129	1-4		8	4.01	1.30	3.87	0.63	1.85	1.10	6.41	0.92	10.8	0.85	14.3	0.34	--	<0.2	13.3	0.60
1T0130	1-9		2	0.09	2.01	0.04	1.56	--	<0.2	--	<0.2	--	<0.2	--	<0.2	0.11	1.46	--	<0.2
1T0139	1-46		3	0.18	0.80	0.16	0.54	--	<0.2	--	<0.2	--	<0.2	--	<0.2	0.18	1.06	--	<0.2
1T0201	1-18		2	0.23	1.82	0.12	1.40	--	<0.2	--	<0.2	--	<0.2	0.06	1.86	0.27	1.36	--	<0.2
1T0221	1-1	s1	9	0.14	1.53	0.09	1.68	0.11	1.80	0.91	1.40	--	<0.2	--	<0.2	0.03	1.10	--	<0.2
1T0222	1-38		2	--	<0.2	N/A	N/A	N/A	N/A	N/A	N/A	N/A	N/A	N/A	N/A	N/A	N/A	N/A	N/A
1T0225	1-40		2	0.10	1.84	0.07	1.36	0.07	1.44	0.27	1.14	--	<0.2	--	<0.2	0.14	1.28	--	<0.2
1T0227	1-15		3	0.15	1.85	0.09	1.36	--	<0.2	--	<0.2	--	<0.2	0.06	1.71	0.19	1.36	--	<0.2
1T0242	1-39		5	--	<0.2	N/A	N/A	N/A	N/A	N/A	N/A	N/A	N/A	N/A	N/A	N/A	N/A	N/A	N/A
1T0248	1-25		2	0.06	1.87	0.04	1.57	--	<0.2	--	<0.2	--	<0.2	3.72	0.26	--	<0.2	--	<0.2
1T0264	1-22		3	0.39	1.96	0.36	1.49	--	<0.2	--	<0.2	--	<0.2	--	<0.2	--	<0.2	--	<0.2
1T0301	1-41		2	0.07	2.09	0.06	1.78	--	<0.2	--	<0.2	--	<0.2	--	<0.2	--	<0.2	--	<0.2
1T0321	1-Single02		1	0.08	2.06	0.05	1.54	0.04	1.63	1.39	0.76	--	<0.2	--	<0.2	0.16	1.29	--	<0.2
1T0325	1-23		2	0.08	2.02	0.05	1.83	0.47	0.29	--	<0.2	--	<0.2	--	<0.2	--	<0.2	--	<0.2
1T0351	1-37		2	--	<0.2	N/A	N/A	N/A	N/A	N/A	N/A	N/A	N/A	N/A	N/A	N/A	N/A	N/A	N/A
1T0371	1-12		3	0.07	1.90	0.05	1.79	0.07	1.70	--	<0.2	--	<0.2	--	<0.2	0.12	1.23	--	<0.2
1T0451	1-7		3	0.08	1.80	0.05	1.87	0.32	0.28	--	<0.2	--	<0.2	--	<0.2	--	<0.2	--	<0.2
1T0455	1-16		3	0.06	1.77	0.06	1.63	--	<0.2	--	<0.2	--	<0.2	0.04	1.35	0.10	1.38	--	<0.2
1T0465	1-1	s1	9	0.11	1.62	0.07	1.65	0.09	1.54	0.18	1.57	--	<0.2	--	<0.2	0.19	1.26	--	<0.2
1T0473	1-14		5	0.24	1.46	0.23	1.59	2.14	0.75	--	<0.2	--	<0.2	0.08	1.34	0.24	1.30	--	<0.2
1T0480	1-42		7	--	<0.2	N/A	N/A	N/A	N/A	N/A	N/A	N/A	N/A	N/A	N/A	N/A	N/A	N/A	N/A
1T0546	1-32		2	0.04	1.54	0.03	1.77	--	<0.2	--	<0.2	--	<0.2	--	<0.2	--	<0.2	--	<0.2
1T0552	1-24		2	10.3	0.33	7.49	0.61	10.5	0.27	13.2	0.21	--	<0.2	--	<0.2	--	<0.2	--	<0.2
1T0554	1-5		6	--	<0.2	N/A	N/A	N/A	N/A	N/A	N/A	N/A	N/A	N/A	N/A	N/A	N/A	N/A	N/A
1T0565	1-28		5	0.05	1.82	0.03	1.80	--	<0.2	--	<0.2	--	<0.2	--	<0.2	--	<0.2	--	<0.2
1T0582	1-6		5	--	<0.2	N/A	N/A	N/A	N/A	N/A	N/A	N/A	N/A	N/A	N/A	N/A	N/A	N/A	N/A
1T0614	1-36		3	--	<0.2	N/A	N/A	N/A	N/A	N/A	N/A	N/A	N/A	N/A	N/A	N/A	N/A	N/A	N/A
1T0623	1-11		2	--	<0.2	N/A	N/A	N/A	N/A	N/A	N/A	N/A	N/A	N/A	N/A	N/A	N/A	N/A	N/A
1T0653	1-Single03		1	--	<0.2	N/A	N/A	N/A	N/A	N/A	N/A	N/A	N/A	N/A	N/A	N/A	N/A	N/A	N/A
1T0655	1-10		2	0.08	1.88	0.07	1.80	1.16	1.38	--	<0.2	--	<0.2	--	<0.2	0.16	1.35	--	<0.2
1T0665	1-35		3	--	<0.2	N/A	N/A	N/A	N/A	N/A	N/A	N/A	N/A	N/A	N/A	N/A	N/A	N/A	N/A
3T0123	3-2		2	1.93	1.09	0.99	1.23	7.15	0.51	--	<0.2	--	<0.2	--	<0.2	0.16	1.23	--	<0.2
3T0135	3-42	s12	2	--	<0.2	N/A	N/A	N/A	N/A	N/A	N/A	N/A	N/A	N/A	N/A	N/A	N/A	N/A	N/A
3T0147	3-46		2	12.1	0.24	--	<0.2	--	<0.2	--	<0.2	--	<0.2	--	<0.2	--	<0.2	--	<0.2
3T0159	3-44		2	--	<0.2	--	<0.2	--	<0.2	--	<0.2	--	<0.2	--	<0.2	--	<0.2	--	<0.2
3T0183	3-6		37	--	<0.2	N/A	N/A	N/A	N/A	N/A	N/A	N/A	N/A	N/A	N/A	N/A	N/A	N/A	N/A
3T0202	3-12	s3	17	0.13	1.91	0.05	1.46	--	<0.2	--	<0.2	--	<0.2	0.03	1.51	0.09	1.34	--	<0.2
3T0209	3-7		12	--	<0.2	N/A	N/A	N/A	N/A	N/A	N/A	N/A	N/A	N/A	N/A	N/A	N/A	N/A	N/A
3T0210	3-6		37	--	<0.2	N/A	N/A	N/A	N/A	N/A	N/A	N/A	N/A	N/A	N/A	N/A	N/A	N/A	N/A
3T0213	3-4		6	--	<0.2	N/A	N/A	N/A	N/A	N/A	N/A	N/A	N/A	N/A	N/A	N/A	N/A	N/A	N/A
3T0215	3-35		2	0.04	1.78	0.04	1.53	0.04	1.22	0.04	1.76	--	<0.2	0.12	1.00	0.07	1.18	--	<0.2
3T0216	3-48		2	--	<0.2	N/A	N/A	N/A	N/A	N/A	N/A	N/A	N/A	N/A	N/A	N/A	N/A	N/A	N/A
3T0227	3-7		12	--	<0.2	N/A	N/A	N/A	N/A	N/A	N/A	N/A	N/A	N/A	N/A	N/A	N/A	N/A	N/A
3T0245	3-22	s4	3	0.07	1.75	0.06	1.53	--	<0.2	--	<0.2	--	<0.2	0.04	1.53	0.09	1.27	--	<0.2
3T0251	3-6		37	--	<0.2	N/A	N/A	N/A	N/A	N/A	N/A	N/A	N/A	N/A	N/A	N/A	N/A	N/A	N/A

Appendix Table 10. Summary of rVSV-ZEBOV-induced antibody binding to Filovirus GPs (continued).

Antibody				GP binding ¹										Binding region ¹					
Name	Clone #	Shared sequence	Number of clonal members	EBOV (Makona)		EBOV (Mayinga)		BDBV		SUDV		MARV		sGP		EBOV ΔMLD		ctrl.	
				EC ₅₀	OD	EC ₅₀	OD	EC ₅₀	OD	EC ₅₀	OD	EC ₅₀	OD	EC ₅₀	OD	EC ₅₀	OD	EC ₅₀	OD
3T0253	3-24		3	0.06	1.78	0.05	1.59	--	<0.2	4.32	0.39	--	<0.2	0.03	1.54	0.07	1.25	--	<0.2
3T0258	3-1		3	0.25	0.82	0.30	0.79	--	<0.2	--	<0.2	--	<0.2	--	<0.2	0.14	0.96	--	<0.2
3T0265	3-19		2	0.06	1.84	0.05	1.66	--	<0.2	--	<0.2	--	<0.2	0.03	1.65	0.10	1.23	--	<0.2
3T0303	3-10		4	--	<0.2	N/A	N/A	N/A	N/A	N/A	N/A	N/A	N/A	N/A	N/A	N/A	N/A	N/A	N/A
3T0325	3-41		2	--	<0.2	N/A	N/A	N/A	N/A	N/A	N/A	N/A	N/A	N/A	N/A	N/A	N/A	N/A	N/A
3T0331	3-26		4	0.10	0.88	0.11	1.18	--	<0.2	--	<0.2	--	<0.2	--	<0.2	0.17	1.15	--	<0.2
3T0338	3-Single02		1	0.10	1.75	0.11	1.47	--	<0.2	--	<0.2	--	<0.2	0.06	1.54	0.26	1.35	--	<0.2
3T0350	3-28		3	0.07	1.75	0.06	1.37	--	<0.2	0.05	1.33	--	<0.2	0.04	1.43	0.24	1.20	--	<0.2
3T0353	3-45		3	--	<0.2	N/A	N/A	N/A	N/A	N/A	N/A	N/A	N/A	N/A	N/A	N/A	N/A	N/A	N/A
3T0368	3-49		4	11.7	0.40	--	<0.2	--	<0.2	--	<0.2	--	<0.2	--	<0.2	2.57	0.22	--	<0.2
3T0376	3-7		12	--	<0.2	N/A	N/A	N/A	N/A	N/A	N/A	N/A	N/A	N/A	N/A	N/A	N/A	N/A	N/A
3T0405	3-34		2	0.06	1.94	0.07	1.49	--	<0.2	4.15	0.28	--	<0.2	--	<0.2	0.12	1.11	--	<0.2
3T0409	3-43		4	--	<0.2	N/A	N/A	N/A	N/A	N/A	N/A	N/A	N/A	N/A	N/A	N/A	N/A	N/A	N/A
3T0411	3-23		2	0.09	1.80	--	<0.2	--	<0.2	--	<0.2	--	<0.2	--	<0.2	--	<0.2	--	<0.2
3T0415	3-30		4	14.4	0.28	--	<0.2	--	<0.2	--	<0.2	3.55	0.38	--	<0.2	--	<0.2	--	<0.2
3T0420	3-29		2	0.04	1.78	0.05	1.84	--	<0.2	--	<0.2	--	<0.2	--	<0.2	--	<0.2	--	<0.2
3T0427	3-38		2	4.10	0.22	--	<0.2	--	<0.2	--	<0.2	--	<0.2	--	<0.2	--	<0.2	--	<0.2
3T0442	3-32		2	--	<0.2	N/A	N/A	N/A	N/A	N/A	N/A	N/A	N/A	N/A	N/A	N/A	N/A	N/A	N/A
3T0458	3-8		2	--	<0.2	N/A	N/A	N/A	N/A	N/A	N/A	N/A	N/A	N/A	N/A	N/A	N/A	N/A	N/A
3T0468	3-12	s3	17	0.10	1.88	0.12	1.72	--	<0.2	--	<0.2	--	<0.2	0.09	1.63	0.12	1.19	--	<0.2
3T0478	3-47		2	2.21	0.35	4.96	0.26	--	<0.2	--	<0.2	--	<0.2	--	<0.2	0.68	0.62	--	<0.2
3T0506	3-39	s11	7	--	<0.2	N/A	N/A	N/A	N/A	N/A	N/A	N/A	N/A	N/A	N/A	N/A	N/A	N/A	N/A
3T0527	3-40		2	--	<0.2	N/A	N/A	N/A	N/A	N/A	N/A	N/A	N/A	N/A	N/A	N/A	N/A	N/A	N/A
3T0553	3-Single01		1	0.12	1.80	0.07	1.83	0.42	1.83	3.61	0.20	--	<0.2	0.08	1.93	0.07	1.36	--	<0.2
3T0611	3-36		2	0.03	1.74	0.06	1.73	--	<0.2	--	<0.2	--	<0.2	--	<0.2	0.12	1.26	--	<0.2
3T0650	3-20		2	0.05	1.67	0.14	1.71	--	<0.2	--	<0.2	--	<0.2	0.08	1.59	0.18	1.35	--	<0.2
3T0662	3-3		2	--	<0.2	N/A	N/A	N/A	N/A	N/A	N/A	N/A	N/A	N/A	N/A	N/A	N/A	N/A	N/A
3T0673	3-21		4	0.05	1.30	0.07	1.68	--	<0.2	--	<0.2	--	<0.2	0.06	1.58	0.11	1.45	--	<0.2
4T0115	4-46		2	0.07	1.86	0.09	1.72	0.14	1.34	--	<0.2	--	<0.2	--	<0.2	0.12	1.05	--	<0.2
4T0154	4-10		2	0.09	1.68	0.12	1.74	0.12	1.36	1.23	1.05	--	<0.2	--	<0.2	0.23	1.2	--	<0.2
4T0159	4-49	s14	3	6.66	1.19	7.21	1.27	6.83	0.62	--	<0.2	--	<0.2	--	<0.2	14.7	0.53	--	<0.2
4T0168	4-Single01		1	3.44	0.21	--	<0.2	--	<0.2	--	<0.2	--	<0.2	--	<0.2	--	<0.2	--	<0.2
4T0171	4-39	s11	3	--	<0.2	N/A	N/A	N/A	N/A	N/A	N/A	N/A	N/A	N/A	N/A	N/A	N/A	N/A	N/A
4T0176	4-49	s14	3	0.08	1.59	0.06	1.82	0.08	1.75	1.25	1.28	--	<0.2	--	<0.2	0.00	1.19	--	<0.2
4T0182	4-6		2	0.46	1.69	0.35	1.72	1.02	1.56	4.39	1.33	--	<0.2	--	<0.2	0.59	1.31	--	<0.2
4T0238	4-Single02		1	--	<0.2	N/A	N/A	N/A	N/A	N/A	N/A	N/A	N/A	N/A	N/A	N/A	N/A	N/A	N/A
4T0243	4-57	s16	3	0.23	1.10	0.34	0.82	6.20	0.23	5.01	0.25	--	<0.2	--	<0.2	0.09	1.17	--	<0.2
4T0262	4-8		2	0.10	1.77	0.13	1.74	0.20	1.48	0.45	1.61	--	<0.2	--	<0.2	0.23	1.16	--	<0.2
4T0269	4-Single03		1	--	<0.2	N/A	N/A	N/A	N/A	N/A	N/A	N/A	N/A	N/A	N/A	N/A	N/A	N/A	N/A
4T0284	4-2	s1	4	0.06	2.00	0.05	1.80	0.08	1.37	0.43	1.27	--	<0.2	--	<0.2	1.37	0.93	--	<0.2
4T0306	4-55		4	0.08	1.54	0.12	1.63	0.29	1.21	5.75	0.81	--	<0.2	--	<0.2	0.23	0.84	--	<0.2
4T0337	4-42		2	--	<0.2	N/A	N/A	N/A	N/A	N/A	N/A	N/A	N/A	N/A	N/A	N/A	N/A	N/A	N/A
4T0341	4-11		2	--	<0.2	N/A	N/A	N/A	N/A	N/A	N/A	N/A	N/A	N/A	N/A	N/A	N/A	N/A	N/A
4T0344	4-24		2	0.05	1.66	0.06	1.80	0.07	1.60	0.12	1.72	--	<0.2	--	<0.2	0.15	1.08	--	<0.2
4T0350	4-41		2	0.04	1.72	0.11	1.65	--	<0.2	--	<0.2	--	<0.2	0.25	1.44	2.35	1.12	--	<0.2
4T0365	4-50		2	0.06	1.70	0.09	1.67	0.11	1.32	0.24	1.45	0.87	0.27	--	<0.2	0.14	1.18	--	<0.2
4T0412	4-Single04		1	0.08	1.60	0.10	1.49	0.20	0.98	--	<0.2	--	<0.2	--	<0.2	0.12	0.88	--	<0.2
4T0417	4-31		3	--	<0.2	N/A	N/A	N/A	N/A	N/A	N/A	N/A	N/A	N/A	N/A	N/A	N/A	N/A	N/A

Appendix Table 10. Summary of rVSV-ZEBOV-induced antibody binding to Filovirus GPs (continued).


Antibody				GP binding ¹										Binding region ¹					
Name	Clone #	Shared sequence	Number of clonal members	EBOV (Makona)		EBOV (Mayinga)		BDBV		SUDV		MARV		sGP		EBOV ΔMLD		ctrl.	
				EC ₅₀	OD	EC ₅₀	OD	EC ₅₀	OD	EC ₅₀	OD	EC ₅₀	OD	EC ₅₀	OD	EC ₅₀	OD	EC ₅₀	OD
4T0421	4-21		2	--	<0.2	N/A	N/A	N/A	N/A	N/A	N/A	N/A	N/A	N/A	N/A	N/A	N/A	N/A	N/A
4T0423	4-47		3	0.11	1.72	0.16	1.62	0.17	1.19	--	<0.2	--	<0.2	--	<0.2	0.29	1.14	--	<0.2
4T0427	4-38		3	0.10	1.46	0.21	1.62	--	<0.2	4.81	0.53	--	<0.2	0.17	1.58	0.36	1.27	--	<0.2
4T0429	4-48		3	0.07	1.90	0.11	1.75	--	<0.2	--	<0.2	--	<0.2	--	<0.2	--	<0.2	--	<0.2
4T0434	4-44		2	0.06	1.69	0.11	1.59	--	<0.2	0.32	1.35	--	<0.2	--	<0.2	0.15	1.05	--	<0.2
4T0437	4-Single05		1	--	<0.2	N/A	N/A	N/A	N/A	N/A	N/A	N/A	N/A	N/A	N/A	N/A	N/A	N/A	N/A
4T0444	4-15	s3	7	0.16	1.55	0.26	1.60	--	<0.2	--	<0.2	--	<0.2	0.17	1.57	0.18	1.16	--	<0.2
4T0452	4-20		3	0.14	1.62	0.18	1.63	--	<0.2	--	<0.2	--	<0.2	0.17	1.61	0.19	1.18	--	<0.2
4T0520	4-32		4	0.04	1.74	0.06	1.70	--	<0.2	--	<0.2	--	<0.2	--	<0.2	--	<0.2	--	<0.2
4T0525	4-Single06		1	0.07	1.46	0.10	1.51	0.18	1.19	0.28	1.18	--	<0.2	0.11	1.21	0.22	0.98	--	<0.2
4T0541	4-Single10		1	0.19	1.67	0.22	1.57	0.46	1.28	0.79	1.09	--	<0.2	0.45	1.27	0.28	1.04	--	<0.2
4T0563	4-51		2	--	<0.2	N/A	N/A	N/A	N/A	N/A	N/A	N/A	N/A	N/A	N/A	N/A	N/A	N/A	N/A
4T0570	4-7		2	0.05	1.89	0.08	1.80	0.12	1.76	--	<0.2	--	<0.2	--	<0.2	0.10	1.17	--	<0.2
4T0578	4-15	s3	7	0.10	1.65	0.17	1.62	--	<0.2	--	<0.2	--	<0.2	0.07	1.24	0.11	1.12	--	<0.2
4T0657	4-58	s5	3	0.07	1.64	0.08	1.86	--	<0.2	0.14	1.49	--	<0.2	0.05	1.49	0.06	1.20	--	<0.2
4T0726	4-2	s1	4	0.14	1.52	0.11	1.70	0.17	1.63	0.64	1.59	--	<0.2	--	<0.2	0.16	1.15	--	<0.2
4T0764	4-Single07	s15	1	0.06	1.69	0.05	1.75	8.07	0.34	--	<0.2	--	<0.2	0.06	1.73	0.00	1.47	--	<0.2
4T0770	4-Single08	s12	1	--	<0.2	N/A	N/A	N/A	N/A	N/A	N/A	N/A	N/A	N/A	N/A	N/A	N/A	N/A	N/A
4T0784	4-Single09	s9	1	0.27	2.04	0.40	1.71	0.86	1.18	--	<0.2	--	<0.2	0.06	1.43	0.09	1.20	--	<0.2
5T0101	5-36		19	--	<0.2	--	<0.2	--	<0.2	--	<0.2	--	<0.2	--	<0.2	--	<0.2	--	<0.2
5T0104	5-1		10	--	<0.2	N/A	N/A	N/A	N/A	N/A	N/A	N/A	N/A	N/A	N/A	N/A	N/A	N/A	N/A
5T0107	5-35		2	1.86	0.30	--	<0.2	0.92	0.26	--	<0.2	--	<0.2	--	<0.2	--	<0.2	--	<0.2
5T0124	5-49		2	--	<0.2	N/A	N/A	N/A	N/A	N/A	N/A	N/A	N/A	N/A	N/A	N/A	N/A	N/A	N/A
5T0139	5-28		2	--	<0.2	N/A	N/A	N/A	N/A	N/A	N/A	N/A	N/A	N/A	N/A	N/A	N/A	N/A	N/A
5T0147	5-39		5	--	<0.2	N/A	N/A	N/A	N/A	N/A	N/A	N/A	N/A	N/A	N/A	N/A	N/A	N/A	N/A
5T0180	5-17		2	0.25	1.91	0.34	1.54	7.40	0.23	--	<0.2	--	<0.2	0.15	1.21	0.44	1.19	--	<0.2
5T0181	5-47		4	--	<0.2	N/A	N/A	N/A	N/A	N/A	N/A	N/A	N/A	N/A	N/A	N/A	N/A	N/A	N/A
5T0202	5-18		3	0.20	1.65	0.26	1.47	--	<0.2	--	<0.2	--	<0.2	0.20	1.25	0.36	1.3	--	<0.2
5T0209	5-13		3	0.13	1.83	0.13	1.48	--	<0.2	--	<0.2	--	<0.2	0.09	1.27	0.13	1.11	--	<0.2
5T0223	5-16		6	0.26	1.93	0.22	1.54	--	<0.2	7.17	0.45	--	<0.2	0.14	1.35	0.21	1.11	--	<0.2
5T0246	5-Single01		1	--	<0.2	N/A	N/A	N/A	N/A	N/A	N/A	N/A	N/A	N/A	N/A	N/A	N/A	N/A	N/A
5T0257	5-Single02	s5	1	1.69	0.85	1.70	0.66	--	<0.2	0.36	1.19	--	<0.2	0.25	1.12	0.64	0.69	--	<0.2
5T0259	5-15		4	--	<0.2	N/A	N/A	N/A	N/A	N/A	N/A	N/A	N/A	N/A	N/A	N/A	N/A	N/A	N/A
5T0278	5-23		2	0.08	1.99	0.06	1.59	10.4	0.22	--	<0.2	--	<0.2	0.06	1.41	0.10	1.12	--	<0.2
5T0322	5-41		10	--	<0.2	N/A	N/A	N/A	N/A	N/A	N/A	N/A	N/A	N/A	N/A	N/A	N/A	N/A	N/A
5T0337	5-25		2	0.31	1.90	0.27	1.70	5.63	0.20	--	<0.2	--	<0.2	0.16	1.55	0.16	1.10	--	<0.2
5T0376	5-Single03	s15	1	0.07	1.62	0.07	1.88	--	<0.2	--	<0.2	--	<0.2	0.07	1.70	0.01	1.40	--	<0.2
5T0377	5-50		2	0.59	0.86	1.25	0.50	--	<0.2	--	<0.2	--	<0.2	--	<0.2	0.16	0.87	--	<0.2
5T0378	5-48	s14	2	0.07	1.75	0.11	1.66	0.16	1.55	2.05	0.88	--	<0.2	--	<0.2	0.12	0.94	--	<0.2
5T0404	5-7		3	0.18	1.29	0.51	1.48	0.53	1.47	1.11	1.05	--	<0.2	0.68	1.36	0.80	0.95	--	<0.2
5T0406	5-8		3	0.36	1.41	0.72	1.38	1.15	1.35	1.36	0.97	--	<0.2	2.51	1.26	0.76	0.92	--	<0.2
5T0420	5-48	s14	2	0.15	1.62	0.08	1.80	0.15	1.75	1.97	1.55	2.12	0.20	--	<0.2	0.11	1.20	--	<0.2
5T0438	5-45		9	--	<0.2	N/A	N/A	N/A	N/A	N/A	N/A	N/A	N/A	N/A	N/A	N/A	N/A	N/A	N/A
5T0451	5-11		3	0.14	1.77	0.18	1.66	1.92	0.21	--	<0.2	--	<0.2	0.13	1.51	0.12	1.18	--	<0.2
5T0459	5-46		2	--	<0.2	N/A	N/A	N/A	N/A	N/A	N/A	N/A	N/A	N/A	N/A	N/A	N/A	N/A	N/A
5T0464	5-6		3	--	<0.2	N/A	N/A	N/A	N/A	N/A	N/A	N/A	N/A	N/A	N/A	N/A	N/A	N/A	N/A
5T0465	5-Single04	s16	1	0.22	0.86	1.04	0.56	--	<0.2	--	<0.2	--	<0.2	--	<0.2	0.82	0.85	--	<0.2

Appendix Table 10. Summary of rVSV-ZEBOV-induced antibody binding to Filovirus GPs (continued).

Antibody				GP binding ¹										Binding region ¹					
Name	Clone #	Shared sequence	Number of clonal members	EBOV (Makona)		EBOV (Mayinga)		BDBV		SUDV		MARV		sGP		EBOV ΔMLD		ctrl.	
				EC ₅₀	OD	EC ₅₀	OD	EC ₅₀	OD	EC ₅₀	OD	EC ₅₀	OD	EC ₅₀	OD	EC ₅₀	OD	EC ₅₀	OD
4m0314	4-69	N/A	2	--	<0.2	N/A	N/A	N/A	N/A	N/A	N/A	N/A	N/A	N/A	N/A	N/A	N/A	N/A	N/A
4m0333	4-58	N/A	5	0.05	1.35	0.08	1.61	--	<0.2	0.13	1.25	--	<0.2	0.06	1.59	0.24	1.22	--	<0.2
4m0357	4-63	N/A	2	--	<0.2	N/A	N/A	N/A	N/A	N/A	N/A	N/A	N/A	N/A	N/A	N/A	N/A	N/A	N/A
4m0361	4-59	N/A	3	0.10	1.52	0.11	1.75	--	<0.2	--	<0.2	--	<0.2	0.08	1.73	0.17	1.33	--	<0.2
4m0365	4-62	N/A	2	--	<0.2	N/A	N/A	N/A	N/A	N/A	N/A	N/A	N/A	N/A	N/A	N/A	N/A	N/A	N/A
4m0368	4-52	N/A	3	0.83	0.70	0.90	0.54	--	<0.2	--	<0.2	--	<0.2	--	<0.2	0.32	1.01	--	<0.2
4m0373	4-12	N/A	6	0.08	1.68	0.10	1.72	0.14	1.53	--	<0.2	--	<0.2	--	<0.2	0.21	1.13	--	<0.2
4m0387	4-68	N/A	2	8.88	1.29	14.4	0.27	--	<0.2	--	<0.2	--	<0.2	--	<0.2	--	<0.2	--	<0.2

¹ Intensity above an OD of ≥ 0.2 was defined as binding

N/A = not analyzed

 = mAbs of shared sequences

 = mAbs with V genes IGHV3-15 and IGLV1-40

Appendix Table 11. Specific peptide sequences of peptide library epitope screening detected by rVSV-ZEBOV-induced mAbs.

Antibodies	Epitope	Peptide sequence	Antibodies	Epitope	Peptide sequence
1T0130	SP	LPRDRFKRTSFFLWV IIL	3T0420	Gly-cap	TPQFLLQLNETIYASGKR
	GP1	SASSGKLG LITNTIAGVA		Gly-cap	NETIYASGKRSNTTGKLI
1T0139	SP	LPRDRFKRTSFFLWV IIL		MLD	ENSSAMVQVHSQGRKAAV
	SP	TSFFLWV IILFQRTFSIP	MLD	VHSQGRKAAVSHLTLAT	
1T0201	SP	MGVTGILQLPRDRFKRTS	3T0427	GP1	GPCAGDFAFHKEGAFFLY
	GP1	EPVNATEDPSSGYSTTI		GP1	FHKEGAFFLYDRLASTVI
	SP	LPRDRFKRTSFFLWV IIL		Gly-cap	NETIYASGKRSNTTGKLI
	SP	TSFFLWV IILFQRTFSIP	3T0468	GP1	AENCYNLEIKKPDGSECL
1T0221	GP1	EPVNATEDPSSGYSTTI		HR1/2	LLQRWGGTCHILGPDCCI
1T0248	SP	LPRDRFKRTSFFLWV IIL	3T0611	GP1	HHQDTGEESASSGKLG LI
	MLD	DNSTHNTPVYKLDISEAT	4m0361	SP	MGVTGILQLPRDRFKRTS
	MLD	VYKLDISEATQVGQHRR	4m0368	GP1	SATKRWGFERSGVPKVVN
1T0264	SP	LPRDRFKRTSFFLWV IIL	4m0373	HR1/2	CIEPHDWTKNITDKIDQI
	MLD	ATQVGQHRRADNDSTAS	4T0159	SP	MGVTGILQLPRDRFKRTS
1T0301	SP	LPRDRFKRTSFFLWV IIL		SP	LPRDRFKRTSFFLWV IIL
	MLD	DNSTHNTPVYKLDISEAT		SP	TSFFLWV IILFQRTFSIP
	MLD	ATQVGQHRRADNDSTAS		GP1	IPLGVIHNSTLQVSDVDK
1T0325	SP	LPRDRFKRTSFFLWV IIL		GP1	STLQVSDVDKLVCRDKLS
	SP	TSFFLWV IILFQRTFSIP	GP1	SVGLNLENGVATDVPSA	
	MLD	DNSTHNTPVYKLDISEAT	4T0168	GP1	AENCYNLEIKKPDGSECL
	MLD	VYKLDISEATQVGQHRR		MLD	AVSHLTLATISTSPQPP
1T0451	MLD	VYKLDISEATQVGQHRR	4T0176	SP	LPRDRFKRTSFFLWV IIL
1T0465	GP1	AENCYNLEIKKPDGSECL		GP1	SVGLNLENGVATDVPSA
	HR1/2	LLQRWGGTCHILGPDCCI		GP1	VNYEAGEWAENCYNLEIK
	HR1/2	CHILGPDCCIEPHDWTKN		HR1/2	LLQRWGGTCHILGPDCCI
1T0546	SP	MGVTGILQLPRDRFKRTS		HR1/2	CHILGPDCCIEPHDWTKN
	SP	LPRDRFKRTSFFLWV IIL	4T0182	IFL	PNLHYWTTQDEGAAIGLA
	MLD	PPTTKTGPDNSTHNTPVY		IFL	QDEGAAIGLAWIPYFGPA
	MLD	DNSTHNTPVYKLDISEAT	4T0243	HR1/2	CHILGPDCCIEPHDWTKN
1T0552	SP	LPRDRFKRTSFFLWV IIL	4T0284	GP1	IPLGVIHNSTLQVSDVDK
	GP1	AENCYNLEIKKPDGSECL		Gly-cap	AFWETKKNLTKIRSEEL
1T0565	MLD	EDHKIMASENSSAMVQVH		GP1	VNYEAGEWAENCYNLEIK
	MLD	ENSSAMVQVHSQGRKAAV	GP1	FFSSHPLREPVNATEDPS	
1T0655	MPER	KNITDKIDQI IHDFVDKT	4T0350	Gly-cap	NETIYASGKRSNTTGKLI
3T0215	Gly-cap	IDTTIGEWAFWETKKNLT		Gly-cap	KRSNTTGKLIWKVNPEID
3T0258	SP	LPRDRFKRTSFFLWV IIL		Gly-cap	LIWKVNPEIDTTIGEWAF
	GP1	AENCYNLEIKKPDGSECL		Gly-cap	IDTTIGEWAFWETKKNLT
	GP1	ILPQAKKDFSSHPLREP	4T0365	HR1/2	LLQRWGGTCHILGPDCCI
3T0331	IFL	VAGLITGGRRTREVIIVN	4T0423	HR1/2	LLQRWGGTCHILGPDCCI
3T0350	GP1	SVGLNLENGVATDVPSA		HR1/2	CHILGPDCCIEPHDWTKN
	GP1	NGVATDVPSATKRWGFERS	4T0429	MLD	PPTTKTGPDNSTHNTPVY
3T0368	SP	LPRDRFKRTSFFLWV IIL		MLD	DNSTHNTPVYKLDISEAT
	3T0405	Gly-cap	LTRKIRSEELSFTAVSNG	4T0520	MLD
MLD		ELSFTAVSNGPKNISGQS	MLD		VYKLDISEATQVGQHRR
3T0411	SP	LPRDRFKRTSFFLWV IIL	4T0525	SP	LPRDRFKRTSFFLWV IIL
	SP	LPRDRFKRTSFFLWV IIL		SP	TSFFLWV IILFQRTFSIP

Appendix Table 11. Specific peptide sequences of peptide library epitope screening detected by rVSV-ZEBOV-induced mAbs (continued).

Antibodies	Epitope	Peptide sequence	Antibodies	Epitope	Peptide sequence
4T0541	SP	LPRDRFKRTSFFLWVIL	5T0465	SP	LPRDRFKRTSFFLWVIL
4T0570	MPER	KNITDKIDQIIHDFVDKT		SP	TSFFLWVILFQRTFSIP
	MPER	QIIHDFVDKTLPDQGDND		GP1	IPLGVIHNSTLQVSDVDK
4T0578	SP	LPRDRFKRTSFFLWVIL		Gly-cap	IDTTIGEWAFWETKKNLT
4T0764	GP1	IKKPDGSECLPAAPDGIR		HR1/2	LNKKAIDFLLQRWGGTCH
	Gly-cap	AFWETKKNLTRKIRSEEL	HR1/2	CHILGPDCCIEPHDWTKN	
	HR1/2	TELRTFSILNRKAIDFLL	ADI-15758	MPER	KNITDKIDQIIHDFVDKT
5T0107	GP1	AENCYNLEIKKPDGSECL	KZ52	SP	TSFFLWVILFQRTFSIP
	HR1/2	TELRTFSILNRKAIDFLL		GP1	IPLGVIHNSTLQVSDVDK
5T0257	SP	MGVTGILQLPRDRFKRTS		IFL	RRTRREVIVNAQPKCNPN
5T0278	GP1	VIYRGTTF AEGVVAFLIL	IFL	VNAQPKCNPNLHYWTTQD	
5T0376	GP1	IKKPDGSECLPAAPDGIR	mAb100	SP	LPRDRFKRTSFFLWVIL
	Gly-cap	AFWETKKNLTRKIRSEEL		GP1	IPLGVIHNSTLQVSDVDK
5T0377	SP	LPRDRFKRTSFFLWVIL		GP1	LITNTIAGVAGLITGRR
5T0378	HR1/2	LLQRWGGTCHILGPDCCI		IFL	RRTRREVIVNAQPKCNPN
5T0420	GP1	SVGLNLEGNVATDVPSA		HR1/2	LQLFLRATTELRTFSILN
mAb114	SP	MGVTGILQLPRDRFKRTS	Gly-cap	AFWETKKNLTRKIRSEEL	
	Gly-cap	AFWETKKNLTRKIRSEEL			

SP: signal peptide

MPER: Membrane proximal external region

Gly-cap: Glycan cap

HR: Heptad repeat

IFL: Internal fusion loop

Appendix Table 12. Summary of rVSV-ZEBOV-induced antibody characteristics.

Antibody				Competition ¹				Peptide Library ²							Summary					Neutra- lization								
Name	Clone #	Shared sequence	Number of clonal members ⁵	ADI-15758		ADI-15999		KZ52		mAb100	GP1	Gly-cap	MLD	GP1	IFL	HR 1	HR 2	MPER	sGP	GP1 (Base/Head)	Gly-Cap	MDL	GP1 (C-terminal)	IFL	HR 1/HR 2	MPER	EBOV ³	SUDV ³
				IC50	IC50	IC50	IC50	KZ52	ADI																			
1T0114	1-26		2	N/A	N/A	N/A	N/A																			N/A	N/A	
1T0116	1-31		2	N/A	N/A	N/A	N/A																				N/A	N/A
1T0129	1-4		8	N/A	N/A	N/A	N/A																				--	--
1T0130	1-9		2	--	--	--	--																				--	N/A
1T0139	1-46		3	--	--	46	77																			7.44	N/A	
1T0201	1-18		2	N/A	N/A	N/A	N/A																				2.63	N/A
1T0221	1-1	s1	9	--	--	--	--																				--	--
1T0222	1-38		2	N/A	N/A	N/A	N/A																				N/A	N/A
1T0225	1-40		2	--	--	--	--																				--	--
1T0227	1-15		3	N/A	N/A	N/A	N/A																				1.86	N/A
1T0242	1-39		5	N/A	N/A	N/A	N/A																				--	N/A
1T0248	1-25		2	N/A	N/A	N/A	N/A																				14.8	N/A
1T0264	1-22		3	--	--	--	--																				--	N/A
1T0301	1-41		2	--	--	--	--																				--	N/A
1T0321	1-Single02		1	--	--	--	--																				--	--
1T0325	1-23		2	--	--	--	--																				2.63	N/A
1T0351	1-37		2	N/A	N/A	N/A	N/A																				N/A	N/A
1T0371	1-12		3	--	--	--	--																				--	N/A
1T0451	1-7		3	--	--	--	--																				2.50	N/A
1T0455	1-16		3	N/A	N/A	N/A	N/A																				1.77	N/A
1T0465	1-1	s1	9	--	--	--	--																				--	--
1T0473	1-14		5	N/A	N/A	N/A	N/A																				2.63	N/A
1T0480	1-42		7	N/A	N/A	N/A	N/A																				N/A	N/A
1T0546	1-32		2	--	--	--	--																				--	N/A
1T0552	1-24		2	--	--	--	--																				--	N/A
1T0554	1-5		6	N/A	N/A	N/A	N/A																				--	N/A
1T0565	1-28		5	--	--	--	--																				--	N/A
1T0582	1-6		5	N/A	N/A	N/A	N/A																				N/A	N/A
1T0614	1-36		3	N/A	N/A	N/A	N/A																				--	N/A
1T0623	1-11		2	N/A	N/A	N/A	N/A																				--	N/A
1T0653	1-Single03		1	N/A	N/A	N/A	N/A																				N/A	N/A
1T0655	1-10		2	173	136	--	45																				0.08	N/A
1T0665	1-35		3	N/A	N/A	N/A	N/A																				N/A	N/A
3T0123	3-2		2	--	--	103	73																				0.52	N/A
3T0135	3-42	s12	2	N/A	N/A	N/A	N/A																				--	N/A
3T0147	3-46		2	--	--	--	--																				--	N/A
3T0159	3-44		2	--	--	--	--																				N/A	N/A
3T0183	3-6		37	N/A	N/A	N/A	N/A																				N/A	N/A
3T0202	3-12	s3	17	N/A	N/A	N/A	N/A																				0.53	N/A
3T0209	3-7		12	N/A	N/A	N/A	N/A																				50.0	N/A
3T0210	3-6		37	N/A	N/A	N/A	N/A																				--	N/A
3T0213	3-4		6	N/A	N/A	N/A	N/A																				N/A	N/A
3T0215	3-35		2	N/A	N/A	N/A	N/A																				--	--
3T0216	3-48		2	N/A	N/A	N/A	N/A																				N/A	N/A
3T0227	3-7		12	N/A	N/A	N/A	N/A																				N/A	N/A
3T0245	3-22	s4	3	--	--	--	--																				0.63	N/A
3T0251	3-6		37	N/A	N/A	N/A	N/A																				N/A	N/A

Appendix Table 12. Summary of rVSV-ZEBOV-induced antibody characteristics (continued).

Antibody			Competition ¹				Peptide Library ²							Summary					Neutra- lization					
Name	Clone #	Shared sequence	Number of clonal members ⁵				GP1	Gly-cap	MLD	GP1	IFL	HR 1	HR 2	MPER	sGP	GP1 (Base/Head)	Gly-Cap	MDL	GP1 (C-terminal)	IFL	HR 1/HR 2	MPER	EBOV ³	SUDV ³
			ADI-15758	ADI-15999	KZ52	mAb100																		
3T0253	3-24		3	N/A	N/A	N/A	N/A															1.31	--	
3T0258	3-1		3	--	--	69	111															0.06	N/A	
3T0265	3-19		2	N/A	N/A	N/A	N/A															0.44	N/A	
3T0303	3-10		4	N/A	N/A	N/A	N/A															N/A	N/A	
3T0325	3-41		2	N/A	N/A	N/A	N/A															N/A	N/A	
3T0331	3-26		4	--	--	116	108															0.01	N/A	
3T0338	3-3-02		1	N/A	N/A	N/A	N/A															1.06	N/A	
3T0350	3-28		3	N/A	N/A	N/A	N/A															--	--	
3T0353	3-45		3	N/A	N/A	N/A	N/A															N/A	N/A	
3T0368	3-49		4	177	124	--	--															--	N/A	
3T0376	3-7		12	N/A	N/A	N/A	N/A															N/A	N/A	
3T0405	3-34		2	--	--	55	30															--	--	
3T0409	3-43		4	N/A	N/A	N/A	N/A															--	N/A	
3T0411	3-23		2	--	--	--	--															--	N/A	
3T0415	3-30		4	--	--	--	--															--	N/A	
3T0420	3-29		2	--	--	--	--															--	N/A	
3T0427	3-38		2	--	--	--	--															--	N/A	
3T0442	3-32		2	N/A	N/A	N/A	N/A															N/A	N/A	
3T0458	3-8		2	N/A	N/A	N/A	N/A															N/A	N/A	
3T0468	3-12	s3	17	N/A	N/A	N/A	N/A															2.1	N/A	
3T0478	3-47		2	--	--	--	--															0.78	N/A	
3T0506	3-39	s11	7	N/A	N/A	N/A	N/A															N/A	N/A	
3T0527	3-40		2	N/A	N/A	N/A	N/A															N/A	N/A	
3T0553	3-3-01		1	--	--	55	35															1.31	--	
3T0611	3-36		2	--	--	--	--															0.78	N/A	
3T0650	3-20		2	N/A	N/A	N/A	N/A															0.74	N/A	
3T0662	3-3		2	N/A	N/A	N/A	N/A															N/A	N/A	
3T0673	3-21		4	N/A	N/A	N/A	N/A															0.53	N/A	
4T0115	4-46		2	--	--	--	--															--	N/A	
4T0154	4-10		2	--	--	--	--															--	--	
4T0159	4-49	s14	3	--	--	--	--															--	N/A	
4T0168	4-3-01		1	--	--	--	--															--	N/A	
4T0171	4-39	s11	3	N/A	N/A	N/A	N/A															--	N/A	
4T0176	4-49	s14	3	--	--	--	--															--	--	
4T0182	4-6		2	36	--	--	--															--	--	
4T0238	4-3-02		1	N/A	N/A	N/A	N/A															N/A	N/A	
4T0243	4-57	s16	3	--	--	89	148															0.01	--	
4T0262	4-8		2	--	--	--	--															--	N/A	
4T0269	4-3-03		1	N/A	N/A	N/A	N/A															N/A	N/A	
4T0284	4-2	s1	4	--	--	--	--															--	--	
4T0306	4-55		4	--	--	--	--															100	--	
4T0337	4-42		2	N/A	N/A	N/A	N/A															N/A	N/A	
4T0341	4-11		2	N/A	N/A	N/A	N/A															N/A	N/A	
4T0344	4-24		2	--	--	--	--															--	--	
4T0350	4-41		2	N/A	N/A	N/A	N/A															--	N/A	
4T0365	4-50		2	--	--	--	--															--	--	
4T0412	4-3-04		1	--	--	--	--															--	N/A	
4T0417	4-31		3	N/A	N/A	N/A	N/A															N/A	N/A	

Appendix Table 12. Summary of rVSV-ZEBOV-induced antibody characteristics (continued).

Antibody			Competition ¹				Peptide Library ²							Summary					Neutra- lization						
Name	Clone #	Shared sequence	Number of clonal members ⁵	ADI-15758	ADI-15999	KZ52	mAb100	GP1	Gly-cap	MLD	GP1	IFL	HR 1	HR 2	MPER	sGP	GP1 (Base/Head)	Gly-Cap	MDL	GP1 (C-terminal)	IFL	HR 1/HR 2	MPER	EBOV ³	SUDV ³
				IC50	IC50	IC50	IC50					KZ52	ADI	GP1	GP2		IC100	IC100							
4T0421	4-21		2	N/A	N/A	N/A	N/A																	N/A	N/A
4T0423	4-47		3	--	--	--	--																	--	N/A
4T0427	4-38		3	N/A	N/A	N/A	N/A																	--	--
4T0429	4-48		3	--	--	--	--																	35.0	N/A
4T0434	4-44		2	--	--	--	--																	--	--
4T0437	4-4-Clone05		1	N/A	N/A	N/A	N/A																	N/A	N/A
4T0444	4-15	s3	7	N/A	N/A	N/A	N/A																	1.20	N/A
4T0452	4-20		3	N/A	N/A	N/A	N/A																	0.88	N/A
4T0520	4-32		4	--	--	--	--																	--	N/A
4T0525	4-4-Clone06		1	N/A	N/A	N/A	N/A																	--	--
4T0541	4-4-Clone10		1	N/A	N/A	N/A	N/A																	--	--
4T0563	4-51		2	N/A	N/A	N/A	N/A																	N/A	N/A
4T0570	4-7		2	187	139	--	128																	0.09	N/A
4T0578	4-15	s3	7	N/A	N/A	N/A	N/A																	0.45	N/A
4T0657	4-58	s5	3	--	--	--	--																	--	--
4T0726	4-2	s1	4	--	--	--	--																	2.56	--
4T0764	4-4-Clone07	s15	1	--	--	--	--																	0.88	N/A
4T0770	4-4-Clone08	s12	1	N/A	N/A	N/A	N/A																	N/A	N/A
4T0784	4-4-Clone09	s9	1	--	--	52	48																	1.86	N/A
5T0101	5-36		19	--	--	--	--																	N/A	N/A
5T0104	5-1		10	N/A	N/A	N/A	N/A																	N/A	N/A
5T0107	5-35		2	--	--	--	--																	--	N/A
5T0124	5-49		2	N/A	N/A	N/A	N/A																	N/A	N/A
5T0139	5-28		2	N/A	N/A	N/A	N/A																	N/A	N/A
5T0147	5-39		5	N/A	N/A	N/A	N/A																	N/A	N/A
5T0180	5-17		2	N/A	N/A	N/A	N/A																	12.5	N/A
5T0181	5-47		4	N/A	N/A	N/A	N/A																	N/A	N/A
5T0202	5-18		3	N/A	N/A	N/A	N/A																	2.5	N/A
5T0209	5-13		3	N/A	N/A	N/A	N/A																	1.77	N/A
5T0223	5-16		6	N/A	N/A	N/A	N/A																	1.86	--
5T0246	5-5-Clone01		1	N/A	N/A	N/A	N/A																	N/A	N/A
5T0257	5-5-Clone02	s5	1	--	--	--	--																	--	--
5T0259	5-15		4	N/A	N/A	N/A	N/A																	N/A	N/A
5T0278	5-23		2	N/A	N/A	N/A	N/A																	0.63	N/A
5T0322	5-41		10	N/A	N/A	N/A	N/A																	N/A	N/A
5T0337	5-25		2	N/A	N/A	N/A	N/A																	2.21	N/A
5T0376	5-5-Clone03	s15	1	--	--	--	--																	12.5	N/A
5T0377	5-50		2	--	--	44	--																	--	N/A
5T0378	5-48	s14	2	--	--	--	--																	--	--
5T0404	5-7		3	N/A	N/A	N/A	N/A																	--	--
5T0406	5-8		3	N/A	N/A	N/A	N/A																	--	--
5T0420	5-48	s14	2	--	--	--	--																	--	--
5T0438	5-45		9	N/A	N/A	N/A	N/A																	N/A	N/A
5T0451	5-11		3	N/A	N/A	N/A	N/A																	1.05	N/A
5T0459	5-46		2	N/A	N/A	N/A	N/A																	N/A	N/A
5T0464	5-6		3	N/A	N/A	N/A	N/A																	N/A	N/A
5T0465	5-5-Clone04	s16	1	--	--	54	123																	0.66	N/A
5T0474	5-27		3	N/A	N/A	N/A	N/A																	N/A	N/A

Appendix Table 12. Summary of rVSV-ZEBOV-induced antibody characteristics (continued).

Antibody				Competition ¹					Peptide Library ²								Summary				Neutra- lization			
Name	Clone #	Shared sequence	Number of clonal members ⁵	ADI-15758	ADI-15999	KZ52	mAb100	KZ52	GP1	IFL	HR 1	HR 2	MPER	ADL	sGP	GP1 (Base/Head)	Gly-Cap	MDL	GP1 (C-terminal)	IFL	HR 1/HR 2	MPER	EBOV ³	SUDV ³
				IC50	IC50	IC50	IC50									GP1	GP2	IC100	IC100					
4m0314	4-69	N/A	2	N/A	N/A	N/A	N/A																N/A	N/A
4m0333	4-58	N/A	5	N/A	N/A	N/A	N/A																--	--
4m0357	4-63	N/A	2	N/A	N/A	N/A	N/A																--	N/A
4m0361	4-59	N/A	3	N/A	N/A	N/A	N/A																--	N/A
4m0365	4-62	N/A	2	N/A	N/A	N/A	N/A																--	N/A
4m0368	4-52	N/A	3	--	--	66	96																0.13	N/A
4m0373	4-12	N/A	6	48	36	--	--																--	N/A
4m0387	4-68	N/A	2	--	--	--	--																--	N/A


¹ Competition was defined as inhibition $\geq 25\%$.

² Intensity above an OD of ≥ 0.125 was defined as binding

³ Neutralization indicated in $\mu\text{g/mL}$

⁵ Including clonal members of EBOV *Makona* GP Δ TM and EBOV *Makona* GP Δ MLD Δ TM

N/A = not analyzed

 = mAbs of shared sequences

 = mAbs with V genes IGHV3-15 and IGLV1-40

 = positive interaction

 = potential binding area